TU WIEN

TECHNISCHE UNIVERSITÄT WIEN

PhD Thesis

Dissertation

Advanced additives for radical photopolymerization

ausgeführt zum Zwecke der Erlangung des akademischen Grades eines
Doktors der technischen Wissenschaften
unter der Leitung von

Univ.Prof. Dipl.-Ing. Dr.techn. Robert Liska

E163

Institut für Angewandte Synthesechemie

eingereicht an der Technischen Universität Wien
Fakultät für Technische Chemie
von

Dipl.-Ing. Paul Gauss

0726206

Scheibenbergstraße 47, 1180 Wien

Wien, 25.02.2019   Dipl.-Ing. Paul Gauss

"Die Wissenschaft fängt eigentlich erst da an interessant zu werden, wo sie aufhört."

Justus von Liebig, „Chemische Briefe"

Abstract

Photopolymerization of (meth)acrylate-based resins is a widespread method for decorative and protective coatings due to the energy efficiency and fast curing of this technology. Common industrial radical photoinitiators are generally based on aromatic ketones with the benzoyl-chromophore as the key constituent. Residual photoinitiators or photo products as ubiquitous contaminants are rising health concerns. In this work a new generation of non-aromatic initiator systems was developed to find an alternative for potentially hazardous aromatic initiators. Therefore different aliphatic α-ketoesters were selected and synthesized. Simple aliphatic ketoesters such as ethyl pyruvate and alkyl oxobutanoates with increasing methylation in β-position were able to compete with or outperform typical industrial Type II initiators in acrylates and methacrylates. The performance could be boosted further with amine coinitiators but in general all ketoesters show limited stability under influence of strong basic aliphatic amines.

By cyclization of aliphatic ketoesters a highly reactive near visible initiator was found which outperformed standard visible light thioxanthone initiator ITX at 400 nm. Ethyl pyruvate EP and cyclic ketoester DDFD are also quite good water-soluble and excellent for polymerizing acrylic hydrogels, additionally the compounds showed excellent biocompatibility. All ketoesters have excellent bleaching properties and did not cause any discoloration of the polymers in UV-aging tests.

To improve the material properties of radical photopolymers it was tried to find new chain transfer agents (CTA) based on addition fragmentation chain transfer (AFCT) and hydrogen abstraction fragmentation chain transfer (HAFCT). In case of the new class of HAFCT CTAs it was tried to prepare dimethoxy cyclohexadienes with different leaving groups. A t-butyl dimethyl silyl cyclohexadiene (SiDCH) was stable and proofed the concept of hydrogen abstraction chain transfer in difunctional methacrylates successfully.

Kurzfassung

Photopolymerisation von (Meth)acrylat basierenden Harzen findet weltweit breite Anwendung im Bereich von dekorativen Beschichtungen und als Schutzschicht. Die schnelle und energieeffiziente Härtung von Formulierungen macht diese Technologie besonders attraktiv. Üblicherweise bestehen die verwendeten Photoinitiatoren aus aromatischen Ketonen mit einem Benzoylchromophor als zentraler funktioneller Gruppe. Die mittlerweile überall nachweisbaren aromatischen Überreste aus Initiatoren und deren Photoprodukten werden zunehmend als Gesundheitsgefahr wahrgenommen. Daher beschäftigt sich diese Arbeit mit der Entwicklung neuer radikalischer Photoinitiatoren die ohne aromatische Substituenten auskommen.

Dazu wurden verschiedene aliphatische α-Ketoester ausgesucht und hergestellt. Einfache Ketoester wie Ethylpyruvat und zunehmend β-methylierte Oxobutanoate waren in der Lage sich mit klassischen Typ II Industrieinitiatoren zu Messen oder diese sogar zu übertreffen. Die Reaktivität konnte zusätzlich durch Zugabe von aminischen Coinitiatoren verbessert werden, allerdings zeigten die meisten Ketoester eine schlechte Lagerstabilität in zu basischen aliphatischen Aminen.

Zyklisierung der Ketoester sorgte für eine hohe Photoreaktivität auch im sichtbaren Bereich. Hier konnte der zyklische Ketoester DDFD sogar den Standard Thioxanthon Typ II Initiator ITX unter Bestrahlung bei 400 nm in den Schatten stellen. Ethylpyruvat und der zyklische Ketoester DDFD waren außerdem gut wasserlöslich und konnten erfolgreich zur Herstellung von Hydrogelen verwendet werden. Zudem zeigen die Initiatoren eine ausgezeichnete Biokompatibilität. Bei der UV-Alterung zeigte sich zusätzlich eine besonders hohe Farbbeständigkeit der mit Ketoestern gehärteten Proben. Damit wurde eine neue Klasse an ungefährlichen aliphatischen Photoinitiatoren gefunden die übliche aromatische Initiatoren in der Industrie ablösen könnten.

Um die Materialeigenschaften von spröden Photopolymeren zu verbessern wurde versucht neue Kettentransferreagenzien (CTA) basierend auf Additions Fragmentierungs Kettentransfer (AFCT) und Wassertsoffabstraktions Fragmentierungs Kettentransfer (HAFCT) zu finden.

Die neue Klasse an HAFCT CTAs basierend auf Dimethoxycyclohexadienen stellte sich vor allem synthetisch als herausfordernd da. Eine stabile Substanz t-Butyldimethylsilylcyclohexadien SiDCH konnte isoliert werden und in difunktionellen Methacrylaten wurde das Konzept des Wassertsoffabstraktions Fragmentierungs Kettentransfer erfolgreich bestätigt.

Danksagung

An dieser Stelle möchte ich mich bei Herrn Univ. Prof. Dr. Robert Liska herzlichst bedanken! Lieber Robert, du hattest nicht nur währen des gesamten Verlaufs meiner Dissertation Zeit und Geduld jede Idee zu diskutieren, sondern auch während vieler freundschaftlicher Stunden abseits des Arbeitsalltags immer ein offenes Ohr für mich. Seit ich 2011 während meiner Bachelorarbeit zu einem Teil dieser Arbeitsgruppe wurde, fühle ich mich wie in einer Familie aufgehoben. Du hast zusammen mit Simone eine Gruppe unglaublich hilfsbereiter und kluger Menschen um dich geschart, die ich alle in mein Herz geschlossen habe. Ich schätze mich sehr glücklich ein Teil davon zu sein, denn nur durch diese enge Zusammenarbeit und die vielen geselligen Stunden konnte diese Arbeit entstehen.

Ich möchte mich auch bei meinen Publikationspartnern Univ. Prof. Dr. Georg Gescheidt, Assoc. Prof. Dr. Aleksandr Ovsianikov, Dr. Markus Griesser und Frau Dr. Marica Marovic herzlichst für die gute Zusammenarbeit bedanken.

Außerdem gilt meinen UnivAss-Kollegen Mia, Christian, Markus, Yazgan, Sarah, Hofi, Olga und Patrick besonderer Dank für die vielen Stunden im und abseits des Otech-Labor. Es hat viel Spaß gemacht mit Euch gemeinsam unsere Nachfolger zu betreuen.

Mein Dank gilt auch all meinen restlichen Laborkollegen mit denen ich nicht nur gemeinsam diskutiert und geforscht habe, sondern auch viele illustre Erlebnisse abseits der Arbeit verbinde: Konzi, Stefan, Stephan, Schnölli, Moritz, György, Sascha, AD, Sebi, Pazi, Kathi, Raffi, Gernot, Chris, Nico, Roland, Johannes, Elise, Suljo, Bettina, Sandra, Davide, Max, Markus und Daniel und Daniel. Es freut mich ganz besonders, dass über die Forschungsarbeit hinaus auch Freundschaften entstanden sind.

Auch bei meinen Bachelor Studenten Max, Roland und Simon möchte ich mich für die schöne Zeit bedanken.

Bester Dank gebührt auch dem nichtwissenschaftlichen Personal Walter, Dagmar, Helena, Andrea, Renée, Danko und Isolde die für einen reibungslosen Betrieb sorgen.

Meine tiefe Verbundenheit möchte ich meinen Eltern Elvira und Peter, sowie meiner Lebensgefährtin Lilly aussprechen, die mich immer nach vollen Kräften unterstützt haben.

Danke!

Macromolecular Chemistry

Table of contents

Introduction

Light induced polymerization is a relatively young method that rapidly developed into a versatile industrial method and is widely used in a broad field of applications. Transforming a liquid formulation into a solid material by light irradiation has many advantages. This process shows low emission of volatile organic compounds, while being fast and energy efficient. The photo-curing of liquid films or bulk material can be conducted with UV-light or visible light at room temperature and pressure. Nowadays LEDs subsequently replace mercury lamps making this process even less energy consuming. Even household lamps or sunlight can be used for some applications. Therefore light curing can be considered as a part of "green chemistry" which represents especially environmental friendly technological processes.

These advantages boost the development of new photopolymerization techniques and the improvement of existing ones to conquer new fields of applications of light induced curing.

Photocurable coatings became a major application for radical photopolymerization. By choosing the right monomer system thin layer coatings such as varnishes or paints can be polymerized on a huge variety of substrates, such as wood, paper, ceramics, polymers or metals. Depending on the application such as decorative coatings, prints on (food)packaging, release coatings on polyolefin films and paper, flooring, etc. a huge variety of products are available on the marked. 2016 not less than 155,000 tons of radiation curing inks and varnishes were produced with an average market value of 2.7 billion US$. Since then the market is steadily growing with 2-3% per year.[1] Because of the high adaptability, everyday products of different materials from food packaging to wooden floor tiles are coated with UV curable varnishes.[2]

Not only more or less simple coatings are relying on light curing formulations. Highly complex technologies in the field of medicine e.g. restorative dentistry, tissue engineering and contact lenses take advantage of fast and space resolved curing.

Space-resolved curing is even more important in the field of nanotechnology and microelectronics. With up-to-date light-mask and laser technology, patterns in the scale of nanometers can be polymerized with high resolution and accuracy. Basically computer technology and the scientific field of analytic devices is based on photopolymerization. (e.g. micro-chips, mirrors, waveguides and other structured materials in the nanoscale size)

Generally spoken a system for photopolymerization can be divided into three parts:

A light source, a polymerizable monomer and a photoinitiator.

Of course, actual systems in industry are far more complicated than this. Normally complex mixtures of different monomers, initiators, fillers, pigments and regulating additives are used to cope with the requirements of the application.

Depending on the field of usage, photopolymer systems need to fulfil certain requirements on the mechanical properties of the resulting polymer. Regarding for example the color, hardness, toughness and scratch resistance of a polymerizate.

To understand the properties of photopolymers the whole process from initiation to the final material has to be understood.

A monomer consists of a molecule carrying reactive moieties with a high level of trapped chemical energy, such as double carbon-to-carbon bonds or epoxides with high ring tension. When a photoinitiator is irradiated with light, the compound is elevated to a higher energy state and decomposes to reactive compounds that attack the monomer terminal-groups. By a chain reaction, the monomer molecules build new covalent bonds, forming a macromolecule.

$I^* + M \rightarrow I\text{-}M^* + M \rightarrow I\text{-}M\text{-}M^* \rightarrow\rightarrow (M)_n$
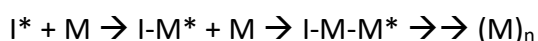
By the mechanism of initiation and chain reaction, the photopolymerization can be divided into the ionic and the radical photopolymerization.

This work will further deal with the radical photopolymerization and the improvement of some inherent disadvantages of this versatile method.

The initiation of radical polymerization starts with the decomposition of an initiator molecule. Such a decomposition requires some kind of activation energy. This could be thermal energy or in the case of photopolymerization: light.

$$I \xrightarrow{h\nu} R\cdot \; + \; M \longrightarrow R\text{-}M\cdot \; + \; M \xrightarrow{M} M_n$$
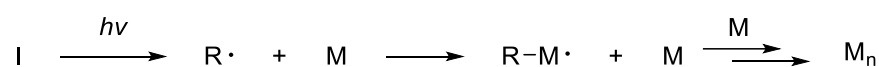
As the initiator decomposes into radicals these radicals (R•) can attack a monomer molecule (M). The radical is passed to the monomer, which adds to the next monomer molecule, which then again adds to the next monomer always passing the radical to the chain end. This process after initiation is called propagation reaction or chain growth.

During the propagation, side reactions occur. Radicals tend to recombinate or disproportionate, forming a covalent bond and terminating the chain growth.

Chain—M· + ·M—Chain ⟶ Chain—M—M—Chain   recombination

Chain—M· + ·M—Chain ⟶ Chain—M—H + M=Chain   disproportionation
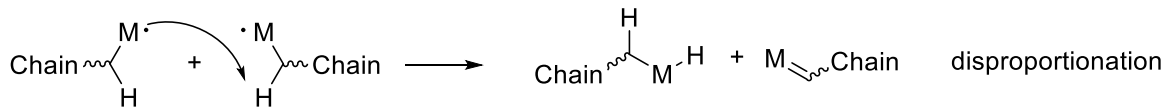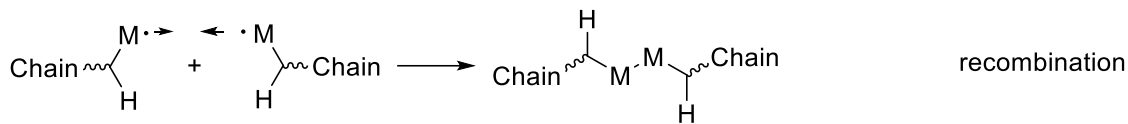
When oxygen is present also recombination reactions with oxygen as a biradical is very likely to happen. This process is called oxygen inhibition, as the resulting species is not efficient in reinitiating chain growth. Therefore, inert atmosphere is needed for radical polymerization in thin layers or additives have to be used to prevent inhibition by oxygen.

Chain—M· + ·O=O· ⟶ M—O—O·   ⟶✗⟶
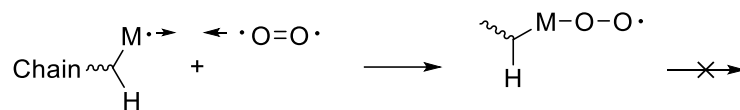
Raw material used for radical photopolymerization in industry normally consist of low molecular weight resins (300-5000 g mol^{-1}) with two or more reactive end groups, so that durable networks are formed during polymerization.[3]

Fast curing, high conversion, low toxicity, neutral odor, low shrinkage stress and low oxygen inhibition during polymerization is essential for industrial applied monomers.[4]

The most common monomer systems used in industry are acrylates. The low steric hindrance and high reactivity of the acrylic group ensures fast and efficient curing. (Scheme 1, a)

a)

acrylates

b)

methacrylates
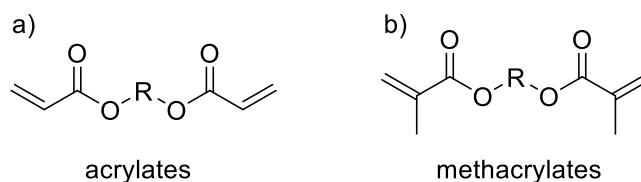
Scheme 1. Typical monomers for radical photopolymerization

Important properties like hardness, flexibility, abrasion-, thermal- and chemical resistance can be adjusted by the structure of the spacer between the reactive groups (R). Most resins consist of acrylated polyepoxides, polyesters, polyethers and polyurethanes. To reduce the viscosity of formulations reactive diluents like low molecular weight hexanediol diacrylate (HDDA) are added. When a higher crosslink density is demanded low molecular weight multifunctional acrylates like trimethylolpropane triacrylate (TMPTA), pentaerythritol tetraacrylate (PETA) and dipentaerythritol pentaacrylate (DPEPA) can be used.[3] (Scheme 2)

Acrylates undergo Michael addition with amines and thiols present in tissue, therefore especially low molecular weight acrylates are irritant and show significant toxicity.[5] Methacrylates are used as less toxic alternative. Due to the steric methyl group and better stabilization of the propagating radical methacrylates are less reactive but exhibit a significantly lower toxicity as methacrylates are not prone to Michael addition.[3]
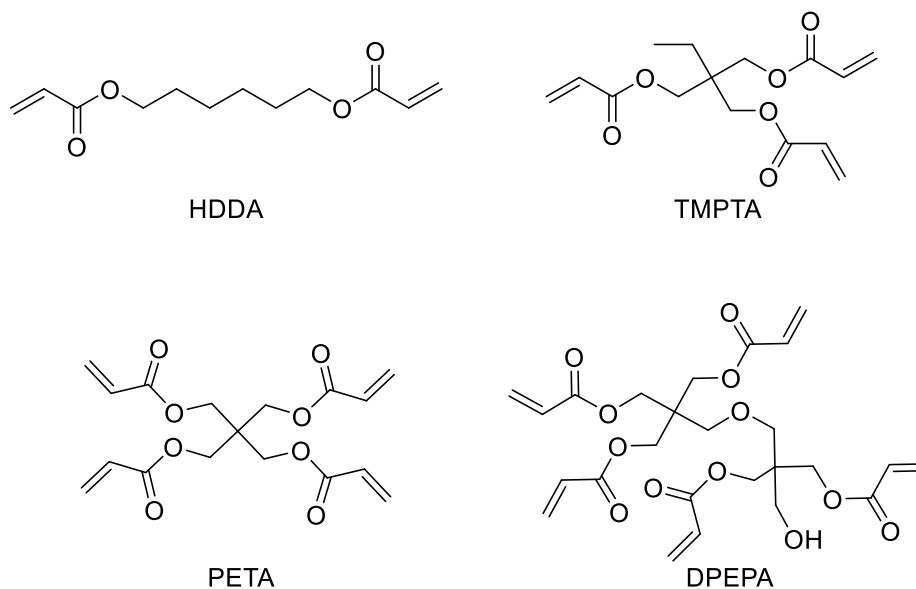
Scheme 2. Typical acrylic reactive diluents

Photoinitaiting Systems for Radical Polymerization

To understand the process of photoinitiation fully, basic physical concepts of photo quantum physics have to be understood.

Any molecule exhibits an absorption spectrum between the UV and infrared spectrum. Such a spectrum shows which wavelengths are absorbed by a substance. By linear combination of atomic orbitals, chemical bonds and resulting molecular orbitals are formed. Heteroatom containing molecules show free electron pairs which are not involved in bonds. These non-bonding electrons exist in non-bonding states and occupy so-called n-orbitals. (Scheme 3)
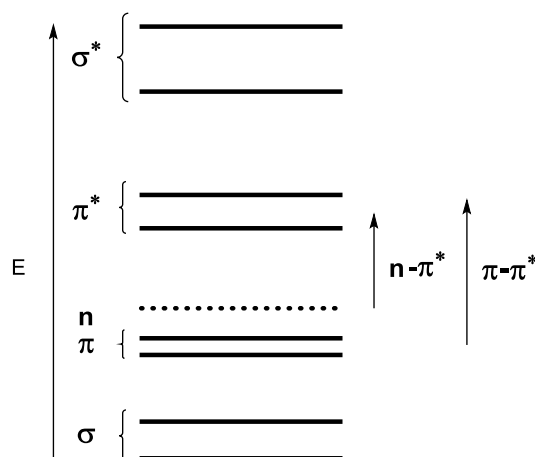
Scheme 3. Molecule orbital scheme of a carbonyl moiety

Any electronic transition solely can happen from occupied to unoccupied orbitals. The orbital in the highest energy state that is still occupied is called HOMO whilst the lowest unoccupied state is called LUMO. Many molecular properties are actually defined by the HOMOs and LUMOs. The energy difference of HOMOs and LUMOs define the wavelength, which has to be absorbed to allow an energy transition. The part of the molecule containing such n or π electrons, which absorb in the UV-Vis region, is called chromophore. As the human eye can only detect light with a wavelength between 400-800 nm, any substance with an absorption band in this region will be colored.

Table 1: Absorption maxima of typical chromophores[6]

Chromophore	λ_{max} π-π* [nm]	λ_{max} n-π* [nm]
C=C	170	-
C=O	166	280
C=N	190	300
N=N	-	350
C=S	-	500

Typical chromophores and absorption maxima of their π-π* and n-π* are shown in Table 1. It is visible that generally π to π* transitions absorb at much smaller wavelengths than n to π* transitions. This can be explained by energy levels of the molecular orbitals. In Scheme 3 it is visible that more energy is needed to elevate a π-electron to the π*-orbital than a nonbonding electron from a n-orbital.[7]

In an example spectrum of benzophenone in Figure 1 it can be easily seen that the absorption of the overlapping π-π* orbitals is much stronger than that of the n-π* transition. This is because

the n- and π* orbitals in the carbonyl are barely overlapping, making the transition less likely. The absorption properties are also dependent on the polarity of the solvent.[8]
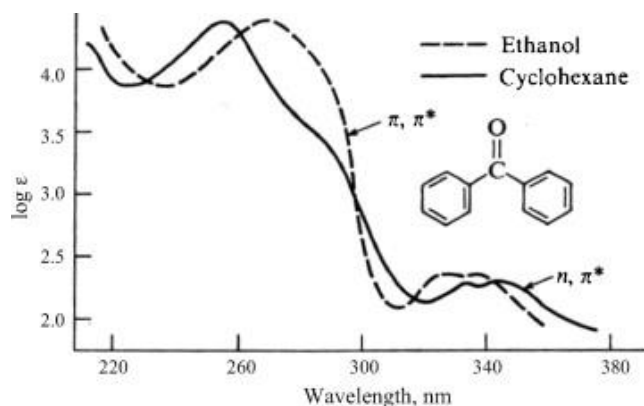
Figure 1. UV-Vis spectrum of benzophenone in ethanol and cyclohexane[8]

By absorbing a quantum of energy (light), electrons are elevated in higher energy states (e.g. S_1, S_2). In the un-exited singlet ground state S_0 all electrons are paired in antiparallel directions. When an electron is elevated to an exited singlet state the spins remain antiparallel.
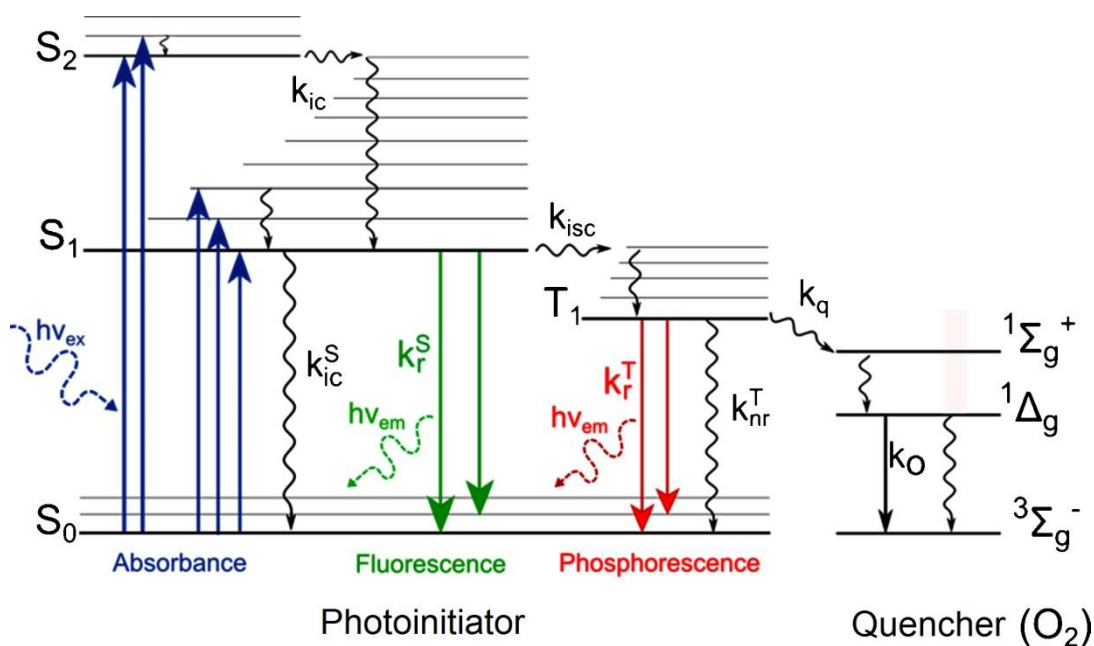
Figure 2. Jablonski diagram[9]

By intersystem crossing (ISC), the molecule can reach an excited triplet state T_1 in which the spins are parallel.

Singlet ground state   Singlet excited state   Triplet excited state
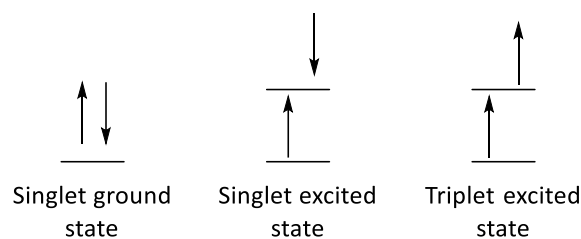
Triplet states are generally more long-lived (> 10^{-6} s) than singlet excited states ($10^{-10} - 10^{-7}$ s) and responsible for the formation of radicals. The formation of radicals is always in competition to other deactivation pathways as the excited molecule tries to get rid of the excessive energy and back to the S_0 state. The deactivation can happen by emission of photons, which is called fluorescence in case of singlet states and phosphorescence in case of triplet states. The excessive energy can also be dissipated by internal conversion to vibrations (heat). (Figure 2)

Triplet stated can also be quenched by third party molecules like molecular oxygen, where the energy is transferred to the third party and dissipated by mentioned pathways.[10]

Generally, two types of radical photoinitiators are distinguished by their mechanism of generating radicals from the triplet state. Generally, it is common knowledge that radical photoinitiators need benzoyl moieties as chromophore to initiate polymerization efficiently.

Norrish Type I photoinitiators consist of molecules with cleavable bonds. Normally an aromatic acyl moiety is attached to either a tertiary carbon or heteroatoms such as phosphorus, germanium, tin or other metals. In addition, peroxy or diazo structures can be used as photoinitiator.[11]

$X= CR_3, POR_2, GeR_3,$
$SiR_3, SnR_3, O\text{-}OR$
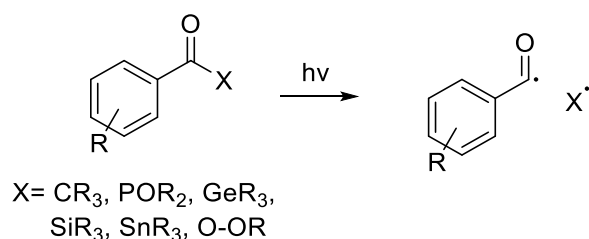
Norrish Type II systems also contain benzoyl chromophores but the acyl moiety does not cleave upon irradiation. In this case, an intermediate biradical is formed in the excited triplet state and a hydrogen atom is abstracted from a coinitiator. This can occur via direct hydrogen abstraction from surrounding molecules or via electron transfer reaction with amine coinitiators. [12]

The class of Type I initiators generally consist of a benzoyl chromophore and some opposing leaving group which is forming rather stable radicals. The first Type I initiators were

acetophenone derivatives, which are active in the UV-range with the typical n-π* transition at around 330 nm. (Scheme 4.)
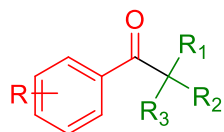
Scheme 4. General structure of carbon based Type I initiators

These types of photoinitiator are further classified by the substituents in the alpha position into benzoin derivatives, diphenyl- or dialkoxy acetophenones, morpholino- and aminoketones and hydroxyl dialkyl acetophenones.

In the 1960s to 1970s Norrish Type I benzoines have been excessively investigated as PIs. The general structure of benzoin initiators can be seen in Scheme 5. Benzoin ethers are more convenient than benzoines with free hydroxyl groups.
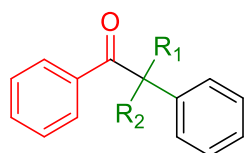
Scheme 5. Basic structure of benzoin photoinitiators

For example 2,2-dimethoxy-2-phenylacetophenone (DMPA, R_1= OMe, R_2= OMe) or benzoin methyl ether (BME, R_1=OMe, R_2= H) have been most widely applied industrially among all UV-initiators for a long time.[10] Benzoin ethers like DMPA exhibit a typical benzoyl n-π* transition at 343 nm and show fast cleavage from the triplet state and are efficient initiators for acrylates. The benzoyl and methyl radicals are efficient in initiation of polymerization, while the dimethoxy radical is rather a chain-terminating reagent.
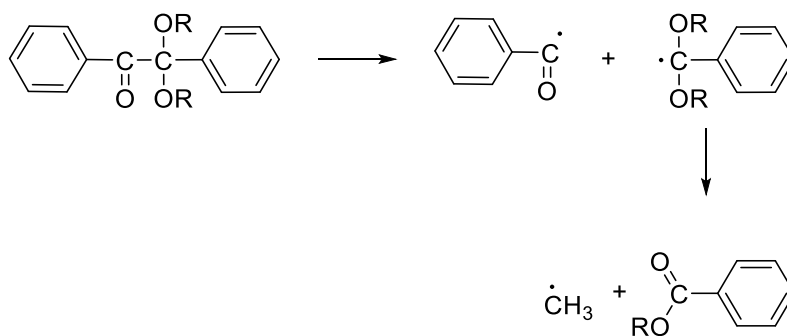
Scheme 6. Photodecomposition of benzoin ether initiators[10]

To improve the reactivity of benzoin ethers a benzyloxybenzyl group was introduced (R_1= O-benzyl, R_2= benzyl) which leads to a more reactive radical. In addition, derivatives with polymerizable groups were developed. (Scheme 6)

Also, dialkoxy/diphenyl acetophenones were used as photoinitiators. Dialkyloxy acetophenones exhibit an especially fast cleavage and a good polymerization quantum yield. While diphenyl acetophenone shows long lived triplet states.[10]

R_1= Ar, Oalkyl
R_2= Ar, Oalkyl

Scheme 7. Basic structure of dialkoxy/diphenyl acetophenone photoinitiators

The initiator diethoxy acetophenone (R_1= OEt, R_2= OEt) can react in a Norrish Type I or Type II mechanism when excited by UV-light. (Scheme 7 and Scheme 8)

Type I   Type II

Scheme 8. Decomposition by light of diethoxy acetophenone[10]

Today mostly hydroxy propiophenones are used as highly reactive unimolecular Type I UV-initiators. Fast homolytic cleavage leads to benzoyl and hydroxy propyl radicals that are very reactive towards (meth)acrylates.[13]

hydroxy propiophenones

For applications in visible light curing acyl phosphine oxides are widely used since the 1980s as highly reactive Type I initiators. Acyl phosphine oxides exhibit an absorption maximum from 350-380 nm extending up to 420-440 nm with a high extinction coefficient in the visible range. This makes these compounds especially suitable for white pigmented systems due to the deeper penetration depth.[11, 14]

TPO-L BAPO

In addition, phosphinoyl radicals show higher reactivity towards acrylates than benzoyl radicals.[15] Most recent initiators for visible light are half-metal and metal acyl compounds such as mono- to tetraacylgermanes[16] and tetraacylstannanes[17], which can initiate up to green light.

The class of Type II initiators or non-cleavable photoinitiators mostly consists of diaryl ketones, ketocumarins or diketones. When these systems are excited by light to the triplet state the molecule does not cleave homolytically but either abstracts a hydrogen from a hydrogen donor such as on alcohols or ethers or reacts with an amine coinitiator by electron and subsequent hydrogen transfer.[13] (Scheme 9)

hydrogen abstraction
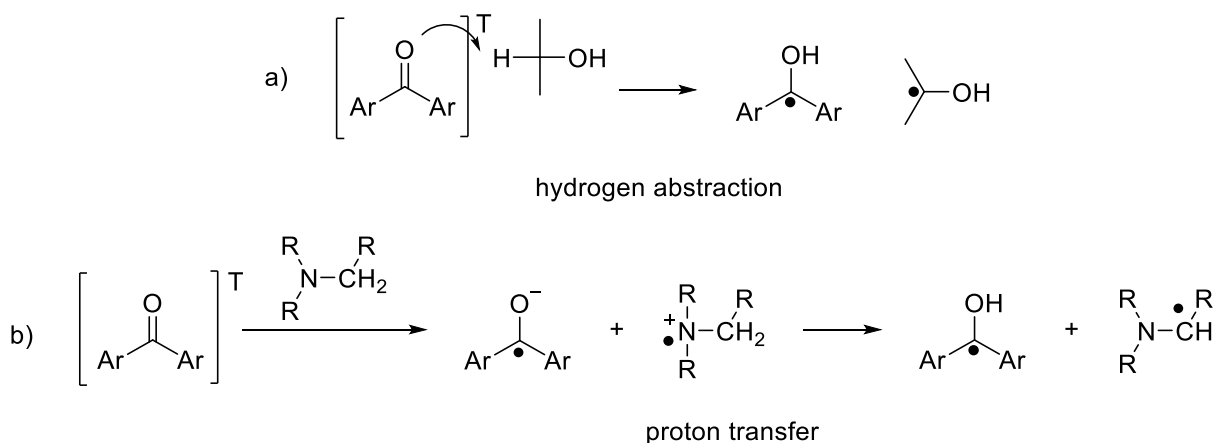
proton transfer

Scheme 9. Reaction mechanism of a Norrish Type II initiator by a) hydrogen abstraction and b) electron/proton transfer[13]

Of course, forming a charge transfer complex and undergoing hydrogen transfer takes time and is first diffusion and then equilibrium controlled. Therefore, Type II systems are generally less reactive than Type I systems. Benzophenones and thioxanthones are among the most used photoinitiators in the field of coating and printing industry.[18]

benzophenones   thioxanthones   anthraquinones

10
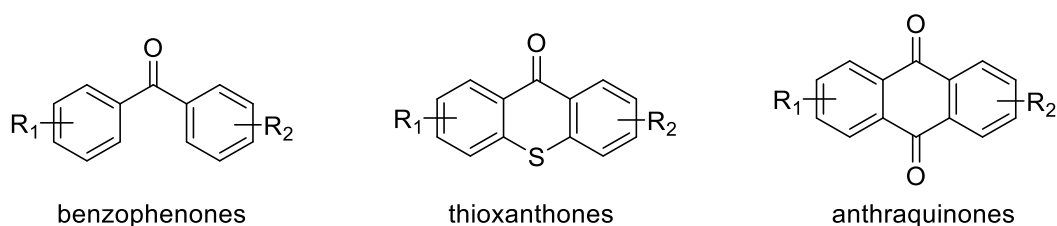
Thioxanthone derivatives such as ITX are the most important Type II initiators and sensitizers for visible light. It has to be mentioned that Type II systems with amine coinitiators are less sensitive to oxygen inhibition.

The only aromat free initiators avaiable are planarized diketones such as camphor quinone, which are widely used in dental applications as long wavelength initiators with aromatic tertiary amines as coinitiator.[19]

The contamination of the environment and products of daily use and therefore human beings with aromatic remains of photoinitiators is an increasingly noticed problem.[20]

The Problem of Oxygen Inhibition

Unfortunately, oxygen from surrounding air is inhibiting the initiation and curing process. Therefore, expansive inert gas solutions or extremely high concentrations of costly (co)initiators have to be used to prevent oxygen inhibition.[21, 22]

Molecular oxygen can diffuse into the monomer formulation up to 60 µm, depending on the viscosity the resin layer. Therefore especially thin layers like varnishes or printings are affected most by oxygen inhibition.[23]

The industrial approach to counterfeit this problem is to use different initiator systems at different wavelengths. To achieve good through cure a photoinitiators absorbing at 365 and 405 nm (e.g. acylphosphineoxide initiators) are used. Oxygen inhibition is compensated at the surface by using a lower wavelength than 350 nm and a highly efficient hydroxy acetophenone initiator. For wavelengths lower than 365 nm, mercury pressure lamps have to be used, as there is still a lack of efficient deep UV LED light sources. This leads to emission of ozone and mercury contaminated waste bulbs.[24] As already mentioned physical methods to create a sufficient oxygen barrier (e.g. inter gas, lamination, sealing liquids) are expensive and circuitous. Fortunately a multitude of chemical additives was found and developed in the recent years which can normally be used in a concentration below 5 wt% and prevent quenching of the propagation by oxygen.

There are multiple strategies to reduce the negative effect of molecular oxygen on the radical polymerization. In the review article "Strategies to Reduce Oxygen Inhibition in Photoinduced Polymerization"[25] and the article "The formulator's guide to anti-oxygen inhibition additives"[26] from 2014 a great overview on the prevention strategies of oxygen inhibition was shown.
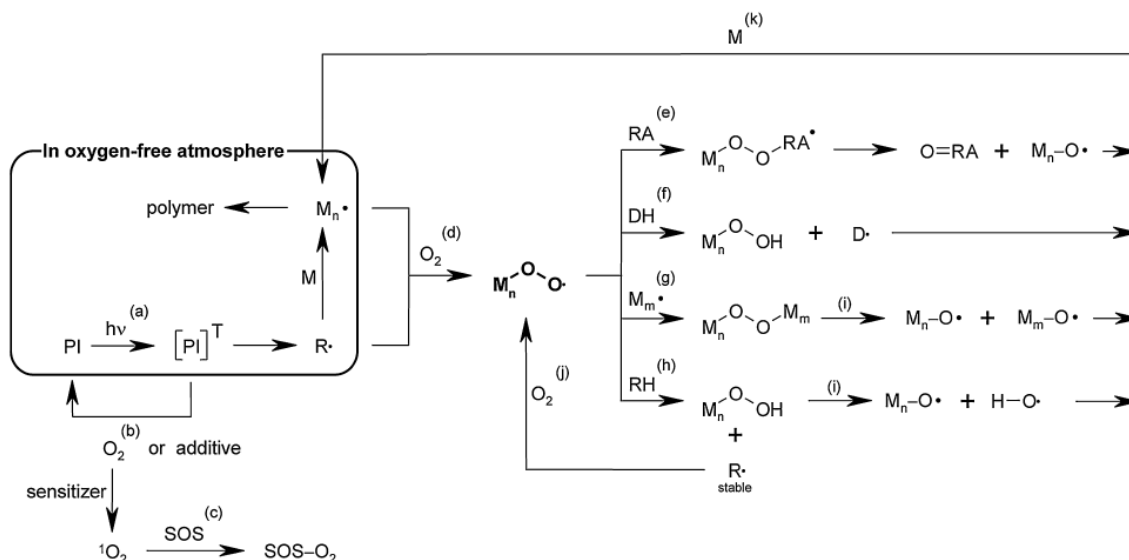
Scheme 10. Mechanistic explanation of oxygen inhibition and strategies to mitigate it: (a) initiation stage strategies (i.e., inerting, lamination, light source, molecular inerting and photoinitiators), (b) quenching of excited state of photoinitiator, (c) singlet oxygen scavengers, (d) formation of unreactive peroxyl radicals from initiating or propagating radical, (e) reducing agents, (f) hydrogen donors, (g) termination by radical–radical recombination, (h) hydrogen abstraction, (i) peroxide decomposition, (j) scavenging of a molecule of oxygen, and (k) reinitiation of polymerization.[26]

During the propagation reaction of radical polymerization, a chain end radical can react with molecular triplet oxygen and form unreactive terminal peroxide radicals. Triplet oxygen is the stable form of oxygen and occurs as biradical. By recombination of the chain end radical with a triplet oxygen radical the terminal peroxide is formed.
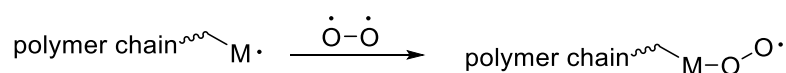
This rather unreactive species can recombine with other chain end or initiator radicals (Scheme 10, g) resulting in the loss of two propagating radicals. Or the peroxyl radicals abstract hydrogens from the surrounding matrix resulting in hydroperoxide end groups. This stable peroxides can be cleaved thermally and release reactive oxyl radical. As photopolymerization is normally not conducted at elevated temperatures the peroxides will not further play a role in the polymerization.

By anti-oxygen inhibition reagents these reactions can be suppressed leading to high double bond conversions even under air.

Reducing agents can be used to lower oxygen inhibition by reducing the peroxyl radical to a much more reactive oxyl radical. (Scheme 10, e) Phosphines are a good example for reducing agents that can be used to suppress oxygen inhibition.
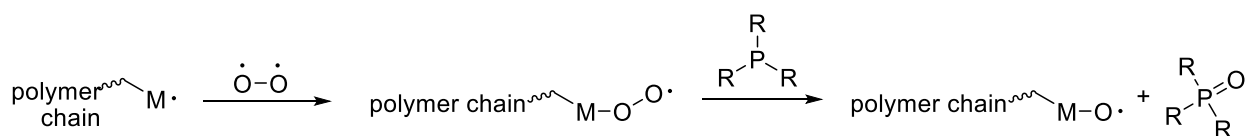
By adding triphenylphosphine (TPP) to an acrylic formulation (TPGDA), the conversion under air atmosphere is subsequently improved with increasing amount of phosphanes.[27] (Figure 3)
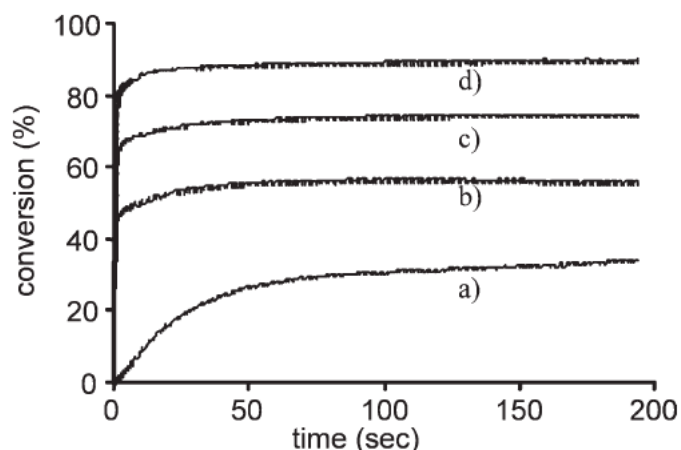
Figure 3. Photopolymerization kinetics of TPGDA under air using different concentrations of TPP. (a) 0 wt%, (b) 1 wt%, (c) 4 wt% and (d) 6 wt%. Photoinitiator: 4 wt% TPO, light intensity: 21 mW/cm2 [27]

Hydrogen donors such as thiols are also powerful anti-oxygen inhibition reagents. In this case the peroxyl radical abstracts a hydrogen from the thiol resulting in a saturated hydro peroxide end group and a highly reactive thiyl radical that is reinitiating the chain growth. (Scheme 10, f)
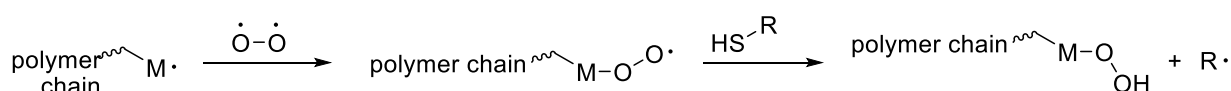
In (meth)acrylic systems 1 to 10% of thiol additive can already reduce the oxygen inhibition dramatically and even very thin layer of some micrometers can be cured.

Although thiols are potent anti-oxygen inhibition reagents, their application is limited due to some inevitable drawbacks like bad odor, limited storage stability of the formulations and reduced modulus of the resulting polymer.

Regulating Radical Photopolymerization

Although there is enormous potential for applications of photopolymers, the technology is dealing with matters concerning the mechanical properties of photo materials. When (meth)acrylic monomers are cured by uncontrolled radical photopolymerization,

13

inhomogeneous networks with a high crosslinking density are achieved. Such material can be very hard but also tend to be rather brittle. This is a critical problem when used as bulk material for example as dental composites or material for additive manufacturing technologies.

The reaction mechanism of radical bulk polymerization must be understood in detail to find solutions against the brittleness of photo materials.

Most industrial (meth)acrylate formulations are liquid at room temperature, therefore the average molecular weight is low and the molar content of reactive doublebonds is high. Multifunctional monomers crosslink during the curing reaction and the formation of new covalent bonds causes shrinkage.
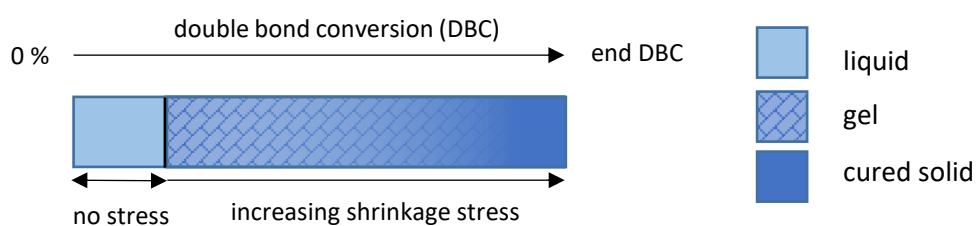
Figure 4. Development of shrinkage stress during curing reaction

As sketched in Figure 4, soon after the initiation due to the high density of functional groups, the liquid formulation gels at rather low conversions. After the solidification, the network domains are no longer mobile and the tensions caused by shrinking cannot be dissipated. Most of the curing reaction propagates in solid state resulting in an inhomogeneous network with lots of inner tensions.[28]

The problem derives from the uncontrolled radical polymerization, resulting in inhomogeneous highly cross-linked networks. (Figure 5) Such materials show typical duromeric thermo-mechanical properties such as high and broad glass transition temperatures and low impact resistance.
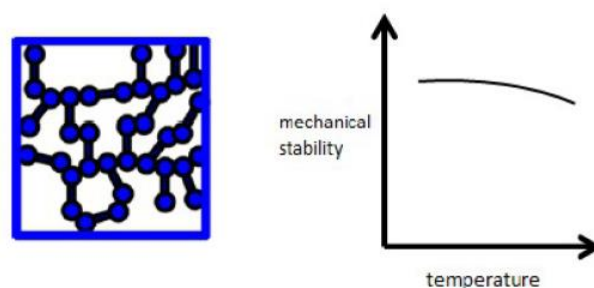
Figure 5. Schematic unregulated inhomogeneous network and broad phase transition[29]

Similar problems were already known for cationic cured epoxy resins, which were overcome with particle-filled systems (rubber-, core-shell- and other particles) or by using block copolymers for phase separation.[30]

In case of radical polymerization, no polarity change can be observed between monomer and polymer. Therefore, phase separation is hard to achieve without losing important mechanical properties. In addition, filled systems can be problematic as the curing depth and accuracy are negatively influenced by light absorption and scattering.

The monomer systems can be tuned by mixing high molecular weight oligomers with reactive diluents or by adding radically ring-opening monomers (ROMP). Still the networks in such polymers stay inhomogeneous and the problems inherent to photo materials cannot be solved to full satisfaction.

The problem is that theoretically every second C-atom in the chain exhibits one crosslink to another chain when only a difunctional monomer is used.[31] (Figure 6)
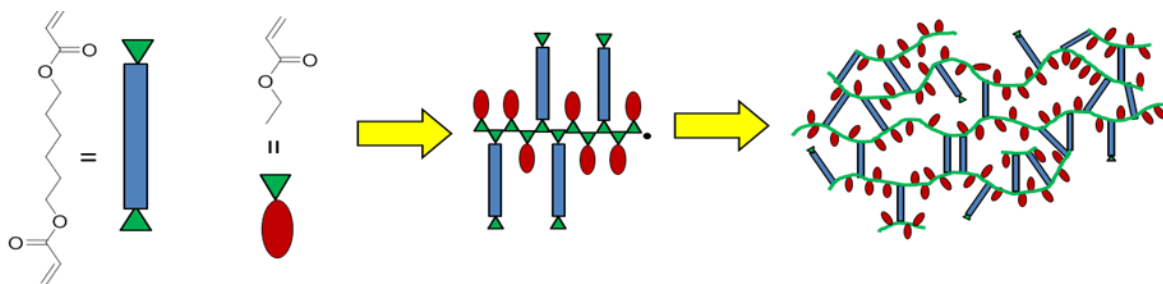
Figure 6. Principle of network formation with mono- and difunctional monomers[31]

To reduce inner tensions and form homogenous networks the gel point has to be shifted to higher DBC by controlling the radical propagation. In this case, the formulation stays liquid up to a higher conversion and the volume of monomer curing in the solid state is reduced. (Figure 7)
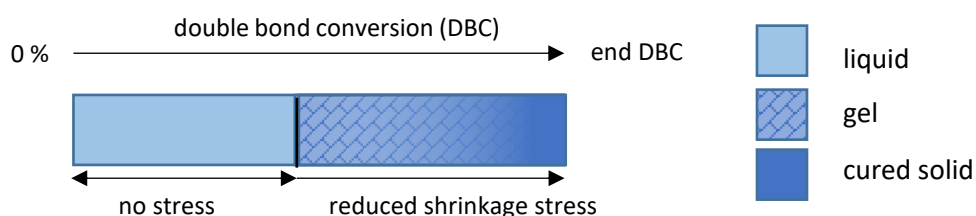
Figure 7. Development of shrinkage stress during regulated curing reaction

For that so-called chain transfer agents (CTA) can be used. Such molecules terminate chain growth and then reinitiate polymerization. (Figure 8)
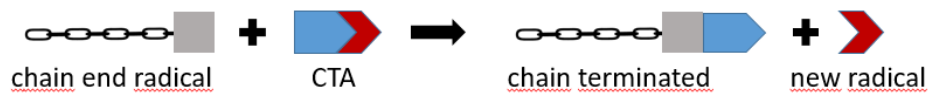
Figure 8. Simplified representation of a chain transfer agent

The termination reaction has to be statistically that means that the probability for a radical to add to a monomer or CTA molecule has to be in the same range. This is defined by the chain transfer constant C_T, the ratio of chain transfer and chain growth reaction of a radical polymerization by their reaction constant, seen in equation 1.

$$C_T = \frac{k_{tr}}{k_p}$$ **Equation 1**

C_T *Chain transfer constant*
k_{tr} *Rate constant transfer*
k_p *Rate constant chain growth by propagation*

When $C_T < 1$, the chain growth is dominating, causing broad molar weight distribution and high molecular weights.

When $C_T > 1$, the chain transfer is favored, causing delay of chain growth and low molecular weights in the beginning of the reaction. After the chain transfer compound is consumed, ratios change during the polymerization causing an inhomogeneous molecular weight distribution.

Keeping this in mind, the CTA has to be chosen according to the monomer system, offering a C_T around 1.
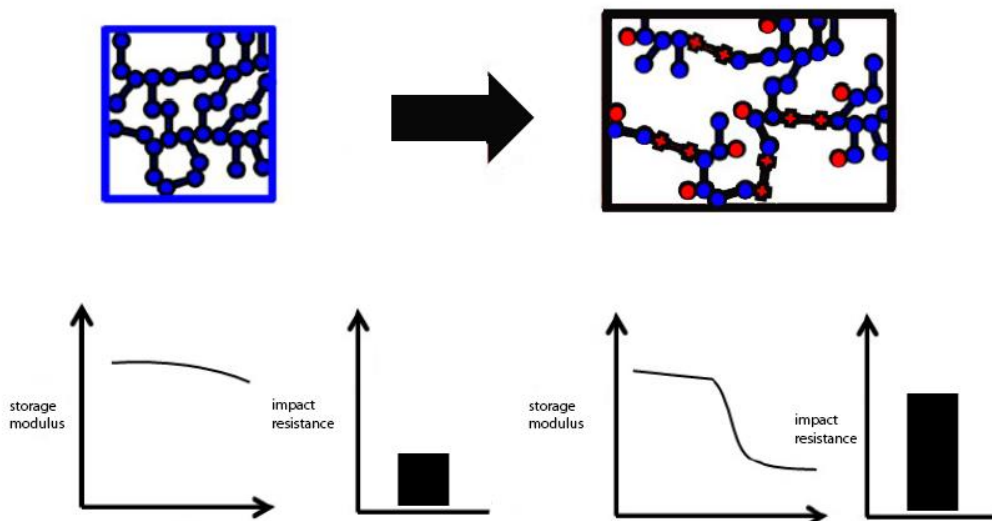
Figure 9. Material properties of unmodified and modified networks[29]

This reduces the average kinetic chain length and cross-linked domains are smaller. Therefore, the DBC at the gel point (DBC$_G$) is higher. In addition, the network structure is more homogenous and narrow phase transitions can be obtained. (Figure 9)

Several concepts to regulate radical polymerization are known:

- NMP – nitroxide mediated polymerization[32, 33]

$$R-O-NR_2 \rightleftharpoons R\cdot \ + \ \cdot O-NR_2$$

$$\downarrow M$$

$$P-O-NR_2 \rightleftharpoons P\cdot \ + \ \cdot O-NR_2$$

M
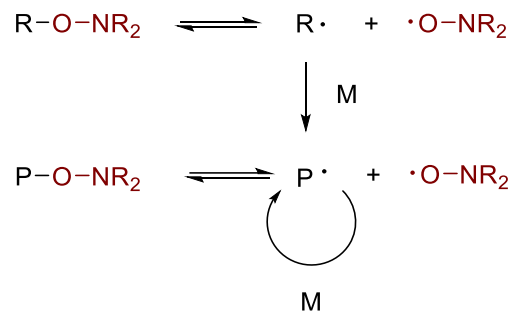
In this case stable nitroxide radicals such as (2,2,6,6-tetramethylpiperidin-1-yl)oxyl (TEMPO) de- and reactivate chain growth by capturing and releasing terminal radicals. The equilibrium is shifted to the non-active bound species, so only few active radicals are present at the same time, reducing side reactions to a minimum. NMP is a controlled polymerization that offers great regulation of molecular weight and can be used to form block copolymers and modify end groups. The propagation on the other hand is very slow so the reaction takes hours also solvents are required. Thus, this method is not usable for bulk photopolymerization.

- ATRP – Atom transfer radical polymerization[34]

$$R-X \ + \ Cu(I)X \rightleftharpoons R\cdot \ + \ Cu(II)X_2$$

$$\downarrow M$$

$$P-X \ + \ Cu(I)X \rightleftharpoons P\cdot \ + \ Cu(II)X_2$$

M
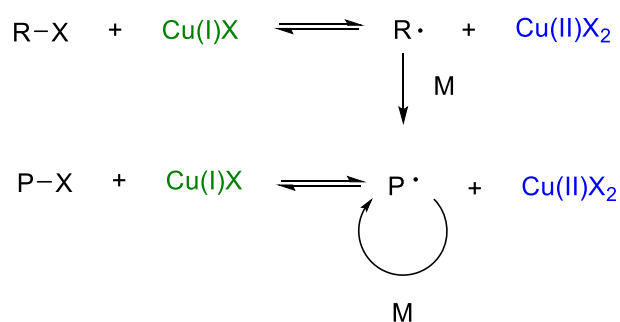
Like NMP, ATRP is a reversible deactivation radical reaction that uses copper(I) salts as catalyst and halogenated initiators. Also this process offers all advantages of living radical polymerizations, such as good control over molecular weight, easy access to tailored block copolymers. Nevertheless, as well as with NMP for this rather slow reaction solvents and elevated temperatures are needed.

- RAFT- Reversible addition fragmentation chain transfer[35]

Weak single bond

Reactive double bond

Z modifies addition and fragmentation rates

R must be a good homolytic leaving group and a good initiating species
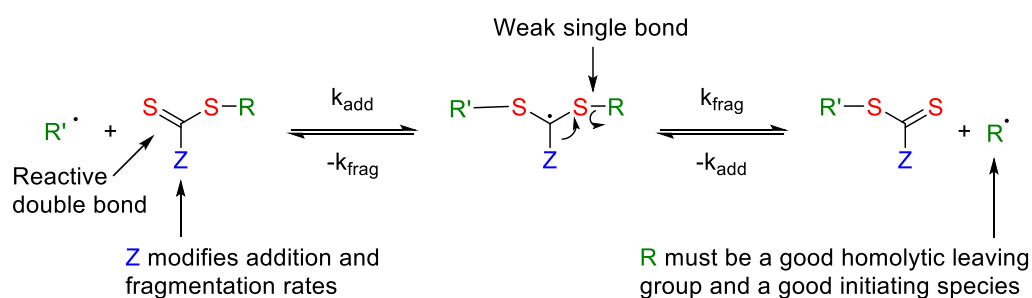
RAFT polymerization uses thio charbonyl-thio compounds such as dithioesters, trithiocarbonates or dithiocarbamates as chain transfer agents. After initiation with a radical initiator the propagation reaction stays in a RAFT equilibrium, in which radicals add to the sulfur double bond and a new radical is release on the opposite side forming a new reactive sulfur double bond. The method offers a high control over molecular weight and distribution, especially because the RAFT agent can be specifically adapted to the class of monomer. In addition, RAFT polymerization is very robust in the sense of solvent, impurities and atmosphere. Generally, RAFT polymerizations are used in solution for block copolymers, grafting polymer brushes from surfaces and other complex polymer architectures. It was already shown that RAFT techniques cannot be applied in bulk photopolymerization, as the slow RAFT reaction causes massive retardation during the curing reaction and most RAFT reagents are strongly absorbing in the UV and blue region of the spectrum. Therefore, photo initiation is not possible in this spectral region.[36]

- AFCT – Addition fragmentation chain transfer[35]
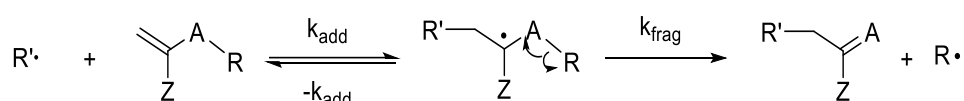
AFCT reagents are similar to RAFT reagents with the great difference that the process is irreversible. Therefore, after addition of a radical, the chain is terminated and a leaving radical is reinitiating polymerization. This means on the one hand that the chain transfer agent is consumed during the reaction and on the other hand the process is faster as no propagation-transfer equilibrium is reached. By choosing the activating group Z the transfer agents can be tuned in the terms of addition and fragmentation rates. For different monomer systems, the reagents have to be chosen to reach a chain transfer contestant of around 1. This guaranties statistic conversion and low PDIs. Depending on the AFCT reagent the reaction can be very fast and is also usable in bulk photopolymerization.[37-39]

- Hydrogen Donors[40]

$$R\cdot \ + \ DH \longrightarrow RH \ + \ D\cdot$$
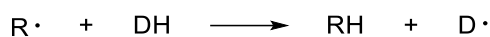
In the simple concept of hydrogen donors, the tendency of radicals to abstract hydrogens is used. The chain end radical can abstract a hydrogen from a hydrogen donor and is terminated while the donor radical can reinitiate chain growth. Therefore, donor molecules need easy abstractable hydrogens and the residual radical must efficiently add to monomer to reinitiate chain growth. Typical hydrogen donors are thiols[40] or group 14 hydrides such as silanes, germanes and stannanes.[41] Also carbon bound hydrogens near hydroxyl or ether groups are efficiently abstracted by radicals.

Depending on the donor hydrogen abstraction and reinitiation can be very fast and works well in bulk systems at room temperature. Storage stability of formulations and reduced young's modulus of resulting materials can be still issues that limit application.

Objective

Radical photopolymerization is a standard curing method that is widely used for protective and decorative coatings in different industrial branches.

Due to the frequent and gaining use of photopolymers for packages in food industry and medical applications from contact lenses to tissue engineering, the search for biocompatible and harmless photoinitiators is very important. The vast majority of applied industrial photoinitiators are based on aromatic ketone structures that are considered potentially harmful including their photoproducts. Aromatic initiators such as benzophenones or thioxanthones and their photoproducts often act as endocrine disruptors in the human body by imitating hormone structures.[42] In addition, a lot of these compounds exhibit potential carcinogenic effect.

benzophenones   phenyl glyoxylates   alpha ketoesters   acetophenones

Type II   Type I
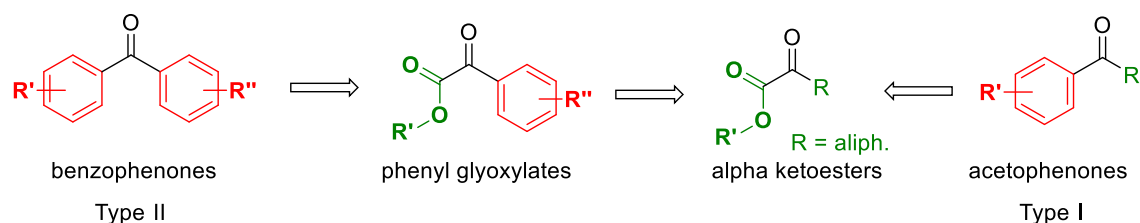
In this work, new concepts for non-aromatic photoinitiators should be explored. Recent publications showed that aliphatic metalloid glyoxylates are efficient photoinitiators. Based on this knowledge non-aromatic ketoesters and related structures should be chosen, synthesized and tested as radical photoinitiators. By modifying aliphatic ketoesters, structure property relations regarding absorption and initiation efficiency can be found. Photo-active compounds need to be deeper investigated by UV-Vis measurements and photo-DSC tests in different monomer systems, at different wavelengths and compared with industrial reference systems. Photolysis tests are ought to reveal further information about initiation mechanisms and the (photo)toxicity should be tested by cell incubation tests.

As a second task, also the material properties of photopolymers have to be further improved. Therefore, the formation of brittle inhomogeneous photopolymer networks needs to be regulated. Regulation of radical bulk photopolymerization is a way to reach higher toughness and make photomaterials competitive with thermoplastic polymers. Different successful strategies were developed to improve photomaterials. For example, regulation of radical polymerization by addition fragmentation chain transfer (AFCT) and thiol-ene chemistry could already successfully improve material properties.

It is known that AFCT reagents with an α-oxy-acrylate base structure and a sulfone leaving group are able to reduce the network density and internal stress of photopolymers and lead to tougher materials with well-defined glass transition.
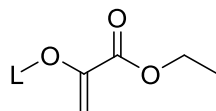
In this work, new AFCT reagents based on oxy-acrylates should be synthesized and tested. Therefore, the introduction of different leaving groups L and examination of the resulting compounds is planned.

Recently, silane-ene chemistry was tested to replace thiol-ene chemistry as the strong odour and the reduced modulus of thiol-ene based materials is a major drawback of this technology. It was found that most alkyl silanes are weak hydrogen donors and that the storage stability under oxygen is limited as silanes are prone to oxidation.

Consequently, stable cyclohexadiene hydrogen donors with a reactive leaving group should be investigated. The mechanism of radical hydrogen abstraction and subsequent fragmentation is already known from silylated cyclohexadienes in hydro silylation reactions.
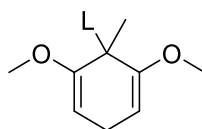
In this work, cyclohexadienes with silyl and other leaving groups should be synthesized and tested as hydrogen abstraction fragmentation chain transfer agents (HAFCT). The compounds need to be fully characterized and tested in different monomer systems. Therefore, studies in monofunctional methacrylates should be conducted to measure the photoreactivity of formations with the new regulators. Subsequent NMR and SEC studies of the polymers will reveal detailed information about the conversion and influence on the molecular weight.

Photo-rheology real-time NIR studies in difunctional methacrylate formulations can give a deep insight into network formation and regulation, by measuring conversion and mechanical properties of the samples at the same time. Dynamic mechanic thermal analysis of bulk polymer sticks polymerized with the new compounds as additives will reveal detailed information about mechanical properties and thermodynamic transitions.

Part 1: Novel photoinitiators based on aliphatic structures

During the last half century, free radical photopolymerization has become one of the most important technologies for protective and decorative coatings. Advantages are the fast and energy-efficient curing of VOC free formulations. In this technology, UV-Vis light is used to activate monomolecular Type I or bimolecular Type II photoinitiators for the curing of (meth)acrylate-based coatings and inks. Regulations for food packaging and medicinal products are especially strict when it comes to substances migrating through the cured material into the product.[43, 44] These restrictions result from the fact that low molecular weight photoinitiators and sensitizers together with their photoproducts are not environmentally friendly and may harm the human body.[43] Benzophenones are among the most used photoinitiators for UV curing in the range of 230-350 nm due to the low price and the rather good performance especially in case of bathochromic shifted derivatives.[12] The International Agency for Research on Cancer (IARC) published a monograph in 2013 about the negative health effects and cancerogenity of benzophenone.[45]

There is evidence that benzophenone, its derivatives and photoproducts act as estrogenic endocrine disruptors in mammals. [46-48] The IACR also found some indications that orally absorbed benzophenones can induce cancer growth in rats. Therefore, benzophenone was categorized as "possibly carcinogenic to humans (Group 2B)".[45]

In 2005 Italian authorities discovered traces of the photoinitiator isopropyl thioxanthone (ITX) within baby milk cartons, resulting in the seizure of more than 30 million liters of milk which has been contaminated by the curable ink from outside the packaging.[49] Furthermore, in a recent US study different photo(co)initiators could be found in 100% of 1000 tested serum samples, showing that these substance are ubiquitous contaminants.[50]

The benzoyl chromophores of cleavable photoinitiators are generally also problematic as various photoproducts are generated during the curing reaction. Especially volatile and odorous compounds such as benzaldehyde can be problematic at the production site or when it comes to food packaging.[43] On the other hand, degradation and recombination products of aromatic initiators are potentially mutagenic or toxic to the human body. Therefore, even safe initiators can lead to substances migrating in the resulting polymer network and becoming hazardous. Therefore, non-aromatic PIs are of high interest for industrial applications. Up to now camphor quinone is the only aromat-free photoinitiator of significant importance.

1.1.   State of the art

In the year 2017 the patent EP 3153150 A1 was published on silicon and germanium based ketoesters as longwave photoinitiators for dental applications.[51] These structures were said to be efficient initiators with an absorption maximum at 430-460 nm. Interestingly the lack of aromatic moieties did not seem to affect the photoreactivity. [51]

M= Si, Ge
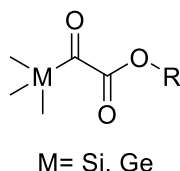
The recent discovery, that silyl glyoxylates function as photoinitiator drew the attention to keto esters in radical photopolymerization in general. Phenylglyoxylates are already well known as low-yellowing Type II radical photoinitiators (e.g. Irgacure 754). In this case, one aromatic moiety of a benzophenone is replaced by an ester group. (Scheme 11) The n-π* transition and extinction coefficient is in the same range (around 330 nm) as of a typical benzoyl chromophore. Interestingly also aliphatic α-ketoesters show a compatible absorption pattern.
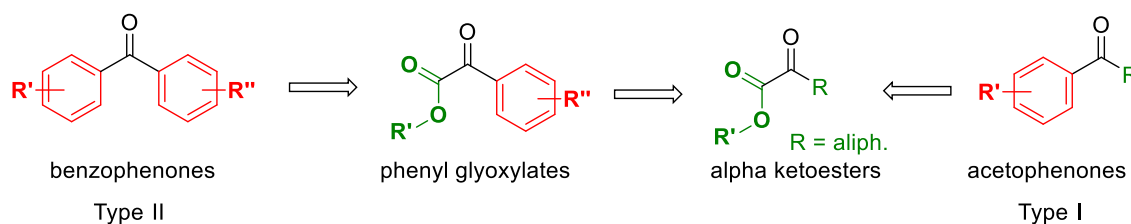
Scheme 11. Structure relation of ketoesters to aromatic initiators

It was unclear up to now if the aromatic moiety at all is necessary for an efficient initiation. This is why the photoreactivity of aliphatic ketoesters and their efficiency as photoinitiators for radical polymerizations has to be investigated. Only a few studies have been reported describing their photodecomposition. The first paper was published by Hammond et. al. in 1961. In these experiments, they were able to show that ethyl pyruvate can be photolysed to CO and acetaldehyde. They also proved that the decomposition can be sensitized by benzophenone and interpreted this as proof for the decomposition of ethyl pyruvate via the triplet state. In this publication neither a reaction pathway was suggested nor were radicals mentioned.[52]

Three years later Leermakers et. al. found similar quantum yields for the decomposition reaction for all alkyl pyruvates (ɸ= 0.15 ± 0.02) and a narrow range of triplet energies around 272 kJ

mol^{-1}. They could also show that a direct hydrogen transfer reaction is not favored upon irradiation, favoring a biradical mechanism for the decomposition and CO release.[53]

Later in 1967 Evans and Leermakers could verify the Type II elimination reaction of α-ketododecanoic acid, decomposing to heptene and pyruvic acid. They also could show that α-keto acids exhibit a unique behavior in comparison to other classes of keto-compounds. Namely, aliphatic α-ketoacids may be characterized by high rates of both intersystem crossing and photoreaction.[54]

Two years later, Nakanish et. al. published the photoreduction of a non-enolisable α-ketoester linked to a ginkgolide. As reaction route an intramolecular hydrogen abstraction creating a biracial was suggested.[55]

The radicals produced upon irradiation of pyruvates in isopropanol were investigated by ESR in 1972 by Samuni et. al. They could not only observe the resulting α-hydroxy radical but also a cis/trans isomerization with the ester moiety.[56]

1981 Davidson et. al. published a paper on the investigation of the Norrish Type II reaction of long chain aliphatic α-ketoesters and –acids. They were able to show that intramolecular hydrogen abstraction leads to a biradical intermediate which further decomposes to alkenes and a pyruvate.[57] (Scheme 12, a)

a)
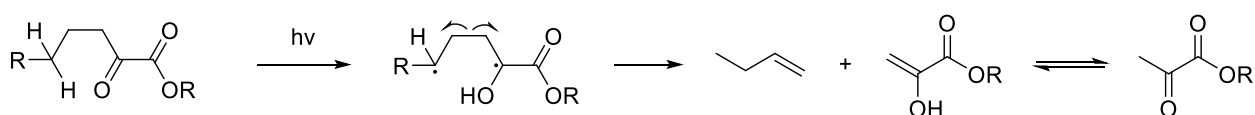
b)
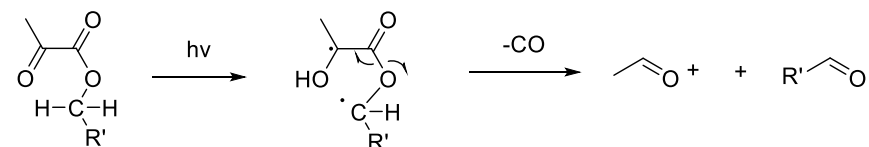
Scheme 12. Photo-decomposition of aliphatic α-ketoesters on the α-carbonyl side (a),[57] photo-decomposition pathway on the ester side (b)[58]

Finally, in the year 2000 Herrmann et. al. could verify that also the aliphatic moiety on the ester side functions as hydrogen donor for the intra molecular hydrogen abstraction. The biradical further decomposes under CO release of the intermediate ketal to aldehydes or an aldehyde and

ketone, respectively.[58] (Scheme 12, b) In both cases relatively long-lived radicals are generated, which potentially could initiate radical polymerization.

This would give an interesting Type II initiation system, as intramolecular hydrogen abstraction and intermolecular hydrogen abstraction are possible. Coinitiators could be used but would not be necessary for this system.

1.2.   Selection of compounds

For the proof of concept, a basic set of aliphatic α-ketoesters with increasing methylation on the β-carbon was chosen for the first tests. Fortunately, all ester compounds were commercially available, except the tert-butyl ketoester MDMOB that was easily synthesized according to literature. Therefore, pinacolone was first oxidized with permanganate to the t-butyl keto acid a and then esterified with methanol.[59, 60]

| Speedcure 73 | EP | MOB | EMOB | MDMOB |
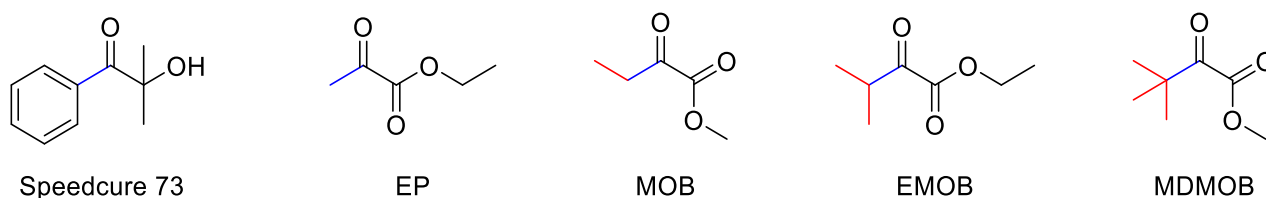
In a simple setup 1 w% of potential initiator was mixed with a equimolar mixture of two dental methacrylates (UDMA and D3MA) and cured at 100% intensity in the broadband Intelliray 600 UV floodlight oven for 100 s. Speedcure 73 was used as high reactive reference sample. To a total surprise, all α-ketoesters lead to perfectly cured samples. (Figure 10) Further, the reference cured with the common initiator Speedcure 73 showed reddish discoloration whilst the ketoester-cured samples remained colorless.
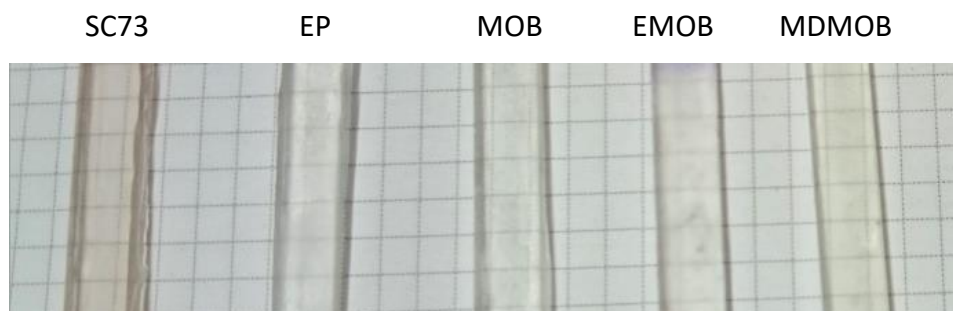
Figure 10. Cured sticks with SC 73, EP, MOB, EMOB, MDMOB top and front view

To prove that ketoesters are different from simple aromatic ketones regarding their photoreactivity, the phenyl analogues the α-ketoesters were tested in the same way.

AP   PP   MPP   DMPP
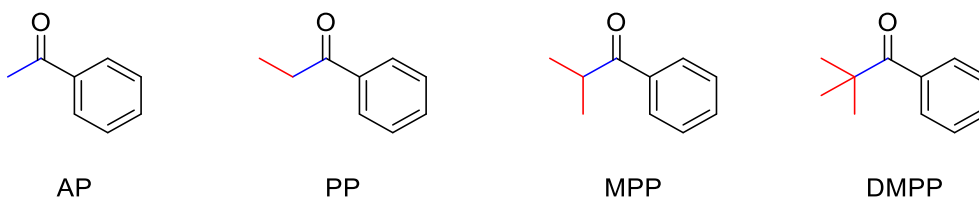
None of the tested benzoyl compounds showed reactivity. The preliminary curing tests in the UV oven revealed only weak reactivity of the t-butyl DMPP, as some curing occurred after 600 s of irradiation. The result was a limp and moist specimen that was barely cured. This shows that the photochemistry is different from mono carbonyl compounds.

After these promising results, a deeper investigation and broad variety of α-ketoesters needed to be tested. Therefore, promising substance were categorized by the variation on the α-ketoester structure. (Scheme 13)

Group a) consists of mostly commercial *simple aliphatic α-ketoesters* that were already used for the preliminary curing tests. Starting with ethyl pyruvate the compounds exhibit increasing methylation on the β-carbon. Also, methyl and ethyl ester were varied. This should give insight into the effect of increasing steric hindrance with increasing methylation and structure reactivity relations between methyl and ethyl esters.

In group b) the influence of *modification of the ester moiety* should be investigated. By introducing hetero atoms as nitrogen and sulphur the absorption spectrum should be shifted and the influence on the reactivity by heteroatoms should be investigated. Also attaching an amine coinitiator by esterification to improve the performance was planned.

Group c) *modification of the alpha carbonyl* consists of ketoesters with different groups in β-position influencing the α-carbonyl. By altering the β-substituent it should be investigated if it is possible to change the initiation mechanism of ketoesters from a Norrish Type II to a Norrish Type I mechanism. Therefore, moieties of known acetophenone Type I initiators such as halides, hydroxy groups and morpholine should be introduced.

In group d) *long wavelength UV initiators* different strategies were tested to cause a bathochromic shift of the absorption spectra. By introducing unsaturated moieties in β-position the absorption should be increased and shifted to higher wavelengths by cross conjugation. Planarized cyclic ketoesters should be tested as the low carbonyl angles should cause a significant shift of absorption. Same effect should be achieved with ketomalonates due to their similarity to triketones and by introducing phosphorus as hetero atom.

Analogue to known silyl and germy glyoxylates, phosphonate and tosyl glyoxylates needed to be investigated in group e) *long wavelength visible initiators*.

a) simple aliphatic ketoesters

EP (c)   MOB (c)   EMOB (c/s)   MDMOB (s)

b) modification of the ester

TBTKE (s)   TKE (s)   KEA (s)   AKE (s)

c) modification of the alpha carbonyl

BrKE (s)   OHKE (s)   MOKE (s)   TFKE (c)

d) long wavelength UV initiators

ACKE (s)   MAKE (s)   DDFD (c)   SQA (c)

DEAP (c)   DEKM (c)

e) long wavelength visible light initiators

SiKE (c)   TMSi (s)   TMGe (s)   PKE (s)   SKE (s)

(c) commercial, (s) to be sythesized
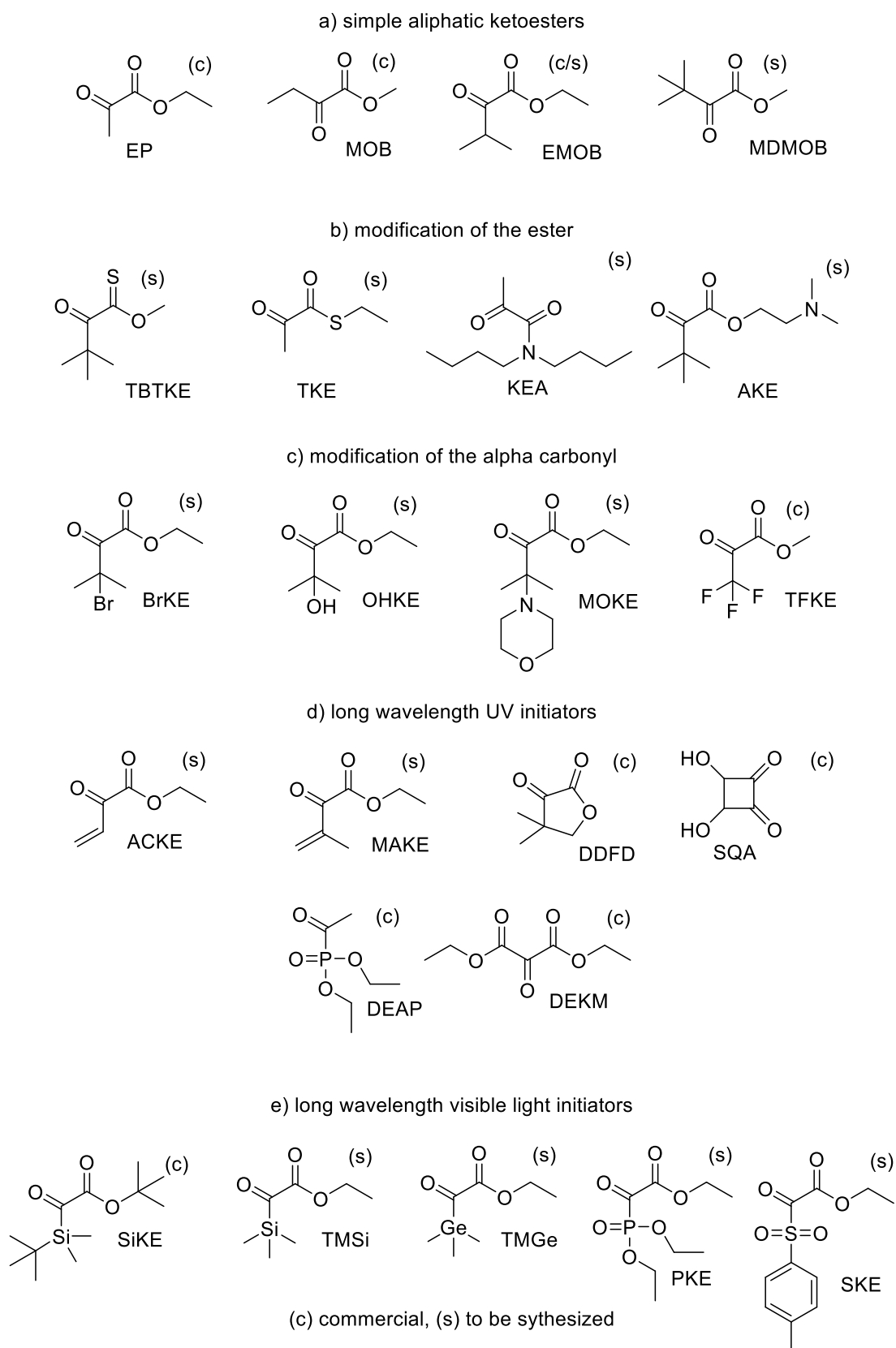
Scheme 13. Compounds selected to be tested as photoinitiators

To compare the reactivity of the novel compounds with industrial standards, typical (co)initiators were selected. (Scheme 14)

UV refrence initiators
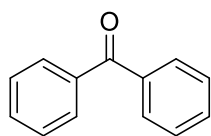
benzophenone
BP
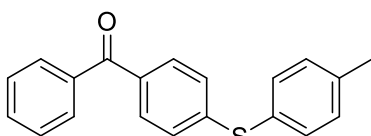
phenyl(4-(*p*-tolylthio)phenyl)methanone
BMS
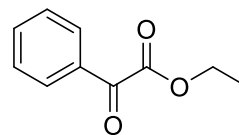
ethyl phenylglyoxylate
PGO

modification of the α-carbonyl
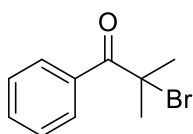
2-bromo-2-methyl-1-phenylpropan-1-one
SCBr
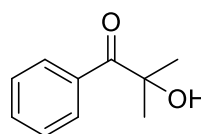
2-hydroxy-2-methyl-1-phenylpropan-1-one
SC73

long wavelength UV initiators
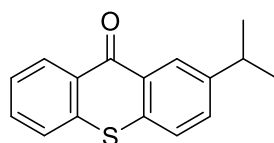
2-isopropyl thioxanthone
ITX

long wavelength visible initiators
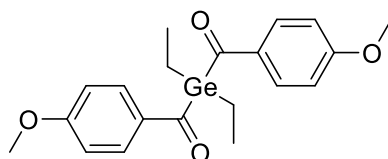
Ivocerin

coinitiators
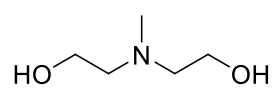
methyl diethanolamine
MDEA
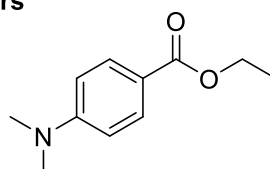
ethyl-p-dimethylamino benzoate
EDB

Scheme 14. Reference (co)initiators for comparison with the novel compounds

Benzophenone BP and benzophenone derivative BMS are widely used Type II photoinitiators for UV curing. The introduction of an aromatic thioether in BMS causes a massive increase in absorption and makes BMS one of the most reactive Type II initiators. These compounds are always used with coinitiators such as methyl diethanolamine MDEA and ethyl dimethylamino benzoate EDB.[61] Phenyl glyoxylates such as ethyl phenylglyoxylate PGO are known Type II initiators based on α-ketoesters. Due to intramolecular hydrogen abstraction, these compounds do not require a coinitiator.[62]

Bromo propiophenone SCBr and hydroxy propiophenone SC73 are typical industrial Type I UV initiators used for fast and efficient curing reactions.[10]

Thioxanthone ITX was selected to compare the new long wavelength UV initiators with. Isopropyl thioxanthone is an efficient Type II initiator in the near visible area and requires a coinitiator.[10]

The long wavelength visible initiators are compared with the highly reactive dental diacyl german Type I initiator Ivocerin.[63]

2. Selection and synthesis of α-keto compounds

2.1. Simple aliphatic α-ketoesters

As a first curing test with ethyl pyruvate was successful, it was of interest to first investigate the reactivity of ketoesters with increasing methylation. For the first proof of concept studies, a small set of aliphatic α-ketoester compounds was chosen.
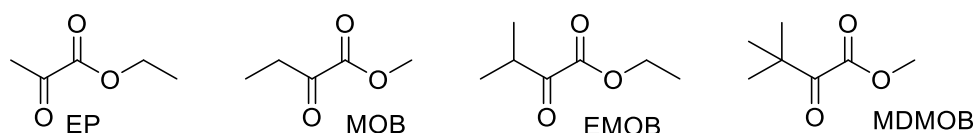
It is known for ethyl pyruvate EP that intramolecular hydrogen abstraction occurs at the ester CH_2. For the excited carbonyl, it needs to be sterically possible to abstract intramolecular hydrogen atoms. Therefore, differences in reactivity should be revealed by varying the aliphatic groups on the ester and α-carbonyl.

Ethyl pyruvate (EP), methyl oxobutanoate (MOB) and ethyl methyl oxobutanoate (EMOB) were commercially available. The compound with two methyl groups EMOB was very expansive and therefore synthesized in a bigger scale. Methyl dimethyl oxobutanoate MDMOB was not available commercially and therefore also synthesized.

2.1.1. Synthesis of dimethyl oxobutanoic acid (1)

Dimethyl oxobutanoic acid (**1**) as a precursor to methyl dimethyl oxobutanoate (MDMOB) is easily prepared by oxidation of 1 eq. pinacolone with 2 eq. potassium permanganate in strong basic conditions identical to literature.[59]
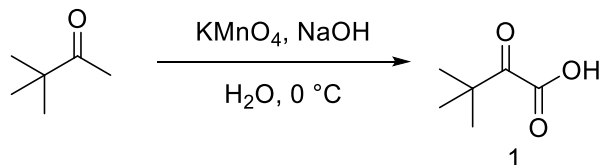
The ketone precursor is dissolved in 2 eq. cold aqueous NaOH and potassium permanganate is added subsequently at 0 °C. The temperature has to be cold and the potassium permanganate has to be added slowly as over-oxidation to pivalic acid is almost inevitable. Unfortunately, it is nearly impossible to remove pivalic acid from the desired product, therefore this step is crucial. After complete addition of permanganate within 4 h, the solution is allowed and warmed up to RT and stirring is continued overnight. The precipitated manganese dioxide is filtered off and the solution is acidified with conc. HCl. Extraction with diethyl ether and distillation in vacuum affords the desired product **1** in 78% of theory with minor impurities of pivalic acid.

2.1.2. Synthesis of methyl dimethyl oxobutanoate (MDMOB)

For the synthesis of MDMOB 1 eq. dimethyl oxobutanoic acid is refluxed in 10-fold amount methanol with catalytic amounts of sulfuric acid identical to literature.[60]
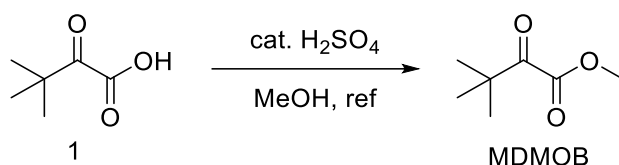
After evaporation of excessive methanol, the crude product is extracted with saturated sodium hydrogen carbonate solution and distilled under reduced pressure to afford the desired ketoester. To completely remove remaining pivalic acid methyl ester fractionated distillation finally yields 38% methyl ester MDMOB as clear liquid.

2.1.3. Synthesis of ethyl methyl oxobutanoate (EMOB)

For the synthesis of ethyl methyl oxobutanoate EMOB a Grignard reaction between diethyl oxalate and isopropyl magnesium bromide (**2**) was chosen as convenient preparation pathway identical to literature.[64, 65]
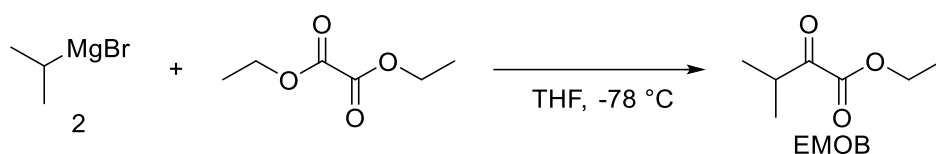
As the Grignard reagent can attack twice on the oxalate and as well on the formed ketoester, different ratios were tested between 1.0 and 2.0 equivalent diethyl oxalate. An excess of 0.5 eq. is sufficient, by that unwanted side products can be successfully avoided. A higher excess is not beneficial as the residue diethyl oxalate is hard to separate from the product. Distillation was not successful and resulted in mixed fractions even when a Vigreux column was used. The product can be isolated with column chromatography (20:1 petrol ether to ethyl acetate as eluent) and is afforded in 36% of theory as colorless liquid.

2.2. Modification of the ester moiety

There is no literature available about light induced formation of radicals with simple aliphatic α-ketoamides like KEA. Therefore, it was of interest to see if this class of compounds can induce radical polymerization and if there is any influence on the light absorption pattern.

The α-carbonyl can also be influenced by modification of the ester group with sulphur. Thioesters TBTKE and TKE were of interest as the photochemistry is not described in literature and the thioesters are known to absorb light in the visible region. The introduction of sulphur atoms was interesting, as the resulting O-alkyl and S-alkyl thioates should exhibit a bathochromic shift.[66] Also the photochemistry of this compound class is not investigated.
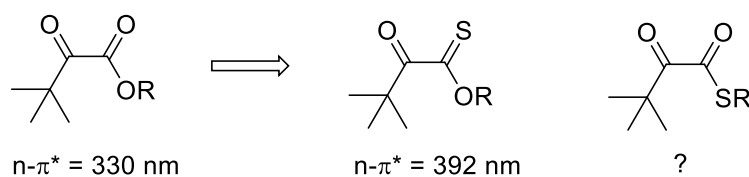
Also the introduction of amines as coinitiator like in AKE was a strategy to increase the curing efficiency.
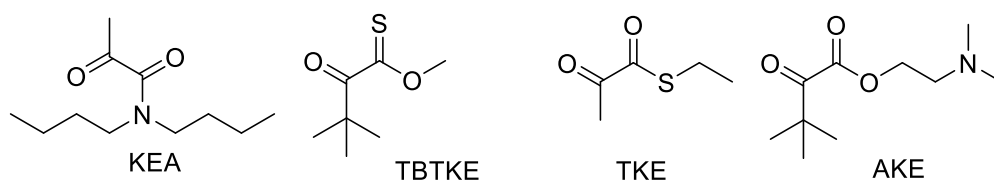
As it is expected that α-ketoesters are Type II initiators, tertiary amine coinitiators could improve the reactivity of the system. Additionally, the previously mentioned radical quenching cleavage reactions could be suppressed by offering an electron/proton transfer moiety.
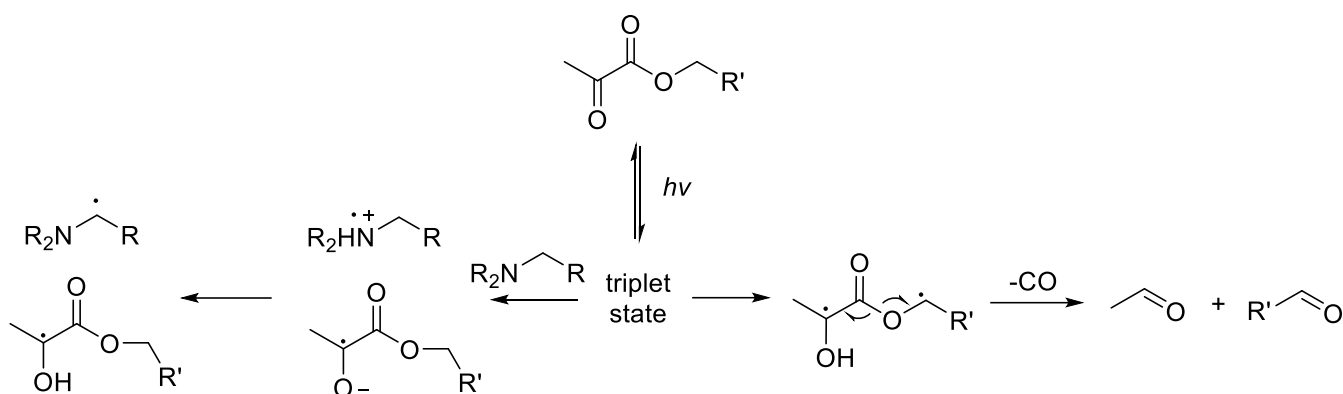
Therefore, it was reasonable to introduce a tertiary amine as functionality on the ketoester to create a monomolecular coinitiating system.

2.2.1. Synthesis of N,N-dibutyl-2-oxopropanamide (KEA)

In preliminary tests pyruvates showed instability under basic conditions. Probably due to aldol reactions[67] the mixture of amines with pyruvates soon turns dark brown and no desired products can be isolated. Therefore, the amide should be prepared via the acid chloride identical to literature.[68, 69]
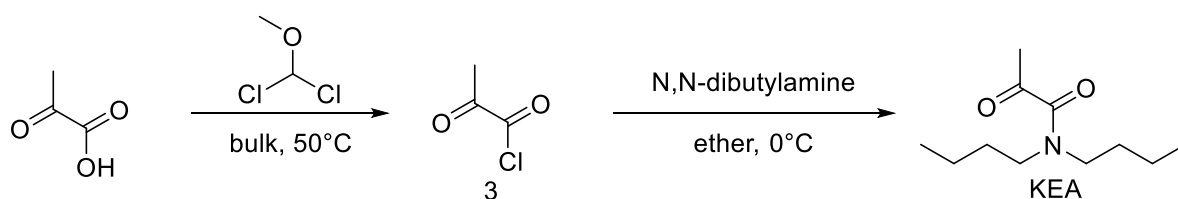
For the synthesis of N,N-dibutyl-2-propane amide (KEA) the corresponding acid chloride of pyruvic acid (**3**) had to be prepared first. As α-keto acids are sensible to harsh reaction conditions, the relatively soft chlorinating agent dichloromethyl methylether was chosen.[46] To the acid the chlorinating agent was added slowly in excess of 1.5 eq., under inert conditions and heated to 50 °C for 30 min after completion of addition. Then the mixture was stirred overnight under argon at room temperature. After evaporation of all volatile residues in vacuum, the pyruvic acid chloride (**3**) was directly used for the next step as it is too sensitive for distillation. Therefore, the acid chloride was slowly added to a 2.1 eq. excess of dibutyl amine in threefold amount of dry ether at 0 °C under argon. The reaction was stirred 1 h while cooling and quenched with diluted HCl. After extraction and evaporation, distillation afforded the ketoamide KEA in 21% yield.

2.2.2. Synthesis of O-methyl S-ethyl 2-oxopropanethioate (TKE)

It was first tried to synthesize the S-ethyl thioketoester TKE by reaction of pyruvic acid chloride with ethane thiol.[70]
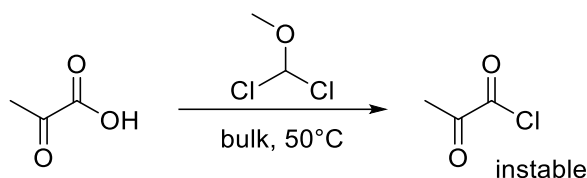
The pyruvic acid chloride was very sensitive. The pyruvic acid previously prepared with the chlorination agent dichloromethyl methylether, decomposed in the fridge.[71, 72]
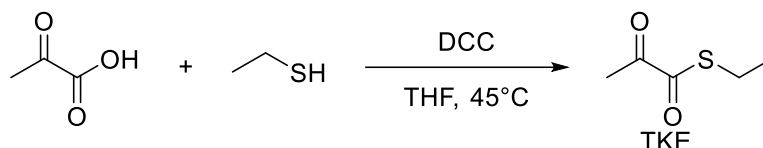
To avoid resynthesis of instable acid chloride, direct reaction of pyruvic acid and ethane thiol with DCC was chosen identical to literature.[73]

One equivalent DCC was dissolved in the tenfold amount dry THF. After the addition of 1 eq. ethane thiol, 1 eq. pyruvic acid was added dropwise diluted in the threefold amount THF. Instant formation of solid urea was visible and the whole reaction mixture turned deeply yellow. After refluxing for 5 min the mixture was cooled and filtrated. After evaporation of the solvent under vacuum, the yellow residual oil was distillated twice, yielding the thio ketoester TKE as yellow extremely smelly oil in 34% of theory.

2.2.3. Synthesis of O-methyl 3,3-dimethyl-2-oxobutanethioate (TBTKE)

For the synthesis of O-methyl thiolate TBTKE a direct one-pot synthesis from pinacolone with thionyl chloride and methanol as reagent was chosen according to literature.[74]
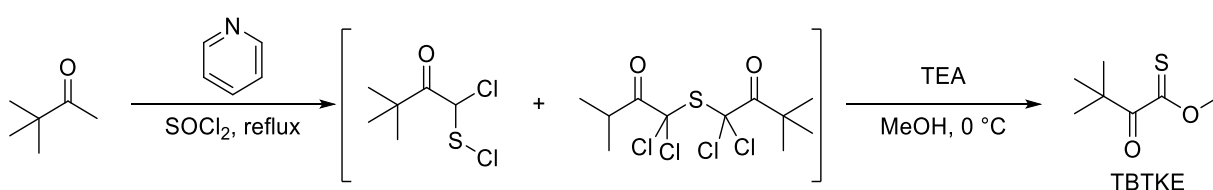
To the 15-fold amount of thionyl chloride pinacolone was added dropwise while stirring at RT together with 2 mol% of pyridine as catalyst. Instantly a lot of gas formation and the reaction turning deeply red was observed. After two hours the excess of thionyl chloride was distilled off under vacuum. The crude intermediate was redissolved in the 20-fold amount of methanol and 4 eq. of triethylamine were added dropwise at 0 °C. After complete addition the reaction was allowed to warm up to RT overnight. The next day the reaction was acidified with 1 N HCl and extracted with ether. After drying of the organic phase the solvent was stripped off in vacuum

and 1.73 g of yellow very smelly raw product was obtained. Further purification with MPLC and ball pipe distillation afforded 8% of pure O-methyl 3,3-dimethyl-2-oxobutanethioate (TBTKE).

2.2.4. Synthesis of 2-(dimethylamino)ethyl 2-oxopropanoate (AKE)

For the synthesis of 2-(dimethylamino)ethyl 2-oxopropanoate (AKE) the dimethyl oxobutanoic acid chloride (4) was used, prepared analogue to pyruvic acid chloride **3**. By esterification of dimethyl aminoethanol to the acid chloride analogue to literature the tertiary amine coinitiator is installed on the ketoester.[75]

For the reaction 2.5 eq. of dimethyl ethanolamine were dissolved in 5-fold amount of dry DCM and cooled to 0 °C. To the mixture 1 eq. acid chloride was added slowly dropwise. The reaction was allowed to warm up overnight. After filtration of the hydrochloride precipitate, the mixture was acidified with 1 N HCl and extracted. The organic phase was dried with sodium sulphate and the solvent stripped off in vacuum. After ball pipe distillation of the crude oil only 17% of theory of 2-(dimethylamino)ethyl 2-oxopropanoate (AKE) was obtained as colorless oil. First it was unclear why the yield was that low. But the product was not stable under the strong basic conditions of the amino end group. Even in the freezer the compound further decomposed within weeks.

2.3. Modification of the alpha carbonyl

From acetophenones it is known that efficient Type I photoinitiators can be created by introducing a leaving group such as halides or isopropyl hetero moieties. The α-cleavage pathway is the most favored but with halogen, sulphur or amino groups also β-cleavage occurs.[11]

34
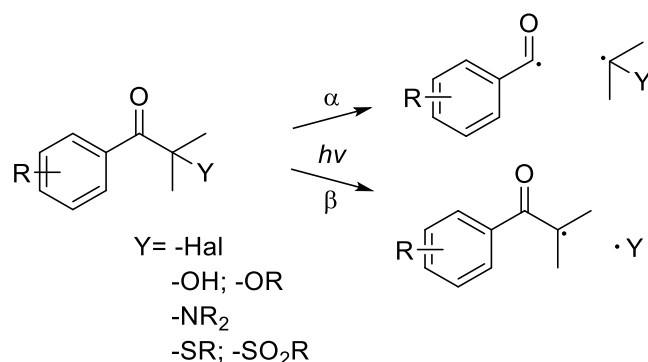
Therefore, it was of interest to synthesize ketoester analogues to the known acetophenone initiators and compare their reactivity.

(c) commercial
(s) to synthesize

SCBr   SC73   PMK

TFKE   BrKE   OHKE   MOKE
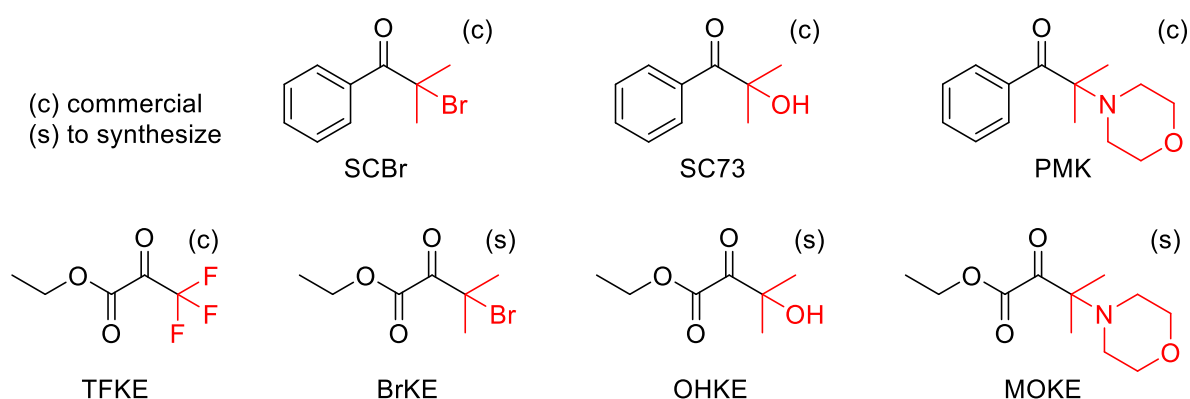
The initiation mechanism for simple ketoesters as pyruvates is most likely a Type II mechanism which was shown in previous works.[52] In the case of α-carbonyl modified silyl glyoxylates a Type I mechanism is dominating.[51] It was really interesting if the modification analogue to Type I acetophenones would lead to an α- or β-cleavage mechanism. Therefore, a bromo (BrKE), hydroxy- (OHKE) and morpholino (MOKE) ketoester should be synthesized. The trifluro ethyl pyruvate was commercially available.

2.3.1. Synthesis of ethyl bromomethyl oxobutanoate (BrKE)

For the modification of the α-carbonyl with a bromine group, previously synthesized ethyl methyl oxobutanoate (EMOB) was chosen as suitable precursor.
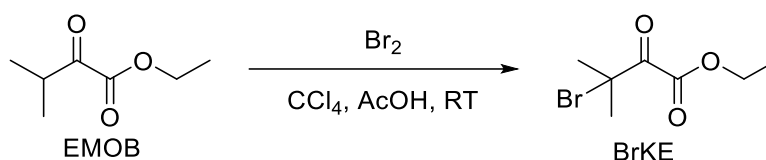
The tertiary hydrogen of EMOB can be easily substituted by bromine at room temperature according to literature.[76] As it is the energetically most favored position, only the tertiary hydrogen is substituted by bromine. For the synthesis, ketoester EMOB is diluted in a 9:1 mixture of tetrachloromethane and acetic acid and one equivalent elementary bromine is added via syringe. After 2 h the solution decolorizes and the bromo ketoester (BrKE) is extracted with chloroform and saturated sodium hydrogen carbonate solution. After removal of the solvents, the product is obtained almost quantitatively (94%) as colorless oil.

2.3.2.   Synthesis of ethyl hydroxymethyl oxobutanoate (OHKE)

In the next step the bromo moiety should be substituted by a hydroxyl group. To use sodium hydroxide seemed to be most convenient way. Therefore, the bromo ketoester was dissolved in THF and stirred at RT with 1 eq. of aqueous NaOH.[77] After 4 h still a lot of precursor is left.
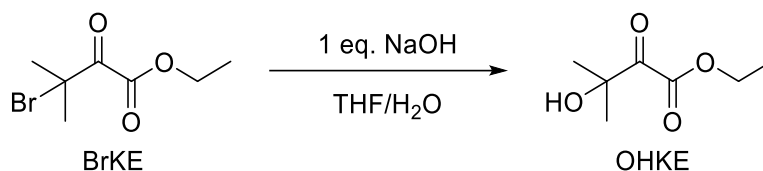
To get a full substitution more NaOH was added and the ester should be transferred into the methylhydroxy sodium oxobutanoate.
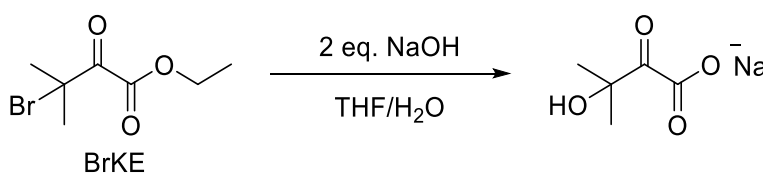
Unfortunately, under strong basic conditions the ketone moiety was destroyed by side reactions and no free acid could be isolated after acidic workup.

A milder way to exchange bromine groups against hydroxyl groups is the reaction with silver (I) oxide in moist acetonitrile analogue to literature.[78]
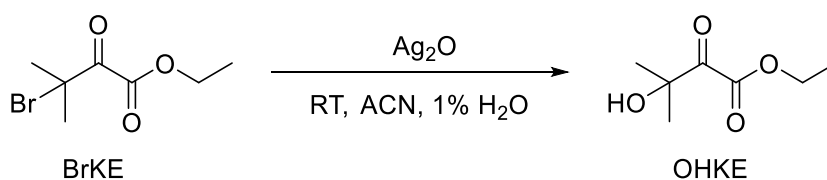
In this heterogeneous reaction the black silver oxide is suspended in the reaction mixture and stirred overnight in darkness. Afterwards the grey solid is filtered off and the mixture is extracted with diethyl ether. After drying and removal of the solvent, ball pipe distillation affords 94% of theory of desired hydroxyl ketoester with minor impurities of precursor.

2.3.3. Synthesis of ethyl morpholino methyl oxobutanoate (MOKE)

For the synthesis of morpholino ketoester MOKE, 1 eq. of previously prepared bromo ketoester BrKE was reacted with 1 eq. morpholine in THF at room temperature similar to literature.[79]
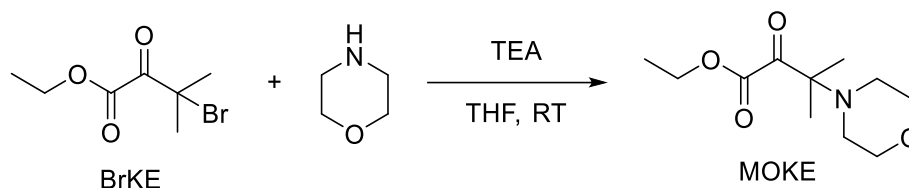
One equivalent triethylamine was used as acid scavenger. Although the precipitation of TEA hydro bromide was a good sign, no product could be isolated, as the basic conditions lead to side reactions of the ketone. It seems that basic conditions are real troublesome for ketoesters, as they readily decompose to a mixture of aldol products.[80]

2.4. Long wavelength UV initiators

Generally, aliphatic ketoester exhibit a low extinction coefficient and the absorption maxima of the n-π* transition is located in the low UV-A region around 330 nm. Since LED technology is gaining huge importance in industrial application and due to higher energy efficiency of light sources in visible region it is of great interest to shift the absorption of photoinitiators to higher wavelengths. By cross conjugation of the carbonyl with C-C double bonds the extinction coefficient and the absorption wavelength of the n-π* transition are increased. (Scheme 15)

λ_{max} = 325 nm λ_{max} = 346 nm
ε = 57 L mol^{-1} cm^{-1} ε = 75 L mol^{-1} cm^{-1}
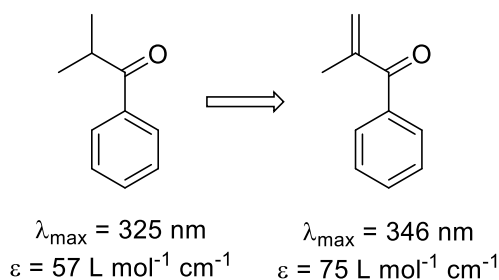
Scheme 15. UV-Vis absorption of alkyl phenyl ketone[81] in comparison to alkenyl phenyl ketone[82]

Therefore, unsaturated ketoesters ACKE and MAKE should be synthesized.

From diketones it is well known, that increasing coplanarity of the carbonyls also causes a strong bathochromic shift and also increases absorption. The highest shift towards longer wavelength can be achieved in five membered rings at a carbonyl angle of 0-10°, as for example in camphorquinone.[83] Linear diketones or α-ketoesters arrange their carbonyls in *trans*-position (180°). As α-ketoesters can be seen as pseudo diketone, planarization via ring structure as in DDFD was also considered as possibility to improve the absorbance of ketoesters.

Also higher conjugated triketones are known to strongly absorb in the visible area due to a major bathochromic shifts. Unfortunately triketones are hydrolytically very unstable and readily form hydrates, which do not exhibit conjugated carbonyls.[84, 85] A variety of similar build ketomalonates are commercially available and also these compounds should be tested as potential photoinitiator.

Diethyl aceto phosphonate DEAP was chosen as analogue to ethyl pyruvate. The phosphonic acid ester could increase absorption and cause a bathochromic shift, known from acyl phosphine oxides.

Based on this knowledge the following four substances were chosen to be tested.
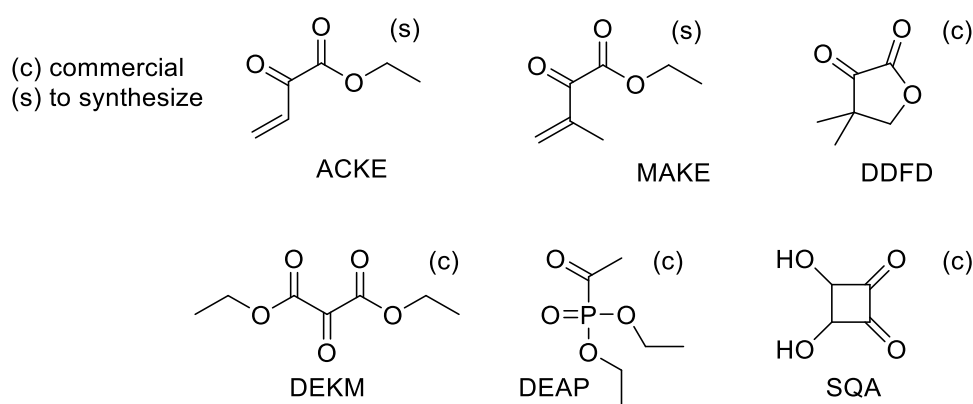
Compounds with unsaturated carbon moieties on the α-carbonyl had to be synthesized. The other compounds were commercially available.

2.4.1. Synthesis of ethyl 2-oxobut-3-enoate (ACKE)

From the synthesis of the dimethyl substituted aliphatic ketoester EMOB it was already known that α-ketoesters can be synthesized from diethyl oxalate and the corresponding Grignard reagent. In the case of EMOB isopropyl magnesium bromide lead to the desired product.

To synthesize ethyl-2-oxo-3-butenoate ACKE from diethyl oxalate, vinyl magnesium bromide or chloride are commercially available as solutions in THF. As vinyl halides are dangerous gases at room temperature, the Grignard reagents cannot be freshly prepared in laboratory scale.
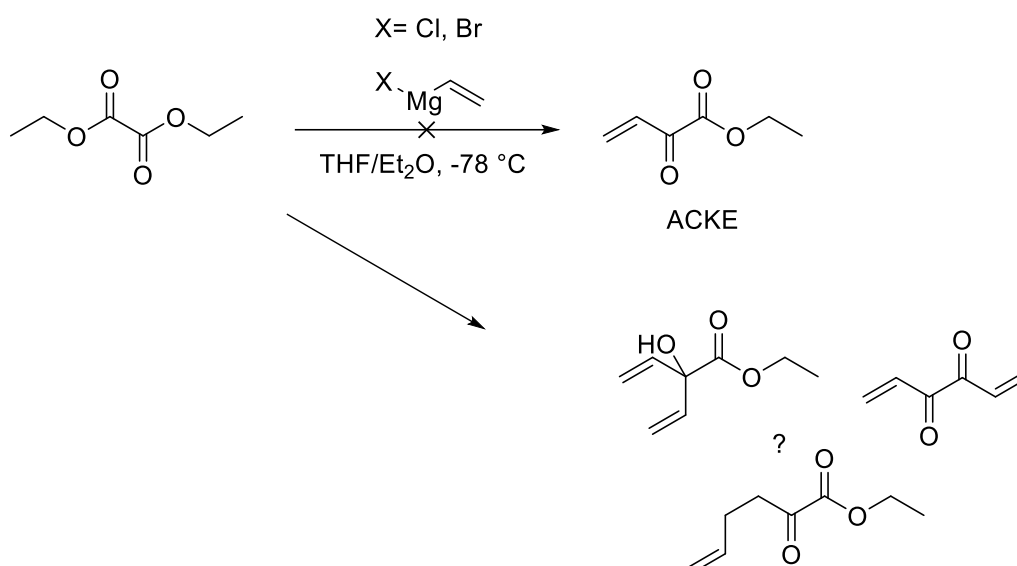
In the first attempt ident to literature,[86, 87] diethyl oxalate was treated slowly with 1 M vinyl magnesium chloride solution in a 1:1 mixture of diethyl ether and THF at -78 °C ident to literature. After 2 h the reaction mixture was warmed up to 10 °C and quenched with 1 N HCl. After extraction with ethyl acetate and saturated $NaHCO_3$ solution, the dried organic phase was stripped off the solvent. The small amount of yellow crude oil (10% of theory) still contained diethyl oxalate. ^{1}H-NMR shows a vinyl group, but the shifts of the double bond hydrogens are too low. GC-MS only peaks with multiple molecular weight of the desired product.

Another possibility was to react ethyl chloro oxalate with vinyl Grignard reagent ident to literature.[88] In this case the acid chloride is even more reactive than the ester side. Also quenching is not necessary as the Grignard reagent directly reacts with the acid chloride and magnesium salts precipitate.
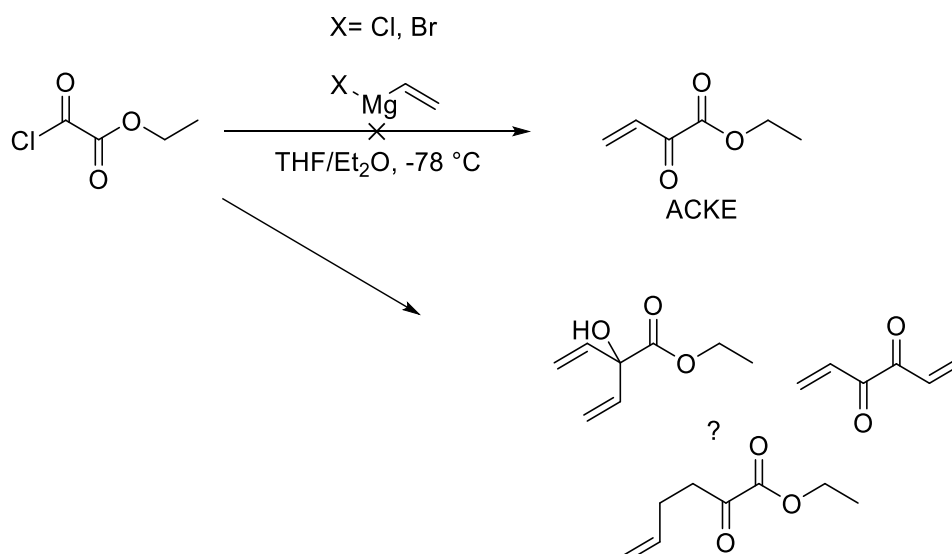
The reaction was done with vinyl magnesium bromide, as well as vinyl magnesium chloride, in presence of an excess of acid chloride. After filtration and extraction with NaHCO$_3$ solution and ether, TLC showed one main product and two side products. The main spot was UV active and quickly reacted with permanganate stain indicating the desired product. After column chromatography with 15% diethyl ether in PE the product isolated was examined by ^{1}H-NMR and GC-MS, revealing that the Grignard reagent attacked twice. It seems the generated ketone is too reactive towards the Grignard reagent. In fact although there are patents and articles stating they could synthesize ethyl oxobutenoate ACKE via this reaction,[89, 90] there is also literature declaring it is nearly impossible to stop these Grignard reactions at the ketone due to their higher reactivity towards nucleophile attack.[91] Literature was found about amine mediated Grignard reactions that stop in the keto stage with aromatic acid chlorides.[92] Therefore a last attempt analogue to literature was done using 2,2'-oxybis(N,N-dimethylethan-1-amine) as complexing agent.

Therefore, the Grignard reagent was slowly added to 1 eq. of amine in THF at -10 °C and stirred for 15 minutes. The solution was dropped slowly to the diethyl oxalate substrate at -60 °C within 20 min. The mixture was warmed up to -20 °C and quenched with ammonium chloride solution. Extraction with ethyl acetate afforded a mixture of addition products but no oxobutanoate ACKE. As the synthesis of ethyl methyl oxobutanoate was possible by Grignard reaction, the lower reactivity of isopropenyl magnesium bromide, which is far more sterically hindered than the vinyl reagent, could be used to obtain an unsaturated ketoester.

2.4.2. Synthesis of ethyl 3-methyl-2-oxobut-3-enoate (MAKE)

For the synthesis of 3-methyl-2-oxobut-3-enoate 1.5 eq. the Grignard reagent isopropenyl magnesium bromide (**4**) had to be prepared. Therefore, magnesium flakes where moisturized with 2 mL dry THF. After diluting 1.3 eq. isopropenyl bromide in tenfold amount of dry THF, 2 mL of the solution were added to the magnesium and heated with a heat gun. After the reaction started, reflux temperature was maintained by dropwise addition of isopropenyl bromide solution.
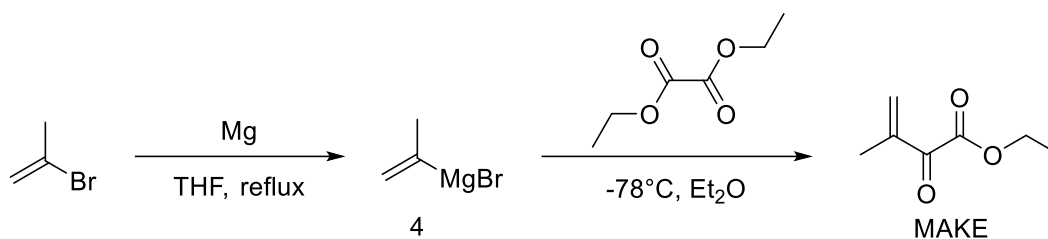
After the Grignard reaction was finished the resulting solution of **4** was added dropwise to a solution of 1 eq. diethyl oxalate in 60 mL 1:1 ether THF at -80 °C ident to literature.[64] As the Grignard reagent can react multiple times with the substrate, TLC monitoring was crucial. After adding ¾ of the solution, subsequent TLCs showed no more diethyl oxalate and the reaction was quenched with 2 N H_2SO_4. After extraction with ether, the combined organic phases were dried and the solvent removed in vacuum. The resulting yellow oil shows some remaining diethyl oxalate and impurities in NMR. After ball pipe distillation, a clear oil was obtained. NMR still showed some precursor and a pure product was obtained by column chromatography in a yield of 34% as slightly yellow oil.

The conversion of diethyl oxalate is hard to follow by TLC as the compound is not visible under UV and hardly stains with any staining reagent. After NMR it was clear that diethyl oxalate was not fully consumed, therefore the yield is lower than expected.

In literature, the compound is described as yellow which made this product especially interesting as the double bond was expected to cause a bathochromic shift.[93, 94] Nevertheless, the color is caused by impurities of diketone, which results from double attack by the Grignard reagent. The yellow very apolar compound can be separated by column chromatography. The pure compound is almost colorless.

2.5. Long wavelength visible light initiators

The initial idea to use ketoesters as initiators came from the previously mentioned patent covering silyl and germyl glyoxylates as photoinitiator.[95] Phophinoxide (PKE) and sulfon (SKE) ketoesters were not covered by the patent and the heteroatom-moiety in α-position could lead to new visible photoinitiators. Therefore, the patented molecules should be compared to new glyoxylates.
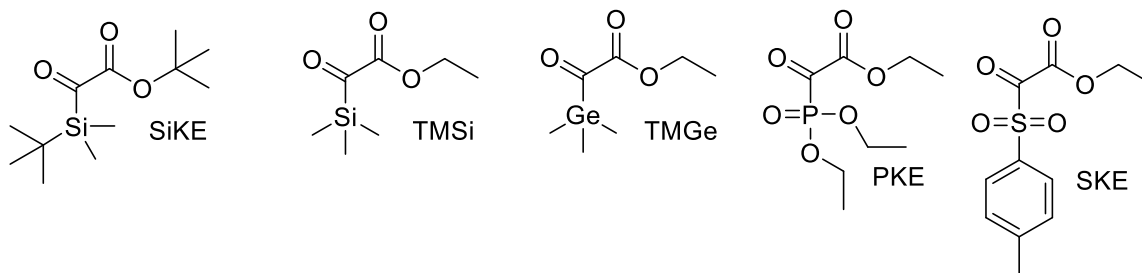
By using diazo acetate and half metal triflates the corresponding α-diazo ester can be easily prepared.[96] The silyl and germyl glyoxylates are then prepared by rhodium acetate catalyzed denitrification of the diazo compounds in presence of oxiranes as oxygen donor.[97]
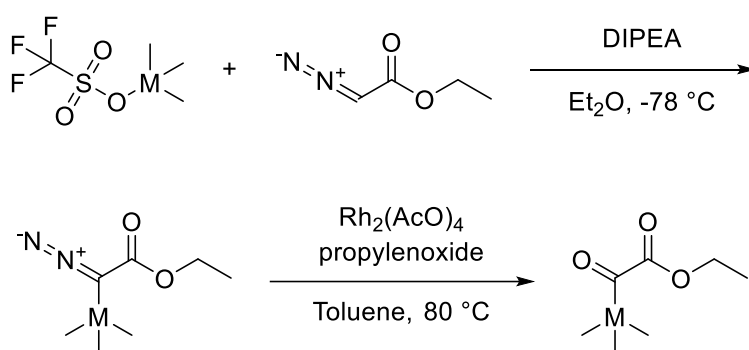
For the synthesis of the phosphine oxide and sulfonyl diazoacetates a different route has to be chosen. In old German literature a very simple synthesis for phosphine oxide glyoxylates was stated by Kreuzkamp.[98]

He suggested the bulk reaction of triethyl phosphite with chloro ethyloxalate.
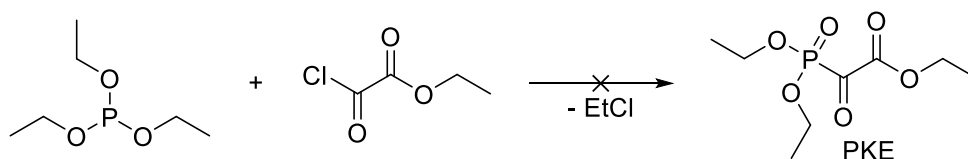
This was falsified years later by McKenna, who showed that this route is not working and the desired product was never synthesized. He suggested a synthesis via triethyl phosphono acetate as the pronounced electron deficiency of the methylene carbon makes it resistant to direct oxidation. Therefore, carbene-mediated oxygen transfer chemistry utilizing the intermediate phosphor diazoacetate with rhodium catalyst and propylene oxide should be used.[97] The resulting triethyl phosphono glyoxylates was described as highly moisture sensitive brilliant yellow oil.

The triethyl phosphono diazoacetate (**10**) can be easily prepared from tosyl azide[99] and commercial triethyl phosphono acetate according to literature.[100]
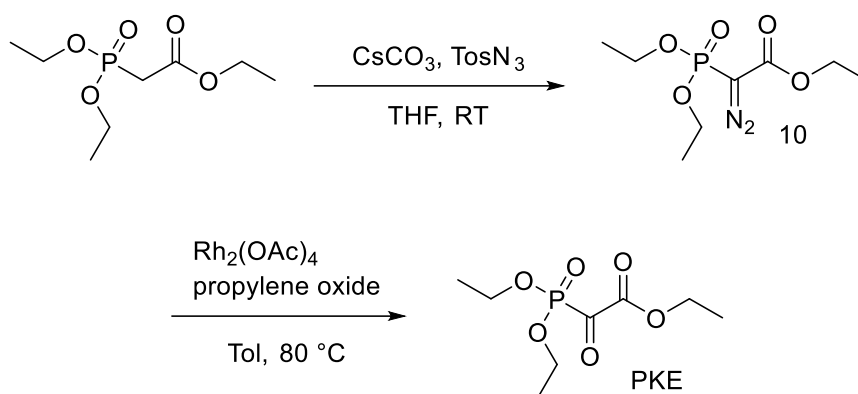
Tosyl diazoacetate can be prepared in the same manner.[101] Also the oxygen transfer via rhodium catalyst should work accordingly but has never been described.
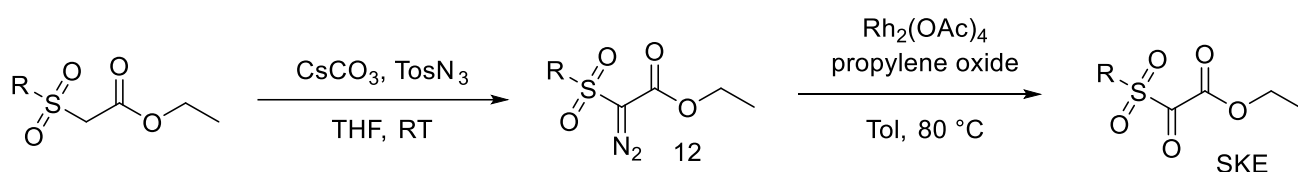
2.5.1. Synthesis of trimethyl silylglyoxylate (TMSi)

For the synthesis of the ethyl trimethyl silylglyoxylate the triflate compound (**5**) had to be synthesized first from trimethyl chlorosilane. Therefore, trimethyl chlorosilane was added at onece to 1 eq. silvertriflate suspended in abs. DCM. The suspension is stirred overnight and filtrated. [96]
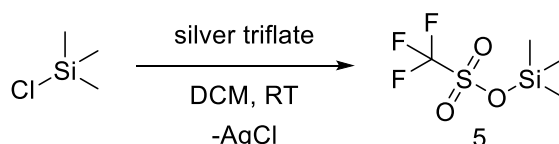
The solution of TMS-triflate (**5**) was then added dropwise to 1 eq. ethyl diazoacetate and 1 eq. ethyl diisopropylamine in 20-fold amount of ether at -78 °C. After 20 min the mixture was warmed up to room temperature and stirred overnight. After filtration of the resulting ammonium salt the solvent was stripped off in vacuum and the crude ethyl diazo(trimethylsilyl)acetate (**6**) was obtained as deep yellow oil. Further purification was not conducted due to stability concerns of the product.
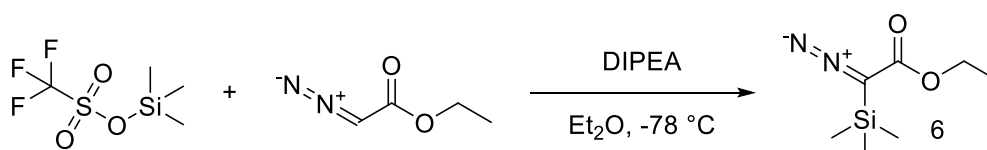
The diazo compound (**6**) was dissolved in toluene and 12 eq. of propylene oxide were added. Then the 2 mol% rhodium catalyst was then added while stirring. Instant formation of gas was

observed. The reaction was then heated to 40 °C overnight and the solvent was stripped of in vacuum.
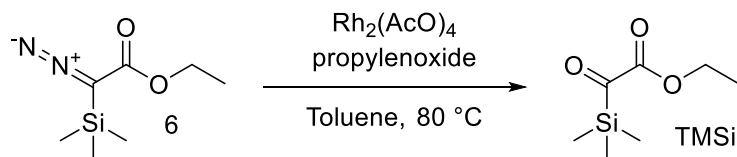
The crude product was flashed over silica with PE/EE 1:25 and after evaporation of the solvent 31% of theory ethyl trimethyl silylglyoxylate TMSi was obtained as brilliant yellow oil.

2.5.2. Synthesis of ethyl trimethyl germylglyoxylate (TMGe)

For the synthesis of ethyl trimethyl germylglyoxylate TMGe, the reaction with trimethyl chlorogermane was conducted exactly as in the reaction with the chlorosilane.
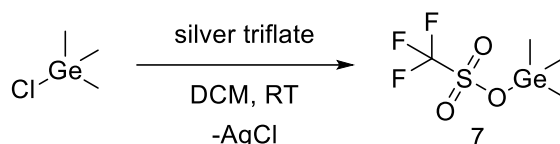
Also, the next step was prepared as the silyl compound. The product (**8**) was then analyzed by GC-MS, NMR and ATR-IR showing the product and minor traces if amine. In the IR the diazo peak was clearly visible at 2075 cm^{-1}.
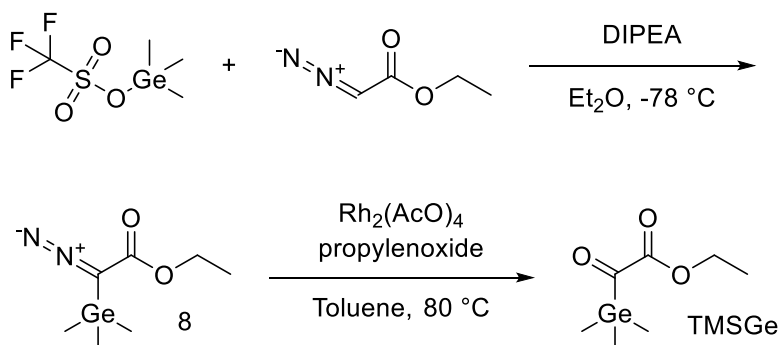
In addition, in this case the yellow diazo intermediate was redissolved in toluene in a Schlenk tube and charged with 12-fold excess of propylene oxide. The gas formation when adding the 2 mol% rhodium acetate was even stronger and almost caused the reaction to foam out of the flask. After stirring at 40 °C overnight, the product was purified by column chromatography with 10% ether in PE after removing the solvent. In the end, 35% of theory of ethyl trimethyl germyl glyoxylate was obtained as brilliant yellow oil.

2.5.3. Synthesis of triethyl phosphono glyoxylate (PKE)

In the case of triethyl phosphono glyoxylates the precursor triethyl phosphono acetate is commercially available. For the diazotation of the compound tosyl azide (**9**) has to be freshly prepared from tosyl chloride and sodium azide.
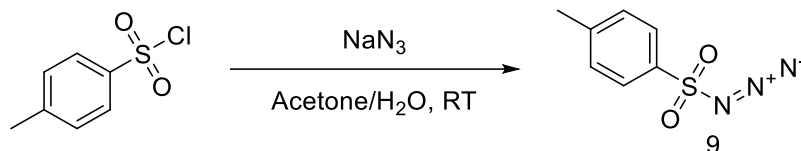
For the preparation of tosyl azide (**9**), sodium azide is dissolved in the 4-fold amount of water and stirred.[102] Tosyl chloride is dissolved in the 2-fold amount acetone and added dropwise to the stirred sodium azide solution cooled to 0 °C. After 1 h the precipitate of NaCl is filtered and the filtrate is extracted with ether. The solvent is then stripped off carefully off the dried organic phase to afford tosyl azide (**9**) quantitatively.
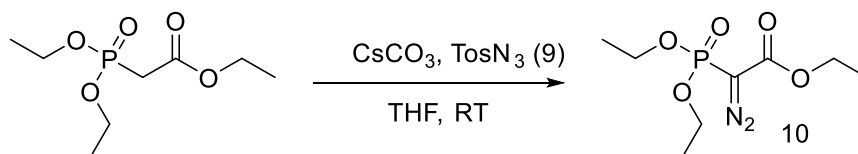
In the next step abs. THF is charged with 1 eq. of triethyl phosphono acetate and 1 eq. cesium carbonate. 1 eq. tosyl azide (**9**) is added quickly and the mixture is stirred at RT for 2 h.[103] Afterwards the reaction is filtered over hyflow to remove the precipitated tosyl amide and the solvent stripped off in vacuum to afford crude triethyl phosphono diazo acetate as yellow oil. NMR analysis showed remaining tosyl amide therefore the compound is redissolved in a small amount of diethyl ether and the same amount of petrol ether is added to precipitate remaining tosyl amide. After filtration and removal of the solvent in vacuum, the diazo compound (**10**) is received in 49% of theory as yellow oil. Small amounts tosyl amide are still present but due to the instability of the compound 92% purity was acceptable for the next reaction step.
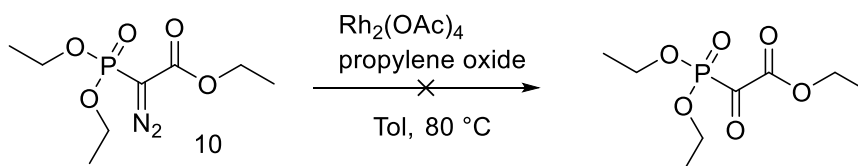
In the third step, 1 eq. triethyl phosphono diazo acetate is redissolved in 40-fold excess of abs. toluene and charged with 12 eq. propylene oxide in a Schlenk tube. After adding 2 mol% of

rhodium catalyst to the reaction, it is stirred at 40 °C overnight.[97] The next day it was tried to filtrate a small amount of the reaction mixture over silica gel in a Pasteur pipette to remove the green catalyst. The eluate is yellow and loses its color within minutes. As the resulting compound seemed to be highly air sensitive the solvent was stripped of by vacuum in the Schlenk tube. It was then tried to get rid of the rhodium salts in the green oil. Unfortunately, the compound was so instable, that filtration lead instantly to the decomposition of the product. Precipitation with small amounts of petrol ether could precipitate some of the rhodium salts. The resulting dark yellow oil already decolorized when it was mixed with NMR solvent or monomer.

Probably the pulling phosphonate and ester groups cause formation of a gemdiol and further decomposition.
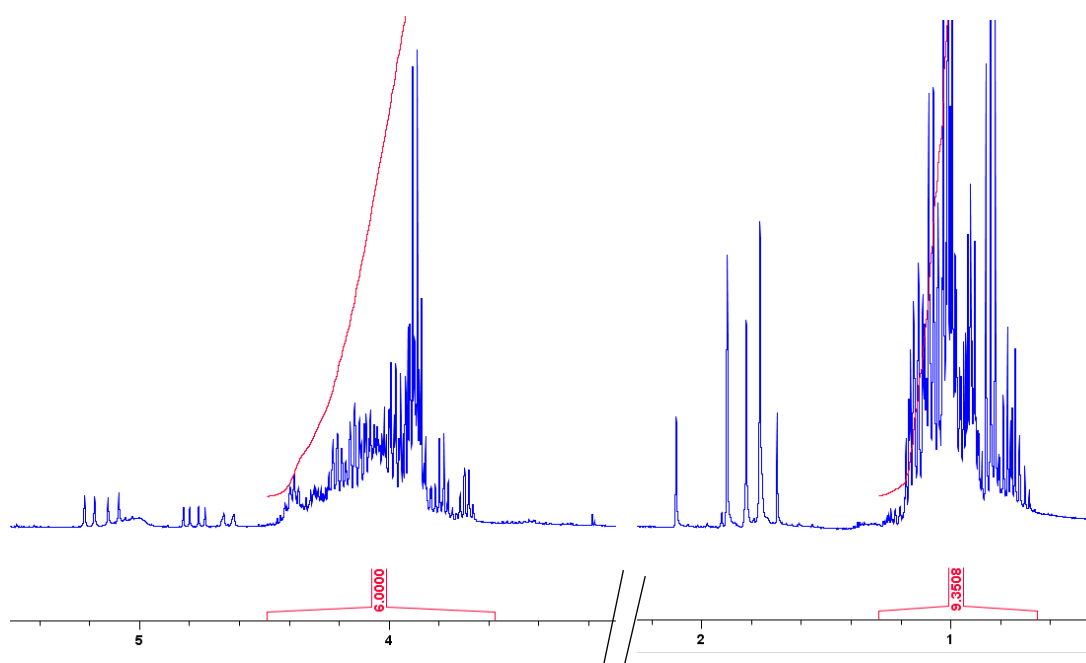
Figure 11. ^{1}H-NMR of decomposed triethyl phosphono glyoxylate (PKE)

The crude product could not initiate polymerization. It seemed that the stated sensitivity to air moisture stated in literature[97, 104] was too severe to isolate and analyze the compound under normal conditions. The NMR in Figure 11 shows the ethyl signals of the decomposed product.

2.5.4. Synthesis of ethyl tosyl glyoxylate (SKE)

The tosyl ethyl acetate (**11**) had to be synthesized previously by the simple reaction of ethyl bromo acetate and sodium toluene sulfinate ident to literture.[105]
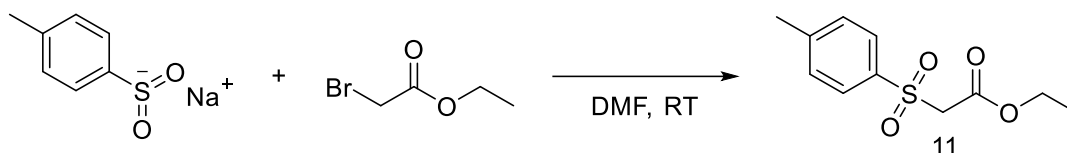
Therefore, the sodium sulfinate was dispersed in 20-fold weight excess of DMF and ethyl bromo acetate is added at once. The suspension gets warm and the solid dissolves quickly. After stirring overnight, the mixture is diluted with half the volume water and extracted with the same amount of ethyl acetate. The solvent is then stripped off the dried organic phase. To remove the remaining DMF the oil was redissolved in diethyl ether and extracted three times with the 4-fold amount of water. After drying and evaporating the organic phase, 70% of theory of tosyl ethyl acetate crystallized as colorless needles.
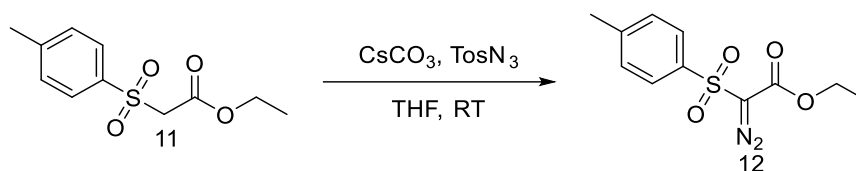
In the next step 1 eq. tosyl acetate (**11**) were suspended with 1 eq. of cesium carbonate in 35-fold amount of THF. An equimolar amount of tosyl azide was added after 30 min stirring at RT and stirred overnight.[106] The next day the deeply orange solution was filtered off the colorless precipitate and the solvent was stripped off in vacuum. The resulting orange oil was filtered over 15-fold amount of silica gel with 1:1 EE/PE as eluent. The solvent was removed again by vacuum and the resulting lemon-yellow oil crystallized. Recrystallization from $CHCl_3$ affords 88% of theory of ethyl tosyl diazoacetate (**12**), with small amounts of remaining tosyl amide.
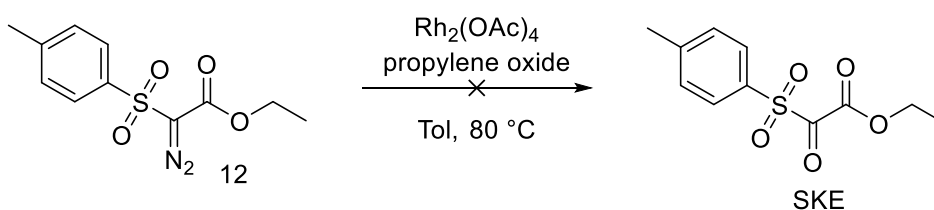
In the third step, 1 eq. ethyl tosyl diazoacetate is redissolved in 40-fold excess of abs. toluene and charged with 12 eq. propylene oxide in a Schlenk tube. After adding 2 mol% of rhodium catalyst to the reaction, it is stirred at 40 °C overnight.[97] After evaporation of the solvent in vacuum, a half-solid orange oil was obtained. HPLC, GC-MS and NMR show about 30 substances, two of them main products. In addition, this glyoxylate is probably very moisture sensitive as it carries two electron withdrawing groups on the ketone. Therefore, column chromatography was not successful. The orange crude product did not initiate polymerization. As can be seen in NMR of

Figure 12, there are a huge number of different products after the reaction with rhodium catalyst and propylene oxide, only the tosyl CH_3 signal at 2.3 ppm is clearly visible.
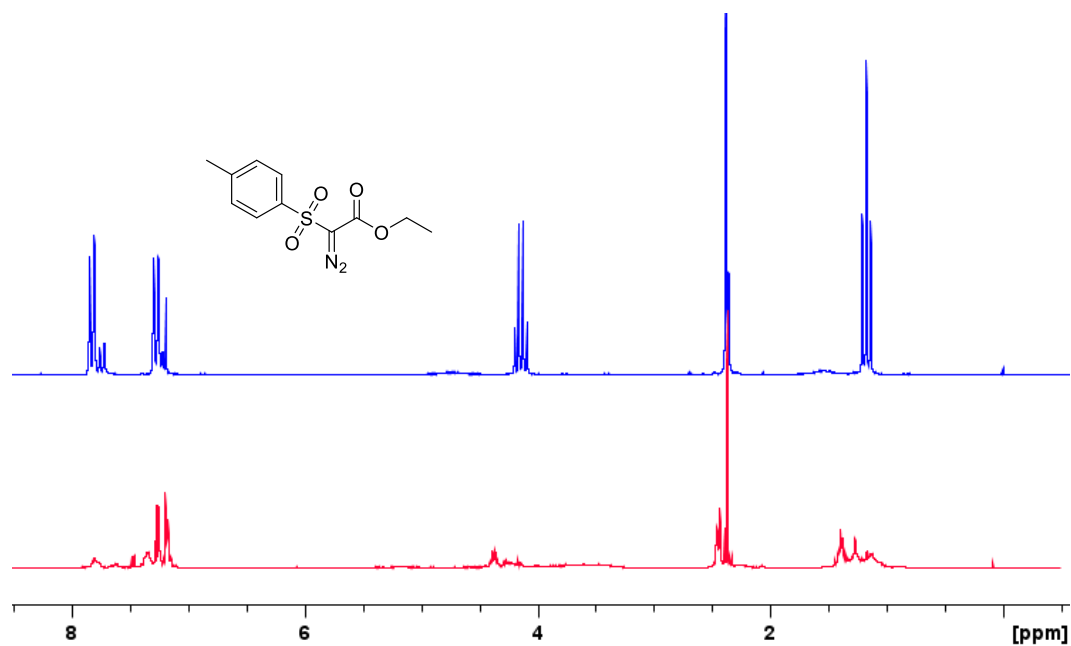
Figure 12. ^{1}H-NMR of ethyl tosyl diazo acetate (blue) and the reaction product afterwards (red)

3. Preliminary curing tests with α-keto compounds

All compounds that were commercially available or could be synthesized were tested in a 1 wt% hexanediol diacrylate formulation by irradiating a 500 μl sample in a silicone mold in a broadband Intelliray 600 UV floodlight oven for 100 s. (Scheme 16)

a) simple aliphatic α-ketoesters

EP (c) MOB (c) EMOB (c/s) MDMOB (s)

b) modification of the ester moiety

TBTKE (s) TKE (s) KEA (s) AKE (s)

c) modification of the alpha carbonyl

BrKE (s) OHKE (s) TFKE (c)

d) long wavelength UV initiators

MAKE (s) DDFD (c) SQA (c) DEKM (c) DEAP (c)

e) long wavelength visible initiators

SiKE (c) TMSi (s) TMGE (s)

(c) commercial
(s) synthesized
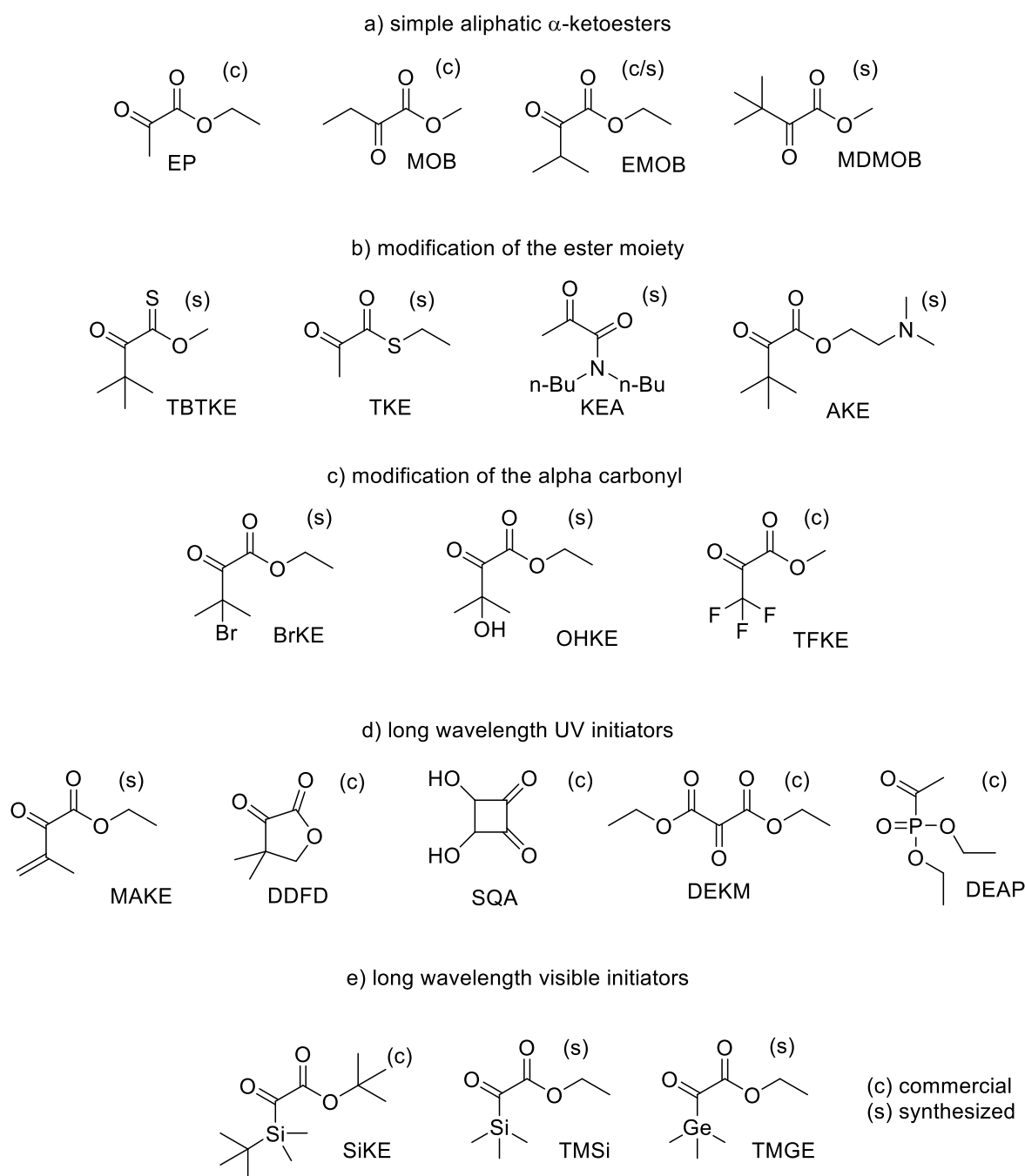
Scheme 16. Available compounds that were tested as photoinitiators.

This curing test ensured to reveal any activity as photoinitiator as the device offers very high broadband light power. Substances that exhibited no curing of the HDDA formulation within 100 s were eliminated from the study. (Table 2)

Table 2. Overview of the reactivity of compounds in preliminary curing tests

compound	initiation
a) simple aliphatic ketoesters	
EP	yes
MOB	yes
EMOB	yes
MDMOB	yes
b) modification of the ester moiety	
TBTKE	no, no bleaching
TKE	incomplete, no bleaching
KEA	no
AKE	yes
c) modification of the alpha carbonyl	
BrKE	yes
OHKE	yes
TFKE	no
d) long wavelength UV initiators	
MAKE	no
DDFD	yes
SQA	no (insoluble)
DEKM	yes
DEAP	yes
e) long wavelength visible initiators	
SiKE	yes
TMSi	almost liquid, no bleaching
TMGe	no, no bleaching

In group a) the *simple aliphatic α-ketoesters* showed good reactivity and no discoloration of specimens.

Exchanging oxygen with sulphur in group b) *modification of the ester moiety* leads to yellow compounds with a bathochromic shift. The t-butyl thio ketoester TBTKE did not show any activity while the thio ketoester TKE showed some reactivity. The yellow color probably derives from an equilibrium with the o-alkyl isomer. This explains why the compound does not show reactivity in the visible range (Ivoclar Lumamat) although it absorbs light in that region. By changing the ester group to an amide (KEA) the photo reactivity completely disappears.

Although amino ketoester AKE is slowly decomposing due to the basic amino group, it showed decent reactivity directly after synthesis.

The *modification of the alpha carbonyl* in group c) with β-bromine (BrKE) or β-hydroxy groups (OHKE) leads to reactive colorless compounds. Interestingly the trifluoro ketoester TFKE did not

show any reactivity. This compound is known to be moisture sensitive due to the highly electronegative rests on the ketone.

The group d) of slightly yellow *long wavelength UV initiators* show very mixed results. The isopropenyl ketoester MAKE is completely unreactive and the formulation does not change upon irradiation. Even longer irradiation in solution did not show any change in the NMR spectrum.

The cyclic structure DDFD shows high reactivity and leads to a colorless polymer. The other cyclic compound, squaric acid SQA, is actually a four membered cyclic dione. It was assumed that the strongly planarized carbonyls would cause a bathochromic shift and visible light reactivity. Unfortunately, the compound was not soluble in any monomer and the supernatant formulations that were decanted after 30 min ultrasonic bath at 50 °C showed no reactivity at all.

The ketomalonate DEKM shoes some activity but the sample seems to be not fully cured. As it is the same problem for all ketoesters with two pulling groups, sensitivity to moisture is a crucial problem. Under non-inert conditions, ketomalonates readily form monohydrates with a gem-diol structure. Initiation is then probably impeded, as the carbonyl chromophore is destroyed.[107]

The phosphorus ester analogue diethyl aceto phosphonate DEAP showed surprisingly good curing and was very active.

In group e) the *long wavelength visible initiators* all had a deep yellow color as neat compound. Also the formulations were yellow. As expected the known silylglyoxylate initiator SiKE was highly reactive and showed good bleaching. The trimethyl silylglyoxylate was barely active and showed only slight bleaching. The specimen was not fully cured, resulting in a soggy specimen. The trimethyl germylglyoxylate was completely inactive and showed no bleaching or conversion.

Brook rearangement
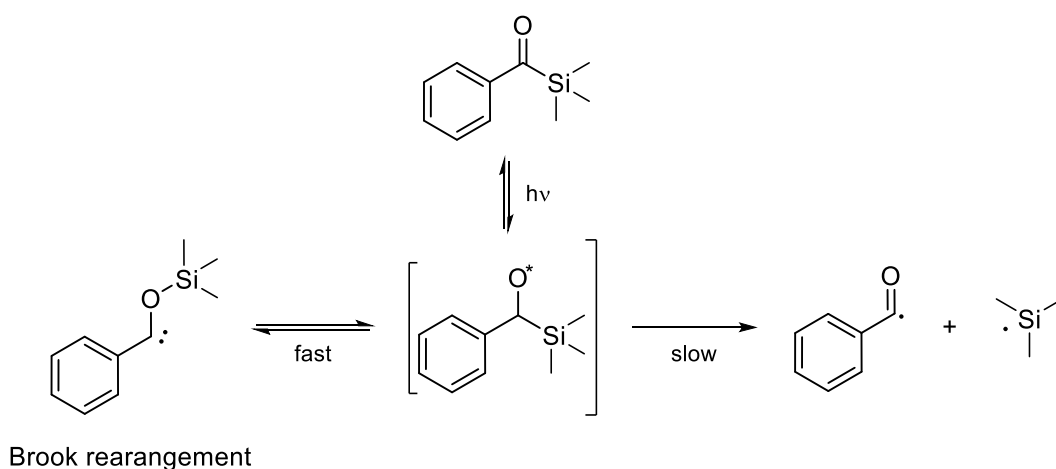
Scheme 17. Photoreaction of benzoyl trimethyl silane: Brook carbine formation, left and hemolytic cleavage right

This can be explained by brook rearrangement that is known from acyl silanes that are not sterically hindered. (Scheme 17) The probability of photo Brook rearrangement arrangement is higher the less sterical demanding moieties are carried by the silane.[108, 109]

The same reaction is also known for acyl germanes, which also undergo Brook rearrangement.[110]

The fact that only the sterically hindered ketoester SiKE is active as radical photoinitiator is a clear sign that trimethyl groups are not bulky enough and also silyl and germyl glyoxylates undergo rearrangement reactions when excited by light.

In total nine compounds were found to be active as photoinitiator and were further investigated.

4. UV-Vis measurements

From all compounds active as photoinitiator, UV-Vis measurements were conducted. The concentration in acetonitrile was chosen, that the maximal absorption was not exceeding 1.0 absorption units. This ensures that the measurement is within the linear region of Lambert-Beer's law.

In Table 3 the absorption maxima of the n-π* transition and the extinction coefficient at the maximum is given. Most compounds show an absorption maximum between 320 and 340 nm.

Table 3. Maxima of the n-π* transition and extinction coefficient of the tested initiators.

Initiator	λ_{max} [nm]	ε [L mol^{-1} cm^{-1}]
reference initiators		
BP	338	140
BMS	312	21600
PGO	343	53
ITX	383	2792
a) simple aliphatic α-ketoesters		
EP	330	17
MOB	325	17
EMOB	331	21
MDMOB	311	25
b) modification of the ester moiety		
TKE	298 / 393	213 / 4.5
c) modification of the α-carbonyl		
BrKE	327	57
OHKE	318	33
d) long wavelength UV initiators		
DDFD	375	28
DEKM	368	30
DEAP	334	38
e) long wavelength visible initiators		
SiKE	434	92

Only bathochromic shifted compounds like cyclic DDFD, visible light initiator ITX and diethyl ketomalonate DEKM exhibit absorption maxima at higher wavelength.

The spectra of the reference initiators benzophenone and phenyl glyoxylate are shown in Figure 13. Benzophenone BP and phenyl glyoxylate PGO show similar absorption pattern. Benzophenone is carrying two phenyl groups and therefore shows a higher extinction coefficient. Phenyl glyoxylate PGO shows a bathochromic shift in comparison to benzophenone. By exchanging one phenyl group to an ethyl ester the absorption is lower but tails out until 405 nm. This can be explained by the interaction of the ketone carbonyl with the ester carbonyl, forming a pseudo diketone. Benzophenone absorbs until 390 nm and therefore cannot be used as photoinitiator in visible light.
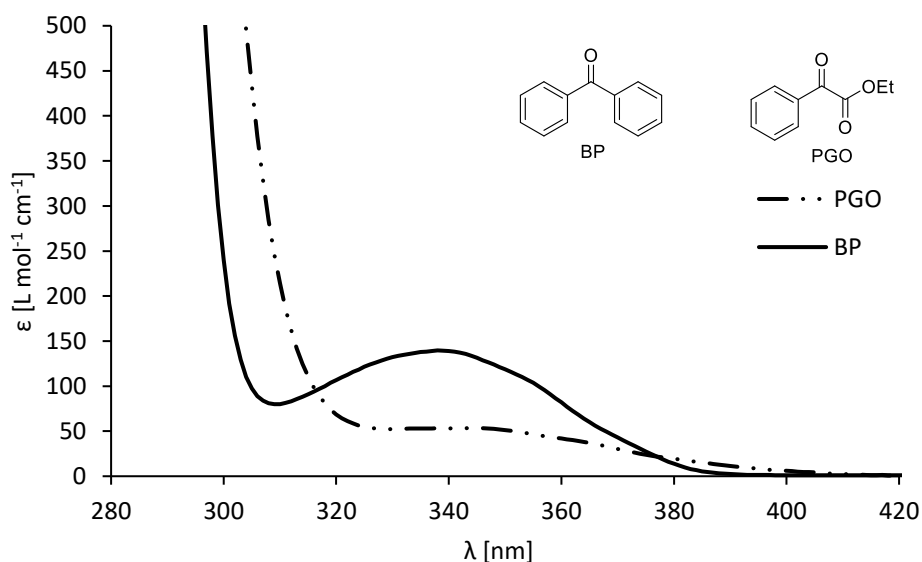
Figure 13. UV-Vis spectrum of benzophenone (BP) and phenyl glyoxylate (PGO).

The compounds with the highest absorption in this study were the benzophenone thioether BMS and thioxanthone ITX. (Figure 14) BMS shows very high absorption in the UV range with a maximum at 313 nm and an extinction coefficient of 21500 L mol^{-1} cm^{-1}. The compound shows a tail out to about 390 nm and does not initiate in the visible light area.
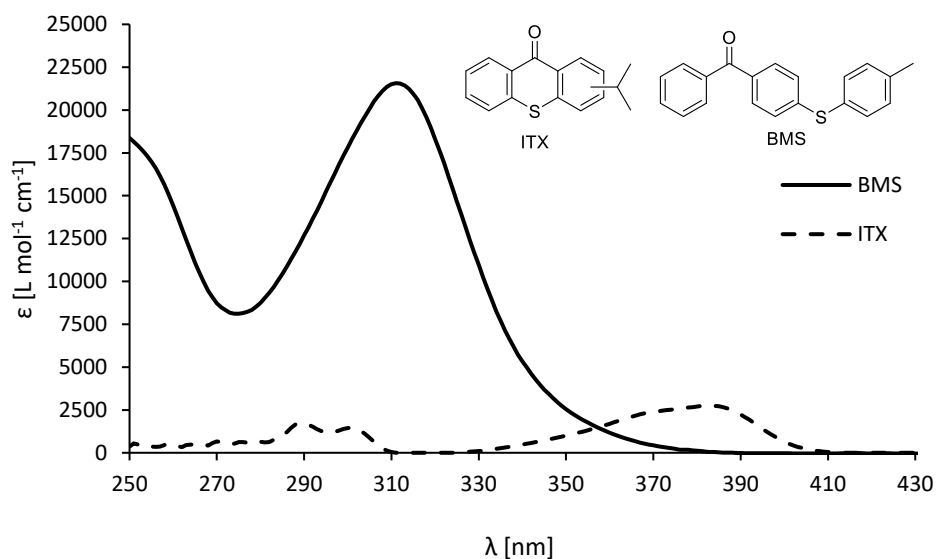
Figure 14. UV-Vis spectrum of benzophenone derivative BMS and thioxanthone ITX.

Thioxanthone ITX has a lower extinction coefficient than BMS but it is still magnitudes higher than the other tested initiators. With an absorption maximum at 383 nm and an extinction coefficient of almost 2800 L mol^{-1} cm^{-1} the absorption tails out to 410 nm in the visible area.

The *simple aliphatic α-ketoesters* all show relative low extinction coefficients of 17 to 25 L mol^{-1} cm^{-1} and similar absorption patterns. (Figure 15) The n-π* transition maximum is around 330 nm, only *t*-butyl derivative MDMOB shows a significant lower shifted maximum at 317 nm and less absorption in the higher UV range.
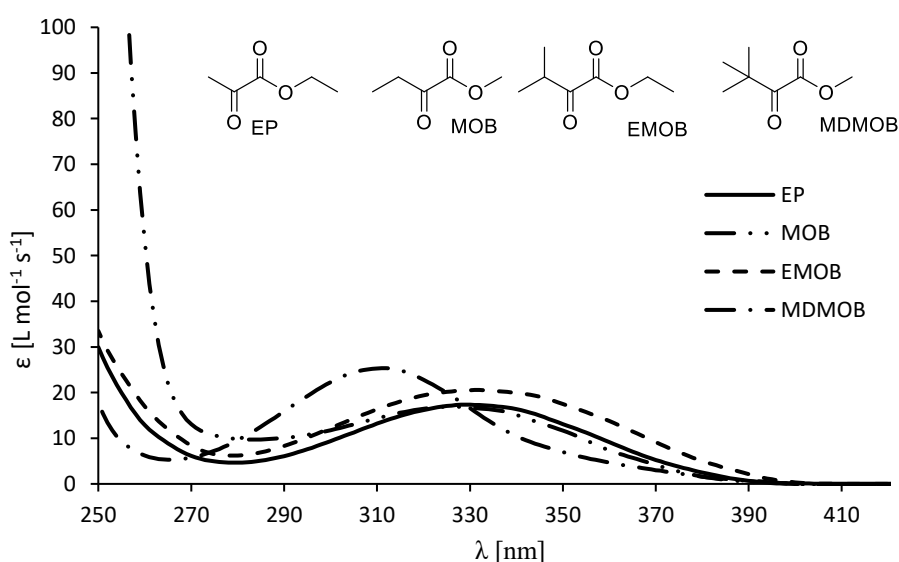
Figure 15. **UV-Vis spectra simple ketoesters ethyl pyruvate EP, methyl oxobutanoate MOB, ethyl methyl oxobutanoate EMOB and dimethyl methyl oxobutanoate MDMOB**

All compounds tail out to 390 – 400 nm and methyl oxobutanoate EMOB shows the highest absorption from 340 to 400 nm.

Modification of the α-carbonyl by introducing a bromine or hydroxy moiety in β-position, the absorption can be increased. (Figure 16) The effect is stronger for the bromo compound BrKE. In comparison to the unmodified ketoester EMOB (Figure 15) the extinction coefficient is more than doubled to 57 L mol^{-1} cm^{-1}. There is no bathochromic shift visible as the n-π* transition maximum is 327 nm but due to the higher overall absorption there is a tail out visible until 405 nm.

The hydroxy ketoester OHKE shows a lower extinction coefficient at the maximum of only 33 L mol^{-1} cm^{-1} at 318 nm. Therefore, the hydroxy group causes a hypsochromic shift in comparison to the unmodified ketoester EMOB.
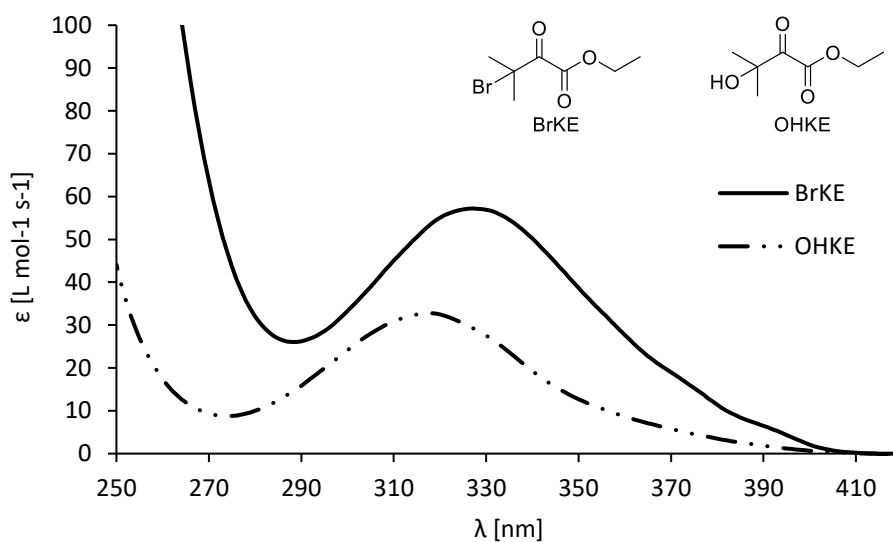
Figure 16. UV-Vis spectra of bromo ketoester BrKE and hydroxy ketoester OHKE

By *modification of the ester moiety*, thioketoester TKE showed a remarkable absorption spectrum. The compound exhibits a strong absorption band in the deeper UV-region at 298 nm with an extinction of 213 L mol^{-1} cm^{-1}.
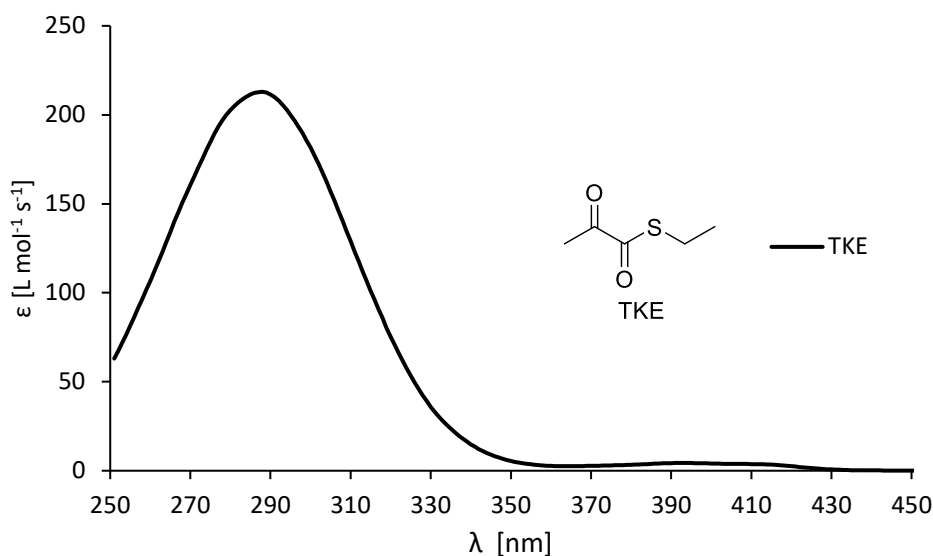
Figure 17. UV-Vis absorption spectra of S-ethyl thioketoester TKE

However, a closer look reveals a transition in the visible light region up to 430 nm. (Figure 18)
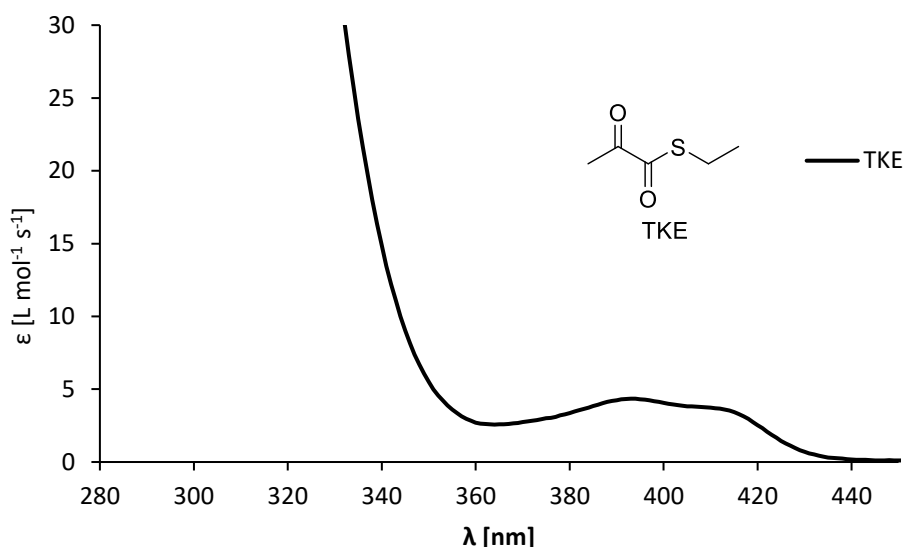
Figure 18. Zoomed-in UV-Vis absorption spectra of S-ethyl thioketoester TKE

The absorption in this region explains the deep yellow color of the compound. The visible maximum is found at 393 nm with a low extinction coefficient of only 4.5 L mol^{-1} cm^{-1}. The maximum is part of a plateau from 390 nm to 420 nm which exhibits almost the same extinction coefficient.

Only two compounds with significant bathochromic shift were active as photoinitiator in the group of *long wavelength UV initiators*. Diethyl ketomalonate DEKM and cyclic ketoester DDFD exhibit very similar absorption pattern. In case of the ketomalonate DEKM the two ester groups together with the ketone form a pseudo triketone. The additional carbonyl in comparison to

pyruvates causes a shift of the maximal n-π* absorption from 330 nm to 368 nm. Due to this shift the compound absorbs light up to 420 nm. (Figure 19)
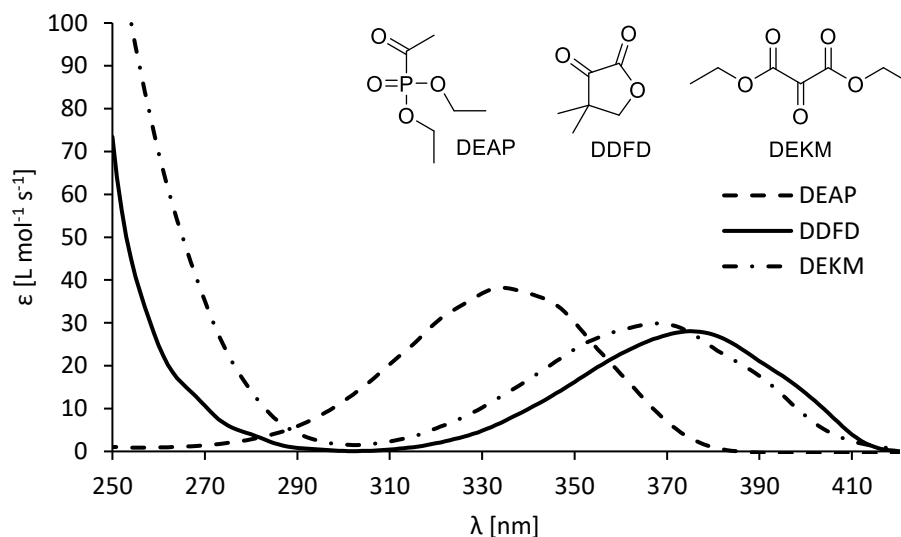
Figure 19. UV-Vis absorption spectra of cyclic ketoester DDFD and diethyl ketomalonate DEKM

Cyclic ketoester DDFD is the cyclic isomer to simple ketoester EMOB. From diketones, it is known that the carbonyl angle determines the absorption pattern of diketones.[111, 112] Higher co-planarity of the carbonyls causes a shift to higher wavelengths. α-Ketoesters can be defined as pseudo diketone.
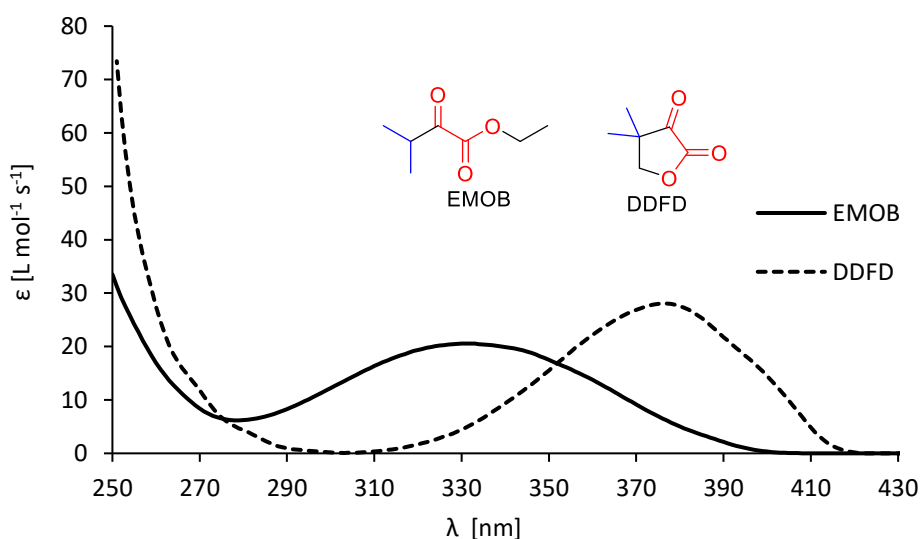
Figure 20. UV-Vis absorption spectra of linear analogue EMOB in comparison to cyclic DDFD.

Cyclisation of a ketoester leads to an increased co-planarity of the carbonyls due to sterical reasons. This causes a bathochromic shift of the UV-Vis absorption, which can be clearly seen in Figure 20 where the absorption of linear ketoester EMOB is compared to cyclic DDFD.

The bathochromic shift is higher than in case of ketomalonate DEKM and leads to the highest absorption in the visible light area among the aliphatic ketoesters.

Aceto phosphonate DEAP shows a maximum at 334 nm with an extinction coefficient of 38 L mol^{-1} cm^{-1}. Unfortunately, the compound only absorbs only until 380 nm. Therefore, the phosphorus does not cause the expected bathochromic shift and the compound cannot be used in the near UV-visible area. This was unexpected as similar aromatic acylphosphine oxides are used as visible light photoinitiator.[63]

Already known silyl glyoxylate SiKE was also tested. In this case, a strong shift of the carbonyl band to visible light is seen. (Figure 21) Inductive effects of the silicon atom on the α-carbonyl of the ketoester cause the strong bathochromic shift.[113]
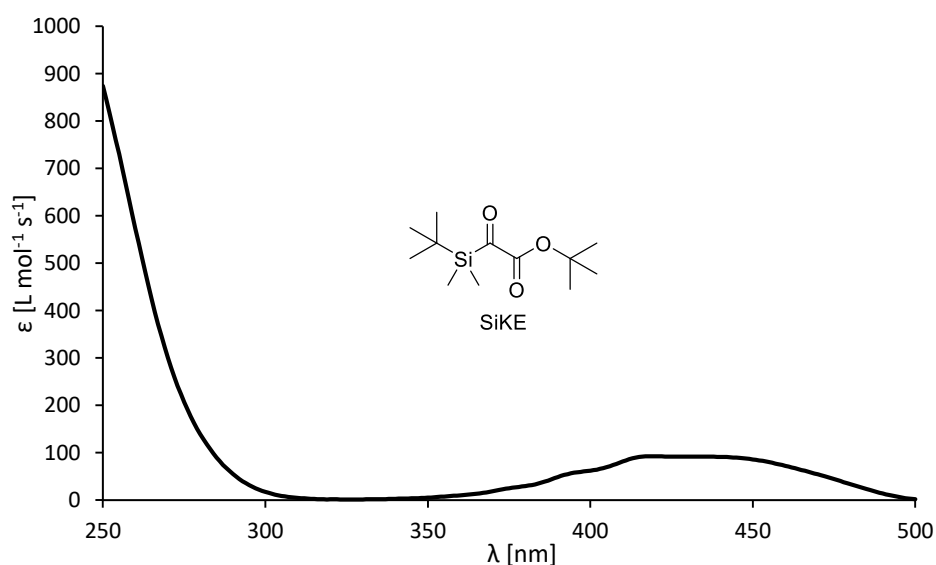
Figure 21. UV-Vis absorption spectra of silyl glyoxylate SiKE

After characterization of the compounds, they were tested in photo-DSC measurements according to their absorption properties.

5. Photo-DSC measurements with α-keto compounds

All initiators were tested by photo-DSC measurements in different monomer systems. To ensure the same molar ratio of initiators to monomer for all tested compounds, ethyl pyruvate (EP) as compound with the lowest molecular weight was used as benchmark. For the photo-DSC measurements, 10 mg (1 wt%, 0.086 mmol) of EP were weighed into a brown glass vial with

1000 mg monomer. All other (co)initiators were weighed into the monomer equimolar to the amount of 1 wt% ethyl pyruvate.

After transferring 10.5 ± 0.5 mg into a DSC pan, the aluminum pan was closed by a glass lid and put into an auto sampler. The samples were irradiated twice for 300 s and a calorigram was recorded. After subtracting the baseline calorigram of the second irradiation period from the first, a baseline corrected calorigram was obtained. From the area under the curve, the total heat evolved during polymerization was given. With the theoretical heat of polymerization for each monomer, the maximal rate of polymerization (R_P), time to R_P, time to 95% end conversion and double bond conversion DBC was calculated.

The rate of polymerization is a good measure to describe the reactivity of a system. A high polymerization rate ensures fast and efficient curing.

5.1. Acrylate system

Acrylates are an important class of highly reactive monomer for radical polymerization. The fast curing and very variable mechanical properties of acrylates are benefits used in surface coatings, decoratives, as well as different printing applications and additive manufacturing technology. With 5 million metric tons produced worldwide, acrylates are still the most used monomers for radical bulk photopolymerization in industrial application.[114]
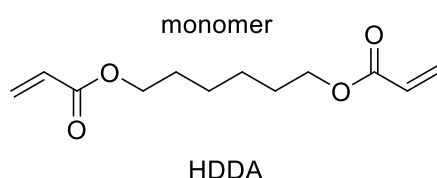
HDDA

For testing the novel photoinitiators in acrylic resins, hexane diol diacrylate (HDDA) was chosen as highly reactive diacrylate that is widespread in different industrial fields.[115]

5.1.1. Simple aliphatic α-ketoesters

To compare the aliphatic α-ketoesters with known industrial initiators, three reference compounds were chosen. Benzophenones BP and BMS are classical Norrish Type II initiators, therefore these initiators required coinitiators. The phenylglyoxylate PGO is a known Type II initiator that is the aromatic analogue to aliphatic ketoesters. It was tested both, with and without coinitiator like all other ketoesters.[62, 116] (Scheme 18)

As coinitiator, the low molecular weight methyl diethanol amine (MDEA) was selected. Tertiary aliphatic amines are often found as coinitiators for electron transfer reactions. Amines tend to have a strong fish-like odor. To circumvent the bad smell tertiary di- or triethanol amines are

used which are less volatile. In dental composites or other medical applications ethyl-4-dimethylamino benzoate (EDB) is used as coinitiator, as it is odorless, less basic than aliphatic amines and considered biocompatible.[117, 118]

initiators
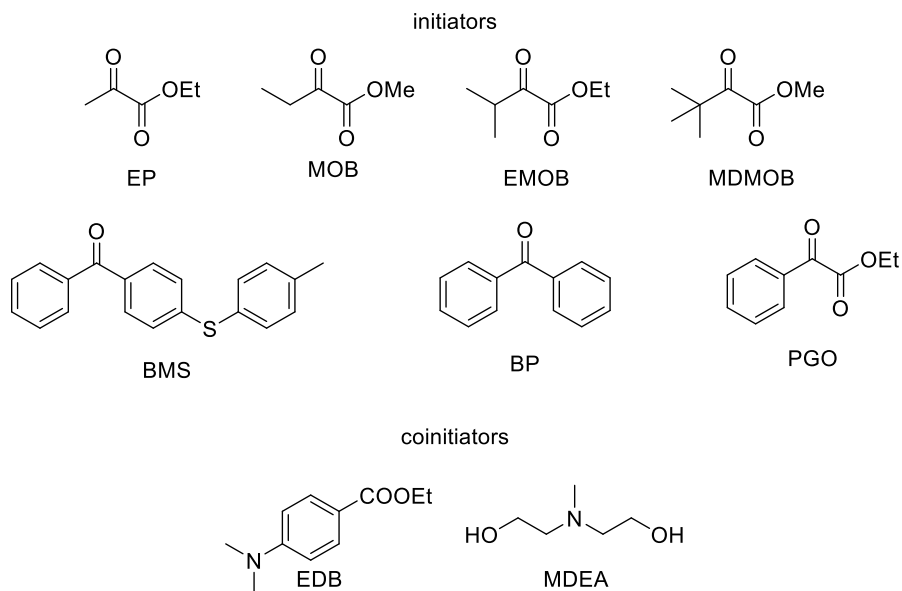
coinitiators

Scheme 18. Test setup for testing α-ketoesters in acrylates

First, the ketoester compounds were tested without coinitiator. Benzophenone BP and benzophenone thioether BMS were tested with the industrial standard coinitiator methyl diethanol amine (MDEA).
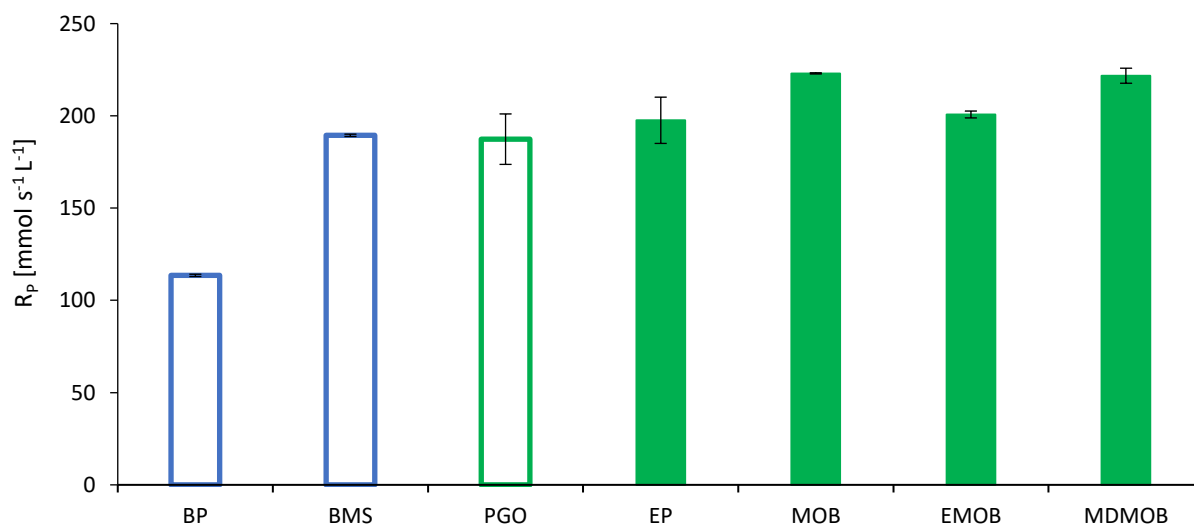
Figure 22. Rate of polymerization of industrial initiators (□) with MDEA, (□) without MDEA and α-ketoesters without coinitiator ■ (green) in HDDA mixtures at 1 W cm^{-2} (320-500 nm). Formulations contain 1 eq. (co)initiator relative to 1 w% EP.

As expected, benzophenone thioether BMS with coinitiator MDEA shows a much higher rate of polymerization (R_P) than benzophenone BP. This is caused by the effect of the thioether that increases the absorption of BMS by two magnitudes compared to benzophenone.

Surprisingly, all tested aliphatic ketoesters can readily compete with the industrial Type II initiators regarding the rate of polymerization even though no coinitiators were used. (Figure 22). This is especially interesting, because analogous phenyl glyoxylates have significantly higher extinction coefficients, still the reactivity of some aliphatic ketoesters is even higher. That is a sign, that the aromatic moiety is responsible for the higher absorption, but not necessary for fast photopolymerization. When no coinitiator is used, the methyl esters MOB and MDMOB are significantly more reactive than the ethyl ester EP and EMOB. This can be explained by intramolecular hydrogen abstraction from the ester alkyl, as the reactivity of primary radicals is higher than that of secondary ones.

Table 4. Photo-DSC results for industrial initiators with MDEA and α-ketoesters without coinitiator in HDDA mixtures at 1 W cm^{-2} (320-500 nm). Formulations contain 1 eq. (co)initiator relative to 1 w% EP.

	R_P [mmol L^{-1} s^{-1}]	t_{max} [s]	t_{95} [s]	DBC [%]
BP_MDEA	114	10.8	77	72
BMS_MDEA	189	6.9	36	60
PGO	187	14.1	63	71
EP	198	8.0	71	67
MOB	223	7.8	45	65
EMOB	201	8.3	70	69
MDMOB	222	8.3	54	67

Taking a closer look at the detailed results in Table 4 reveals that the time to reach maximal rate of polymerization t_{max} is the lowest in case of state of the art Type II initiator BMS (6.9 s). Interestingly, the aliphatic ketoesters also show very low values and reach maximal R_P after around 8 s. This is significantly faster than the aromatic ketoester PGO. To compare how fast a curing reaction is, the time to 95% total conversion (t_{95}) is used. Here it is clearly visible that the reaction initiated by methyl ketoesters MOB and MDMOB is significantly faster than the ethyl esters and the industrial ketoester PGO. The benzophenone derivative BMS is still the fastest but the difference is to the fastest ketoester MOB is less than 10 s. The overall double bond conversion DBC is similar for all compounds (64-67%) only benzophenone BP and phenyl glyoxylate PGO reach about 70%.

After these first very promising results, it was of great interest to use coinitiators to boost the reactivity. As aliphatic tertiary amines like MDEA are known to be highly efficient coinitiators for Type II reactions, it was a logic step to test it with ketoesters. It was problematic that easily enolizeable α-ketoesters such as ethyl pyruvate EP or methyl oxobutanoate MOB and also phenylglyoxylate PGO rapidly decomposed by aldol reactions and lost their ability to initiate. Shortly after mixing, the sample became turbid and a brownish oil precipitated. The higher substituted ketoesters like ethyl methyl oxobutanoate EMOB and methyl dimethyl oxobutanoate MDMOB could be measured as they decomposed much slower.

As can be seen in Figure 23, indeed the coinitiator could further improve the reactivity. This is a clear hint that the polymerization is initiated by a Type II reaction mechanism.
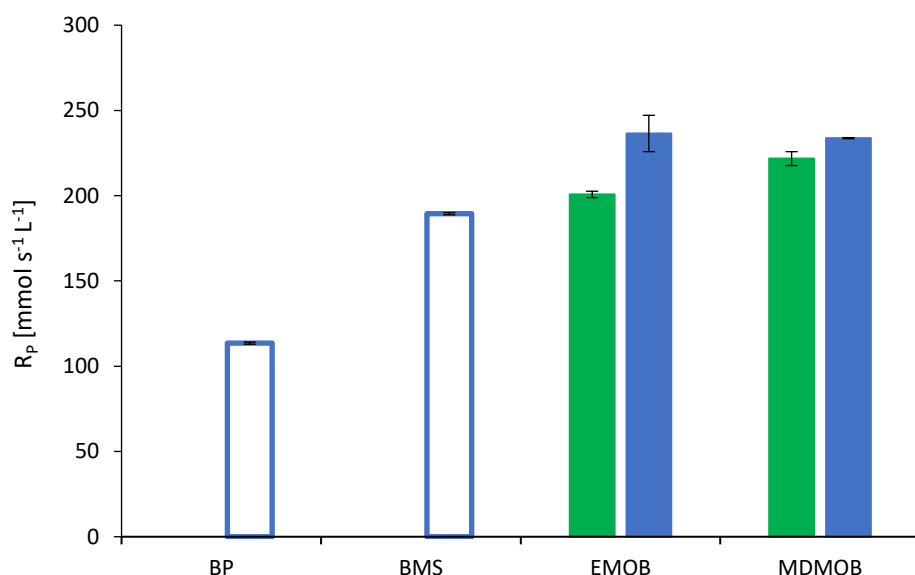
Figure 23. Rate of polymerization of industrial initiators □ (hollow), α-ketoesters without coinitiator ■ (green) and α-ketoesters with MDEA as coinitiator ■ (blue) in HDDA mixtures, at 1 W cm^{-2} (320-500 nm). Formulations contain 1 eq. (co)initiator relative to 1 w% EP.

The detailed results with MDEA as coinitiator are displayed in Table 5. One will notice that not only the R_P is improved but also the t_{max} and t_{95} is much faster with coinitiator, while the DBC remains unchanged. The oxobutanoate EMOB shows a t_{max} even lower than highly reactive reference BMS.

Table 5. Photo-DSC results for industrial initiators and α-ketoesters with MDEA as coinitiator in HDDA mixtures at 1 W cm⁻² (320-500 nm). Formulations contain 1 eq. (co)initiator relative to 1 w% EP.

	R_P [mmol L⁻¹ s⁻¹]	t_{max} [s]	t_{95} [s]	DBC [%]
BP	114	10.8	77	72
BMS	189	6.9	36	60
EMOB	237	6.7	57	68
MDMOB	234	7.7	41	65

initiator

EP

coinitiator

EDB   Gly   Thiol   Iod
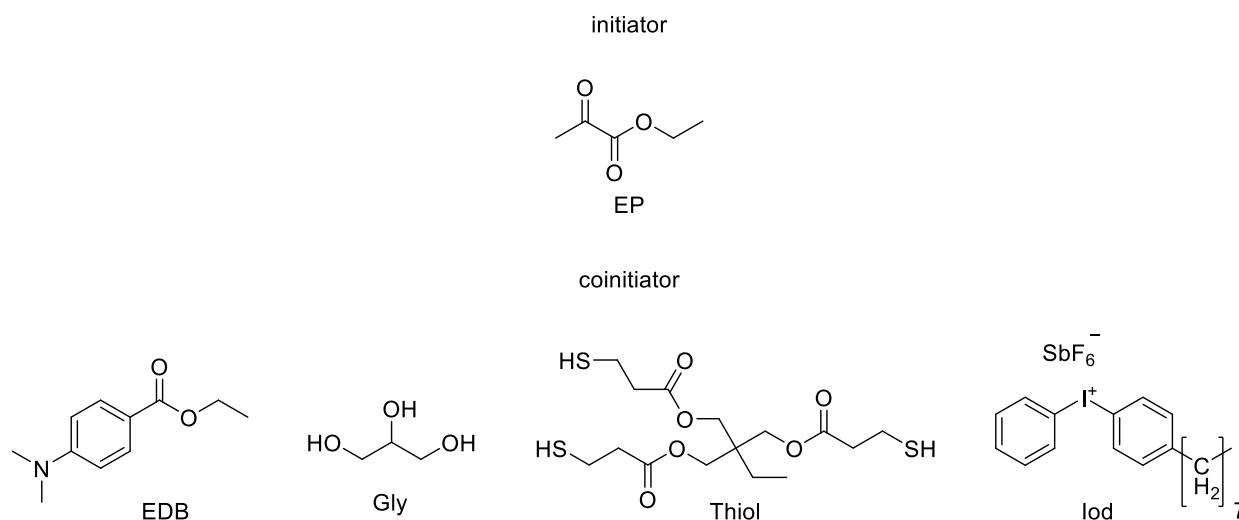
To test other substances as coinitiators a test series with ethyl pyruvate EP was conducted. Therefore, 1 wt% of ethyl pyruvate was used with one equivalent coinitiator. (Figure 25)
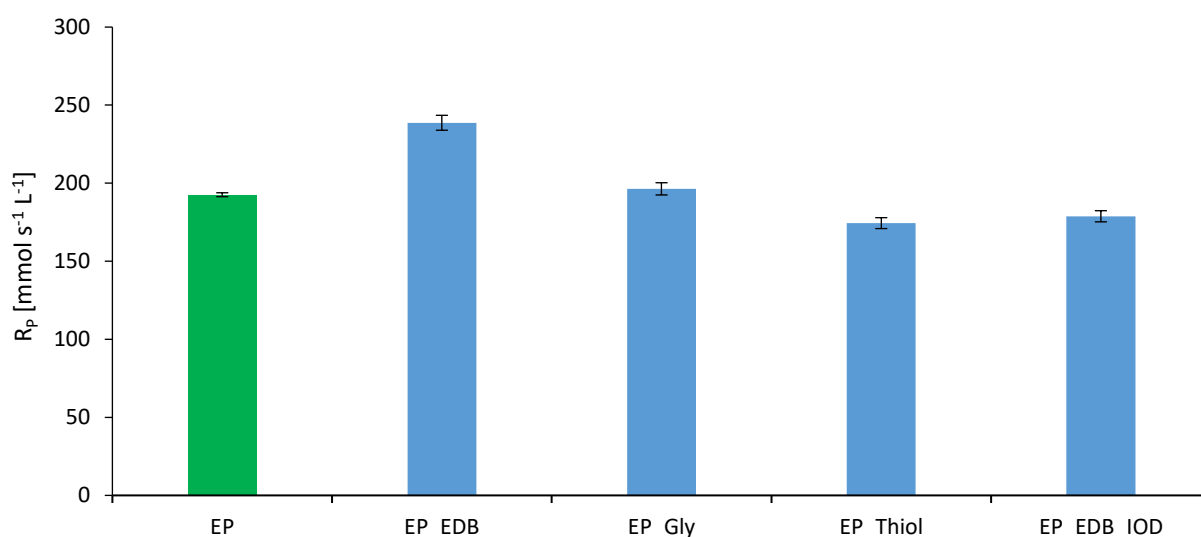
Figure 24. Rate of polymerization of ethyl pyruvate EP without coinitiator ■ (green) and ethyl pyruvate with coinitiators ■ (blue) in HDDA mixtures, at 1 W cm⁻² (320-500 nm). Formulations contain 1 eq. (co)initiator relative to 1 w% EP.

It was found that the ketoesters are stable when ethyl dimethyl amino benzoate (EDB) was used as coinitiator. The aromatic amine is less basic and does not carry alcohol groups that can react. This coinitiator is used with camphor quinone in dental restorative composites. It is not used in coating industry due to the strong yellowing during photoreaction and aging of the coating. Nevertheless, it can give deeper insight how coinitiators influence the curing efficiency of α-ketoesters. In case of ethyl pyruvate the aromatic amine EDB clearly shows a positive effect and increases reactivity. (Table 6)

Table 6. Photo-DSC results of ethyl pyruvate EP with different coinitiators in HDDA mixtures at 1 W cm^{-2} (320-500 nm). Formulations contain 1 eq. coinitiator relative to 1 w% EP.

	R_P [mmol L^{-1} s^{-1}]	t_{max} [s]	t_{95} [s]	DBC [%]
EP	193	8.5	56	66
EP_EDB	239	7.3	39	66
EP_Gly	196	8.1	52	65
EP_Thiol	174	12.6	55	65
EP_EDB_IOD	179	9.9	45	67

Glycerol (Gly) was tested as highly biocompatible coinitiator. The triol contains easy abstractable hydrogens and should act as simple hydrogen donor. There is some positive effect, as the R_P is slightly increased. But the effect is very little and therefore it is not suitable as coinitiator. Also a macro trithiol (Thiol) was tested, as thiols are well known hydrogen donors. In this case, there is no positive effect visible. This can be explained by the high molecular weight thiol that may not be suitable for diffusion controlled hydrogen donation. In addition, the compound interferes with the polymerization and causes retardation in acrylates due to chain transfer reactions.

Aryl iodonium salts can be used with coinitiators and Type II initiators, as the initiator can decompose iodonium salts by electron transfer. Complicated decomposition patterns form several reactive radical species.[119] Therefore, (4-octylphenyl)(phenyl)iodonium hexafluoro antimonate was tested as coinitiator together with EDB. In case of ethyl pyruvate, no increase of reactivity was observed with this iodonium salt.

In Figure 25 the R_P of the initiators without coinitiator is compared with results obtained when the aromatic amine EDB was used as coinitiator. Interestingly the ethyl esters including reference initiator PGO profited from addition of EDB. The methyl esters MOB and MDMOB did not benefit from the aromatic amine. In contrary, the rate of polymerization was even lower. Two possible reasons for that are: First, the aromatic amine absorbs in the same region as the ketoesters. This

could reduce the quantum yield of the initiation, as photons are absorbed by the coinitiator. If this would be the case, all ketoesters should show a reduction of efficiency, which is not the case.
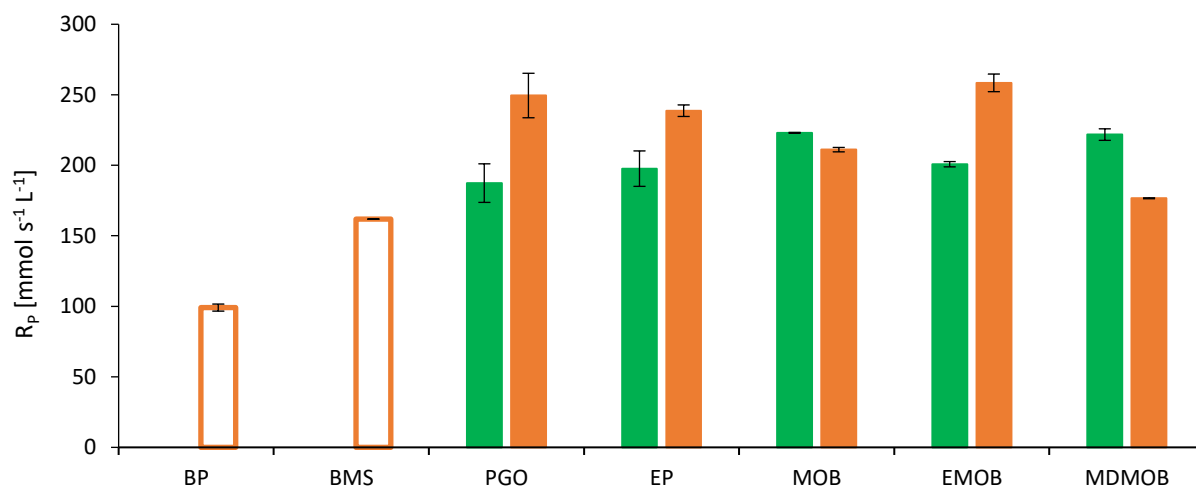
Figure 25. Maximal rate of polymerization of industrial initiators ☐ (hollow) and α-ketoesters with EDB as coinitiator ■ (orange) in HDDA mixtures at 1 W cm^{-2} (320-500 nm). Formulations contain 1 eq. (co)initiator relative to 1 w% EP.

The second, more plausible explanation could be found in the difference of methyl and ethyl radicals. A closer look at the result in Table 7 reveals that also the values of t_{max} and DBC of the methyl esters are also worse with coinitiator. Maybe the formation of methyl radicals by direct hydrogen abstraction is faster and more efficient that the slower process of electron charge transfer reactions with the amine. As the reactivity of methyl ester MDMOB clearly improved by using an aliphatic amine as coinitiator, it could also be that the triplet state of the methyl esters can be quenched to some extent by aromatic amines.

Table 7. Photo-DSC results for industrial initiators and α-ketoesters with EDB as coinitiator in HDDA mixtures at 1 W cm^{-2} (320-500 nm). Formulations contain 1 eq. (co)initiator relative to 1 w% EP.

	R_P [mmol L^{-1} s^{-1}]	t_{max} [s]	t_{95} [s]	DBC [%]
BP	99	10.1	86	63
BMS	162	7.2	44	72
PGO	249	7.1	36	68
EP	239	7.3	39	66
MOB	211	8.5	41	66
EMOB	258	6.8	42	69
MDMOB	177	10.6	43	60

As visible in Table 7, the ethyl ketoesters clearly benefit from adding EDB. The methyl oxobutanoate EMOB reaches the highest R_P of 258 mmol L^{-1} s^{-1}, a higher value than the commercial initiator PGO.

Although the addition of aromatic coinitiator EDB is beneficial for some ketoesters, it is not necessary, as the reactivity is already higher than that of industrial Type II initiators when no coinitiator is used.

5.1.2. Modification of the ester moiety

The modification of the ester moiety by heteroatoms should reveal influence on the initiation by changing absorption properties ort the efficiency of the compounds. As o-methyl ketoesters and ketoamides did not initiate polymerization, only two substances were tested by DSC.

initiators
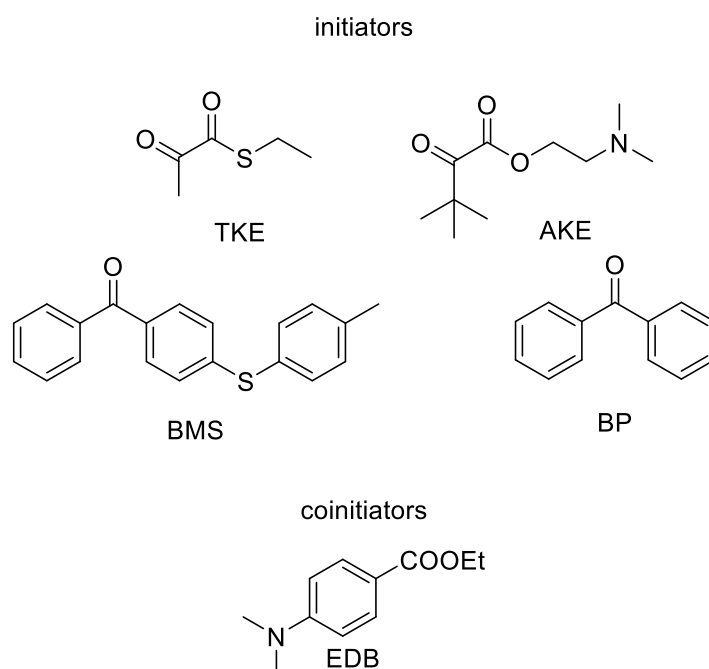
coinitiators

Also these two compounds were not as successful as expected. As clearly visible in Figure 26 the rate of polymerization of the new compound is significantly lower than that of the reference initiators. In case of dimethyl amino ketoester AKE, this is probably caused by the basic self-decomposition of the compound, which was observed after synthesis.

The thioketoester TKE showed higher activity but still was less reactive than the references, adding coinitiator EDB could improve the reactivity slightly but still the performance was disappointing. As previously mentioned in chapter 3, the compound is in the equilibrium between the O-alkyl and S-alkyl thioester. As O-alkyl thiono ketoesters do not initiate, it is possible that

the unreactive isomer is shielding light from the active S-alkyl species. The initiation is likely to be a Norrish Type II reaction as amine coinitiator EDB increases the reactivity.
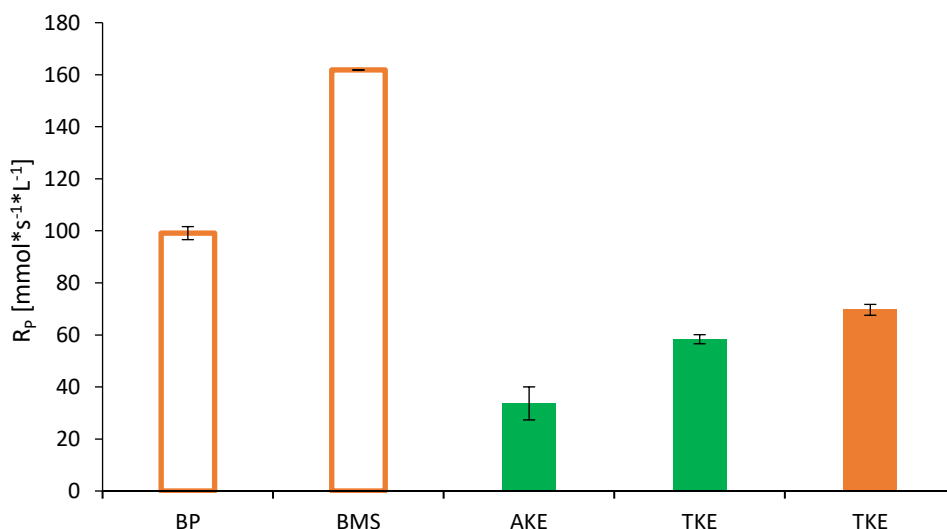
Figure 26. Rate of polymerization of industrial initiators ▢ (hollow) and new compounds with EDB as coinitiator ■ (orange), without coinitiator ■ (green) in HDDA mixtures at 1 W cm^{-2} (320-500 nm). Formulations contain 1 eq. (co)initiator relative to 1 w% EP.

In Table 8 the results are summarized. Here it is visible that the polymerization with the new compounds is slower and reaches lower DBCs compared to the industrial reference initiators.

Table 8. Photo-DSC results for industrial initiators and new compounds with EDB as coinitiator in HDDA mixtures at 1 W cm^{-2} (320-500 nm). Formulations contain 1 eq. (co)initiator relative to 1 w% EP.

	R_P [mmol L^{-1} s^{-1}]	t_{max} [s]	t_{95} [s]	DBC [%]
BP_EDB	99	10.1	86	63
BMS_EDB	162	7.2	44	72
AKE	34	33.6	162	41
TKE	58	26.7	112	52
TKE_EDB	70	23.6	104	51

5.1.3. Modification of the α-carbonyl

Two α-ketoesters were modified analogue to typical industrial Type I photoinitiators. Type I initiators show homolytic cleavage upon irradiation. Therefore, the initiation is much more efficient, leading to higher rates of polymerization. Typical Type I initiators are hydroxy propiophenone like Speedcure 73 (SC73) which is widely used and its bromo precursor SCBr. In a DSC measurement with HDDA as monomer, the substances were compared.
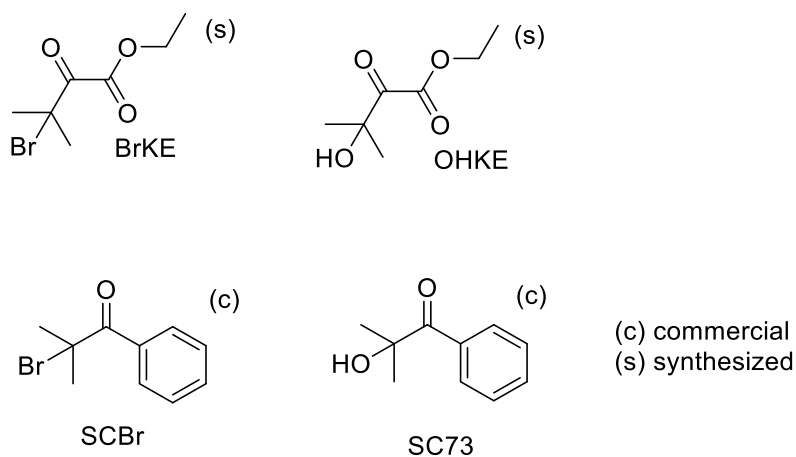
In Figure 27 the rate of polymerization of the tested formulations is shown. The formulation with industrial Type I initiator SC73 shows an unbeatable high rate of polymerization. But interestingly the mixture with bromo ketoester BrKE shows the highest rate of polymerization upon all ketoesters tested without coinitiator. The R_P is significantly higher than that of the bromo propiophenone SCBr.
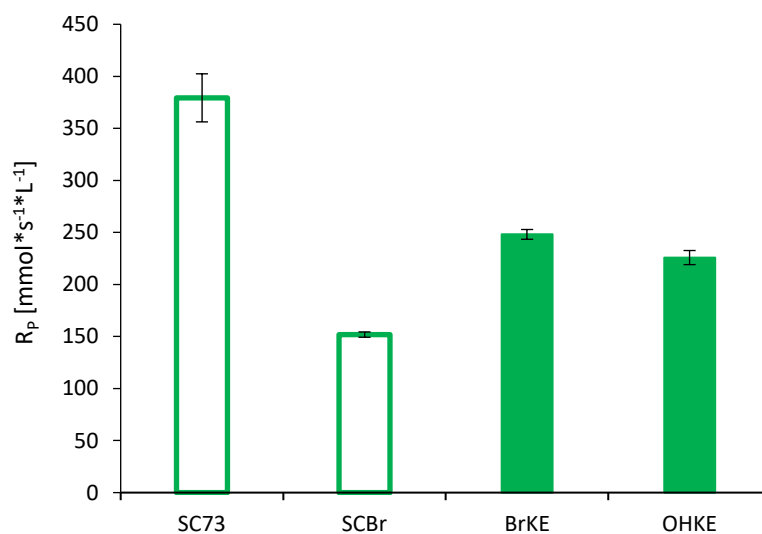
Figure 27. Rate of polymerization of industrial initiators ☐ (hollow) and α-carbonyl modified ketoesters without coinitiator ■ (green) in HDDA mixtures at 1 W cm^{-2} (320-500 nm). Formulations contain 1 eq. initiator relative to 1 w% EP.

The formulation with hydroxy ketoester OHKE shows a lower R_P comparable to the simple ketoesters measured before in 5.1.1. Although the new ketoester compounds are very reactive and show better results than the bromo compound SCBr, it is not clear by reactivity if these compounds are initiating by a Type I mechanism. In case of bromo ketoester BrKE a β-cleavage mechanism could be the reason for a significant higher reactivity than all other tested simple ketoesters.
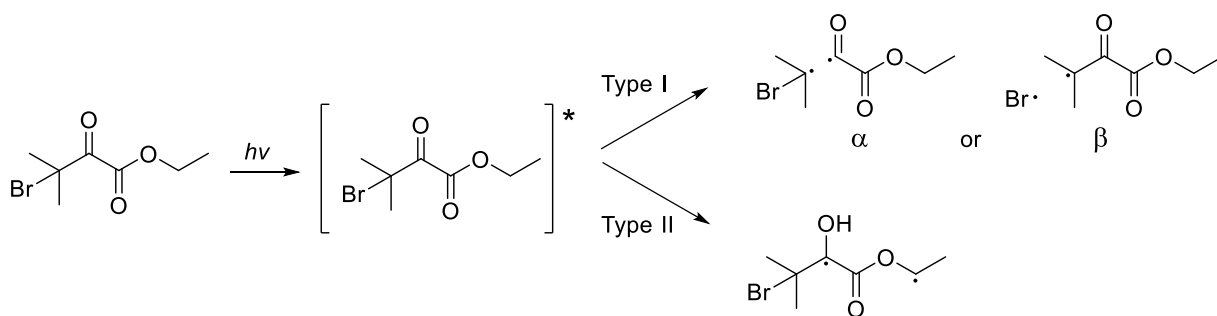
It was tried to add amine coinitiators to see if the reactivity is increased. Unfortunately, the bromo ketoester BrKE was instantly decomposing when amines were added. The hydroxy compound could be measured with amines and the results are visible in Table 9.

Table 9. Photo-DSC results for industrial Type I initiators and new compounds in HDDA mixtures at 1 W cm^{-2} (320-500 nm). Formulations contain 1 eq. (co)initiator relative to 1 w% EP.

|	R_P [mmol L^{-1} s^{-1}]	t_{max} [s]	t_{95} [s]	DBC [%]
SC73	379	3.0	24	67
SCBr	152	7.3	63	60
BrKE	248	5.9	40	64
OHKE	226	6.0	73	66
OHKE_MDEA	128	12.7	81	60
OHKE_EDB	85	19.0	74	61

Surprisingly the addition of amines significantly reduced the reactivity, which could indicate a Type I reaction that is disturbed by adding coinitiator. In Table 9 it is also shown that the ketoesters used without coinitiator, show very short t_{max} and high conversions. Nevertheless, the compounds cannot compete with the state of the art Type I initiator SC73.

5.1.4. Long wavelength UV initiators – broadband tests

It was of great interest to find highly reactive UV initiators that absorb in the long wavelength UV region. Three of the tested substances showed activity in preliminary tests. To compare the reactivity to commercial UV initiators, the substances were first tested with broadband photo-DSC measurements.
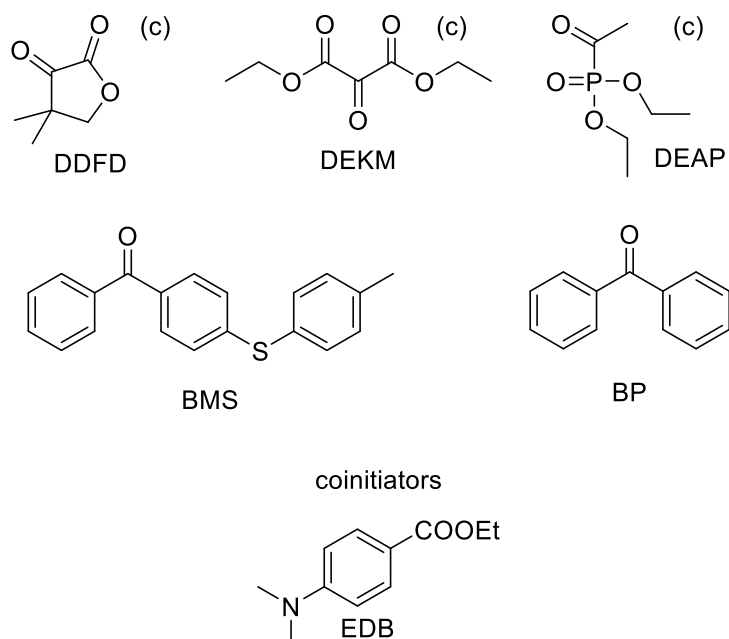
coinitiators

In Figure 28 the rate of polymerization R_P of the formulations is visible. Ethyl pyruvate EP was also tested to compare the reactivity with the phosphorus analogue DEAP. All new compounds were tested without and with EDB as coinitiator.
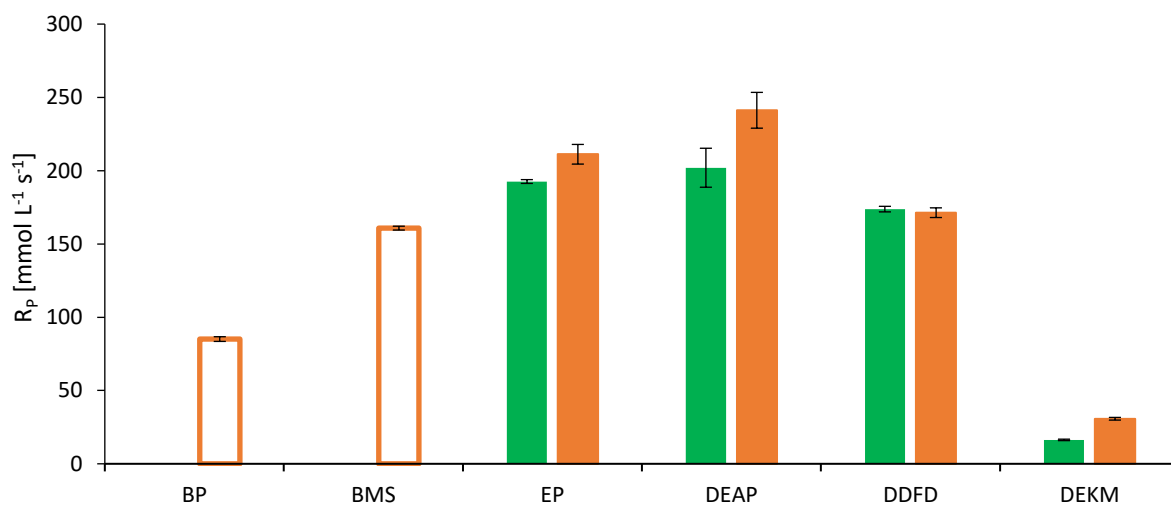
Figure 28. Rate of polymerization of industrial initiators □ (hollow) and α-ketoesters without coinitiator ■ (green) and with EDB as coinitiator ■ (orange) in HDDA mixtures at 1 W cm^{-2} (320-500 nm).

Surprisingly, without coinitiator, diethyl phosphono acetate shows high reactivity, comparable to ethyl pyruvate EP. The compound outperforms the industrial references BP and BMS by a lot. Adding EDB as coinitiator further boosts the R_P by 20% and leads to a significantly higher reactivity than ethyl pyruvate EP.

The ring-structured ketoester DDFD is less reactive than the linear ethyl pyruvate. The reactivity is comparable to benzophenone derivative BMS, which is already a good result. Interestingly just

as with the methyl esters MOB and MDMOB in previous studies, cyclic DDFD does not benefit from adding amine EDB. Probably the polymerization is directly induced by radicals, formed by hydrogen abstraction.

Diethyl ketomalonate DEKM was also tested as initiator, but the results were disappointing. Although coinitiator EDB could double the rate of polymerization, the compound shows less than half the reactivity than benzophenone BP. The low reactivity is probably caused by the high moisture sensitivity of the compound. Under non-inert conditions, ketomalonates readily form monohydrates with a gem-diol structure. Initiation is then impeded, as the carbonyl chromophore is destroyed.[107]

In Table 10 the results are summarized and it is clearly visible that the low rate of polymerization of keto malonate DEKM correlates with the very slow polymerization leading to low DBC.

Table 10. Photo-DSC results for industrial Type I initiators and new compounds in HDDA mixtures at 1 W cm^{-2} (320-500 nm). Formulations contain 1 eq. (co)initiator relative to 1 w% EP.

	R_p [mmol*L^{-1}s^{-1}]	t_{max} [s]	t_{95} [s]	DBC [%]
BP_EDB	85	11.1	69	66
BMS_EDB	161	8.0	44	65
EP	193	8.5	56	66
EP_DMAB	211	7.7	42	63
DEAP	202	8.2	43	61
DEAP_EDB	241	6.7	37	64
DDFD	174	11.6	58	63
DDFD_EDB	171	11.3	54	62
DEKM	16	68.4	117	28
DEKM_EDB	31	37.5	152	38

The mixture containing phosphorus compound DEAP and coinitiator EDB was the most efficient, exhibiting the lowest time to maximal rate of polymerization and the fastest conversion. The DBC is comparable to the industrial references.

5.1.5. Long wavelength UV initiators - 400 nm LED tests

Photoinitiators that are active in and near the visible light spectrum are especially important for energy efficient state of the art LED curing systems. Isopropyl thioxanthone (ITX) with amines as coinitiator is one of the most important industrial Type II initiator systems for visible light polymerization.

ITX   DDFD   EP

coinitiator

MDEA
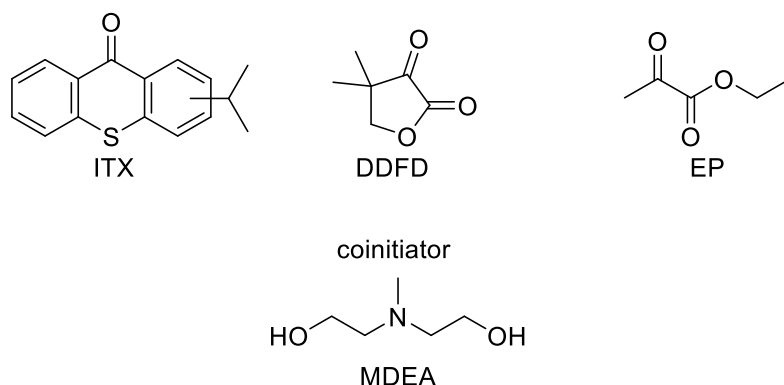
Therefore, it was very interesting to see how ketoesters perform near the visible spectrum. The only active substance found with the right absorption pattern was cyclic ketoester DDFD. As visible in Table 11, the extinction coefficient of ITX is 48 times higher than that of cyclic ketoester DDFD. Ethyl pyruvate EP barely absorbs any light at 400nm. Still, both substances were compared with ITX in a 400 nm LED photo-DSC measurement at 0.38 W cm^{-2}.

Table 11. Extinction coefficient at 400 nm of different initiators.

Initiator	ε_{400} [L Mol^{-1} cm^{-1}]
ITX	677
DDFD	13.6
EP	0.10

The results for the rate of polymerization R_P of the mixtures are shown in Figure 29 and utterly surprising. The formulation containing cyclic ketoester DDFD exhibits a significant higher reactivity than the mixture with ITX and coinitiator MDEA. This is again a good example that the extinction coefficient does not correlate with the efficiency. However, even more unexpected is the mixture with ethyl pyruvate. Although the compound barely absorbs at 400 nm the rate of polymerization is still comparable with benzophenone at broadband irradiation.
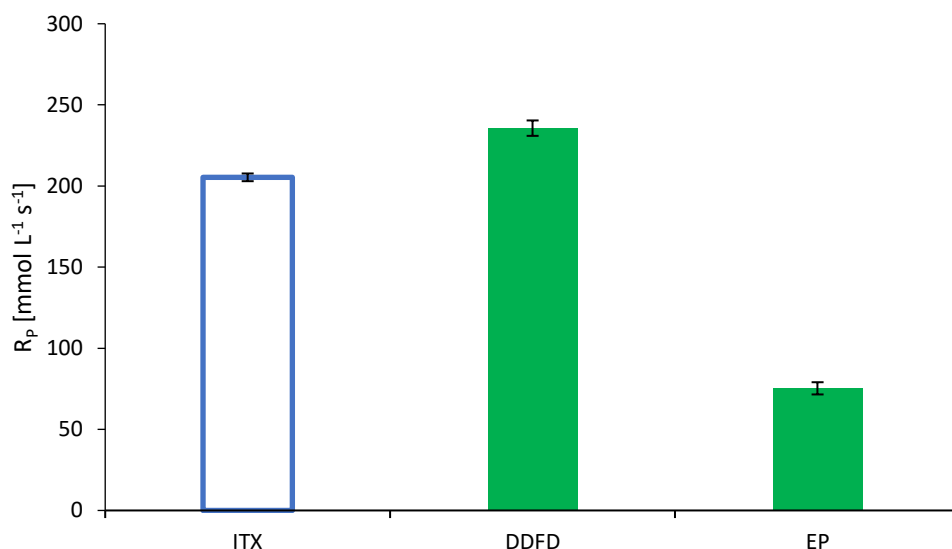
Figure 29. Rate of polymerization of industrial initiator ITX with MDEA as coinitiator ☐ (hollow), α-ketoesters without coinitiator ■ (green) in HDDA mixtures at 0.38 W cm^{-2} (400 nm LED). Formulations contain 1 eq. (co)initiator relative to 1 w% EP.

In Table 12 detailed results of the measurements are shown. The mixture with ITX and coinitiator MDEA reaches t_{max} one second earlier than cyclic DDFD, but the polymerization with DDFD is almost twice as fast with a t_{95} of only 38 s. In the end, the DBC reached with the one compound system DDFD is 6% higher than that of ITX with 64%.

Table 12. Photo-DSC results for industrial Type II initiator ITX and new compounds EP and DDFD in HDDA mixtures at 0.38 W cm^{-2} (400 nm, LED). Formulations contain 1 eq. (co)initiator relative to 1 w% EP.

	Rp [mmol*L^{-1}s^{-1}]	t_{max} [s]	t_{95} [s]	DBC [%]
ITX	109	8.1	62	58
DDFD	245	9.1	38	64
EP	75	21.0	73	49

Ethyl pyruvate EP is much slower and only reaches a DBC of 49%. Still the fact that a descent polymerization is initiated by ethyl pyruvate at 400 nm shows how potent ketoesters are as one component initiation systems.

5.1.6.   Measurements at the same absorbance

It was tried to compare selected initiators not only by equimolar mixtures but also by extinction at a certain wavelength. For the measurements the extinction coefficient at 365 nm was measured and afterwards the amount of initiators was chosen to fit 1 wt% of benzophenone BP.
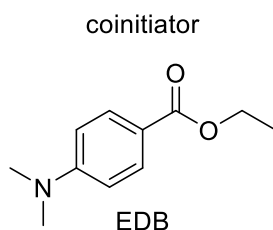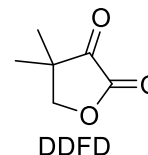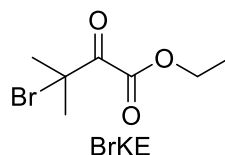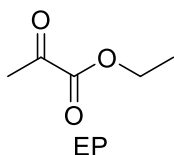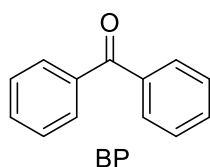
Benzophenone was chosen as benchmark, as the compound with the highest extinction coefficient. (Table 13)

Table 13. Extinction at 365 nm and factor F relating to benzophenone

Initiator	ε_{365} [L·mol^{-1}·cm^{-1}]	Factor F [ ]	initiator [wt%]	coinitiator [wt%]
BP	59.9	1.00	1.0	1.1
EP	7.1	0.12	4.4	9.0
BrKE	22.8	0.38	3.2	x
DDFD	25.3	0.42	1.7	2.5

By dividing the molar amount of 1 wt% benzophenone by factor F, the equiabsorbant amount of initiator is calculated. Benzophenone was measured with aromatic amine EDB as coinitiator, so also ketoesters could be measured with coinitiator. Bromo compound BrKE was not measured with coinitiator, because it decomposes even under mild basic conditions, as previously mentioned. The results for the rate of polymerization R_P are shown in Figure 30. Benzophenone in a concentration of 1 wt% shows a rather low rate of polymerization. Due to the low absorption of ethyl pyruvate EP 4.4 wt% were used.
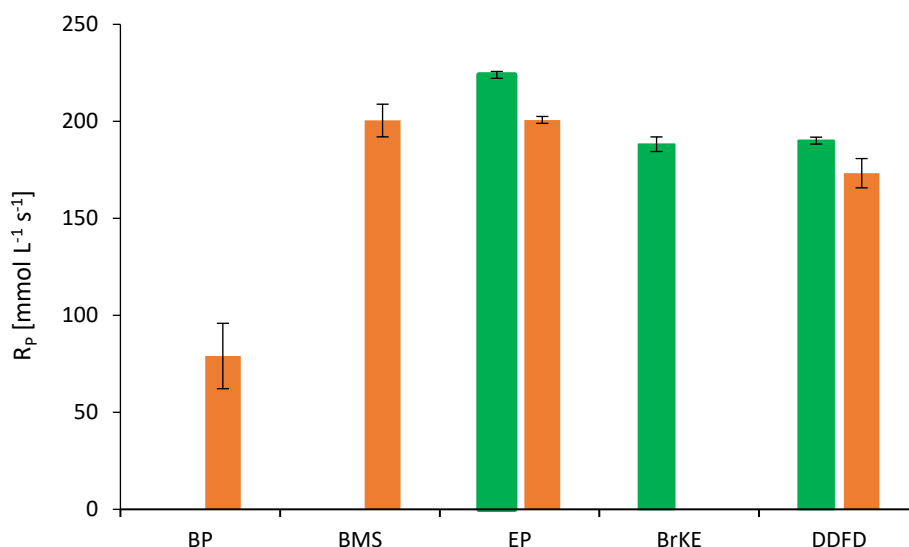
Figure 30. Rate of polymerization of industrial initiators □ (hollow) and α-ketoesters without coinitiator ■ (green) and with coinitiator EDB ■ (orange) in HDDA mixtures at 1 W cm^{-2} (365 nm). Formulations contain equi-absorbant amounts of initiator relative to 1 w% benzophenone BP. Coinitiators were used equimolar to the amount of initiator.

The high amount of initiator significantly increases the R_P of the formulation in comparison to 1 wt% measured in previous series. Nevertheless, the gain of reactivity is not correlating with the amount of initiator added, which indicated that the absorption with 1 wt% EP is almost saturated and cannot be improved much further. Adding coinitiator EDB is even negative in this case. Due to the high molecular weight of the aromatic amine in comparison to ethyl pyruvate, 9 wt% EDB had to be added for an equimolar mixture. This is a problem as the amine EDB exhibits a strong absorption in the same region as the initiator EP. The lower reactivity of the mixture with EDB is for sure caused by a light shielding effect through the coinitiator.

Although, the mixture with bromo ketoester BrKE is far more reactive than benzophenone, the high concentration is surprisingly less efficient than the lower concentrated previous mixture.

Cyclic ketoester DDFD shows significantly higher reactivity than in the broadband measurements when used at the same absorbance of 1 wt% benzophenone, also in this case a coinitiator is not beneficial.

In the details in Table 14 it gets clear that ethyl pyruvate EP is the most efficient initiator when used in amount equiabsorbant to benzophenone BP. The ethyl pyruvate mixture EP not only shows the highest rate of polymerization, it also exhibits the fastest time to maximal rate of polymerization and reaches the highest DBC with 64%.

Table 14. Photo-DSC results for industrial Type I initiators and new compounds in HDDA mixtures at 1 W cm^{-2} (365 nm). Formulations contain equiabsorbant amounts of (co)initiator relative to 1 w% benzophenone BP.

	Rp [mmol L^{-1} s^{-1}]	t$_{max}$ [s]	t$_{95}$ [s]	DBC [%]
BP_EDB	79	14.2	67	55
BMS_EDB	200	7.1	36	61
EP	224	5.6	43	64
EP_EDB	201	6.9	39	60
BrKE	188	6.4	41	59
DDFD	190	7.7	45	60
DDFD_EDB	173	8.0	45	56

Mixtures with cyclic ketoester DDFD without coinitiator are again slower than the linear aliphatic ketoesters but compared to industrial benzophenone very good results were achived.

5.2. Methacrylates

Methacrylates are the second most important class of monomers used for radical photopolymerization. The methyl moiety at the double bond increases the sterical hindrance, causing a lower reactivity than acrylates. Due to the better biocompatibility of methacrylic groups compared to acrylates, methacrylates are often used in medical applications such as bone adhesives or dental composites.

First hexanediol dimethacrylate (HDDMA) was considered as suitable monomer for the following DSC studies. Unfortunately, the physical properties of HDDMA were unsuitable for measuring DSC. The formulations with the monomer tended to creep along the aluminum pans and reached the sealing glass plates, causing a "fisheye" as the formulation was stuck between glass and the edge of the pan. (Figure 31)
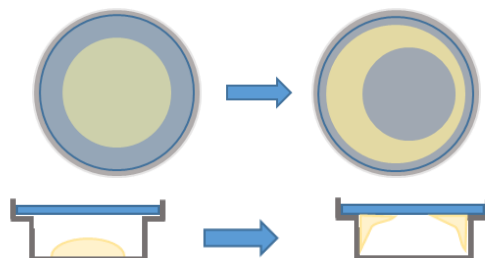
Figure 31. Creeping of formulations with HDDMA (yellow) to the glass lid of the DSC pans.

This effect took about 2 h to happen, considering that one measurement took 30 minutes means that after four samples all other samples in the auto sampler were immeasurable.

To prevent the formulations from creeping, it was tried to hydrophobize DSC pans with C_8-trichlorosilane. (Figure 32) Therefore, the pans were stirred for 4 h in a 1 wt% trichloro octyl silane toluene solution. After rinsing with toluene and drying, the pans were hydrophobic and water droplet would pearl off the pans.
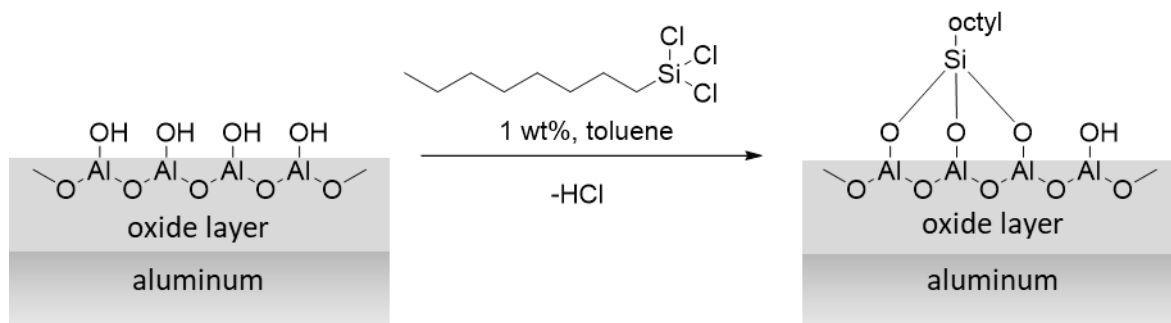
Figure 32. Hydrophobization of aluminum with trichloro octyl silane

The hydrophobization was successful, but as DSC pans are not perfectly planar, the formulations tended to form a droplet at the side of the pan. As the thermo sensor of the DSC device is located at the middle of the pans, this was also no solution to the problem. (Figure 33)
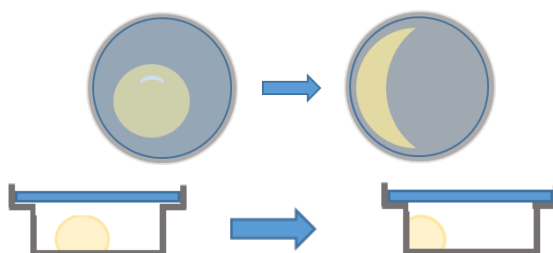
Figure 33. Creeping of formulations with HDDMA (yellow) to the edge of the hydrophobized DSC pans.

As the problem of creeping monomer could not be solved to full satisfaction, a different methacrylic monomer system had to be used for the formulations.

A more viscos equimolar mixture of dental methacrylates UDMA and D3MA was prepared and is further known as DMM. Formulations of DMM were perfectly measureable and did not creep even after 12 hours. As they are used for dental composites and 3D printing, the new photoinitiators can be tested close to the field of application in DMM.

methacrylate system:
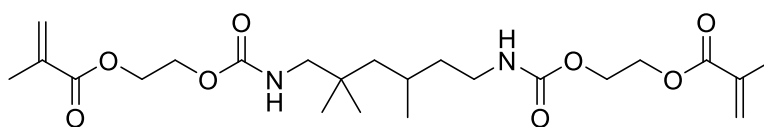
UDMA
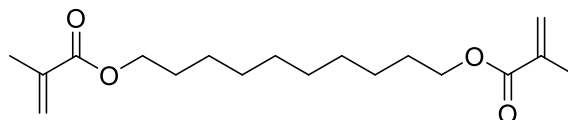
D$_3$MA

1:1 = DMM

5.2.1. Simple aliphatic α-ketoesters

To compare the aliphatic α-ketoesters with known industrial initiators, the same three reference compounds were chosen as for the acrylate study. Benzophenones BP and BMS are classical Norrish Type II initiators, therefore these initiators required coinitiators. The phenylglyoxylate PGO is a known Type II initiator that is the aromatic analogue to aliphatic ketoesters. It was tested both, with and without coinitiator like all other ketoesters.[62, 116]

initiators
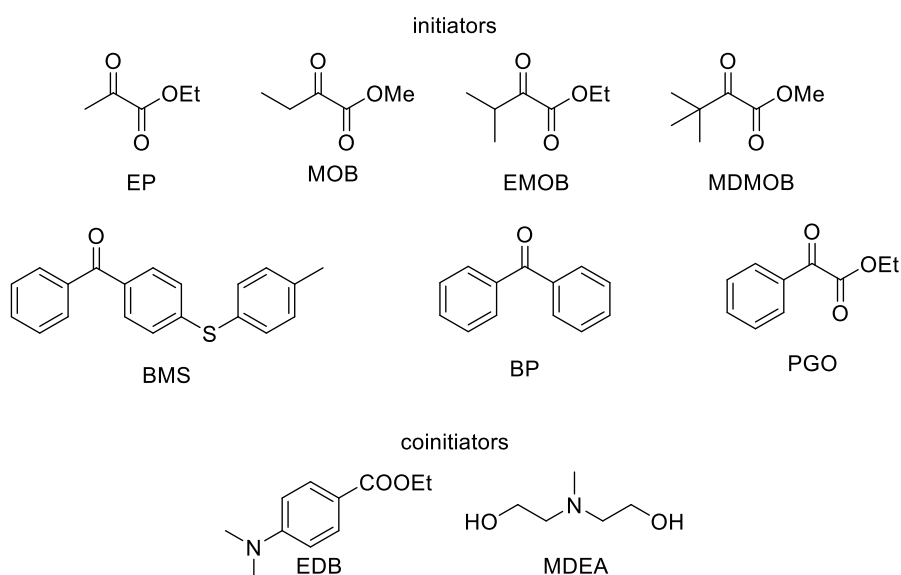
coinitiators

First, the ketoester compounds were tested without coinitiator. Benzophenone BP and benzophenone thioether BMS were tested with the industrial standard coinitiator methyl diethanol amine (MDEA).
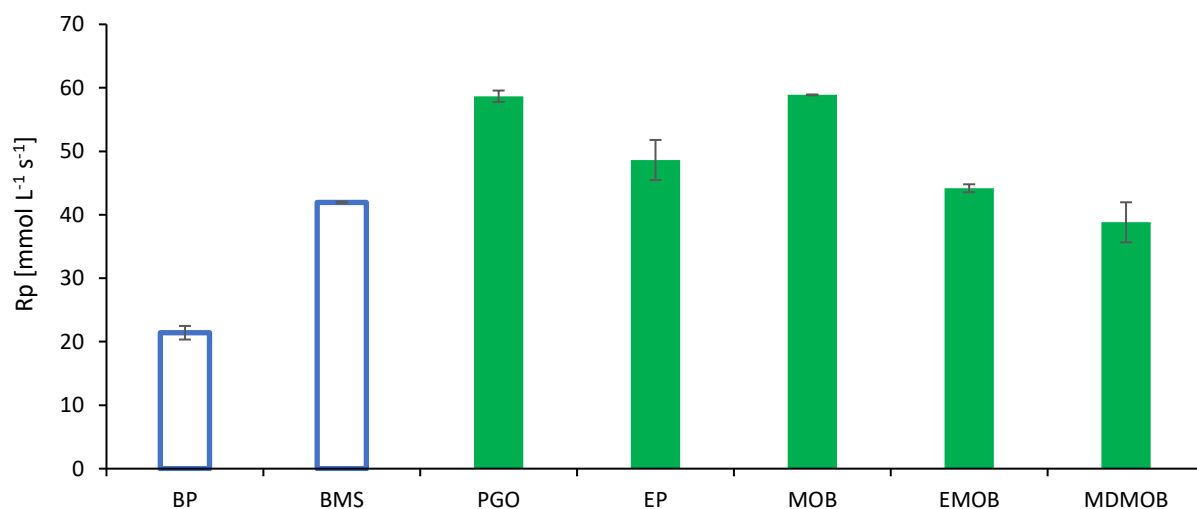
Figure 34. Rate of polymerization of industrial initiators (□) with MDEA, (□) without MDEA and α-ketoesters without coinitiator ■ (green) in methacrylic DMM mixtures at 1 W cm⁻² (320-500 nm). Formulations contain 1 eq. (co)initiator relative to 1 w% EP.

Methacrylates generally exhibit a lower rates of polymerization than acrylates, which is clearly visible in Figure 34. All formulations with α-keto esters including industrial initiator PGO perform better than the benzophenones BP and BMS. Also in methacrylate DMM the new ketoesters show impressive performance. However, due to the higher steric demands of methacrylates, the ketoesters with the highest amount of methyl groups in the β-position, EMOB and MDMOB, are less reactive. Only methyl oxobutanoate MOB is as reactive as the most reactive industrial reference PGO.

Table 15. Photo-DSC results for industrial initiators with MDEA and α-ketoesters without coinitiator in methacrylate DMM mixtures at 1 W cm⁻² (320-500 nm). Formulations contain 1 eq. (co)initiator relative to 1 w% EP.

	R_P [mmol L⁻¹ s⁻¹]	t_{max} [s]	t_{95} [s]	DBC [%]
BP_MDEA	21.4	21.8	140	49
BMS_MDEA	41.9	13.2	94	51
PGO	58.7	14.9	117	67
EP	48.6	18.8	139	57
MOB	58.9	15.5	106	57
EMOB	44.2	17.3	121	54
MDMOB	38.8	20.0	102	52

In following Table 15 the detailed results of the measurements are shown. Although, phenylglyoxylate PGO and methyl oxobutanoate MOB show the highest rate of polymerization, the benzophenone derivative BMS shows the fastest polymerization overall. The time to maximal

R_P (t_{max}) and the time to reach 95% of total conversion is significantly shorter than that of the other initiators. However, mixtures with benzophenone BP and benzophenone thioether BMS reach the lowest double bond conversion (DBC) among the compounds with around 50%. The ketoesters reach 52 – 57% DBC, while phenyl glyoxylate PGO reaches impressing 67%.

Hence, it was exciting if the performance of ketoesters can be enhanced when aromatic amine EDB is used as coinitiator.

On the first sight, it is evident in Figure 35 that the reactivity of the formulations can be improved a lot. Reference phenyl glyoxylate PGO shows the highest polymerization rate. Nevertheless, the ethyl ketoesters EP and EMOB benefit the most from coinitiator. The reactivity of mixtures with ketoester EMOB is almost doubled by the coinitiator. Interestingly the methyl esters show less improve of R_P when a coinitiator is added, which was also observed in acrylates.
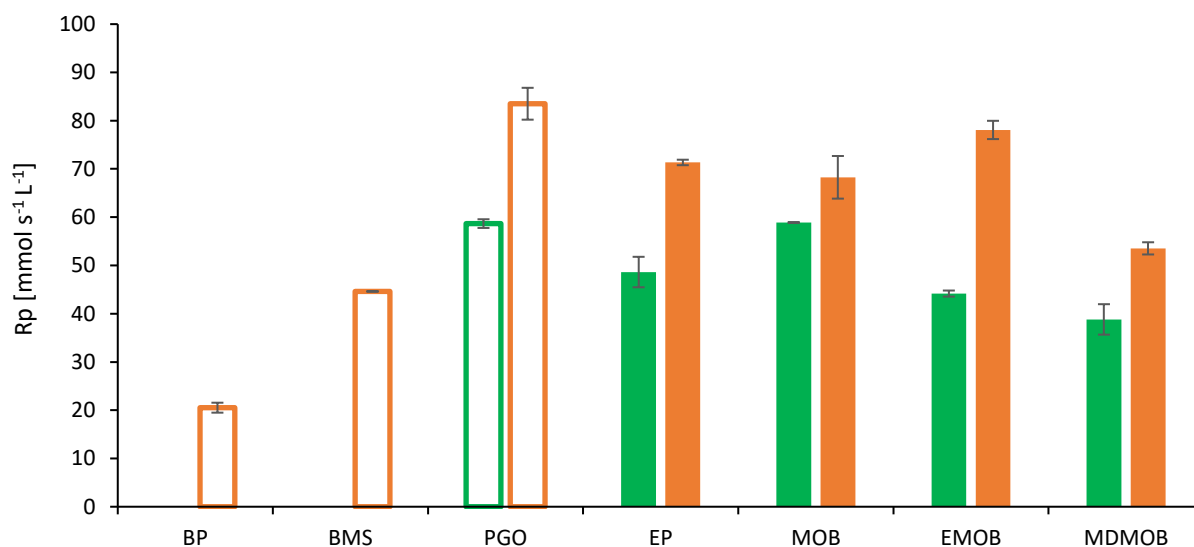
Figure 35. Rate of polymerization of industrial initiators ▢ (hollow) and α-ketoesters with EDB as coinitiator ■ (orange) in DMM mixtures at 1 W cm^{-2} (320-500 nm). Formulations contain 1 eq. (co)initiator relative to 1 w% EP.

In Table 16 it becomes clear that industrial initiator BMS still reaches t_{max} the fastest but all ketoester improved a lot. Ethyl ketoester EMOB reaches the maximal R_P even faster than highly reactive phenyl glyoxylate PGO. The most sterical hindered ketoester MDMOB again shows the lowest reactivity among the ketoesters, resulting in longer tmax and t95 and a DBC of only 51%. All other mixtures with novel compounds show faster time to 95% total conversion than the industrial references and reach 57% DBC, which is more than that of the benzophenone compounds BP and BMS. Again, glyoxylate PGO reaches the highest DBC with 66%.

Table 16. Photo-DSC results for industrial initiators and α-ketoesters with EDB as coinitiator in DMM mixtures at 1 W cm^{-2} (320-500 nm). Formulations contain 1 eq. (co)initiator relative to 1 w% EP.

	R_P [mmol L^{-1} s^{-1}]	t_{max} [s]	t_{95} [s]	DBC [%]
BP	20.5	18.5	147	50
BMS	44.6	10.8	96	54
PGO	83.5	11.2	93	66
EP	71.3	11.9	83	57
MOB	68.3	12.2	86	57
EMOB	78.1	11.0	59	57
MDMOB	53.5	14.9	70	51

The reason for the lower response of methyl esters to the coinitiator could be the fast formation of methyl radicals, which are very reactive. This could lead to fast monomolecular initiation, therefore a coinitiator which reaction is diffusion controlled cannot improve this reaction. This would explain the higher reactivity of methyl oxobutanoate MOB in comparison to ethyl pyruvate EP. Ethyl ketoester EMOB is more sterically hindered as it carries two methyl groups in beta position. With coinitiator similar R_P values for all three compounds are reached. Methyl ketoester MDMOB is the most sterically hindered compound and therefore generally less reactive towards bulky methacrylates.

This theory is supported by the fact, that if smaller aliphatic amine MDEA is used, the rate of polymerization can be further improved in case of base-stable compounds EMOB and MDMOB. This can be explained by faster diffusion of MDEA compared to bulky aromatic EDB. Again, the more hindered methyl ester MDMOB shows lower reactivity than the less bulky ketoester EMOB, but this time the reactivity is almost doubled. The ethyl ester EMOB shows twice the R_P in methacrylate DMM when MDEA is added and reaches the same value as industrial phenyl glyoxylate PGO with EDB as coinitiator. (Figure 36)
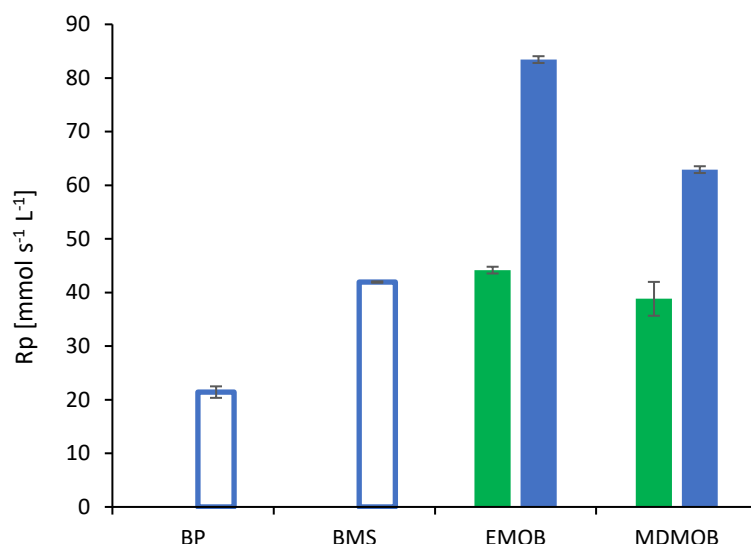
Figure 36. Rate of polymerization of industrial initiators □ (hollow), α-ketoesters without coinitiator ■ (green) and α-ketoesters with MDEA as coinitiator ■ (blue) in DMM mixtures, at 1 W cm^{-2} (320-500 nm). Formulations contain 1 eq. (co)initiator relative to 1 w% EP.

The detailed results in Table 17 are quite impressive. The mixture with ethyl ketoester EMOB and coinitiator MDEA exhibits outstanding reactivity. With more than the double R$_P$ than reference BMS, the mixture reaches maximal rate of polymerization (t$_{max}$) faster than any other compound. In addition, the conversion (DBC) of 63% is much better than that of industrial state of the art initiator BMS. Also, the performance of bulky ketoester MDMOB is significantly higher than when no coinitiator or aromatic amine EDB is used as additive.

Table 17. Photo-DSC results for industrial initiators and α-ketoesters with MDEA as coinitiator in DMM mixtures at 1 W cm-2 (320-500 nm). Formulations contain 1 eq. (co)initiator relative to 1 w% EP.

	R$_P$ [mmol L^{-1} s^{-1}]	t$_{max}$ [s]	t$_{95}$ [s]	DBC [%]
BP	21.4	21.8	140	49
BMS	41.9	13.2	94	51
EMOB	83.4	10.4	99	63
MDMOB	62.9	13.2	93	56

Overall, the new α-ketoester initiators also show very good performance in the methacrylic system. They can easily compete with the standard industrial benzophenones, even the reactivity of special phenyl glyoxylate initiator PGO can be reached with some formulations.

5.2.2. Sensitation of initiation

Although the quantum yield of decomposition for alkyl pyruvates is relatively low (ϕ= 0.15 ± 0.02),[53] the initiation efficiency is surprisingly good. 1961 Hammond et. al. described the sensitation of the photo decomposition of ethyl pyruvate by benzophenone. The quantum yield could be increased from 0.17 to 0.32 when benzophenone was added. In addition, it was described that benzophenone did not decompose when ethyl pyruvate was present, which indicates direct energy transfer.[52] It was of great interest to see if the efficiency of α-ketoesters can be improved by sensitizing. It was decided to test sensitation of pyruvates in methacrylate systems, as it was expected, that the effect of a sensitizer can be easier seen in a less reactive monomer.

| benzophenone | 2-isopropyl thioxanthone | quinine | triphenyl methane |
| BP | ITX | Chin | TPM |
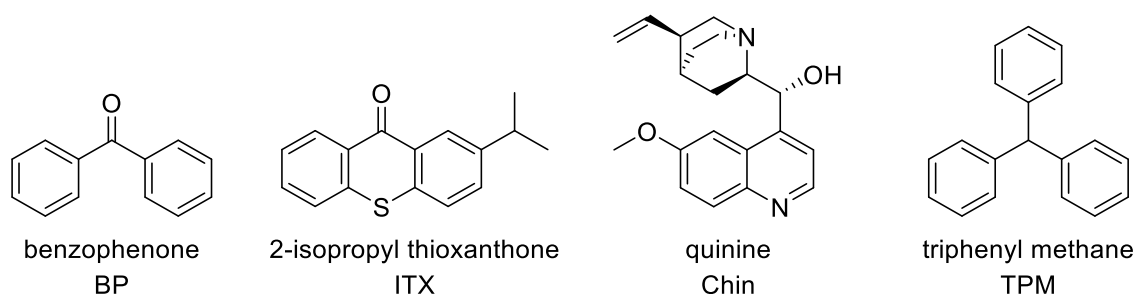
The triplet energy E_T of ethyl pyruvate is 272 kJ mol^{-1} that of benzophenone BP is 284.5 kJ mol^{-1}.[120] Therefore, the energy transfer is possible. Due to the high triplet energy of pyruvates, it was hard to find suitable substances for sensitizing these. Classic photo sensitizers like thioxanthones (ITX) only have an E_T of 256 kJ mol^{-1} and should not sensitize ethyl pyruvates, but were still tested.[121] Quinine (Chin) is a known biocompatible compound with a strong absorption in the same region as pyruvates.[122] There is no triplet energy found in literature so the compound was also tested as sensitizer.

Triphenyl methane TPM exhibits a very high triplet energy of 339 kJ mol^{-1} and is known to sensitize photoreactions.[123] Therefore, it should be able to sensitize pyruvates and was tested as well.
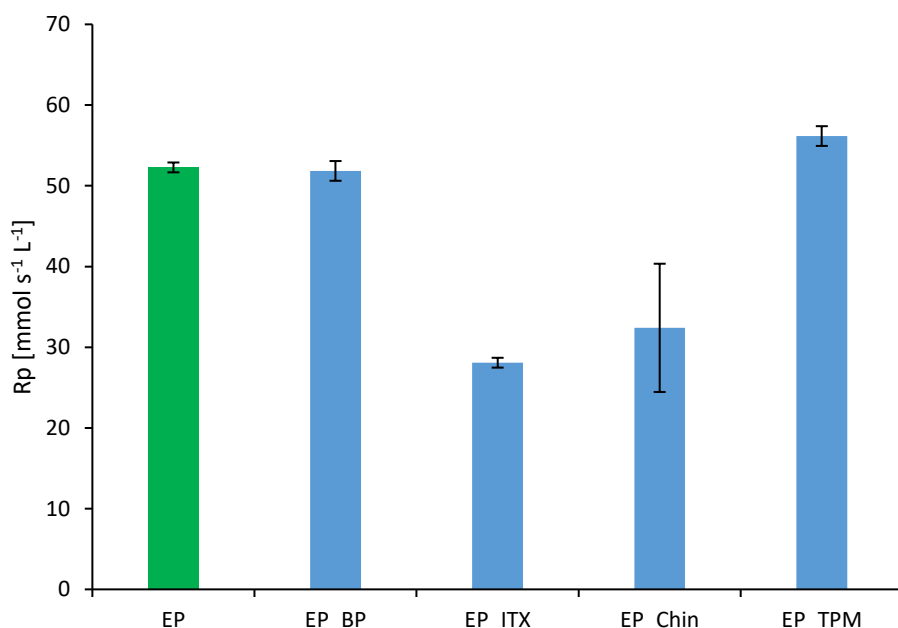
Figure 37. Rate of polymerization of ethyl pyruvate EP without additive ■ (green) and ethyl pyruvate with additive ■ (blue) in DMM mixtures, at 1 W cm^{-2} (320-500 nm). Formulations contain 1 eq. additive relative to 1 w% EP.

Although the photodecomposition of ethyl pyruvate EP sensitized by benzophenone in benzene solution is described in literature, there is no sign of higher reactivity in Figure 37. The addition of benzophenone caused no significant difference in the speed of polymerization or DBC, which can be seen in Table 18.

It is plausible, that the high absorption of benzophenone is shielding light from the initiator EP. As benzophenone itself is a weak initiator without coinitiators it does not contribute to the polymerization. In addition, the relatively polar urethane methacrylate in DMM could directly quench excited benzophenone by hydrogen transfer. It seems the results from experiments in low viscous, apolar and almost inert benzene cannot be directly applied in bulk polymerization of resins.

The addition of thioxanthones is definitely reducing the reactivity of the formulation. The lower E_T and high absorption of thioxanthone ITX, together with the lack of coinitiator, that is necessary for ITX to initiate lead to decreased efficiency of the mixture. This confirms that the energy transfer from ITX to pyruvate EP is not possible in this combination.

Also the nontoxic quinine shows poor results as sensitizer. Probably the triplet energy is too low for sensitizing pyruvates. In addition, quinine is known for its strong fluorescence, which prevents the molecule from entering the triplet state via inter system crossing.

Table 18. Photo-DSC results for 1 wt% ethyl pyruvate without coinitiator in DMM mixtures at 1 W cm⁻² (320-500 nm). Formulations contain 1 eq. sensitizer relative to 1 w% EP.

	R_P [mmol L⁻¹ s⁻¹]	t_{max} [s]	t_{95} [s]	DBC [%]
EP	52	17.0	118	57
EP_BP	52	17.8	101	56
EP_ITX	28	25.3	124	48
EP_Qui	32	18.9	142	50
EP_TPM	56	16.2	108	58

The only tested compound that had a slight positive effect was triphenyl methane TPM. The compound increased the rate of polymerization by ~8%. The effect is not strong but visible. Considering that benzophenone did not have a positive influence, this is a sign that TMP could be more potent under the right conditions. The low concentration of initiator and sensitizer as well as viscosity and polarity of the used monomer system probably limits the achievable effect. The mixtures were also tested with coinitiator EDB present but no beneficial effect by any potential sensitizer could be observed.

Considering that, the novel α-ketoesters, should replace potentially toxic aromatic photoinitiators, it is anyway questionable to use aromatic compounds as benzophenones or other multiple aromatic compounds as sensitizers.

5.2.3. Modification of the α-carbonyl

The β-bromo and β-hydroxy ketoesters were tested in less reactive methacrylates as well. Again, they were compared to commercial Type I initiators. Hydroxy compound OHKE was also tested with the amine coinitiator EDB to see if the reactivity can be improved.
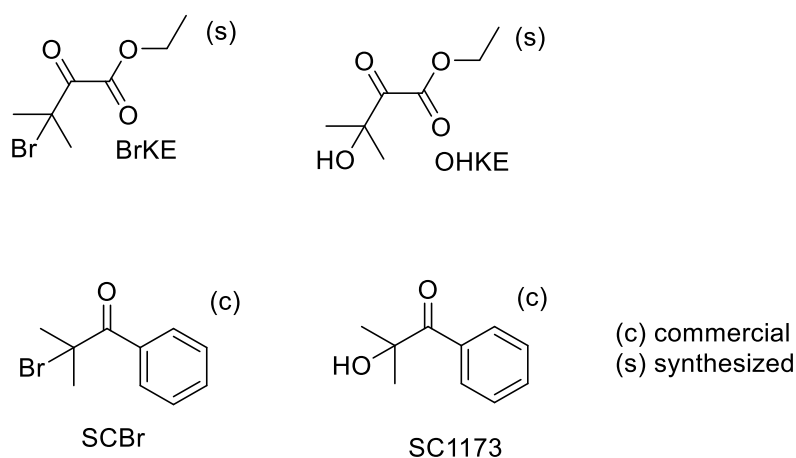
The results for the rate of polymerization R_P of these mixtures is shown in Figure 38. State of the art UV Type I initiator SC73 is similar to the acrylate mixtures the most reactive. The formulation

containing commercial bromo derivative SCBr shows a much lower reactivity and cannot compete with new bromo ketoester BrKE. Compared to the simple ketoesters tested before, the compound shows exceptional high reactivity. Only the mixture of ketoester EMOB with MDEA as coinitiator (5.2.1) could produce a similar rate of polymerization. Considering that in case of bromo ketoester BrKE no coinitiator is used, the exceptional high reactivity compared to other ketoesters makes it plausible that a Type I reaction takes place.
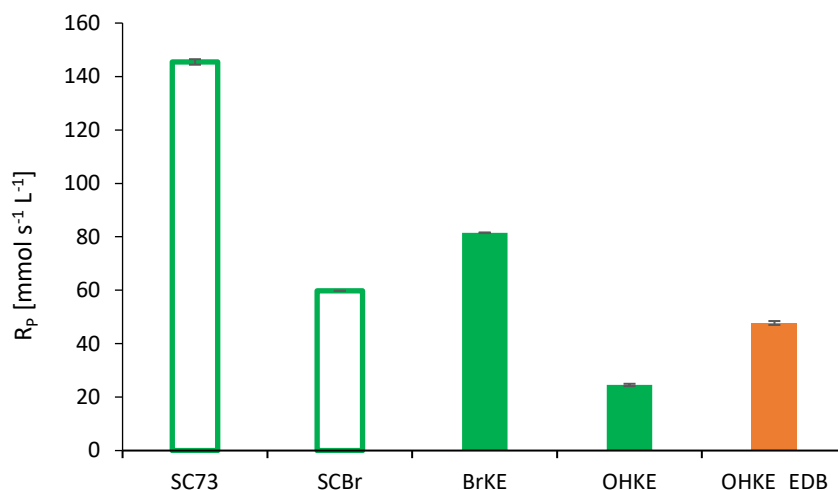
Figure 38. Rate of polymerization of industrial initiators □ (hollow) and α-carbonyl modified ketoesters without coinitiator ■ (green), with EDB ■ (orange) in DMM mixtures at 1 W cm^{-2} (320-500 nm). Formulations contain 1 eq. initiator relative to 1 w% EP.

The hydroxy ketoester OHKE performed significantly worse than the bromo derivative. By adding aromatic amine EDB as coinitiator, the reactivity could be doubled.

Table 19. Photo-DSC results for industrial initiators and α-ketoesters in DMM mixtures at 1 W cm^{-2} (320-500 nm). Formulations contain 1 eq. (co)initiator relative to 1 w% EP.

	R_P [mmol L^{-1} s^{-1}]	t_{max} [s]	t_{95} [s]	DBC [%]
SC73	145	5.64	49	64
SCBr	60	12.2	129	51
BrKE	82	10.2	107	57
OHKE	25	31.6	128	39
OHKE_EDB	48	20.2	141	51

In acrylic systems, only a small difference in reactivity was observed between the bromo and the hydroxy compound and adding coinitiator did not improve the performance. It seems that the hydroxy ketoester OHKE reacts mainly by a Type II mechanism in more polar and less reactive methacrylates. That explains the lower reactivity and good response to the coinitiator.

Also in the detailed results shown in Table 19 it is clear that Type I initiator SC73 shows the highest reactivity by far. Still bromo ketoester BrKE reaches t_{max} faster than the industrial bromo reference SCBr. Also the significant higher conversion of 57% is reached faster than with the aromatic analogue compound. The hydroxy ketoester OHKE shows the slowest polymerization and cannot exceed a conversion of 51% even with coinitiator.

5.2.4. Long wavelength UV initiators – broadband tests

The new compound absorbing in the higher UV-range were also tested with broadband light in methacrylates and compared to commercial Type II initiators.
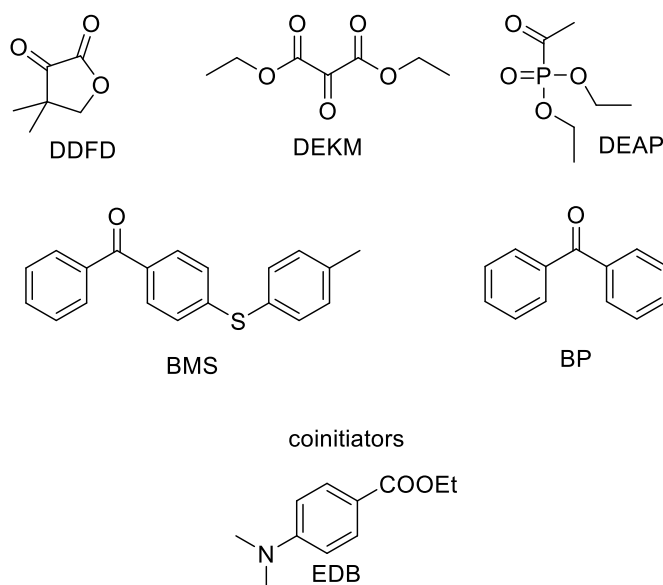
Diethyl ketomalonate DEKM showed very poor reactivity in diacrylate HDDA and did not show any reactivity in methacrylate mix DMM. Therefore, no maximal rate of polymerization is shown for this compound.

In methacrylate DMM also phosphonate DEAP showed lower reactivity than the industrial initiator BMS. (Figure 39) The R_P is still higher than benzophenone when no coinitiator is used. Adding aromatic amine EDB as coinitiator has a very positive effect on the reactivity. The mixture with phosphonate DEAP and coinitiator is almost twice as reactive and exceeds the R_P of the industrial reference initiators. This shows that direct initiation is not favored in case of this compound. Cyclic ketoesters DDFD shows a higher maximal rate of polymerization by direct initiation than phosphonate DEAP. Still the value of R_P is lower than that of the industrial references. Also in case of cyclic DDFD the addition of coinitiator increases the reactivity beyond the industrial references.
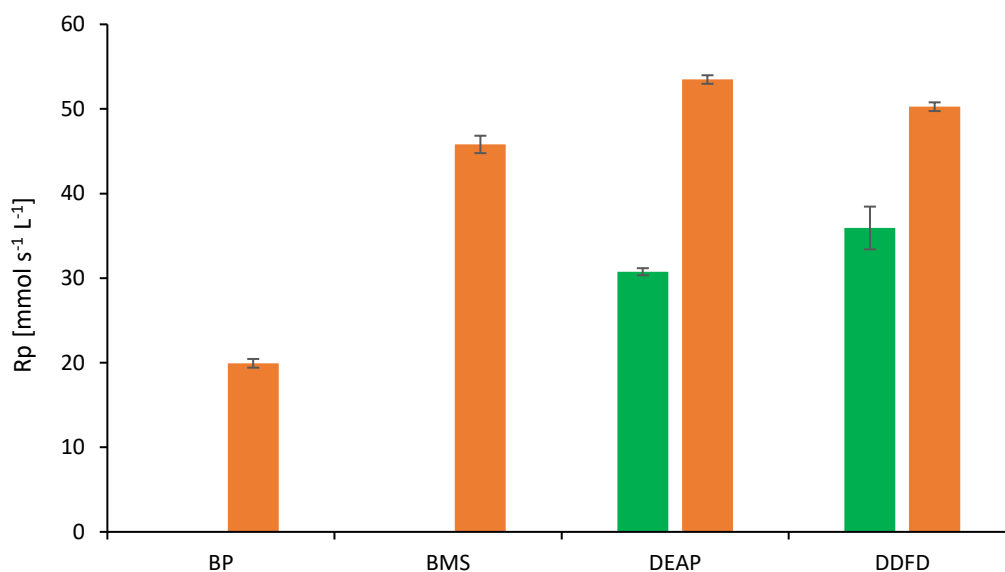
Figure 39. Rate of polymerization of industrial initiators ☐ (hollow) and α-ketoesters without coinitiator ■ (green) and with EDB as coinitiator ■ (orange) in DMM mixtures at 1 W cm^{-2} (320-500 nm).

The sterical hindrance and lower reactivity of the methacrylate formulation makes direct initiation by inter or intra molecular hydrogen abstraction less efficient. Adding a coinitiator is therefore more beneficial than in acrylic monomers.

This is also clearly visible in Table 20, were all results are shown. Without coinitiator no novel compound can beat the industrial references regarding the time to R_P or the DBC.

Table 20. Photo-DSC results for industrial initiators and α-ketoesters in DMM mixtures at 1 W cm^{-2} (320-500 nm). Formulations contain 1 eq. (co)initiator relative to 1 w% EP.

	R_P [mmol L^{-1} s^{-1}]	t_{max} [s]	t_{95} [s]	DBC [%]
BP	20	18.2	143	49
BMS	46	11.1	115	57
DEAP	31	26.7	133	43
DEAP_EDB	53	14.3	104	51
DDFD	36	27.5	110	47
DDFD_EDB	50	18.2	90	54

With coinitiator EDB both substances DDFD and DEAP are comparable or faster than benzophenone BP but not than BMS which shows the fastest t_{max}. The benzophenone derivative BMS also shows the highest conversion with a DBC of 57%. Cyclic ketoester DDFD with EDB gets close, reaching a DBC of 54% with a significantly faster t_{95}.

5.2.5. Long wavelength UV initiators - 400 nm LED tests

Isopropyl thioxanthone (ITX) with amines as coinitiator is one of the most important industrial Type II initiator systems for visible light polymerization. Therefore, it was very interesting to see how cyclic ketoester DDFD performs near the visible spectrum at 400nm in less reactive methacrylates. Photo-DSC studies with a 400 nm LED were conducted. Each sample was irradiated at 0.38 W cm^{-2} twice for 300 s.
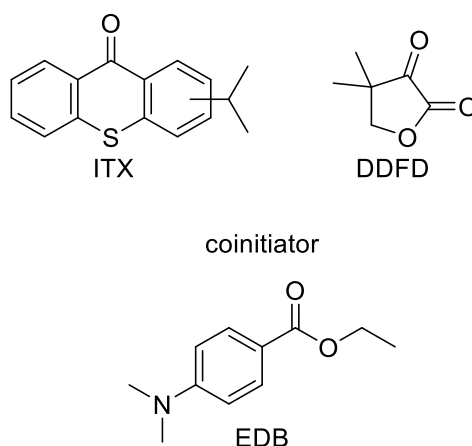
In Figure 40 the maximal rate of polymerization for DMM mixtures with thioxanthone ITX and cyclic ketoester DDFD is shown. Thioxanthones are classic Type II initiators and need a coinitiator to function efficiently. Usual amine coinitiator MDEA was used equimolar to ITX.
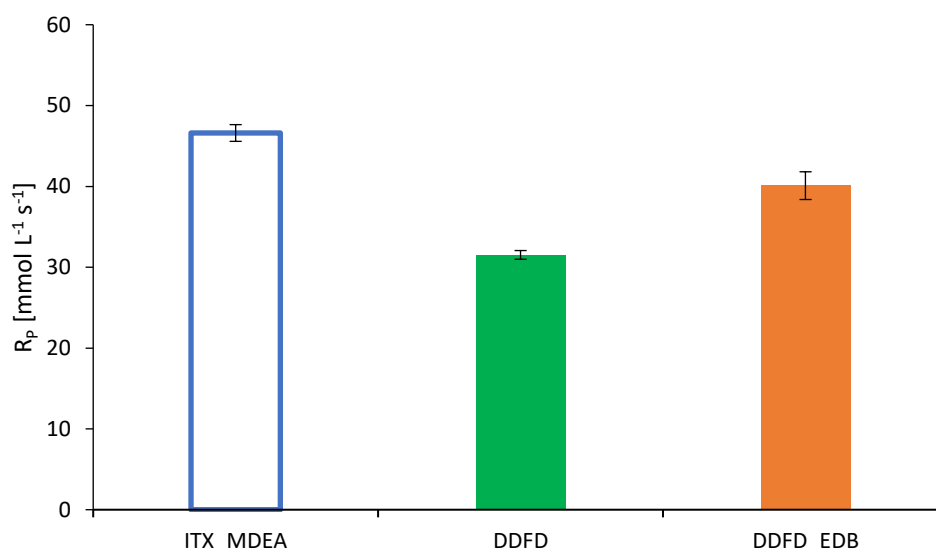
Figure 40. Rate of polymerization of industrial initiator ITX ☐ (hollow), α-ketoester DDFD without coinitiator ▪ (green) and with EDB ▪ (orange) in DDM mixtures at 0.38 W cm^{-2} (400 nm LED). Formulations contain 1 eq. (co)initiator relative to 1 w% EP.

In opposite to the LED measurements conducted in acrylate mixtures, the mixture with cyclic ketoester DDFD shows lower reactivity than the mixture with thioxanthone ITX + MDEA. The

maximal rate of polymerization of the ITX mixture is twice as high. The low reactivity of ketoester DDFD in methacrylates was also observed in the broadband studies. Adding aromatic amine EDB as compatible coinitiator to the mixture with cyclic ketoester DDFD does improve the reactivity but the effect is too small to compete with the reactivity of ITX.

Table 21. Photo-DSC results for industrial initiator ITX with MDEA as coinitiator and cyclic α-ketoester DDFD with and without EDB as coinitiator in DMM mixtures at 0.38 W cm^{-2} (400 nm). Formulations contain 1 eq. (co)initiator relative to 1 w% EP.

	R_P [mmol L^{-1} s^{-1}]	t_{max} [s]	t_{95} [s]	DBC [%]
ITX_MDEA	47	12.0	100	53
DDFD	32	31.5	129	49
DDFD_EDB	40	21.1	124	50

In Table 21 it can be seen that cyclic ketoester DDFD performs significantly slower than thioxanthone ITX. It has to be considered that in case of DDFD the less reactive and more bulky coinitiator EDB had to be used which explains the lower reactivity compared to ITX with more reactive amine MDEA.

5.2.6. Long wavelength visible light initiators

Based on the novel silyl glyoxylate SiKE Type I initiator for dental application it was tried to synthesize other visible light initiators based on glyoxylates. As the synthesis of phosphono and sulfonyl glyoxylates was unsuccessful and trimethyl silyl and germyl derivatives did not show sufficient reactivity in preliminary tests, only silyl glyoxylate SiKE was compared to a standard dental initiator Ivocerin.

For comparison, equimolar mixtures of both compounds were prepared with dental methacrylate mixture DMM. 1 wt% Ivocerin was used for calculation of the molar amounts. The samples were then irradiated in the DSC device at 400-500 nm with 1 W cm^{-2} at the end of the light guide and the kinetic data was compared.
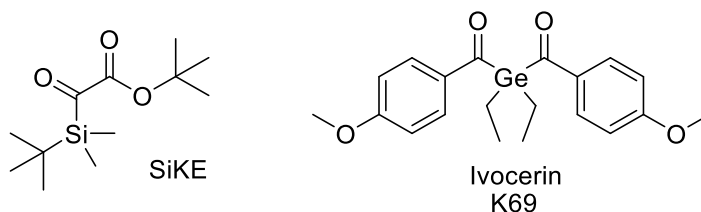
On the first sight it is visible that the silyl glyoxylate SiKE shows much lower reactivity. The maximal rate of polymerization of the mixture with Ivocerin is four times higher. Also in the calorigram (Figure 41, right) shows a much slower polymerization.
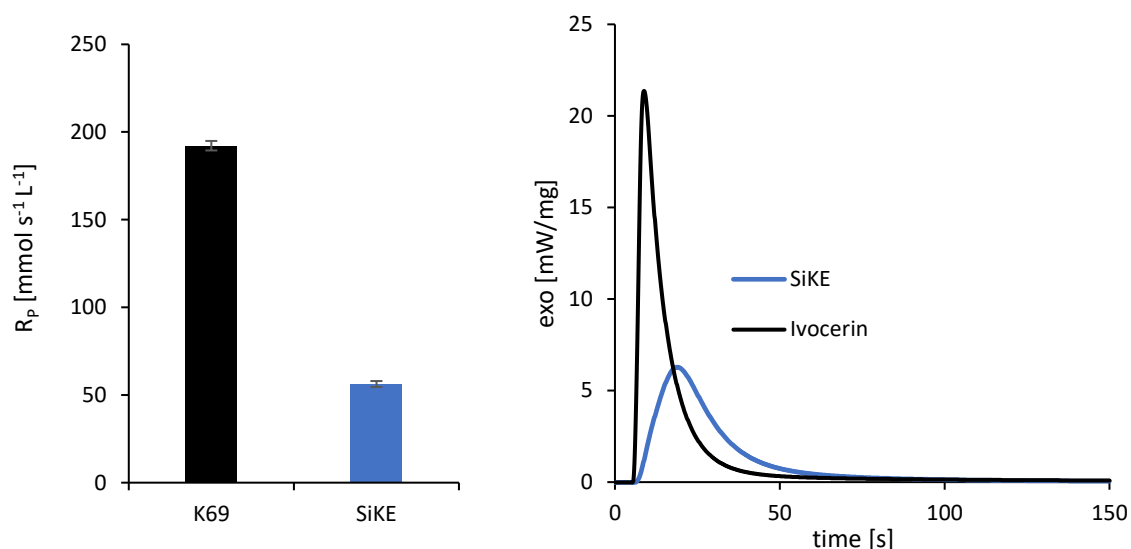
Figure 41. Maximal rate of polymerization R_P (left) and calorigram (right) of mixtures of Ivocerin and silyl glyoxylate SiKE in methacrylate DMM.

The mixture of silyl glyoxylate SiKE reached a DBC of 50% while the mixture with Ivocerin as initiator achieved 72% DBC.

Even if it is considered that Ivocerin forms the double amount of radicals compared to silyl compound SiKE, it is clear that the reactivity of ketoesters in methacrylates is limited. This is well supported by Table 22 which displays the detailed results. Dental initiator Ivocerin (K69) reacts much faster and reaches more than 70% conversion while the slower silyl glyoxylate only reaches 50% DBC.

Table 22. Photo-DSC results for visible light initiator Ivocerin (K69) and silyl glyoxylate SiKE

	R_P [mmol L^{-1} s^{-1}]	t_{max} [s]	t_{95} [s]	DBC [%]
K69	192	3.8	44	72
SiKE	56	14.5	74	50

It is known that silyl glyoxylate SiKE initiates by Type I mechanism,[124] but it seems that the cleavage reaction or resulting radicals are less efficient than that of acyl germanes.

5.3. Hydrogels

Hydrogels are materials, with a widespread use in industry. The most common product made from hydrogels are soft contact lenses but also other products such as medical electrodes, wound dressings and hygiene products are made from hydrogels. Newer applications like drug delivery and tissue engineering are gaining importance.[125]

monomer

PEG700DA

initiators

IC2959

BPQ

EP

DDFD

coinitiator

MDEA
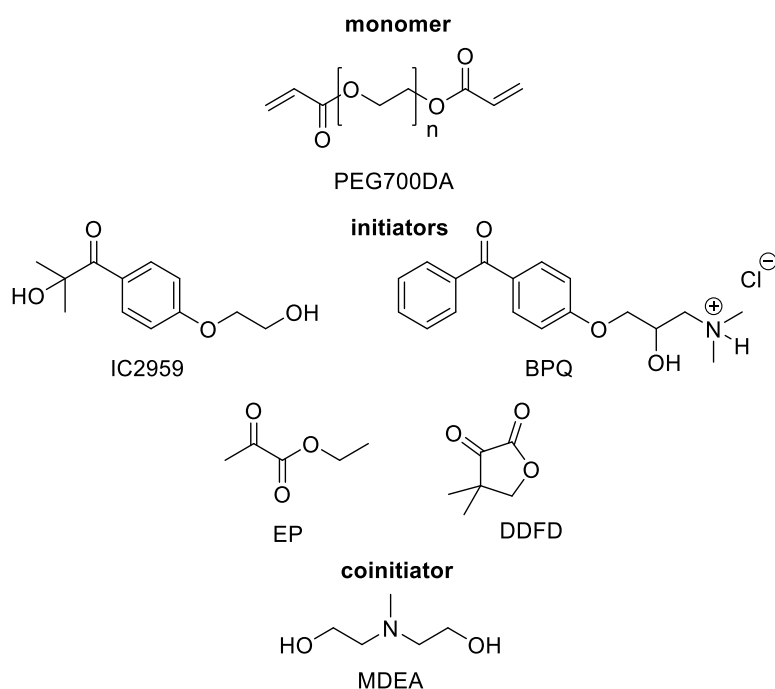
For photo curing in the presence of cells, biocompatibility of the initiators is essential. Ethyl pyruvate EP is water soluble up to 1 wt% in pure water and cyclic DDFD is water soluble at even higher concentrations. The solubility is further increased in formulations containing water soluble monomers.

50 wt% solutions of water soluble diacrylate PEG700DA with the different initiators were prepared and tested at 320-500 nm and 1 W cm^{-2}. Water soluble Type I initiator Irgacure 2959 and Quantacure BPQ, a bimolecular Type II initiator with MDEA as coinitiator, were used as reference initiators. The amount of (co)initiators was calculated equimolar to 1 wt% EP.
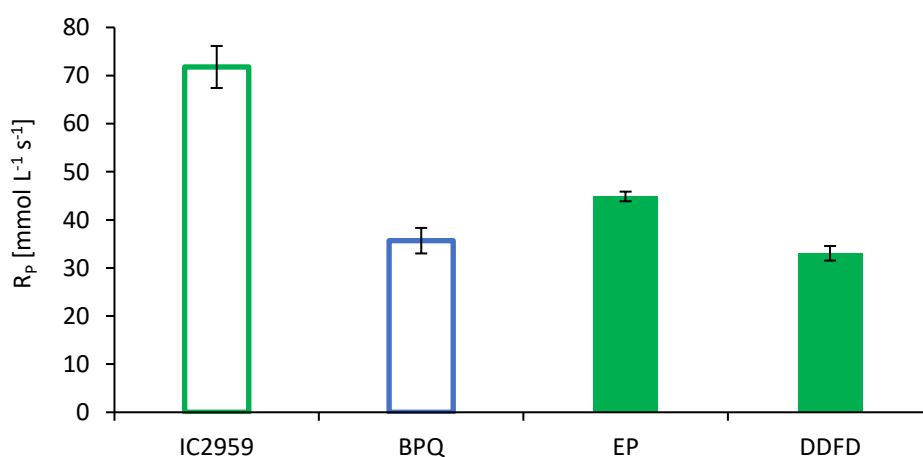
Figure 42. Rate of polymerization R_P of industrial initiators (□) with MDEA, (□) without coinitiator and α-ketoesters without coinitiator ■ (green) in methacrylic DMM mixtures at 1 W cm^{-2} (320-500 nm). Formulations contain 1 eq. (co)initiator relative to 1 w% EP.

As can be seen in Figure 42 and Table 23 that ethyl pyruvate EP and cyclic ketoester DDFD can compete with the commercial water-soluble Type II system BPQ/MDEA. The performance is sufficient even without coinitiator. Ethyl pyruvate EP shows a higher reactivity than cyclic initiator DDFD, which also was observed in acrylate HDDA. This results in shorter times to reach R_P and also shorter t_{95} than that of benzophenone BP and cyclic DDFD. An average DBC of 88 ± 2% was reached for the Type II systems. As expected the Type I system shows a higher polymerization rate the highly reactive initiator IC2959 reached almost full conversion of 95% in a shorter time than all other compounds.

Table 23. Photo-DSC results of hydrogels with water-soluble industrial initiators IC2959 and BPQ as well as water-soluble ketoesters EP and DDFD

	R_P [mmol L^{-1} s^{-1}]	t_{max} [s]	t_{95} [s]	DBC [%]
IC2959	72	3.7	23	95
BPQ_MDEA	36	7.6	42	90
EP	45	6.4	37	87
DDFD	33	10.3	46	86

Ethyl pyruvate is a FDA approved food additive and the compound as well as its photoproducts are harmless to the human body. Considering the field of application for hydrogels, the water-soluble ketoesters could be highly biocompatible initiator replacements for water-based formulations. Due to the absorption spectrum near the visible light of cyclic ester DDFD even more harmless light sources with higher wavelength in presence of cells could be used.

6. UV-aging of polymers

For coatings and decorative applications of light curable formulations, it is important that the cured formulations do not change their appearance with time or undergo discoloration during the curing process. Yellowing therefore is a well-known problem when it comes to cure clear surface coatings, especially when thioxanthones are used as sensitizers and/or amine coinitiators are used in Type II curing systems.[126] [127]

Photoinitiators of coatings and inks cause discoloration of the system. Especially pale pigmented inks and clear coatings are more prone to discoloration by the photoinitiators and their photoproducts since it is common practice to use around a 7 ± 10% photoinitiator level to attain the fast curing systems demanded by the printing ink industry.[128]

A simple test was used to see how color-stable the cured samples were upon longer UV exposure. Therefore, the formulations used for DSC measurements were put into silicon molds and cured in an Intelliray UV flood oven for 100 seconds. The cured specimens were then taken out of the mold and irradiated for additional 120 minutes.

After the UV aging process, the specimens were glued on a white sheet of paper and photographed in a flatbed scanner to obtain pictures with neutral white balance.

In Figure 43 the specimens cured without coinitiators are shown. On the first sight, very good results were obtained with all formulations. The polymers are clear and almost colorless. The mixture with Type I initiator SC73 showed a pinkish color after curing, this discoloration vanished during 120 min UV aging. Probably some colored diketone recombination products formed, that further decomposed during irradiation.
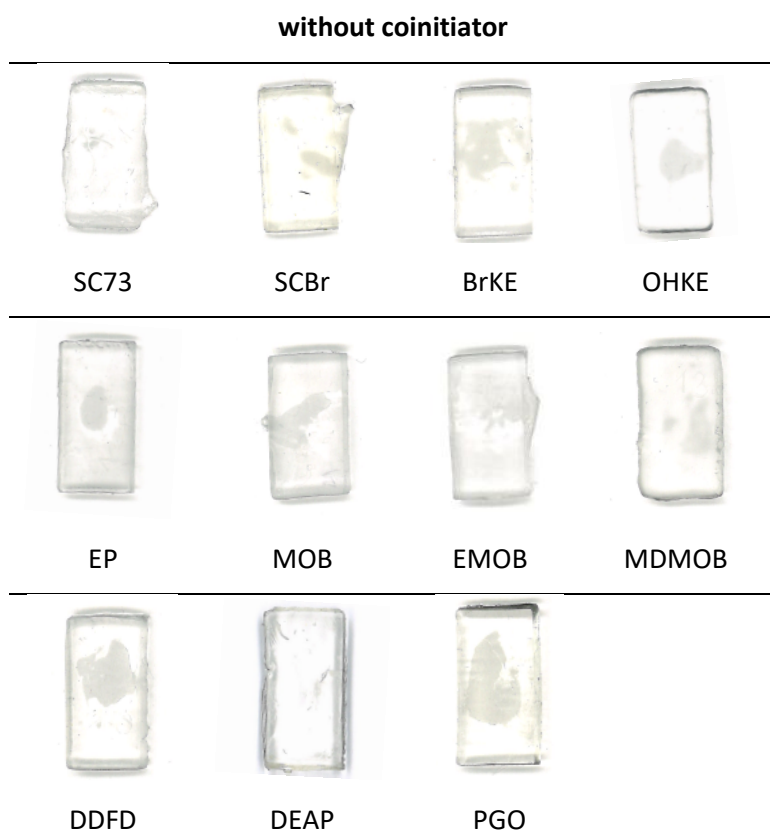
Figure 43. Polymer specimens from DMM with 1 wt% initiator and without coinitiator after 120 min of irradiation

A closer look shows that the bromo compounds SCBr and BrKE show some slight yellowing. It is plausible that released bromine or bromo side products are responsible for that color. Also in case of phenyl glyoxylate some yellow shimmer is visible. As already described above, initiators with aromatic chromophores tend to produce side products which absorb in the visible range.

MDEA as coinitiator

BP/MDEA BMS/MDEA ITX/MDEA

EP/MDEA EMOB/MDEA MDMOB/MDEA
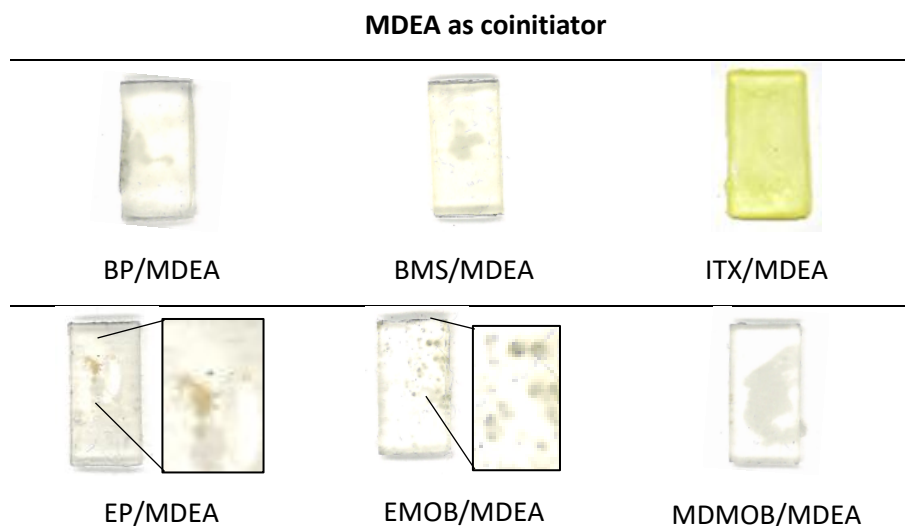
Figure 44. Polymer specimens from DMM with 1 wt% initiator and 1 eq. MDEA as coinitiator after 120 min of irradiation

All mixtures with simple ketoesters and the hydroxy ketoester OHKE result in very clear and colorless specimens that did not show any discoloration.

When industrial Type II initiators and novel ketoesters are used with aliphatic amine MDEA as coinitiator, significant yellowing occurs. From the industrial reference compounds benzophenone showed the lowest discoloration, while benzophenone derivative BMS shows significant yellowing. As BMS contains an aromatic thioether is possible that colored thio compounds are formed. The strongest discoloration is shown by the mixture containing ITX. The thioxanthone is yellow on its own and known for photo oxidation of amines leading to severe yellowing. (Figure 44, first row)

The mixtures containing ethyl pyruvate EP and ketoester EMOB are examples for decomposition by the nucleophilic amine MDEA. As already mentioned, enolizeable ketoesters tend to decompose under the influence of MDEA. The decomposition is very fast for mixtures with ethyl pyruvate EP. The more stable ketoester EMOB can be used with MDEA as coinitiator, but after storage for one week at 4 °C the slower decomposition also leads to formation of brown oily precipitate visible in the magnified pictures. In comparison the stability of sterical hindered ketoester MDMOB, does not show signs of decomposition or discoloration. (Figure 44, second row)

EDB as coinitiator

BP/EDB   BMS/EDB   PGO/EDB   EP/EDB

MOB/EDB   EMOB/EDB   MDMOB/EDB   DEAP/EDB   DDFD/EDB
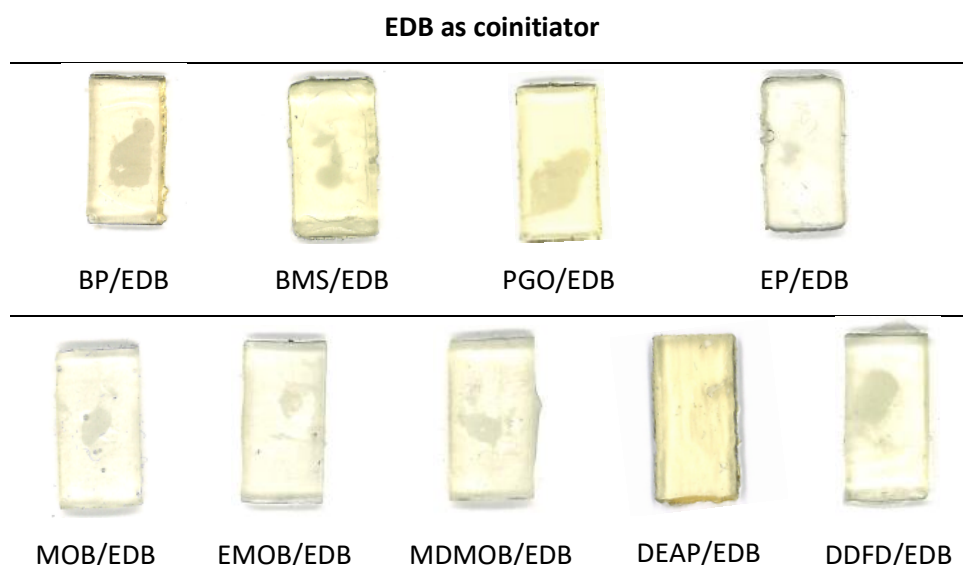
Figure 45. Polymer specimens from DMM with 1 wt% initiator and 1 eq. EDB as coinitiator after 120 min of irradiation

As already expected the aromatic amine coinitiator EDB caused the strongest discoloration. All mixtures containing EDB showed yellow discoloration. Nevertheless, the initiators containing aromatic moieties caused the strongest discoloration together with phosphonate DEAP. When amine EDB is used with α-ketoesters the yellowing is significantly lower. (Figure 45)

Considering that, α-ketoesters show higher reactivity without coinitiator than commercial systems with coinitiator this new class of photoinitiators combines high reactivity with perfect color stability. If the reactivity has to be further increased by usage amines as coinitiator with aliphatic ketoesters, the discoloration is still lower than with hitherto existing Type II systems.

7. Photolysis studies

To get a deeper insight into the mechanism of initiation, photolysis studies were conducted by Markus Griesser in the group of Georg Gescheidt at the TU Graz.

Although there are some mechanistic studies on the photodecomposition of α-ketoesters, there is no literature about the initiation process of radical polymerization. In addition, the photochemistry of cyclic α-ketoesters with planarized carbonyl groups is generally not described. Therefore, the reaction of the cyclic ester DDFD with styrene was chosen as the ideal paradigm for establishing the mechanism of polymerization initiated by α-ketoesters, as the compound is less prone to side reactions and has characteristic methyl groups. Styrene (other than common (meth)acrylates), carries no methyl groups, hence resonances stemming from the growing

polymer chain and styrene-based byproducts do not deteriorate the assignment of signals in the methyl group region. Accordingly, the corresponding NMR signals exclusively reflect conversions based on DDFD.

The NMR spectrum of DDFD/styrene (Figure 46) presents four new signals in the "methyl region" with only one (1.24 ppm, largest) corresponding with the reference spectrum of pure irradiated DDFD (Figure 47). The peak at 0.5 ppm indicates aliphatic protons in close vicinity to a phenyl group (strong shielding). In the following Scheme 19 two different addition modes are shown: Based on the radical pair **RA/RB** generated upon irradiation, styrene can add to both radicals and starting the polymerization. For simplicity, only products **A** and **B** in are presented in Scheme 19. A longer polystyrene homopolymer chain does not further influence the assignment of the NMR resonances attributed to the methyl groups, therefore the scheme is simplified.
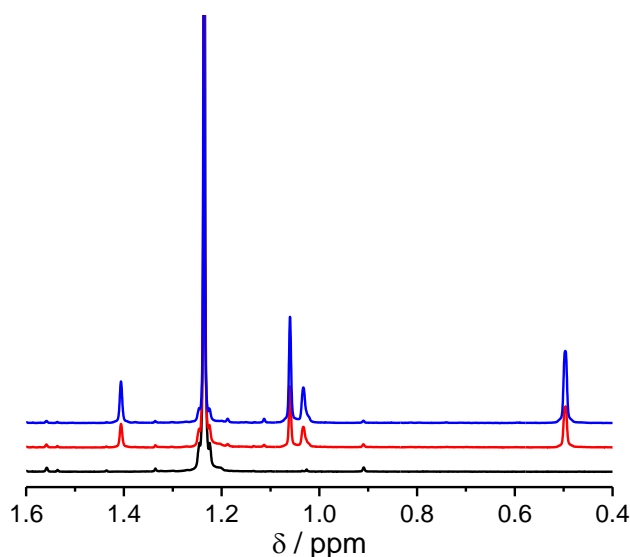
Figure 46. ^{1}H-NMR spectra taken before (black), after 30 min (red), and after 60 min (blue) of continuous irradiation with an LED (365 nm). Initiator DDFD 45 mM, styrene 110 mM, solvent CD$_3$CN.

Upon reaction, the two 4-methyl groups in DDFD (red) become non-equivalent in **A** and **B**. Accordingly, the four emerging peaks at 0.50, 1.03, 1.06, and 1.41 ppm (Figure 46) indicate methyl-group-based resonances of DDFD-type end groups **A** and **B** respectively.
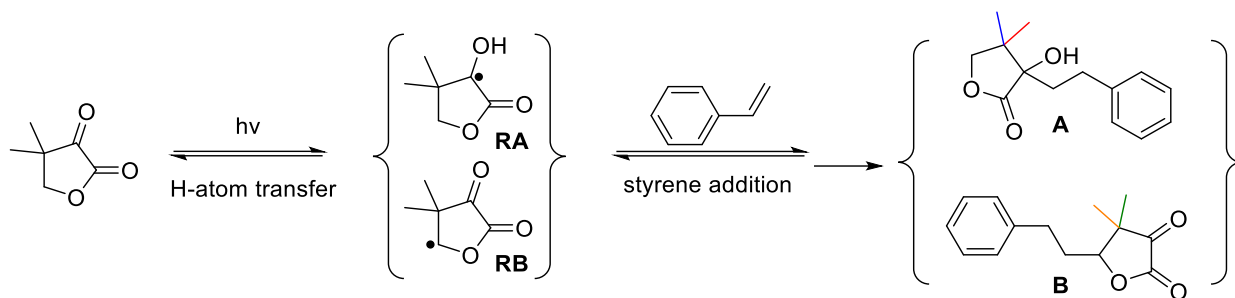
Scheme 19. Photo-induced (intermolecular) hydrogen atom transfer of DDFD forming the radical Pair RA/RB followed by their addition to styrene and H-atom addition. The colored indicates the two equivalent methyl groups of DDFD, which become non-equivalent in the addition products A and B (red and blue in A, green and orange in B). Only the head additions are shown

These observations point to DDFD initiating the polymerization via, intermolecular hydrogen-atom transfer (Type II, Scheme 19). Analogous performed reactions with N-vinylpyrrolidone, butyl acrylate, methyl methacrylate, and 3,3-dimethyl-2-methylenebutanoate are corroborating the results with styrene. However, the substantially higher number of methyl groups present in the latter monomers renders it very complicated assigning the observed resonances, which is visible in Figure 47 to Figure 49.
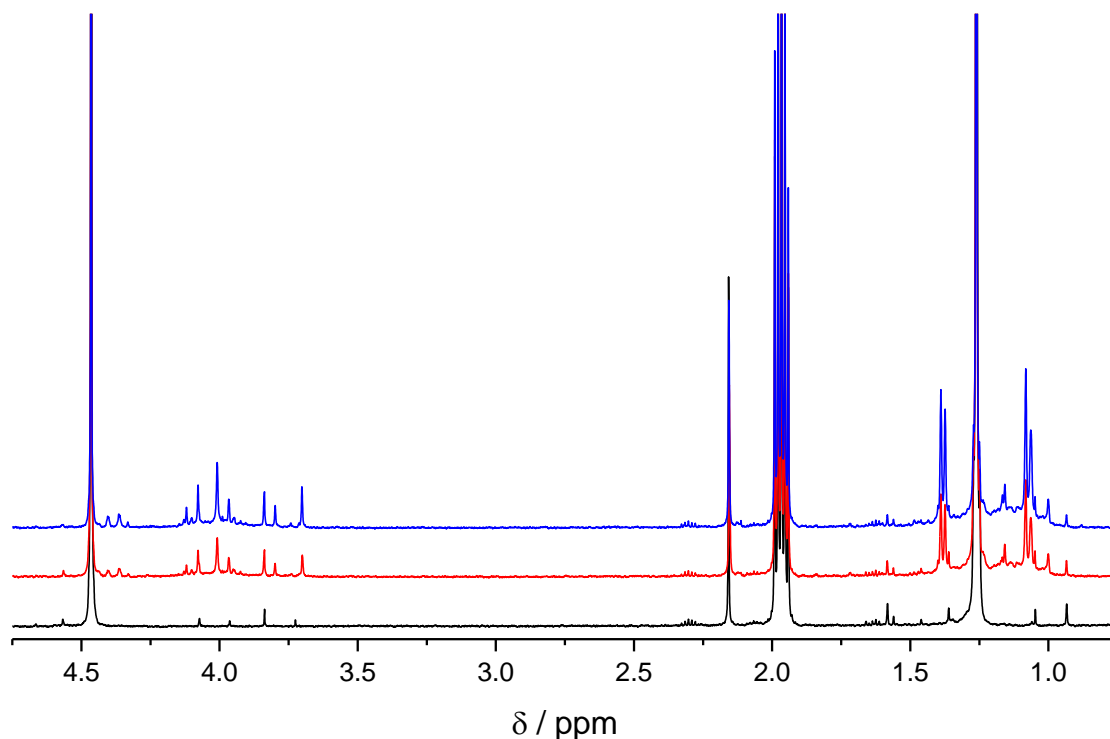
Figure 47. ¹H NMR taken of DDFD (40 mM) before (black), after 30 min (red), and after 60 min (blue) of continuous irradiation with an LED (365 nm).

The observations are in line with previous spectroscopic studies on aliphatic α-ketoesters indicating that pyruvates are not likely to undergo Type I α-cleavage reactions but rather react via triplet-state hydrogen transfer.[57, 129, 130]
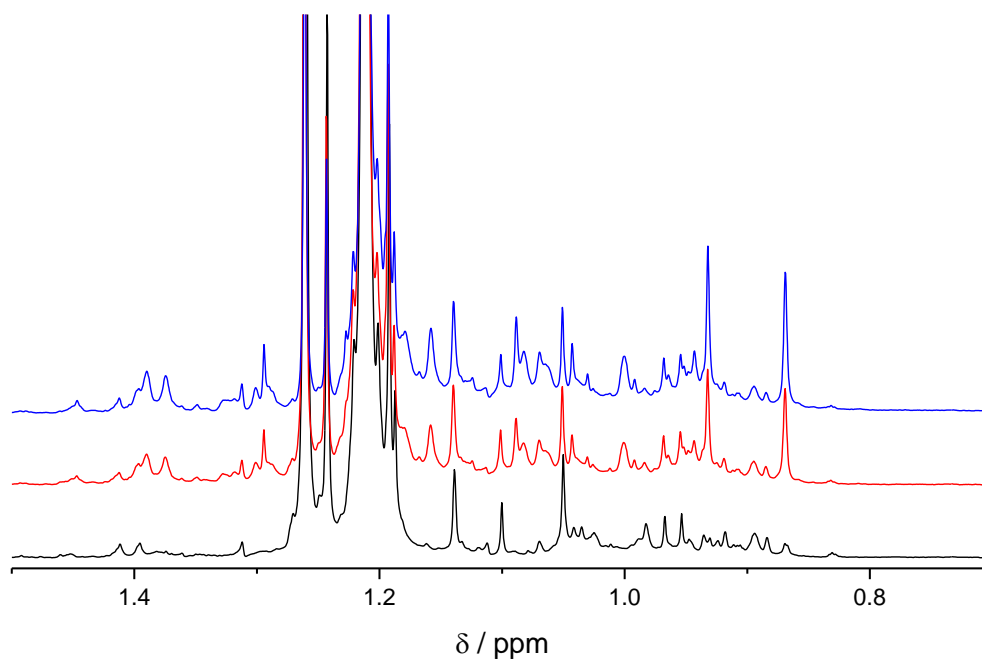
Figure 48. ^{1}H NMR spectra obtained upon irradiating DDFD (27 mM) in the presence of 3,3-dimethyl-2-methylenebutanoate (83 mM). Spectra taken before (black), after 30 min (red), and after 60 min (blue) of continuous irradiation with an LED (365 nm).
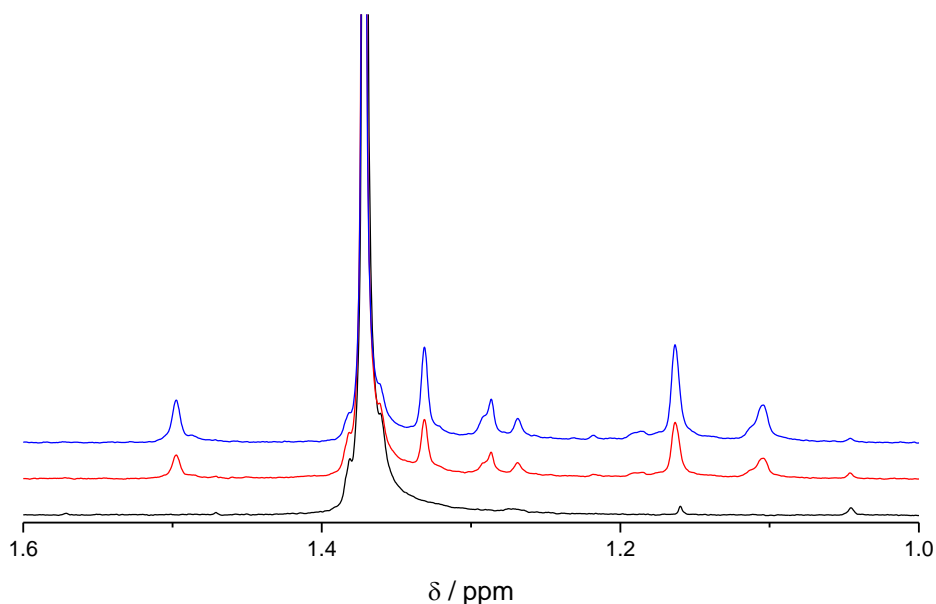
Figure 49. ^{1}H NMR spectra obtained upon irradiating DDFD (46 mM) in the presence of N-vinylpyrrolidone (155 mM). Spectra taken before (black), after 30 min (red), and after 60 min (blue) of continuous irradiation with an LED (365 nm).

In case of cyclic ketoester DDFD intra molecular hydrogen abstraction is not possible due to sterical reasons. This would explain the lower reactivity compared to linear aliphatic ketoesters.

8. Cytotoxicity

For testing the biocompatibility of the novel water-soluble initiators, cytotoxicity tests were performed by Marica Marcovic in the group of Aleksandr Ovsianikov at the TU Wien with mouse fibroblast cell line L929. The compounds were compared to the most common commercial water-soluble Type I initiator Irgacure 2959 and the commercial water-soluble Type II benzophenone ammonium salt system BPQ with MDEA as coinitiator. Equimolar stock solutions of the initiators were prepared standardized on a 40 mg/L (17.84 mM) solution of IC2959. In a dilution series, the toxic concentrations with and without previous 10 min UV-irradiation at 365 nm were determined.
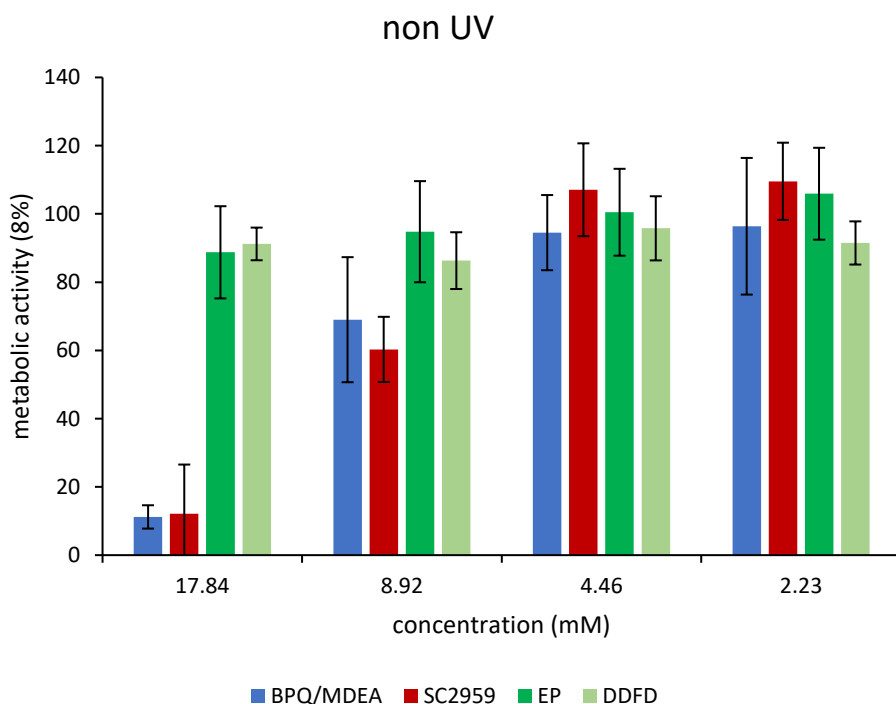
Figure 50. Cell viability after 24 h incubation in initiator solutions without initial irradiation at 365 nm
Left to right: ■ **BPQ/MDEA,** ■ **IC2959,** ■ **EP and** ■ **DDFD.**

As visible in Figure 50 and Figure 51, the reference initiators BPQ/MDEA and IC2959 can be considered as biocompatible from 4.46 mM and lower, as the metabolic activity of treated cells (also after UV) was above 80%. The new photoinitiators ethyl pyruvate EP and the furandione DDFD can be considered nontoxic even at the highest concentration of 17.84 mM and also after

UV irradiation. This indicates that the compounds themselves and also photoproducts are not harmful.
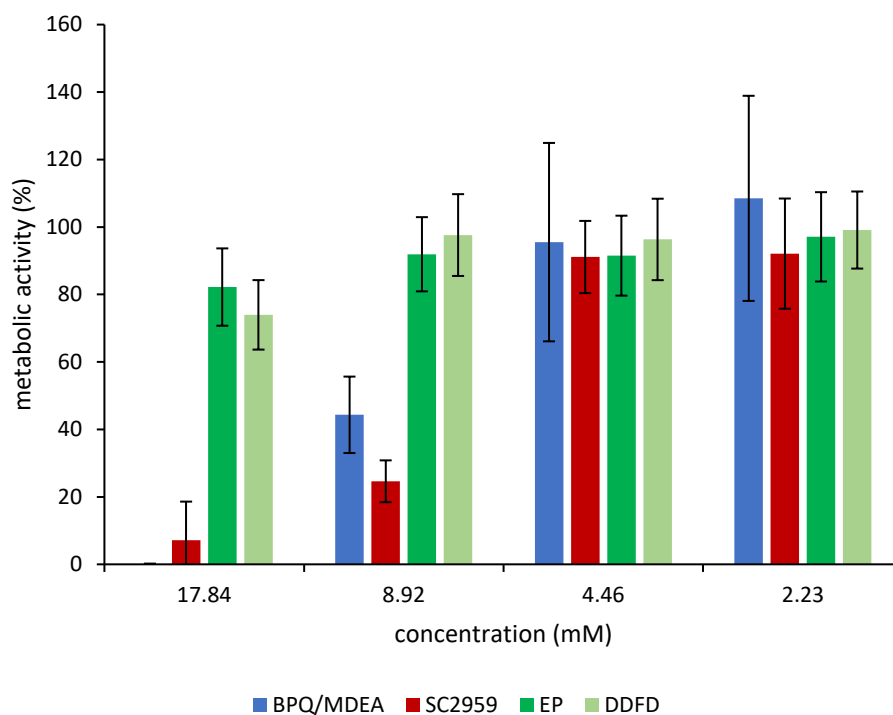
Figure 51. Cell viability after 24 h incubation in initiator solutions after 10 min initial irradiation at 365 nm Left to right: ■ BPQ/MDEA, ■ IC2959, ■ EP and ■ DDFD.

These good results show that aliphatic α-ketoesters have high potential as biocompatible photoinitiators.

Part 2: Improving network properties with chain transfer reagents

Radical polymerization is a very fast and uncontrolled process. Side reactions as chain transfer by hydrogen abstraction and termination reaction cause a broad distribution of kinetic chain lengths. The formation of new covalent bonds causes a reduction of intermolecular interspace and therefore a shrinkage of cured materials. Shrinkage forces and inhomogeneous chain lengths lead to rather brittle materials with broad glass transitions. To improve material properties of radical photopolymers, regulation of the curing reaction is necessary. Different mechanisms for regulation of radical polymerization are known. All of these methods share terminating a propagating chain and reinitiation of new chain growth. So far only addition fragmentation chain transfer and hydrogen donation are fast enough to be applied in bulk photopolymerization.

1. Addition fragmentation chain transfer (AFCT)

1.1. State of the art

In recent years, AFCT gained a lot of interest as research topic. Due to the wide application of photomaterials, improving the material properties of photopolymers became important. Due to high reactivity, good mechanical properties and relatively low toxicity of methacrylates in comparison to acrylates, methacrylic monomers play an important role in the field of dental composites and additive manufacturing technologies. This is why this work will further focus on chain transfer agents that can be used with methacrylates.

Since the late 1980s when AFCT was described to control radical polymerization for the first time[131, 132] a huge number of reagents have been described in literature.

Hee Young Park et al. already reported AFCT modified dental composites 2010.[133] It is described that the produced composites showed low (40-50 °C) and very sharp glass transitions and that the shrinkage stress can be reduced significantly. These results were achieved by combining AFCT and thiol-ene chemistry.
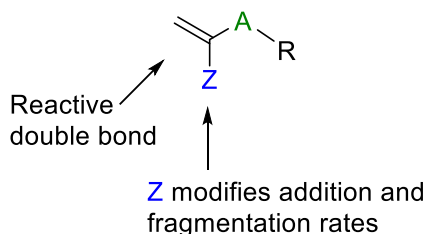
The principal structure for most AFCT reagents is the same. There has to be a reactive double bond, usually carbon, on which a radical can add and a good homolytic leaving group R. The addition and fragmentation speed is determined by the activating Z-group. Depending on the

AFCT structure the chain transfer constants can be varied in monomer systems. It is crucial that the addition rate is in the same order of magnitude as the monomer addition constant. This guaranties statistic consumption of the reagent. Also very important is that the fragmentation reaction is much faster than a potential copolymerization which could happen if the intermediate radical is too long lived and reactive towards monomer.

In Scheme 20 a radical polymerization with an AFCT reagent is shown. After cleavage of the initiator an initiator radical I• starts the polymerization. Depending on the initiator, this happens with the certain addition rate k_{ini}. The propagation of the reaction starts with the addition rate of a chain-end to monomer k_{prop}. During the polymerization, a terminal radical can also add to an AFCT molecule with k_{add}. The intermediate chain transfer agent radical can now undergo two reactions in competition to each other. Either the intermediate radical adds to monomer with the copolymerization addition rate k_{cp} or the leaving group R cleaves off with the fragmentation rate k_{frag}. After fragmentation, the rate of reinitiation k_{reini} is dependent on the chemical structure of the leaving group.
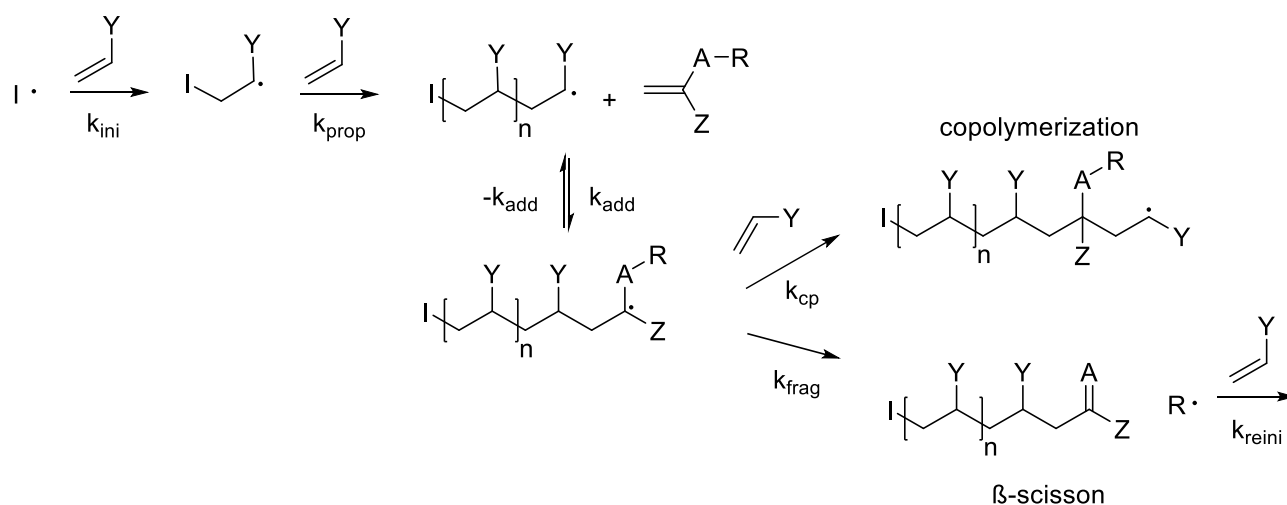
Scheme 20. Possible reaction pathways of radicals with AFCT reagents

Normally chain transfer agents are used as additive up to 20 mol%. Therefore, it is possible but rather unlikely that an initiator is directly adding to a CTA. This is why that case is not shown in Scheme 20.

$$C_T = \frac{k_{tr}}{k_{prop}} \qquad \textbf{Equation 2}$$

$$k_{tr} = \frac{k_{add}*k_{frag}}{-k_{add} + k_{frag}} \qquad \textbf{Equation 3}$$

C_T.................. Chain transfer constant
k_{tr}.................. Rate constant transfer
k_{prop}.............. Rate constant chain growth by propagation
k_{add} .... Rate constant of addition reaction
k_{frag} .... Rate constant of fragmentation reaction

For good regulation of radical polymerization statistical consumption of AFCT molecules is crucial. This is defined by the so-called chain transfer constant C_T, the ratio of the addition rate constant of terminal radicals to monomer k_{prop} (propagation reaction) and the rate constant for the transfer reaction k_{tr}. (Equation 2) For homogenous consumption, the quotient should be around 1.

The transfer rate constant is given by the reversible addition rate constant k_{add} and the fragmentation rate constant k_{frag}. (Equation 3) Copolymerization has to be extremely unlikely, so it does not interfere with the transfer rate constant. Therefore, the fragmentation rate constant k_{frag} has to be magnitudes higher than the copolymerization rate constant k_{cp}. The addition of radicals to a CTA molecule is reversible. The fragmentation rate constant has to be as high as possible to ensure the cleavage reaction happens before the reverse addition reaction can take place.

The leaving radical R• should be highly reactive towards the monomer to ensure efficient reinitiation. In addition, the addition of a leaving radical to a transfer agent is possible but unlikely due do an excess of monomer double bonds.
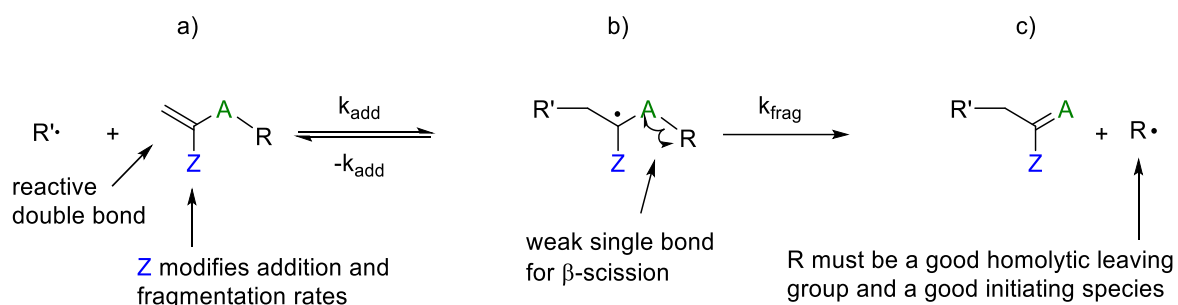
Scheme 21. Structure and reactivity relation of an AFCT reagent

These rate constants can be influenced by the chemical structure of the AFCT reagents. The addition rate of a radical to the double bond is highly dependent on the structure of the Z moiety. (Scheme 21) On the one hand, it must stabilize the intermediate radical well enough to provide

high addition rates on the other hand it must be instable enough to ensure fast β-scission. The fragmentation is also dependent on the bond strength between the leaving group and atom A. Highly stabilized intermediate radical tend to retard the cleavage reaction, slowing down the whole polymerization reaction. Too strong A-R bonds cause copolymerization instead of chain transfer.[134]

In Table 24 some typical AFCT classes that can be used for methacrylates, and chain transfer constants C_T are shown.

Table 24: Chain transfer rates of different β-scission AFCT reagents in methacrylates[135]

Subtance class	Activating group Z	Atom attached to leaving group A	Leaving group R	Chain transfer constant C_T
vinyl ethers	Ph	O	CH_2Ph	0.76^{136}
vinyl peroxides	Ph	O	O-tBu	0.83^{137}
allyl sulfides	CO_2Et	CH_2	S-tBu	0.74^{138}
allyl halides	CO_2Et	CH_2	Br	1.45^{136}
Allyl sulfones	CO_2Et	CH_2	SO_2Tol	1.1^{136}

Chain transfer constants found in literature are usually calculated from thermal polymerizations in solvents. The behavior of CTAs in bulk photopolymerization can therefore not be derived directly from these experiments. Promising classes of AFCT reagents were already tested in previous works. (Scheme 22)

Vinyl ethers need an activation group such as a radical stabilizing phenyl moiety. It was shown in previous work that these reagents tend to fragment slowly and cause massive retardation of polymerization in bulk polymerization of methacrylates.[139]

vinyl ether   vinyl peroxide   allyl sulfide

allyl halide   allyl sulfone
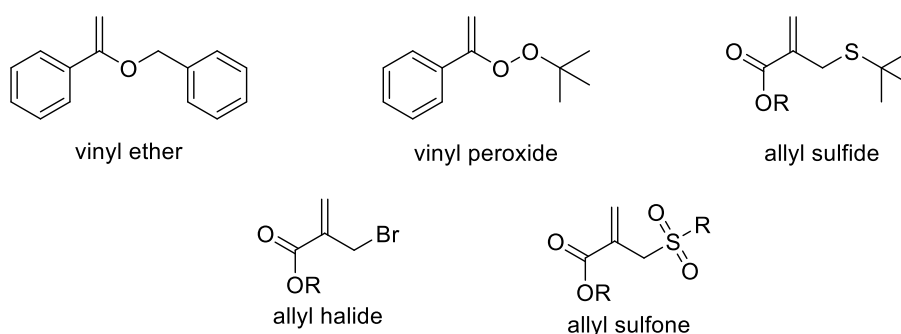
Scheme 22. Examples for some classes of AFCT reagents

Vinyl peroxides show similar transfer constants as vinyl ethers. Due to the labile peroxide bond, the elimination reaction is facilitated. Unfortunately, peroxo compounds show thermal lability, which reduces the storage stability of formulations and the heat of polymerization in bulk can

lead to decomposition of the peroxides. Therefore, the AFCT reagent would act as initiator instead of regulating the network.[140]

Allyl sulphides activated with ester or phenyl moieties show activity as chain transfer agents. Unfortunately the polymerization regulated by these compounds shows strong retardation and resulting materials have a much lower modulus than the unregulated reference networks.[139]

Thiyl radicals are known to efficiently reinitiate methacrylates but the resulting thioethers exhibit very flexible bonds reducing the modulus of resulting materials.[141]

Allyl halides such as ester activated allyl bromides show high transfer constants but halogen radicals are not very reactive towards methacrylates. Also organic bromo compounds are light sensitive and potentially toxic.

Four years ago, β-allyl sulfones were found to be very efficient chain transfer agents for photopolymerization of methacrylates.[37] The sulfonyl radical is among the most reactive radicals towards (meth)acrylates. Different activating groups were tested to optimize reactivity and regulation. Finally it was shown that ester groups as activating moiety are most beneficial for forming homogenous networks with good mechanical properties.[142]

$$R\cdot \; + \quad \overset{k_{add}}{\underset{-k_{add}}{\rightleftharpoons}} \quad \overset{k_{frag}}{\underset{-k_{frag}}{\rightleftharpoons}} \quad + \quad$$

R = Tos, Me
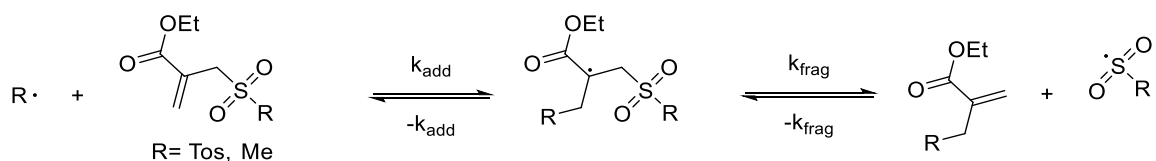
Although allyl sulfones are potent network modifiers and work well in methacrylic bulk networks the polymerization is still retarded in comparison to neat materials, when higher amounts of CTA are added.[36] The cause for that delay is the new double bond formed after cleavage of the leaving group. Due to sterical reasons, this double bond is less reactive than methacrylic end groups and the fragmentation reaction is reversible.[29]

Introducing an oxygen instead of the CH_2 in α-position improves the reactivity a lot. Vinyl sulfonates were found to be even more potent than allyl sulfones and show fast and well-regulated polymerization for acrylates and methacrylates.[143] In the case of vinyl sulfonates the fragmentation reaction leads to formation of a ketogroup, which is irreversible and does not interfere with the radical polymerization.
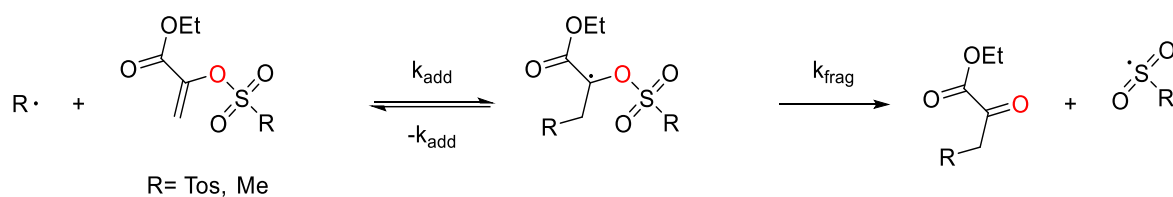
After fragmentation of the intermediate radical, different reaction pathways are possible. Homopolymerization of the CTA is not possible as the fragmentation is favored and much faster. After fragmentation, the sulfonyl radical can reinitiate chain growth but other than allyl sulfones, also self-consumption is possible. (Scheme 23) In this case, the leaving group radical attacks another CTA molecule, leading to chain reaction, which consumes CTA. It was shown that this happens solely when no monomer is present or if high concentrations of CTA (> 20 db%) are used. As long as reactive monomer is present, reinitiation is favored due to the high reactivity of sulfonyl radicals towards (meth)acrylates.[139]
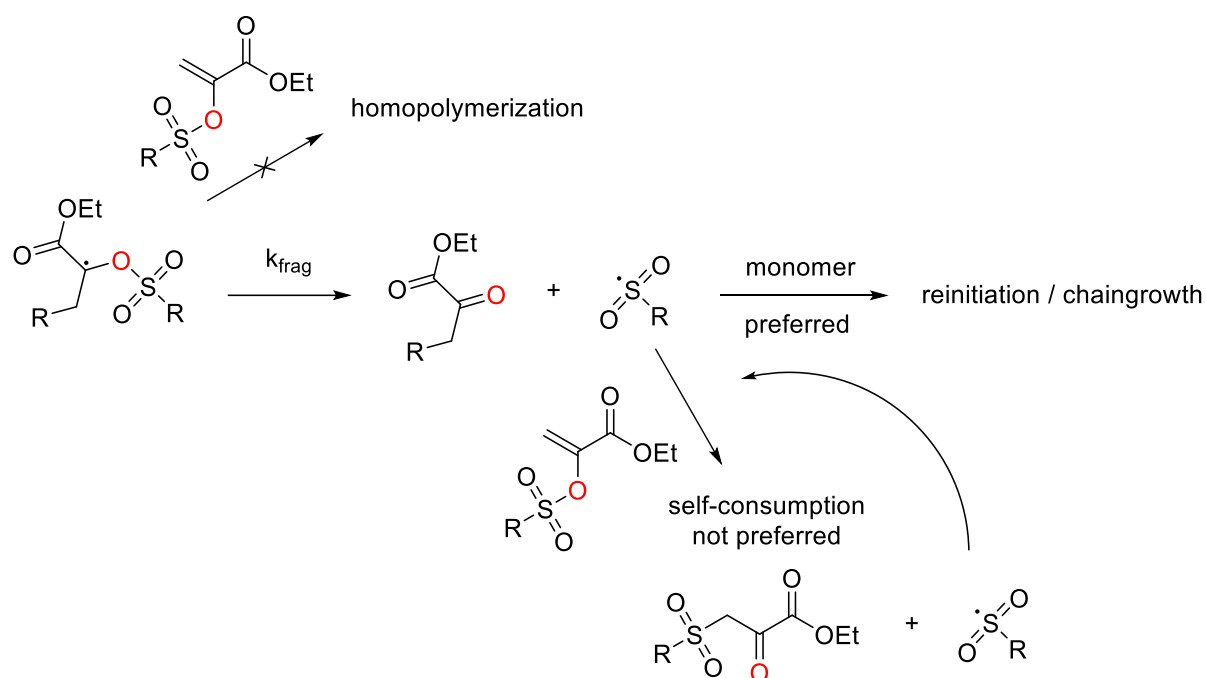
Scheme 23. Reaction pathways of the intermediate radical of vinyl sulfonates

The combination of an irreversible fragmentation step and a highly reactive sulfonyl radical as leaving group is the key to high curing speed and a well-regulated network with significantly better mechanical properties.[143]

A major drawback of sulfonates is, that these esters show an alkylation potential and are therefore considered to be carcinogenic, which can be shown by Ames test.[144, 145]

1.2. Selection and synthesis of AFCT compounds

As it is already known from previous studies, the oxygen between the double bond and the leaving group is optimal for fast and efficient chain transfer due to an irreversible cleavage reaction. As sulfonate esters (L= SO$_2$R) are potentially toxic other leaving groups (L) attached to an oxyacrylate were investigated.
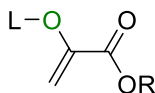
Various oxyacrylates can be prepared via nucleophilic attack of the enol oxygen on an electrophile. The enolisation is conducted via tertiary amine base, which is also needed as acid scavenger for the acidic elimination-product of the electrophile.
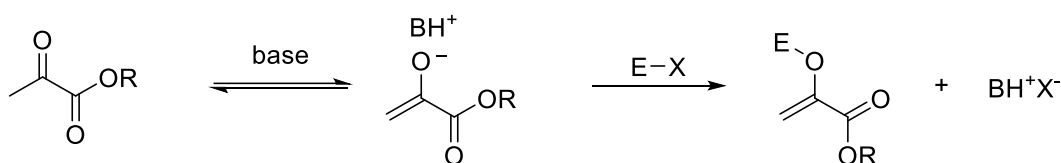
For the silane-ene chemistry it is already shown, that silyl radicals are efficient reinitiating radicals. Therefore, CTAs carrying silyl groups should be investigated. A trimethyl silyl group with low sterical hindrance and a tri(trimethylsilyl)silyl group which showed high reactivity as radical in silane-ene polymerization was chosen as leaving group.

1.2.1. Synthesis of silanoxy ethyl acrylates

The preparation of TMS oxyacrylates is quite simple. The pyruvate is enolised by 1.1 eq. trimethylamine in dichloromethane at room temperature and directly reacted with 1.1 eq. trimethyl clorosilane.[146] After filtration and distillation the TMS oxyacrylate TMSA is obtained in a yield of 82%.
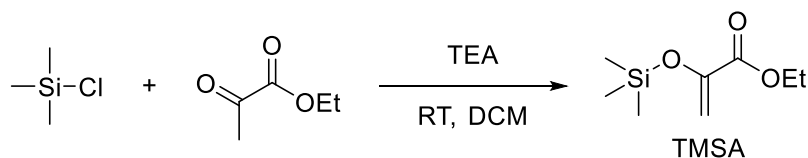
Interestingly the product polymerized within days during storage at 4 °C in the dark. This is surprising as bulk polymerization with a radical initiator was unsuccessful. The resulting polymer had an exceptional high molecular weight (> 100000 Da) and a low polydispersity index (<2). The experiment was repeated four times, BHT was used as inhibitor in all cases, still two batches polymerized without known reason. The high molecular weight and low polydispersity indicates

ionic polymerization, rather than a radical mechanism. The batches that did not polymerize within the first week of storage, showed a shelf-life of several years.

The synthesis of a tri(trimethylsilyl) oxy acrylate SSA was conducted in the same way as for the TMS derivative TMSA. Unfortunately due to the high sterical hindrance and the low reactivity of the tris(trimethyl silyl) chlorosilane no product could be isolated.
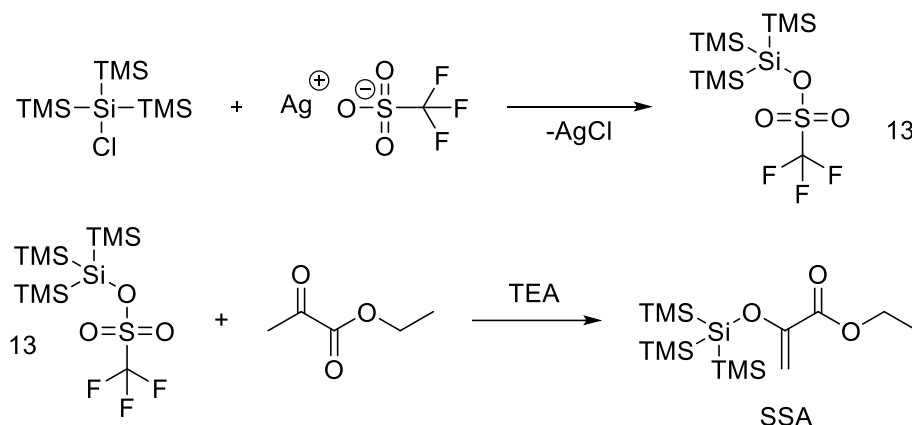
To increase the reactivity of the electrophile, the chloro moiety had to be replaced by a triflate, which is a better leaving group for the nucleophile attack.[147] Therefore, 1.1 eq. chlorosilane was stirred overnight with 1.1 eq. silver triflate in absolute DCM under argon and the filtrated solution of tris(trimethyl silyl)silyl triflate (**13**) was added to 1 eq. ethyl pyruvate in dichloromethane with 1.1 eq. trimethylamine as base without further purification. After extraction and column chromatography 70% of the supersilyl oxyacrylate SSA was obtained.

1.2.2. Synthesis of boron oxy ethyl acrylates

Boryl radicals also seem suitable as reinitiating leaving group. It was already shown that boranes can be used as coinitiator with benzophenone similar to silanes. The initiation is described as very efficient with acrylates.[148] In addition, boron compounds show a low toxicity in general. [149] Therefore, a CTA based on vinyl borates should be synthesized.

The chemistry of boron is different from carbon or silicon based chemistry as boron has an empty p orbital that interacts with bonds attached to the boron atom. For example, oxygen-boron bonds exhibit a semi double bond character as the lone pairs of oxygen interact with the empty p-orbital. Organo boranes are known to be sensitive to oxygen and hydrolysis as in fact, B-C bonds (323 kJ/mol) are weaker compared to C-C bonds (358 kJ/mol), whereas B-O bonds (519 kJ/mol) are much stronger than C-O bonds (384 kJ/mol).[150] With increasing oxygen moieties the stability of boron compounds is increased.

This is why pinacolo borates should offer higher hydrolytic stability. The cyclic structure of this ester offers additional protection and therefore, first a pinacolo vinyl borate was to be synthesized.
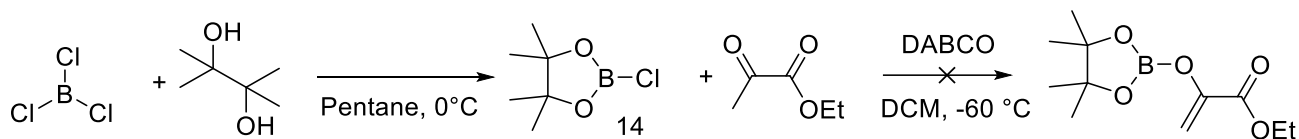
In the first step according to literature 1 eq. dry pinacol was dissolved in dry pentane at 0 °C in argon atmosphere, afterwards a commercial solution of 1 eq. boron trichloride in hexane was added carefully.[151] The unavoidable sideproduct of diborane was filtered of and the residue solution was distilled quickly under inert conditions. Pinacolo chloroborane is meta stable and can be kept at -80 °C for two days under slow decomposition. To avoid decomposition the afforded distillate was kept in action ice slurry at – 80 °C under argon and directly used for the second step of the reaction. In the second step the chloroborane was added slowly at - 60 °C to 2 eq. ethyl pyruvate with 1.5 eq. DABCO as base in abs DCM and slowly warmed up to RT analogue to the synthesis of the silanoxy compounds. After evaporation of the solvent, the residue showed no signs of doublebonds in the NMR.

As dicyclohexyl chloroborane was commercially available and this compound is thermally stable, the reaction with pyruvate was also tested with this organic chloroborane. Therefore, 1 eq. of a commercial solution of dicyclohexyl chloroborane was slowly added to a solution of 1 eq. ethyl pyruvate and 1.1 eq. DABCO at -60 °C under inert atmosphere analogue to the silanoxy compounds. After evaporation of the solvent again no doublebonds were found in the crude product.
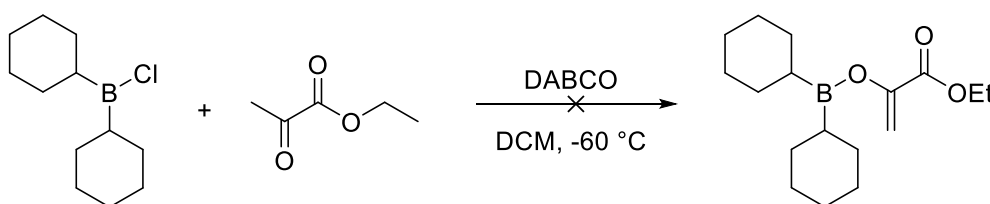
It seems to be very likely that the ethyl pyruvate never reacted, as the formation of a boronic salt with the base is very likely. This salt is then unreactive towards nucleophiles as the boron is negatively charged.
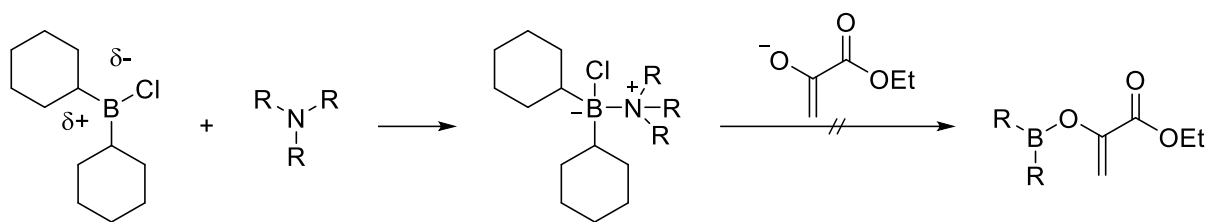
To avoid basic conditions it was reasonable to use the TMS trapped enol which can be insitu deprotected by potassium fluoride and crown ether.[152, 153]
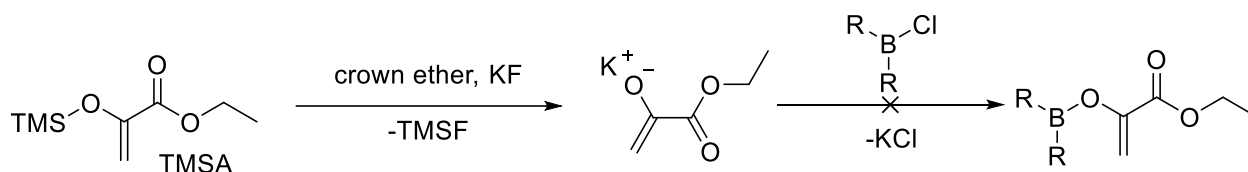
As already shown the stable TMS enolether TMSA can be easily prepared from ethyl pyruvate and TMSCl. In the next step the enol was added dropwise to a solution of chloroborane, crown ether and potassium fluoride in DMF at 50 °C and stirred for three hours. After extraction with ethyl acetate the solvent was removed in vacuum and the residual oil showed no double bonds in NMR.

This was the case for pinacolo chloroborane as well as for the dicyclohexyl chloroborane.

The synthesis routes were also repeated with the dicyclohexyl boron triflate which was prepared analogue to the supersilyl triflate, in the hope that reactivity can be improved but also in this case no product could be isolated.

It seems that boron compounds are very instable and also the chemical procedures cannot be directly transferred from silicon and carbon based chemistry. As it was unclear if the boron compounds are stable at all and no synthesis pathway could be found, no further synthesis with boron compounds was done.

1.2.3. Synthesis of sulphur oxy ethyl acrylates

In literature, alkyl and aryl sulfenates are found. Sulfenates are isomeric to sulfoxides and could be an interesting functional group for CTAs as the radical resulting from irreversible cleavage is well known from thiol-ene chemistry.
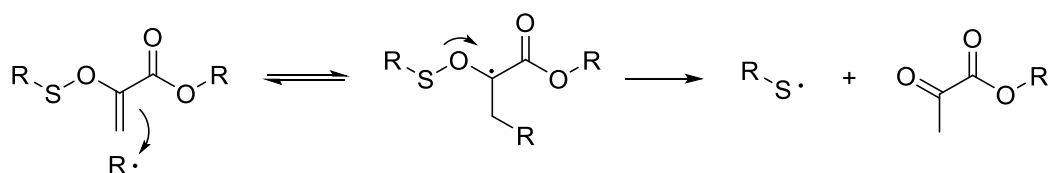
The stability of sulfenate esters is questionable, as it is known that such compounds tend to rearrange to sulfoxides.[154]
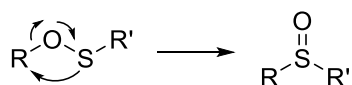
For a synthesis attempt, first phenyl sulfenyl chloride (**15**) was synthesized by refluxing 1 eq. diphenyl disulphane in 2 eq. sulfuryl chloride.[155]
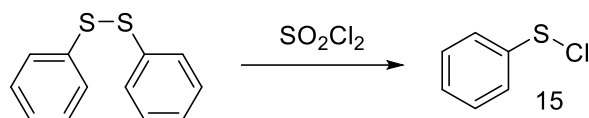
After removal of excessive sulfuryl chloride, 40% of theory sulfenyl chloride (**15**) can be distilled as blood red metastable liquid. Decomposition of the distillate in the freezer overnight leads to a yellow solid and gas formation. So 1 eq. freshly distilled sulfenyl chloride was added to a cooled solution of 1 eq. ethyl pyruvate with 2 eq. DABCO in dry DCM resulting in a black tar of unidentifiable composure.
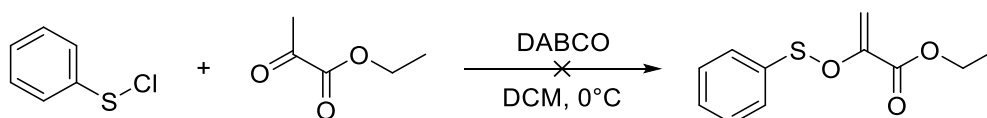
Either stability of sulfenate esters is too low or the desired compound never formed, however no product could be isolated.

Further literature research showed that sulphur monochloride (S_2Cl_2) readily reacts with alcohols to form stable oxy disulphides (R-O-S-S-O-R). More than hundred stable oxy disulphides were found, including propinyl or allyl derivatives.[156] As no enol-like structures were found, it was interesting to test if sulfur monochloride can also react with enols to form enoxy disulphides.
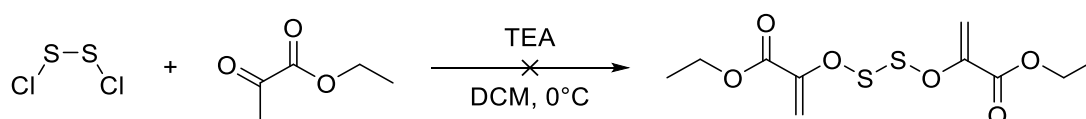
Therefore, 1 eq. sulphur monochloride was added to a cooled solution of 2 eq. ethyl pyruvate and 4 eq. trimethylamine in dry DCM.[157] Unfortunately, also in this case a black tar was formed that showed S_8 rings in GC-MS. No traces of product were found in NMR or GC-MS.

1.2.4. Synthesis of phenyl oxycarbonyl ethyl acrylate (PCA)

It was also considered to test new carbon centered AFCT reagents, as carbon based CTAs should be less problematic regarding stability and toxicity.

Structure derivatives of vinyl esters like benzoyl vinylester VE5 have shown disappointing results as chain transfer agents in previous work, due to the strong C-O ester bond that has to be cleaved.[139]
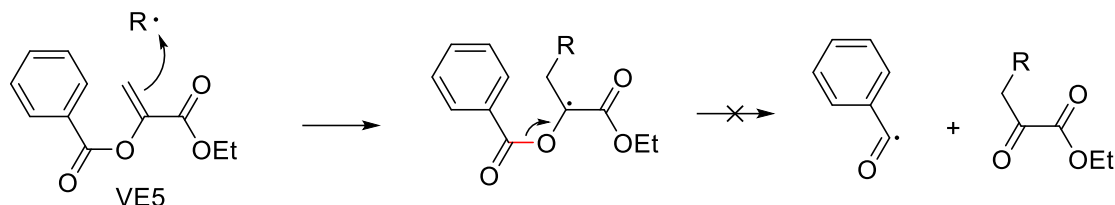
Alternative vinyl carbonate structures are easily available via chloroformates. E.g. Phenyl chloroformate. Only few similar structures are known from publications in the field of inorganic synthesis[158], but have never been tested as CTA. Decarboxylation of the intermediate radical could add a driving force to cleave the C-O bond of these vinyl carbonate based CTAs compared to vinyl esters.
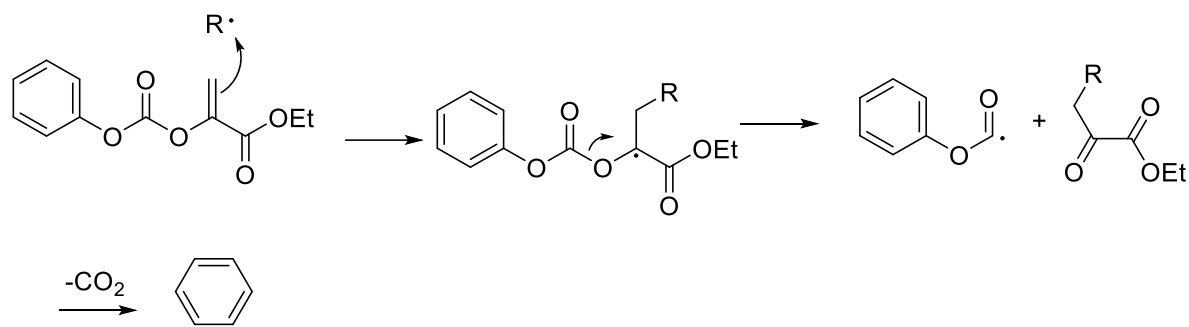
In first synthesis attempts 1 eq. ethyl pyruvate was enolised with 1.5 eq. DABCO or 1.5 eq. TEA in DCM and 1.1 eq. phenyl chloroformate were added dropwise while cooling analogue to the synthesis of vinyl sulfonates.[143] The mixture was then stirred overnight. Filtration and extraction with 1N HCl, bicarbonate and brine resulted in low yields with many side products, difficult to separate, after evaporation of the dried organic phase.
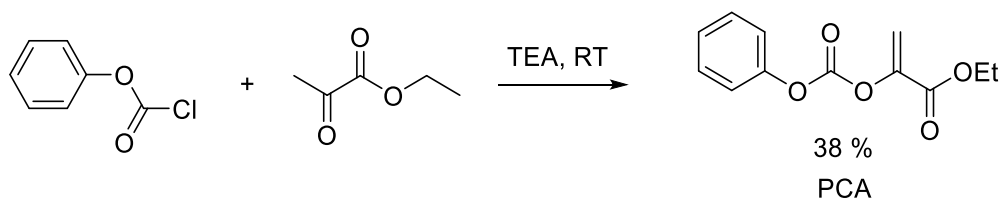
A very successful way to synthesize PCA was finally found, after testing different amine bases, by using a mix of 1.5 eq. pyridine and 1.5 eq. DABCO 1:1 as base. Probably due to the stronger

enolisation by DABCO and the catalytic effect of pyridine 90% yield could be achieved in less than an hour by the same procedure.

PCA
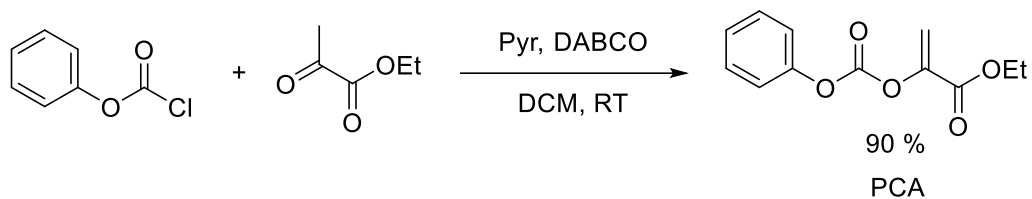
It was also tried synthesize an aliphatic tert-butyl vinyl ester and carbonate as, the lack of stabilization by phenyl groups could lead to more efficient cleavage of the leaving group. Therefore, pivalic acid chloride was added to ethyl pyruvate and triethylamine in dry DCM. Soon the solution turned yellow and precipitation of trimethylamine hydrochloride started. After 12 h the yellow mixture was extracted with 1 N HCl and saturated NaHCO₃ solution. After removing the solvent of the dried organic phase in vacuum, the crude product was examined by NMR and GC-MS. Unfortunately, the product was not stable or never formed and therefore could not be isolated as only traces were found.
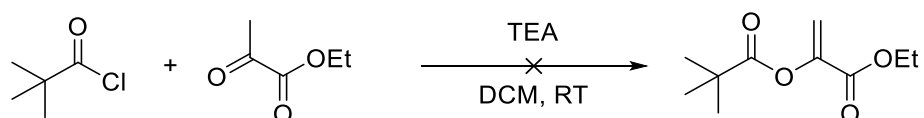
For the synthesis of tert-butyl vinyl carbonate, di-*tert*-butyl dicarbonate (diboc) was reacted with ethyl pyruvate under basic conditions with potassium carbonate. [159]
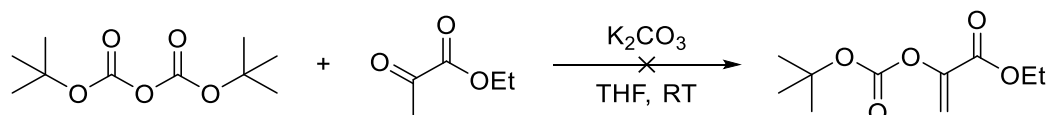
The potassium carbonate was suspended in dry THF and ethyl pyruvate was added. To the mixture, Diboc was added at once. After stirring for 12 h under argon at RT the solution was deeply brown and no desired product could be found after standard workup.

In the end only three new AFCT reagents were prepared successfully and could be further tested.

TMSA　　　　　SSA　　　　　PCA

VP2　　　　　VE5
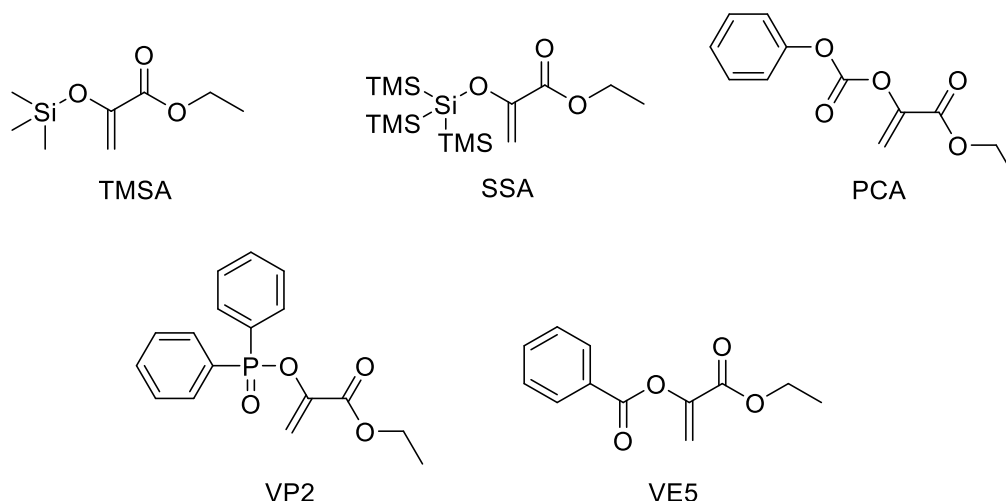
A vinyl phosphate from previous work was also included in the study, as it has not been examined in monofunctional systems before. Also the vinyl benzoate VE5 was tested as reference to the carbonate PCA. Both reagents were previously synthesized by Konstanze Seidler in the course of her thesis.[139]

1.3. Testing AFCT reagents in monofunctional systems

1.3.1. Photo-DSC

In a first study in monofunctional monomer, the reagents should be tested in a photo-DSC experiment. Monofunctional monomers form soluble linear polymers that can be further investigated by NMR and SEC studies. Benzyl methacrylate was selected as monomer as this compound has a high boiling pint of 276 °C and fewer disturbing NMR signals in the lower ppm scale.[142] In addition, the retention properties of poly-BMA are similar to polystyrene and therefore SEC can be measured with polystyrene standards to determine molecular weights. As photoinitiator 1 wt% of Ivocerin was used to guarantee efficient initiation with visible light, as the influence of UV light on the aromatic CTAs was unknown. To see a clear effect by the chain transfer agents it was decided to use 20 db% of additive.

After mixing chain transfer agents and initiator with the monomer, 12 ± 0.5 mg of sample were weighed into aluminum DSC pans and closed with a glass lid to prevent monomer and additives from evaporation.

TMSA   SSA   PCA

VP2   VE5
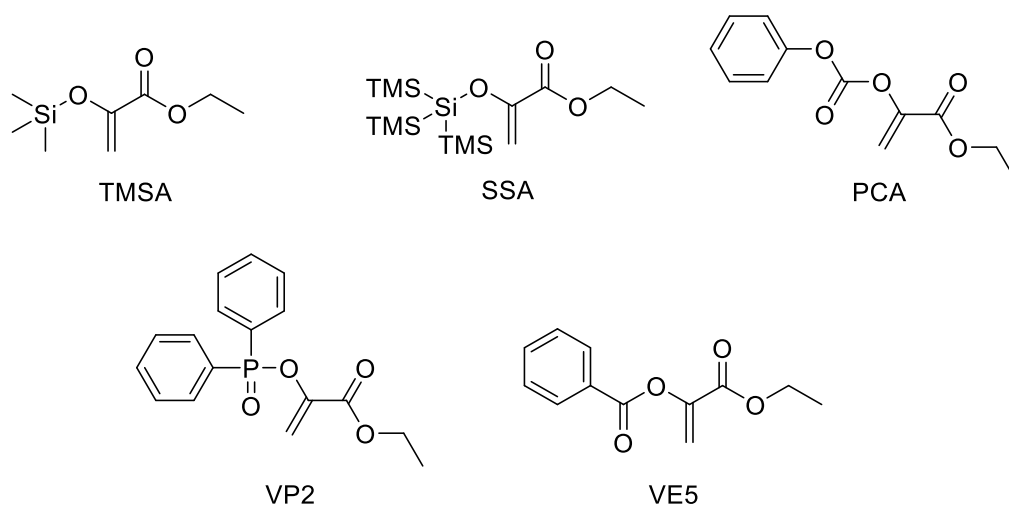
The samples were irradiated at 400-500 nm 1 W/cm^2 at the tip of the light guide twice for 300 s. The heat of polymerization was recorded against the time.
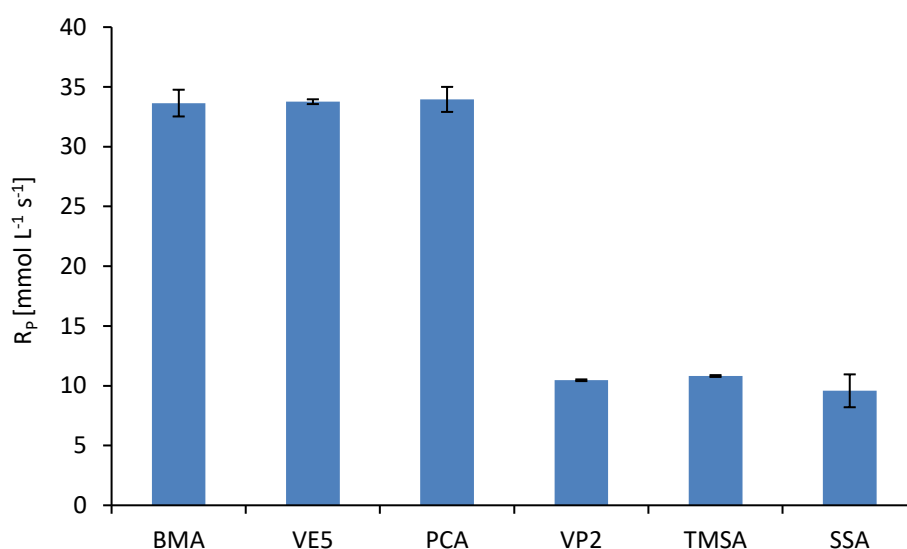
Figure 52. Rate of polymerization of BMA and mixtures with 20 db% additive

Already by comparison of the rate of polymerization great differences are visible in Figure 52. The CTAs with carbon based leaving groups, the vinyl ester VE5 and the carbonate PCA, barely have any influence on the rate of polymerization. But the formulations of CTAs with hetero atom based leaving groups, the phosphate VP2 and the two silyl compounds TMSA and SSA, cause an equal reduction of the rate of polymerization. As shown in Figure 53, this does not affect the time to reach maximal rate of polymerization t_{max} and the time to 95% overall DBC t_{95}. Only the trimethylsilyl compound TMSA showed both lower t_{max} and lower t_{95}.

116
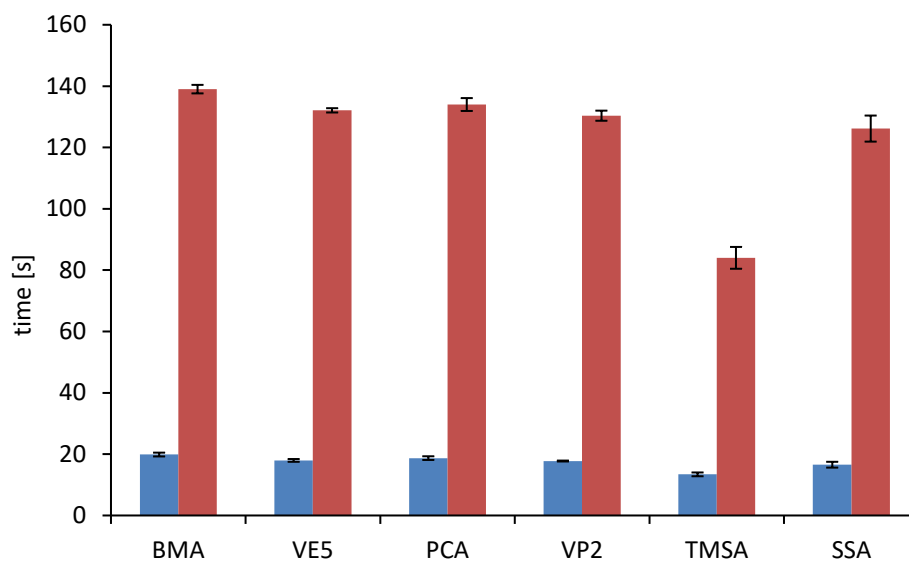
Figure 53. Time to maximal rate of polymerization (t_{max}) ■ **(blue) and time to 95%** ■ **(red) of overall double bond conversion (t_{95}) of BMA and mixtures with 20 db% CTA**

As could already be expected from the low rates of polymerization, the double bond conversion of the heteroatom based CTAs is significantly lower than that of the carbon based.
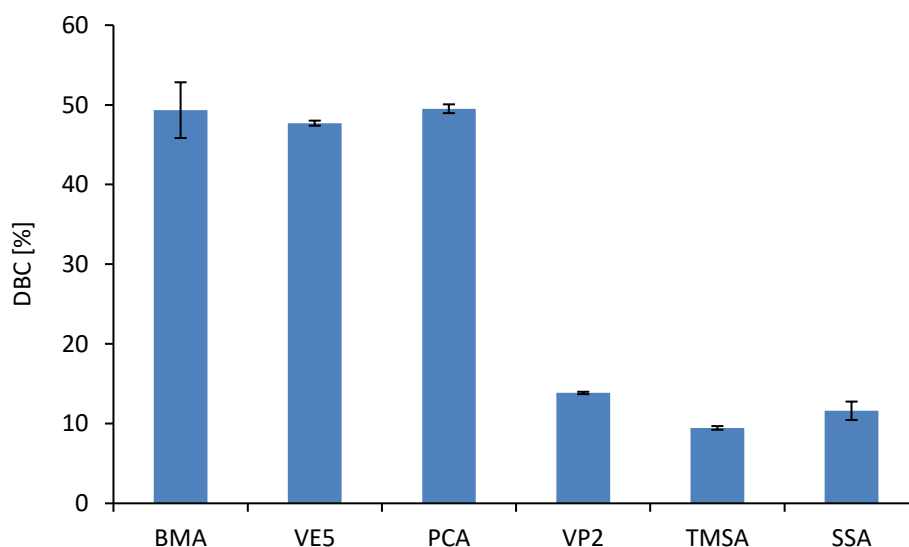
Figure 54. Double bond conversion (DBC) of BMA with 20 db% additive in comparison to neat BMA

Calculated from the heat of polymerization only about 10% conversion was reached. The other formulations of the vinyl ester VE5 and vinyl carbonate PCA reached similar conversions as neat BMA of 50%. This is disappointing, as it seems that the phosphate VP2 and the silyl oxyacrylates TMSA and SSA inhibit the polymerization of BMA. The chain transfer reactions were expected to be energy neutral.[37] (Figure 54)

1.3.2. NMR

As the heat of polymerization and chain transfer is unknown for the formulations with CTA and to see if the CTAs are consumed in an equal rate to monomer, NMR spectra were recorded of the resulting polymers. The spectra were compared to non-irradiated mixtures. By comparison of the standardized double bond signals, the conversion of BMA and CTAs was calculated. The conversion of VE5 could not be calculated separately from the monomer BMA as the double bond signals directly overlapped, therefore a combined conversion is shown.
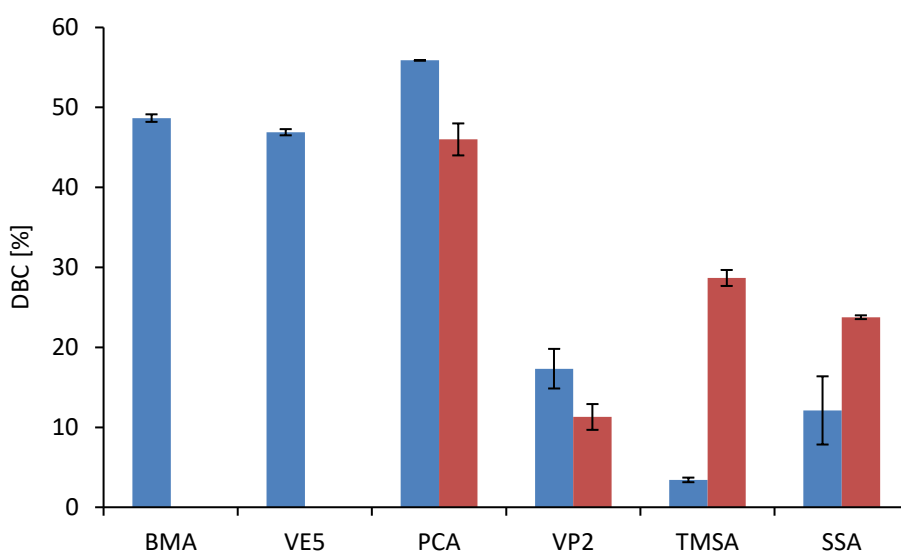
Figure 55. Conversion (DBC) of BMA ■ (blau) and chain transfer agents ■ (red) evaluated by [1]-H-NMR of resulting polymers from the DSC

The conversion of BMA calculated from NMR visible as blue bars in Figure 55, generally shows the same trend as the evaluation by DSC visible in Figure 54. Interestingly the formulation containing the carbonate PCA shows a little higher conversion of BMA in NMR than in DSC measurements, which indicated that the reaction with PCA is not entirely energy neutral causing an endothermic effect. The carbonate PCA is built into the polymer quite homogenously, as the conversion of CTA is also high and close to that of BMA. The vinyl phosphate VP2 shows low conversion of CTA and monomer. Therefore, it seems that this compound generally inhibits polymerization. In the case of trimethyl silyl compound TMSA the conversion of CTA is much higher than that of BMA. This means the heat of polymerization in the DSC measurements must derive from the CTA in case of this sample. 28% of CTA was consumed, while only 3% of monomer polymerized. It looks like the initiator radicals preferably react with TMSA, which mainly undergoes homo reactions. In the case of the more bulky silyl SSA the DBC of monomer was

significantly better with 12% but still twice as much chain transfer agent was consumed. This means that not only the polymerization is inhibited but also these silyl chain transfer agents are not consumed homogenously.

As almost no monomer was consumed in the case of the trimethyl silyl compound TMSA, the reagent was also irradiated with only initiator and no BMA present to see if homopolymerization or self-consumption occurs.
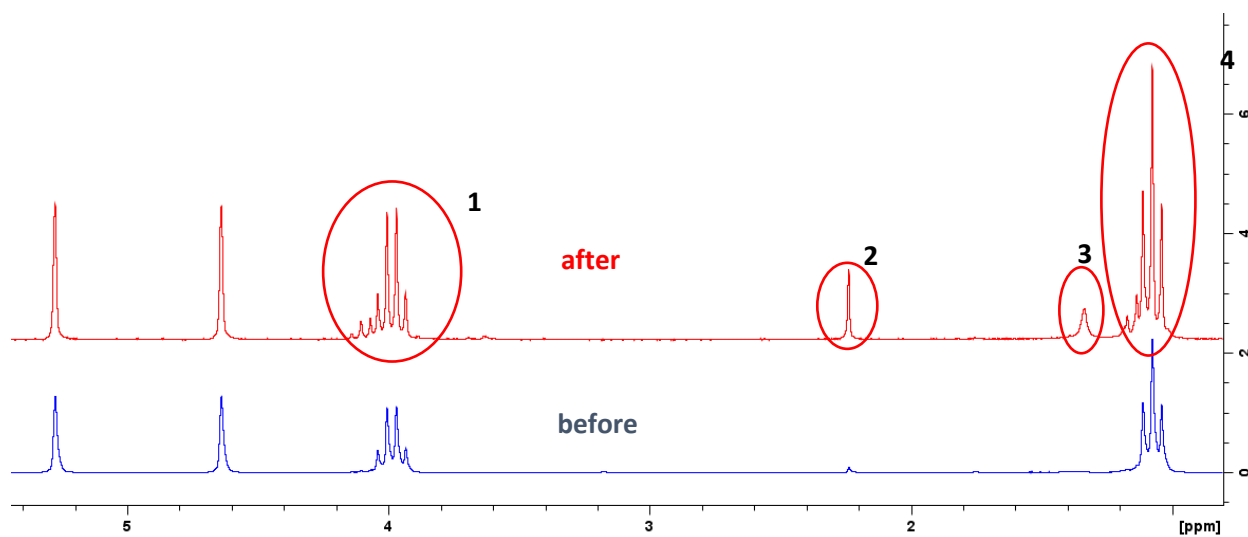
Figure 56. NMR of trimethyl silyl CTA TMSA with 1 wt% Ivocerin before and after 600 s irradiation at 400-500 nm

In case of silyl compound TMSA it seems, that a mixture of both homopolymerization and self-consumption is happening.

In Figure 56 signal 1 and signal 4 show new overlapping slightly higher shifted ester signals. These signals together with the new signal 2 indicate self-consumption, as shown in Scheme 24.
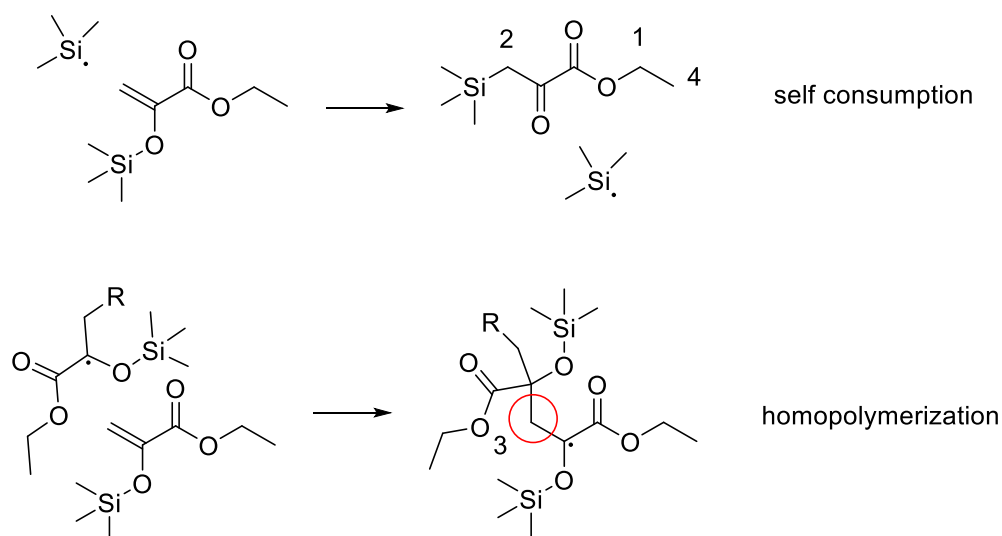
Scheme 24. Radical reactions of silyl acrylate TMSA leading to specific NMR signals

The singlet 3 in Figure 56 is an indicator for homopolymerization as it is shifted much lower. As the signal of self-consumption is bigger than that of the homo polymerization, it is highly probable that only oligomers are produced. The conversion is lower when no monomer is present, then the double bond conversion reaches only 18%.

It is interesting that the self-consumption mechanism cannot be suppressed by the presence of monomer, which is the case for vinyl sulfonates.[143] This can maybe explained by the much lower reactivity of silyl radicals in comparison to sulfonyl radicals towards methacrylate double bonds. Therefore, even at a concentration of 20 db% the polymerization is almost completely inhibited and only self-consumption and homopolymerization of the CTA takes place.

In the case of the bulky supersilyl SSA, no self-reaction could be found and significantly more polymerization of monomer took place. Probably the very bulky supersilyl radical is too sterically hindered to attack another CTA molecule. The consumption of CTA is still favored also in the case of SSA.

1.3.3. Size exclusion chromatography (SEC)

To see if the new CTAs are able to regulate the radical polymerization of benzyl methacrylate, the NMR samples were diluted with THF. From that samples size exclusion chromatography spectra were recorded on a THF SEC device with a refractive index detector and a styrene standard calibration.

From the chromatograms the number average molecular weight Mn and the polydispersity index PDI was determined.
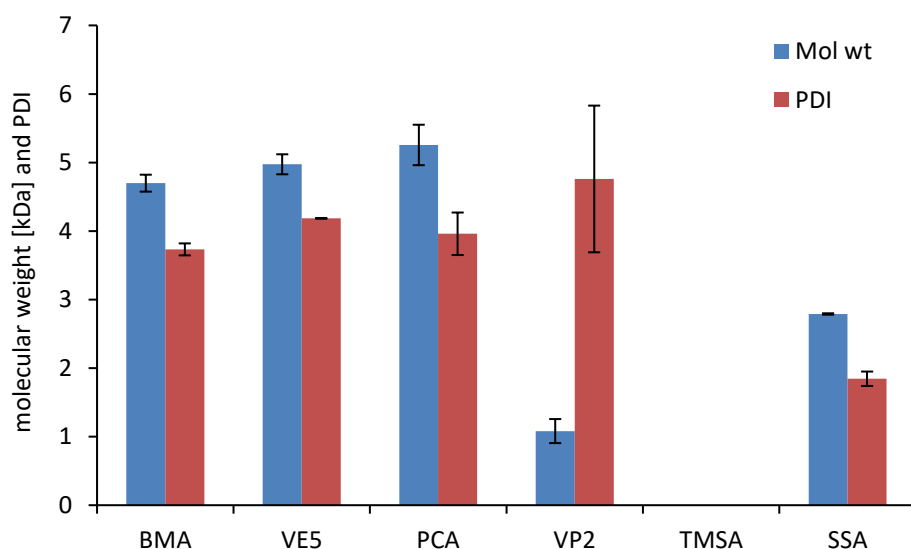
Figure 57. Molecular weight and polydispersity index (PDI) of resulting polymers from the DSC measurements.

As can be seen in Figure 57 the molecular weight of the carbon based CTAs VE5 and PCA is about the same or slightly higher than that of neat BMA. Also the PDI remains unchanged in these samples, which indicates that these compounds undergo copolymerization rather than chain transfer. The phosphate VP2 has no positive influence on the PDI but caused a massive reduction of the molecular weight. Therefore, it inhibits the chain growth but does not regulate the polymerization. The formulation of trimethyl silyl compound TMSA did not yield any polymer. This could be expected, as there was almost no polymerization of BMA visible in NMR.

The only reagent that showed some regulation is the super silyl compound SSA. The molecular weight was almost bisected and the PDI was reduced to only 1.8, which is surprisingly low.

1.4. Testing AFCT reagents in difunctional systems

To see how the network formation in difunctional methacrylates is influenced by the new compounds, a mixture of dental methacrylates D3MA and one equivalent UDMA was prepared (DMM). The CTAs were used in a concentration of 20 db%, with 0.3 wt% Ivocerin as initiator.

methacrylate system:

UDMA

D$_3$MA

1:1 molar mixture = DDM

Ivocerin
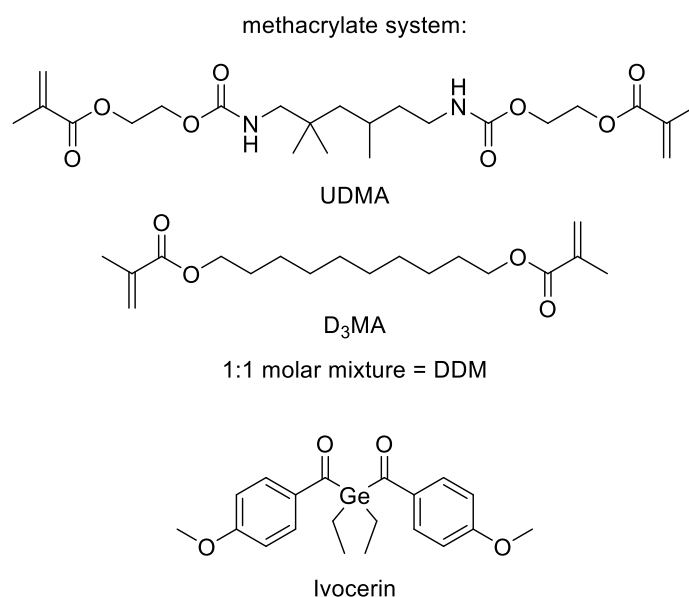
1.4.1. RT-NIR photorheology

For further investigation of the new CTAs, coupled RT-NIR-photorheology measurements were conducted. By coupling of RT-NIR spectroscopy with photorheology a very potent tool is created, that can be used to characterize the photopolymerization of resins. From these measurements the time until gelation (t_G), conversion at gel point (DBC$_G$), final conversion (DBC) and shrinkage stress (normal force measurements, FN) can be obtained. By combination of these parameters a polymerizable system can be deeply investigated.

120 µl of the formulations were irradiated on a RT-NIR photorheometer at 400-500 nm at 0.5 W/cm^2 for 300 s at a constant gap of 100 µm with a deflection stress of 1% at 1 Hz. The storage modulus G' and loss moduls G'' as well as the normal force were recorded with time. At the same time IR-spectra of the curing formulations were recorded to determine the DBC with time. From the intersection of G' and G'' the gel point was determined.

In Figure 58 examples of conversion curves of the dimethacrylate mixture DMM with and without CTAs is shown versus the time. As in the measurements with the monofunctional system, great differences can be seen between the formulations containing carbon centered CTAs and the hetero atomic compounds. Both the vinyl ester VE5 and the carbonate PCA increase the double bond conversion slightly from 72.2 ± 0.1 for neat DMM to 77.5 ± 0.4 and 79.6 ± 0.5 respectively. The effect is stronger for the mixture with the vinyl carbonate PCA, which also shows a little delay in the onset of polymerization.
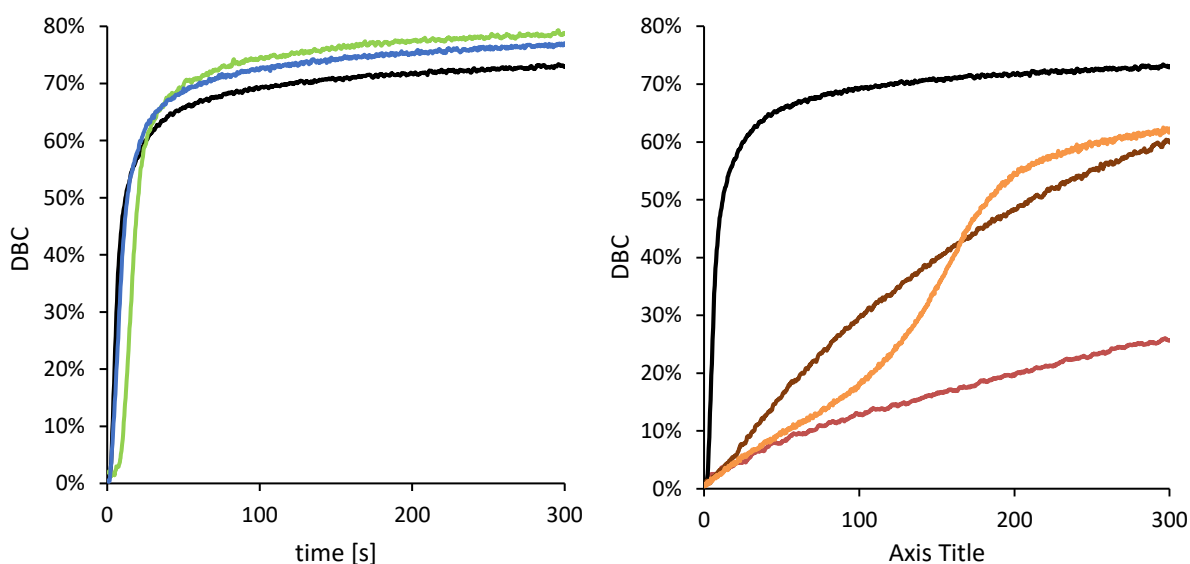
Figure 58. Double bond conversion DBC versus time of dimethacrylate DMM with 20 db% of chain transfer agents calculated from RT-IR: — DMM neat, —VE5, —PCA, —VP2, —TMSA, —SSA

As could already expected from DSC measurements the formulations containing the heteroatom CTAs show massive retardation in curing compared to neat methacrylate DMM and generally reach lower conversions. The polymerization of the phosphate formulation VP2 is the slowest and only reaches 26.2 ± 0.6% DBC. Adding 20 db% of trimethyl silyl compound TMSA slows down the polymerization in the beginning, but probably when all CTA is reacted the polymerization speed increases and a final conversion of 62.0 ± 1.2 can be achieved. The super silyl compound SSA shows constant but also slow polymerization and achieves 62.8 ± 1.4% DBC.

Looking at the time to gelation t_G in Figure 59, the same trend is visible. The neat methacrylate DMM shows very fast gelation, after only 4.0 ± 0.2 s the formulation is solid. The vinyl ester VE5 does not influence the time to gelation much and reaches nearly the same value with 5.1 ± 0.1. The carbonate PCA causes a delay in gelation, which can be explained by the delayed onset of polymerization. The formulation reaches solid state after 12.3 ± 0.1 s.

Due to the much slower polymerization the hetero CTAs cause a massive retardation of gelation. The phosphate is the slowest with 125 ± 2 s. The formulation containing trimethyl silyl CTA TMSA is faster and gels after 63 ± 1.3 s. The fastest hetero CTA mixture is the super silyl formulation which reaches the gel point after 42 ± 3.5 s.
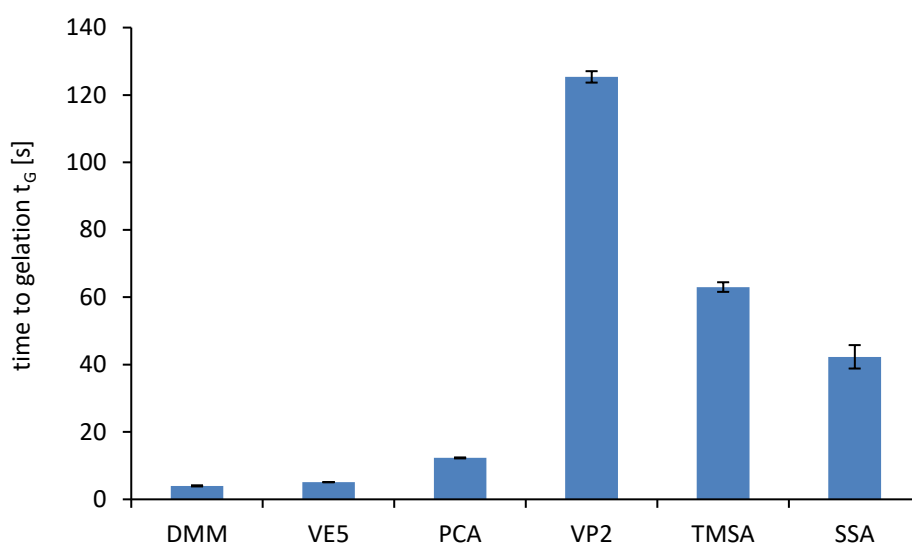
Figure 59. Time to reach the gelpoint t_G of the neat formulation DMM and the formulations containing 20 db% of CTA

In an optimal case of chain transfer, gelation is not delayed but shifted to higher conversions. Therefore, the double bond conversion at the gel point DBC_G was determined and plotted in Figure 60.

Only the carbonate PCA was able to shift the gel point to a little higher conversion. The effect is not very strong, but could indicate that PCA acts as chain transfer reagent in difunctional systems.
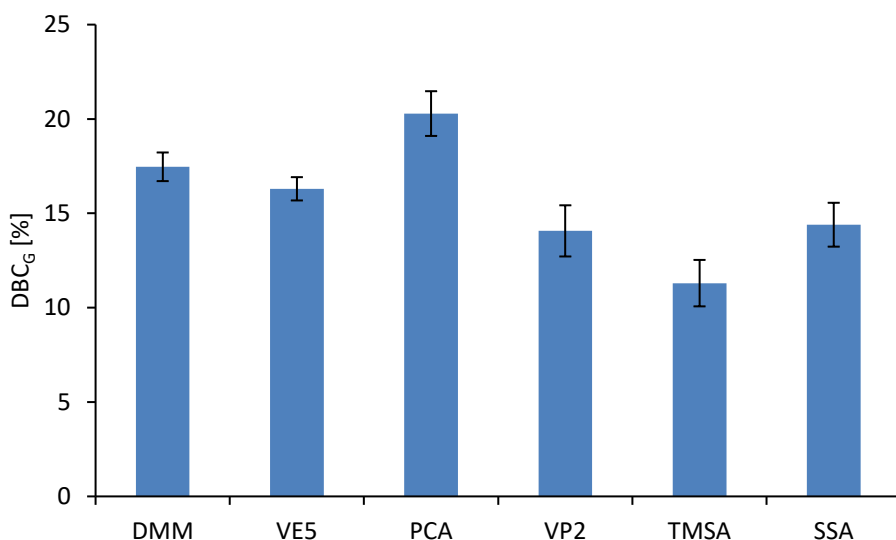
Figure 60. Double bond conversion at the gel point DBC$_G$ of the neat formulation DMM and the formulations containing 20 db% of CTA

The hetero CTAs show lower DBC$_G$ than the neat DMM. This can maybe explained by the very slow polymerization, giving the system more time to form a gel and therefore reach the point of gelation at lower conversion. This indicates that the phosphate and silyl compounds do not act as chain transfer agents at all.

The same trend is visible at Figure 61 where the time to 95% of DBC is shown. Interestingly vinyl ester VE5 and vinyl carbonate PCA accelerate the curing of these formulations in comparison to neat methacrylate DMM. Considering the higher DBC of these formulations, the curing is definitely improved by these substances. It could be that the carbon centered CTAs are acting as reactive diluent and the small monofunctional compounds stay mobile even up to higher conversions. The hetero CTAs show the expected delay of polymerization.
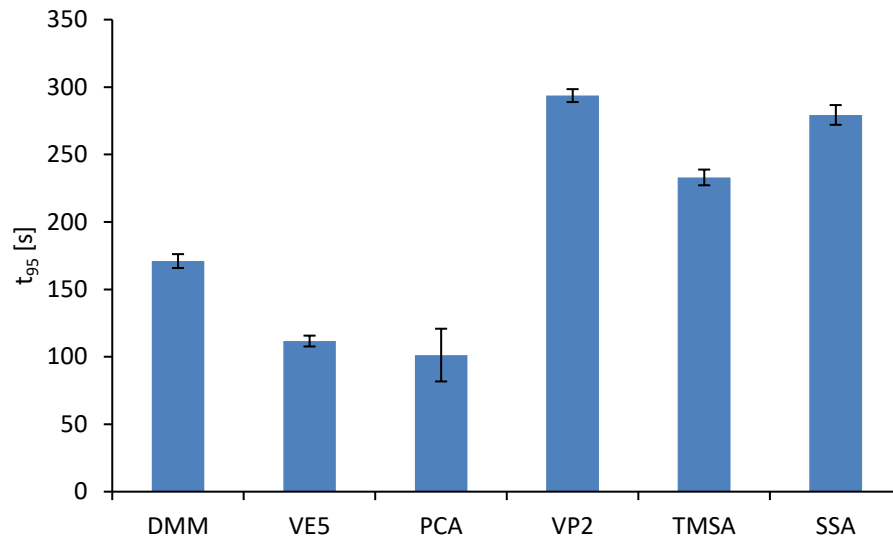
Figure 61. Time to 95% overall DBC t_{95} of the neat formulation DMM and the formulations containing 20 db% of CTA

Also the mechanical properties and shrinkage behavior show great differences depending on which reagent was used.

Unfortunately the shrinkage stress, measured as normal force on the rheometer plate, is not reduced significantly by the carbon centered CTAs. (Figure 62 and Figure 63)
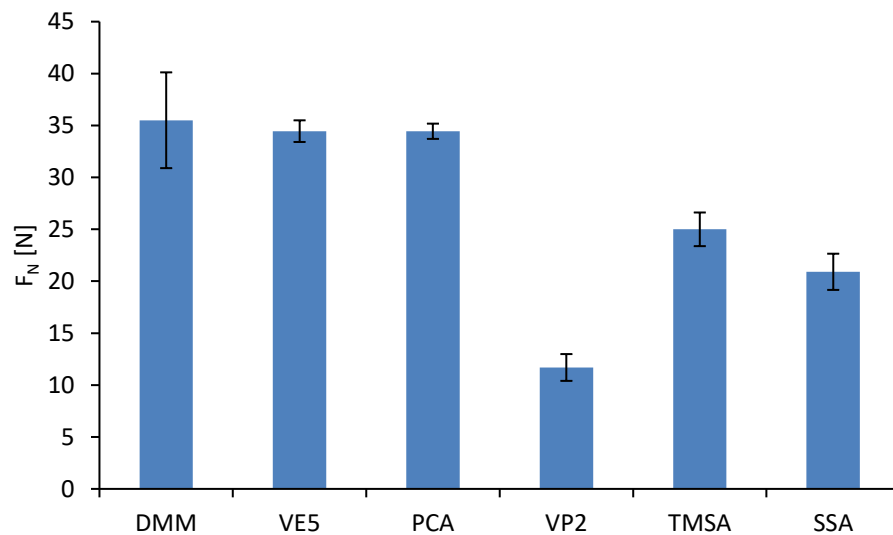
Figure 62. Maximal normal force F_N developed by the neat formulation DMM and the formulations containing 20 db% of CTA

Due to the slow and incomplete polymerization of formulations containing vinyl phosphate or silyl compounds, the shrinkage stress is reduced in these samples. The slow polymerization and therefore slow development of stress is clearly visible in Figure 63.
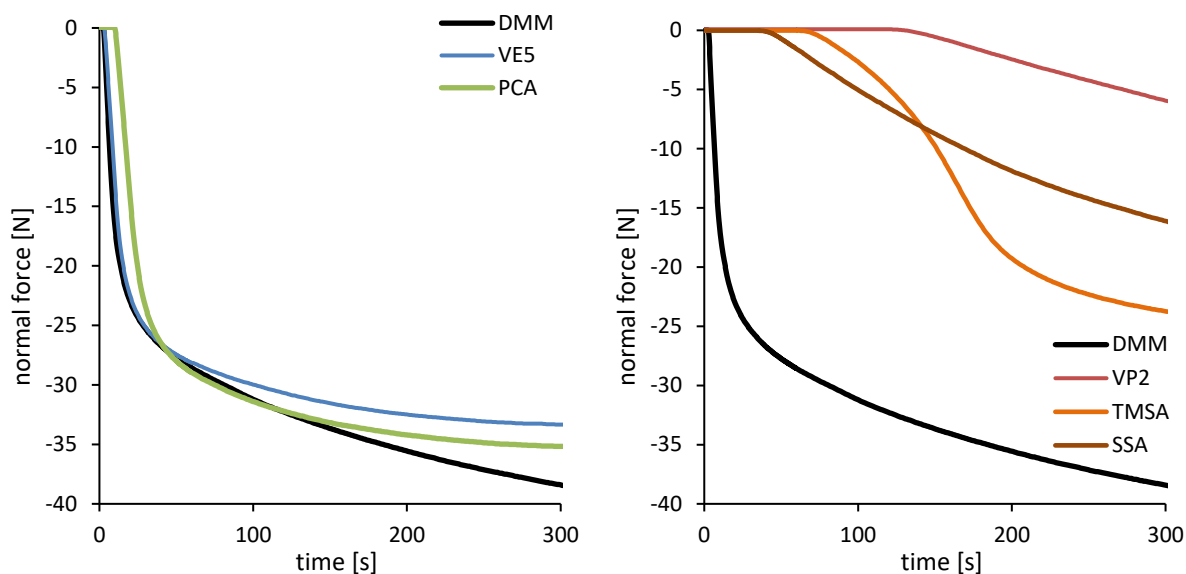
Figure 63. Normal force F_N of the neat formulation and the formulations containing 20 db% of carbon-centered CTAs —VE5 and —PCA (left) and the formulations containing 20 db% of hetero atom CTAs phosphate —VP2, trimethyl silyl compound —TMSA and supersilyl compound —SSA

The final storage modulus G' of networks containing carbon centered CTAs, VE5 and PCA, is comparable to the neat DMM polymer. The measurements of VE5 show some delamination from the rheometer plate, therefore the measured modulus drops after about 150 s. (Figure 64, left diagram)
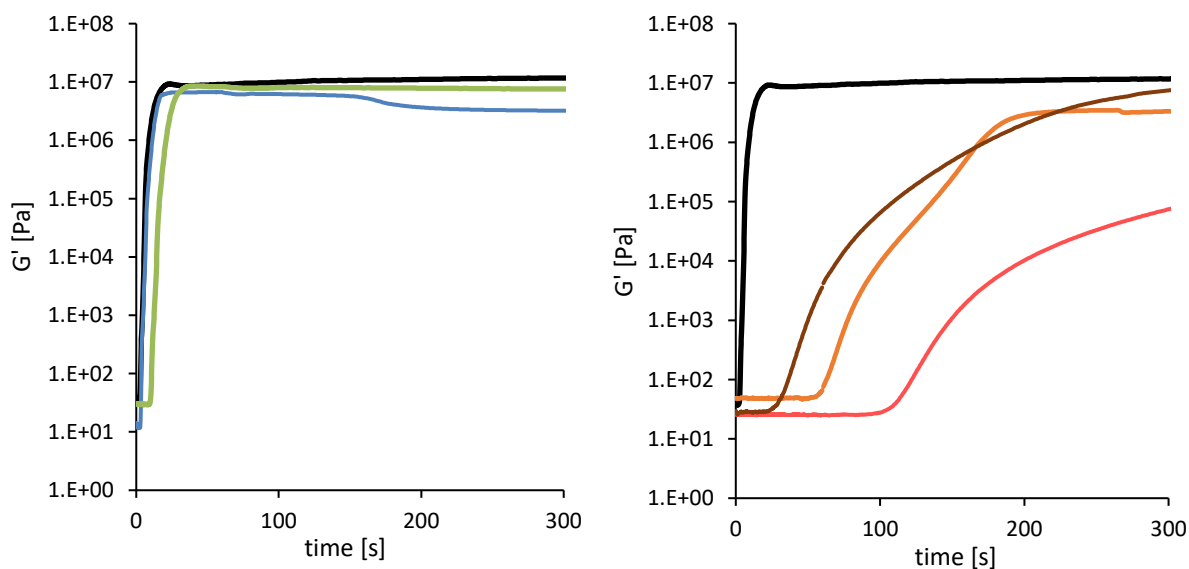
Figure 64. Storage modulus G' measured by rheology of the neat formulation —DMM and the formulations containing 20 db% of carbon-centered CTAs —VE5 and —PCA (left) and the formulations containing 20 db% of hetero atom CTAs phosphate —VP2, trimethyl silyl compound —TMSA and supersilyl compound —SSA (right)

The formulations containing vinyl phosphate VP2 and trimethyl silyl compound TMSA reach significantly lower moduli than the neat polymer DMM. Only the sample with supersilyl CTA SSA reaches a similar G' as the unmodified network.

1.4.2. Dynamic mechanical thermal analysis (DMTA)

Dynamic mechanical thermal analysis of duromeric networks can give a lot of information about the architecture of a network. Therefore, sample sticks (1.5 x 5 x 40 mm) were prepared in a silicon mold at 400-500 nm blue light irradiation, containing 20 db% regulator together with 1 wt% initiator and were compared to the unmodified DMM network.

During DMTA measurements, the sample bars were heated from -100 °C to 200 °C while torsion strain of 1% at 1 Hz was applied to the material. The storage modulus G' and dissipation factor tan δ were recorded with temperature.

In Figure 65 the storage modulus and dissipation factor tan δ of the different networks is plotted versus the temperature. In the left diagram the carbon centered CTAs are compared with the unmodified methacrylic network DMM. The neat polymer shows a typical broad glass transition of highly cross-linked duromers. The glass point T_G can be defined as the maximum of the dissipation curve tan δ. In case of DMM the maximum of the extremely broad transition is at 150 °C with an FWHM of 155 °C. The network containing vinyl ester VE5 shows similar properties at room temperature (25 °C), but a higher modulus is visible at elevated temperatures. The mixture with VE5 reaches the glass point significantly later than the neat polymer at about 170 °C. Also the glass transition is much sharper with an FWHM of only 60 °C. It seems like VE5 is acting as T_G modifier as this reagent just copolymerizes and does not regulate the polymerization. Due to the high rigidity of the bulky phenyl group, the modulus is increased and the glass transition is shifted to higher temperatures.

The network modified with vinyl carbonate PCA shows similar properties as the unmodified network up to 90 °C then a rather sharp glass transition is visible that reaches its maximum at the glass point at 145 °C. The FWHM is rather narrow with 50 °C.
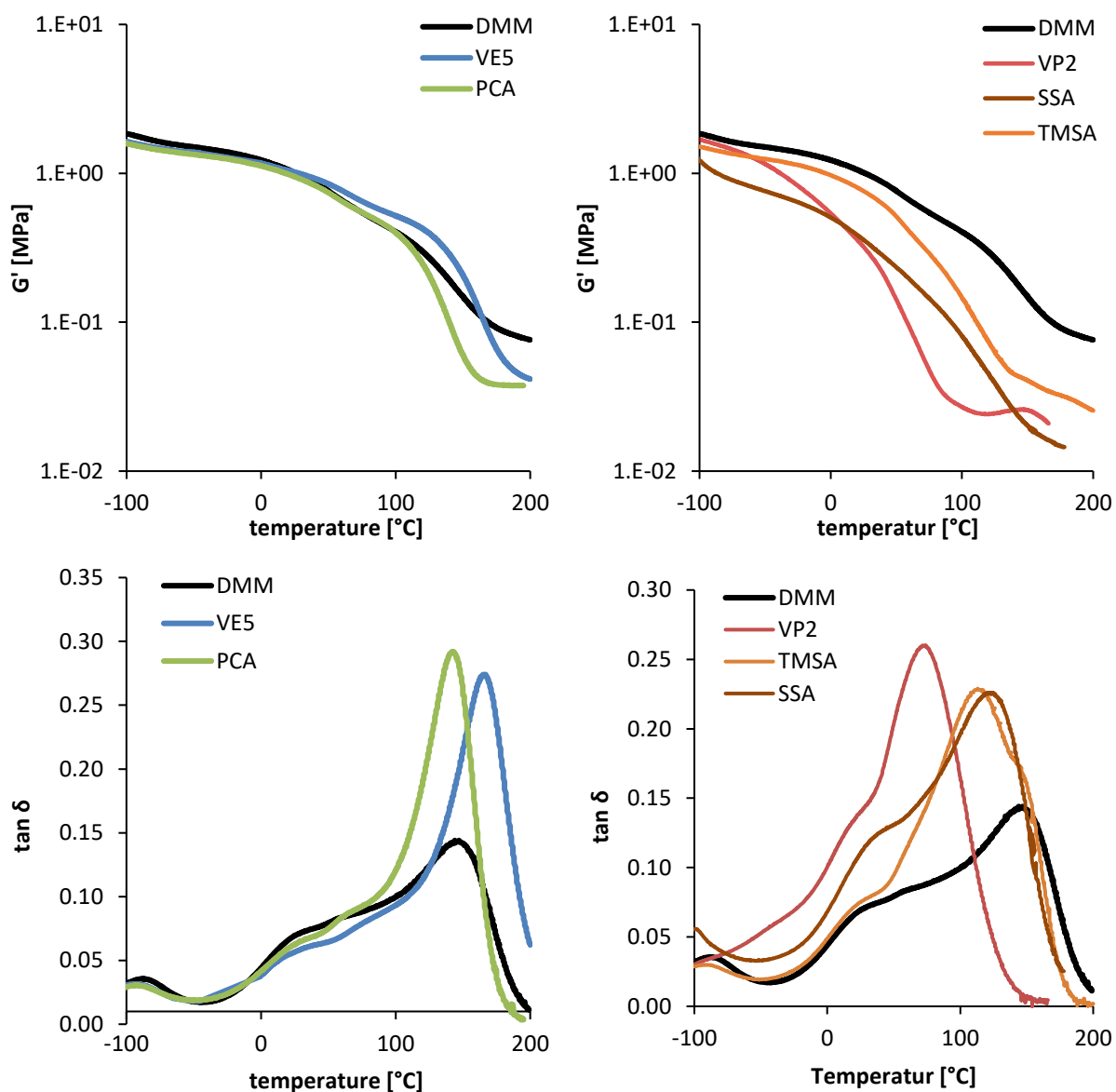
Figure 65. Storage modulus G' and tan δ of the neat formulation —DMM and the formulations containing 20 db% of carbon-centered CTAs —VE5 and —PCA (left) and the formulations containing 20 db% of hetero atom CTAs phosphate —VP2, trimethyl silyl compound —TMSA and supersilyl compound —SSA (right)

All formulations with hetero atoms show a lower modulus over the whole temperature range. As can be seen in the right diagrams of Figure 65, the vinyl phosphate VP2 shows a low glass transition temperature of only 69 °C with a broad FWHM of 90 °C. This is or sure caused by incomplete conversion, which results in a softer network. Also the polymer with trimethyl silyl compound TMSA shows a lower glass transition temperature of 118 °C with an FWHM of 96 °C. The broad glass transition and the lowered modulus makes it clear that this substance is not regulating the network, which could already be expected.

The storage modulus of the network containing 20 db% supersilyl compound SSA exhibits a much lower modulus than the neat polymer of DMM. The T_G is at 128 °C and the broadest with an

FWHM of 130 °C. Also it is visible, that more than one tan δ peaks are overlaying each other, indicating a very inhomogeneous network.

In conclusion the carbon centered CTAs showed high reactivity and build into the network homogenously. It seems that the vinyl ester VE5 is just copolymerizing, but acting as T_G modifier leading to higher T_G and sharper glass transition. The carbonate PCA could improve the DBC_G and also the overall conversion. The material showed a significantly sharper glass transition in the same range of the neat material but the shrinkage force is not reduced significantly. Tests in monofunctional methacrylate BMA did not show evidence of chain transfer as the molecular weight and polydispersity was not changed by carbonate PCA. Therefore, it is likely that also this reagent acts as reactive diluent and not as CTA.

All hetero CTAs showed massive retardation of the polymerization and caused significantly lower conversion. Only the supersilyl CTA SSA showed some evidence of regulation in monofunctional systems and reached acceptable conversion and modulus in the difunctional monomer DMM. Due to the lower conversion and slower polymerization this CTA was able to reduce the shrinkage a lot, but DMTA revealed that the material regulated by SSA was much softer and inhomogeneous than the neat network.

2. Hydrogen abstraction fragmentation chain transfer (HAFCT)

2.1. State of the art

Thiol-ene chemistry is based on well abstractable hydrogens in thiols. With this well applicable method, high yields, high reaction rates, sharp glass transitions, high tolerance in oxygen inhibition and the possibility of visible light polymerization can be achived.[160]

As one of the most influential chemist in the field of thiol-ene chemistry, Hoyle and his co-authors presented this radical mechanism as an improvement for methacrylate based photocurable formulations. Instead of classical radical polymerization, thiol-ene systems show a mixed chain growth/step growth reaction. The combination of the addition of a thiyl radical to an ene-group and the hydrogen transfer to chain end carbon radicals are the base of the thiol-ene step growth reaction. (Scheme 25)
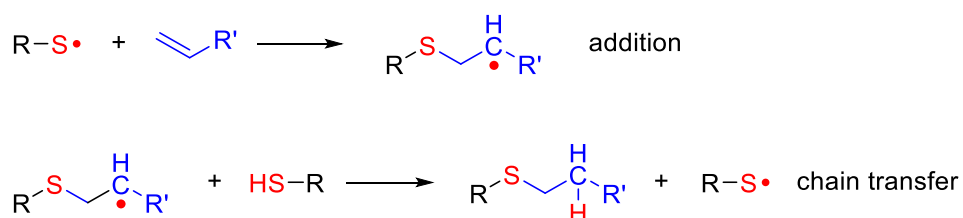
Scheme 25. Thiol-ene chain transfer reaction by hydrogen abstraction

Of course, the formed carbon radical can also continue normal radical chain growth. (Scheme 26) Which of the reactions is the more preferred, depends on the chemical structure and concentration of the monomer and thiol groups.
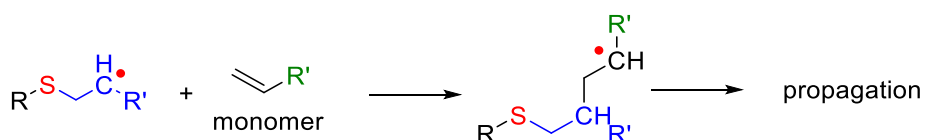
Scheme 26. Normal radical chain growth reaction

By combining monomers, thiol compounds and concentrations, the polymer network architecture and properties are adjustable on a wide range. This would not be possible with conventional radical photopolymerization.[40] With thiol-ene reaction it comes to a shift of the gel point to higher conversions, which reduces the network inherent shrinkage forces and generally leads to high overall conversions of double bonds. Rapid photo-induced polymerization, forming homogenous polymer networks, with sharp glass transition temperature and high impact strength, is possible by thiol-ene chemistry. These are good arguments for using thiol-ene systems is the field of photopolymerization to improve mechanical properties of photomaterials.

On the other hand, using thiols entails some major drawbacks. Thiols show more or less strong odor and tend to colorize polymers with aging. As well, premixed thiol formulations show a low shelf life and tend to polymerize during storage, even if stored in a fridge under exclusion of light.[161] Although toughness can be significantly improved, the highly flexible thioether bonds in the network reduce the young's modulus of the resulting materials.

To circumvent the drawbacks of thiol-ene technology other elements were already tested as hydrogen donor.

In the chase of phosphorus, thiols are replaced with phosphorus compounds carrying abstractable hydrogens. The principle is the same as for thiol-ene chemistry. Hydrogens can be easily abstracted from phosphorus compounds. But unlike thiols there are various phosphorus compounds available in different oxidation states that carry hydrogens. The oxidized compounds can also contain a sulphur double bond instead of oxygen.

| phosphanes | phosphinites | phosphinites | phosphane oxides | phosphinates | phosphonates |
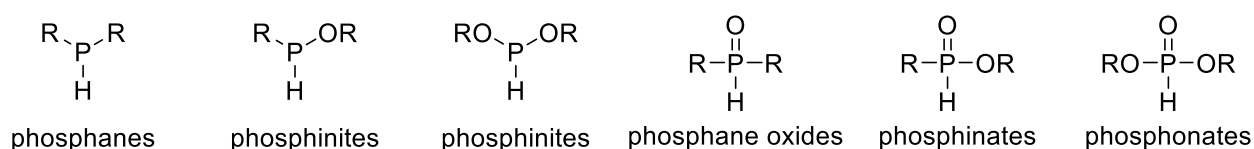
As can be seen in Scheme 27 the polymerization cycle with phosphonate-ene chemistry is similar to thiol-ene chemistry. [162]
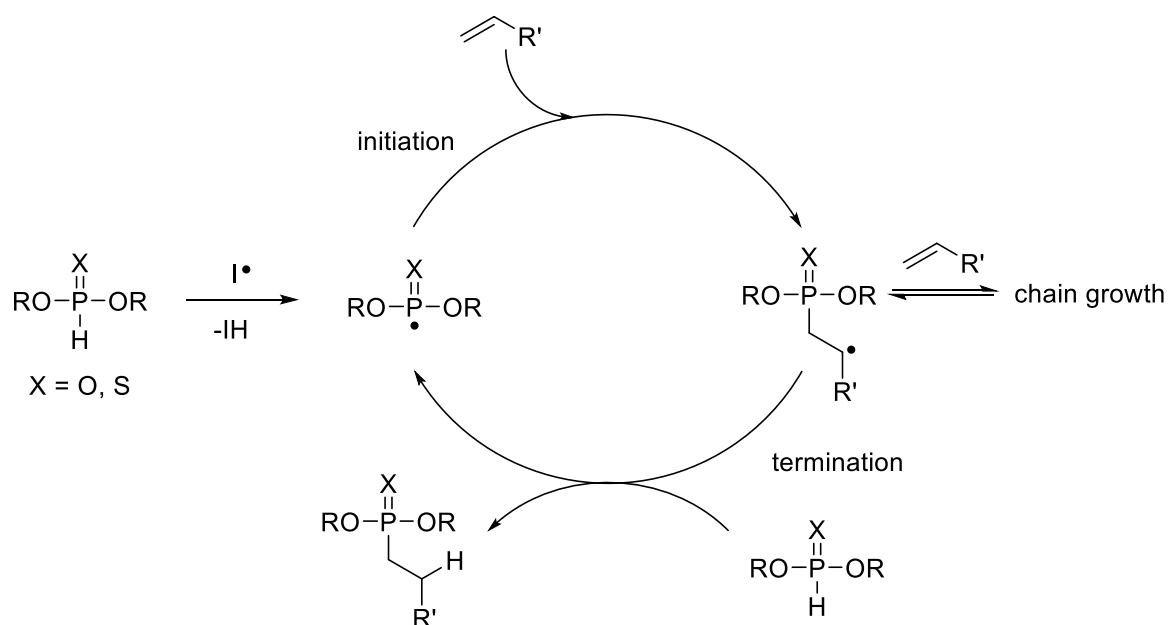
Scheme 27. Mechanism of hydrophosphonylation

After a polymerization was started with an initiator or phosphonate radical chain growth takes place until a hydrogen is abstracted from a phosphonate and the chain is terminated. The

phosphonate radical is then efficiently reinitiating polymerization. By modifying and selecting the phosphorus compound a wide variety of reagents are available.

Phosphanes carrying two hydrogens can even undergo abstraction reactions twice and phosphane end groups can be modified after polymerization changing mechanical properties for example by oxidation. Also ^{31}P atoms are well detectable by (solid-state) NMR and offer a lot of information about the chemical structure of a polymer.[163]

Unfortunately aromatic phosphanes are too unreactive for radical polymerization due to high stabilization of the intermediate radical. Also un-oxidized phosphorus compounds are very sensitive towards oxidation and have to be handled in inert atmosphere. Formulations tend to polymerize spontaneously under air and therefore show a short shelf life. [163]

In the end the strong odor, volatility and often high toxicity of phosphorus containing hydrogen donors limits application drastically.

Also group 14 element hydrides (R$_3$MeH) of Si, Ge and Sn can be used as chain transfer agents similar to thiol-ene reactions.[164] Unfortunately organo tin hydrides are extremely toxic and therefore are not usable for industrial application in more than catalytic amounts.

Germanes are nontoxic and germyl radicals are very efficient initiating radicals.[165] Keeping in mind that germanium is a very expansive element, germanes can be used in small amounts for photoinitiaiting systems but not as additive in a two digit percentage scale.

Interestingly also much cheaper silanes can also be used as hydrogen donors and were already deeply investigated. (Scheme 28)
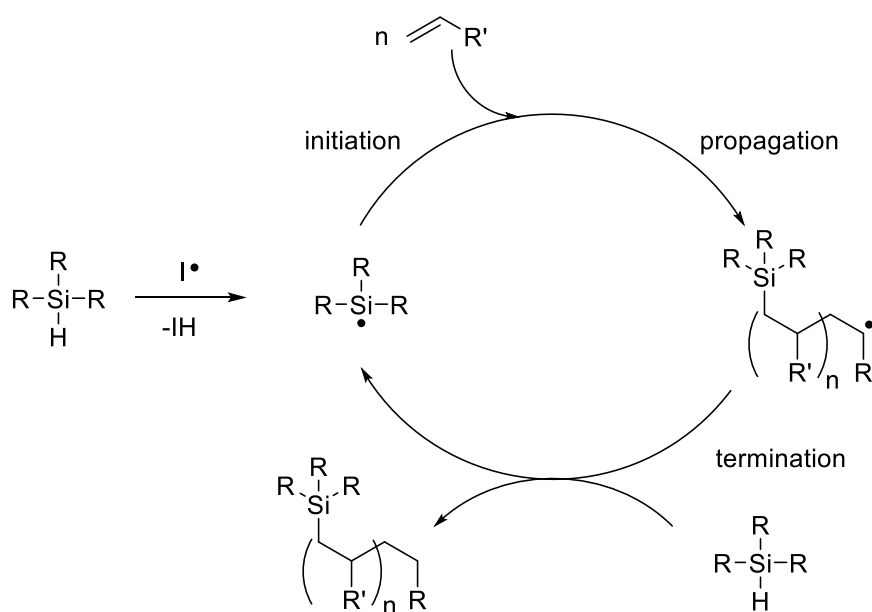
Scheme 28. Mechanism of silane-ene reaction

A silane-ene mechanism was first mentioned in 2008 by Allonas' group. They found out that silyl radicals are very reactive towards electron rich and poor alkenes and mentioned that the reaction is surprisingly insensitive to air.[166] As oxygen inhibition is a huge problem in industrial applications when it comes to polymerize thin layers, this is a big advantage of silane-ene chemistry. The complex reaction can be seen in Scheme 29. Besides chain transfer silanes can terminate unreactive peroxyl chain ends (4) and a silyl radical can also scavenge molecular oxygen. By rearrangement the oxygen is incorporated in the silicon compound (6) and a reactive radical species is generated.[167]
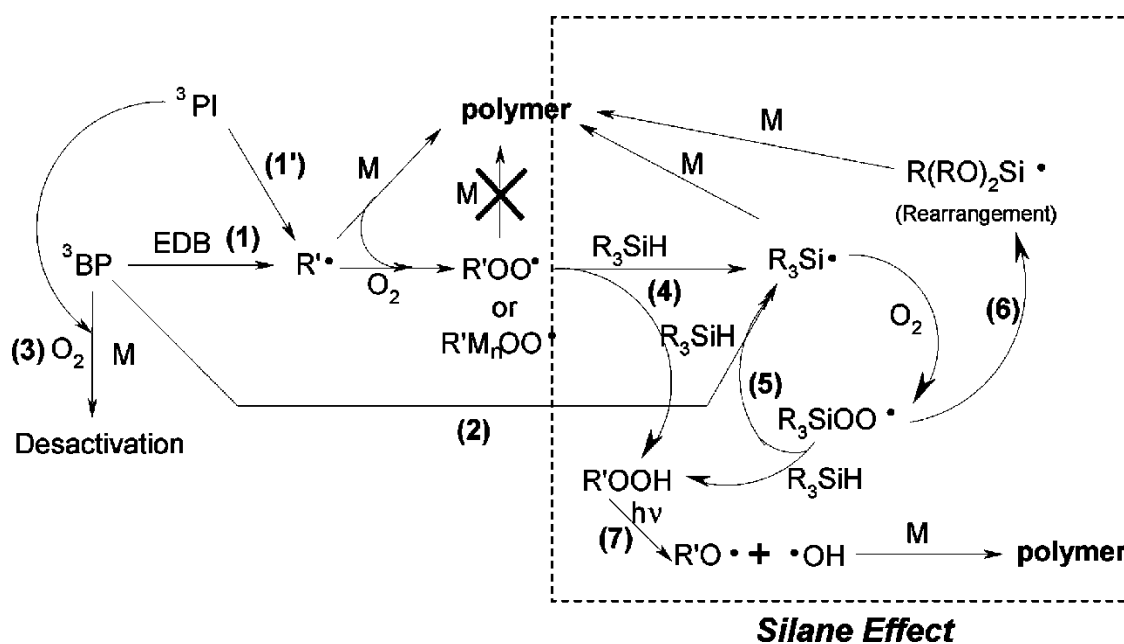
Scheme 29. Silane effect against oxygen inhibition[167]

Unfortunately, the chain transfer reaction was not favored and therefore significant homopolymerization occurred. The explanation for the low abstraction rate was the bond dissociation energy (BDE) between the hydrogen and silicon atom. [166]

In Figure 66 the BDEs of hydrogens on different silanes are shown correlated with the IR vibrations. Trimethylsilane shows a high BDE comparable to silanes with higher numbers of hydrogens. By introducing TMS groups in the silane the BDE is lowered.[168]

Also the conformation of the radicals changes from a tetrahedral to a more planar structure while the stability of the radical is increased by d_π-p_π interaction and hyper conjugation of the Si-atoms.[169, 170]
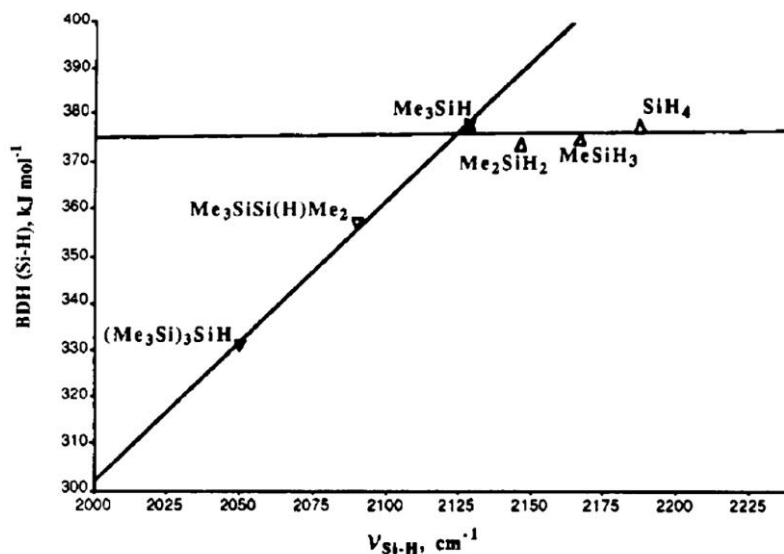
Figure 66. Bond dissociation energy of silane hydrogens and their IR vibration[168]

2007 Semchikov et al found that the electron density on the H atom of silanes is responsible for the reactivity of macro radicals towards hydrogen abstraction. The higher the e⁻ density on the hydrogen the better radicals can abstract that hydrogen. That was also shown in this work by thermal polymerization of methyl methacrylate in presence of different silanes and organosilicon hydrides.[167] (Figure 66)

It was already shown that electron rich silanes with TMS groups can be used as chain transfer agents in bulk polymerization of acrylates and methacrylates, improving mechanical properties of the formed networks. Bulky silanes such as tri(trimethylsilyl)silane can be problematic when it comes to polymerize sterically hindered monomers like norbornene.[171, 172]

A drawback for these systems is the autoxidation of silanes under exposure to air. Although the reactivity of the resulting siloxane hydride is still given, autoxidation is a radical mechanism and can lead to initiation of polymerization and therefore reduced shelf life under air.[173-175]

2.2. Selection and synthesis of HAFCT compounds

A new class of hydrogen donors had to be developed which should not inherent the same drawbacks of thiol-ene and silane-ene chemistry. Cyclohexadienes came to mind as they carry easily abstractable hydrogens. By adding a leaving group in para position of the abstractable hydrogens, aromatization of the ring structure could be a strong driving force for releasing a reactive radical to reinitiate chain growth[176]
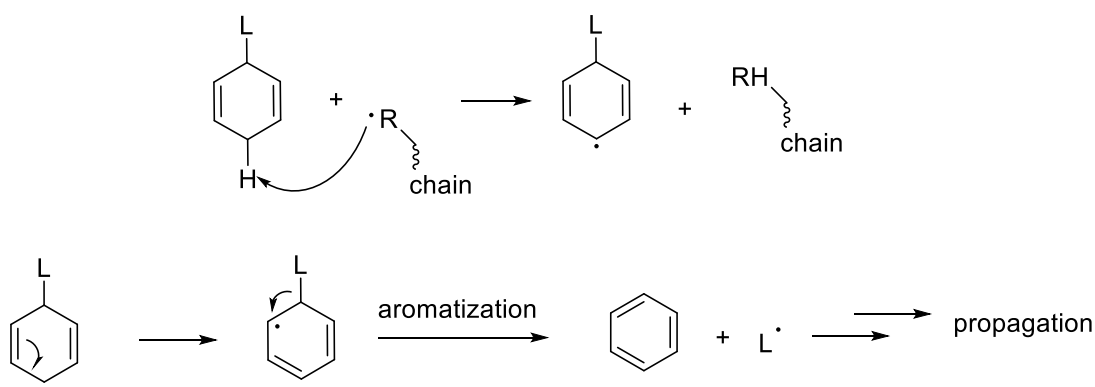
The structure of the cyclohexadienes is crucial for the system to work. There are four possibilities how the doublebonds can be arranged in the ring regarding the leaving group L.

2-L-1,3-diene   5-L-1,3-diene   3-L-1,4-diene   1-L-1,4-diene
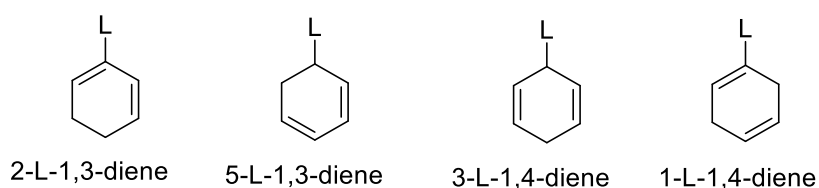
Only cyclohexa-1,4-dienes with the leaving group in the 3-position can function that way, as the intermediate radical has to be in ortho position to the leaving group.

Cyclohexadienes can be synthesized by Birch reduction in liquid ammonia with alkali metals.[177] Depending on the substitution of the aromatic precursor, the doublebonds can be directed in different positions. Direct reduction of the benzene derivative already functionalized with a leaving group L would not lead to the wanted configuration of doublebonds.[178]
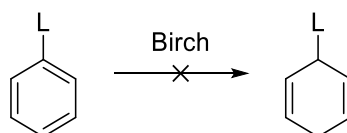
On the other hand, it is already known that polar effects of electron donating groups such as methoxy moieties facilitate the abstraction and especially fragmentation of the leaving group.

In EPR studies performed by the group of Prof. Dr. J. C. Walton of the University of St. Andrews (UK) the radical chemistry of substituted cyclohexadienes was deeply investigated at different temperatures. It was shown that silylated dimethoxy cyclohexadienes, even at the lowest temperature of 102 K, fragment so fast after hydrogen abstraction, that the intermediate cyclic radical cannot be detected. The silyl cyclohexadienes without methoxy group did not fragment at all until temperature was raised to 360 K (87 °C). Then the radical fragmentation products could be found.[179, 180] This effect was used for radical organic synthesis but never tested in polymer chemistry.

As quick fragmentation is crucial for radical polymerization 1,3-dimethoxy benzene was chosen as precursor for the Birch reaction. The resulting dimethoxy cyclohexadiene can be further modified in the 2-position by lithiation and corresponding leaving group electrophile.[179]
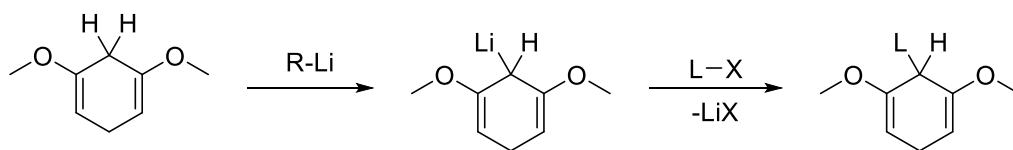
In the next step a methyl group has to be added to prevent radicals from abstracting the preferred hydrogen close to the leaving group L.[181]
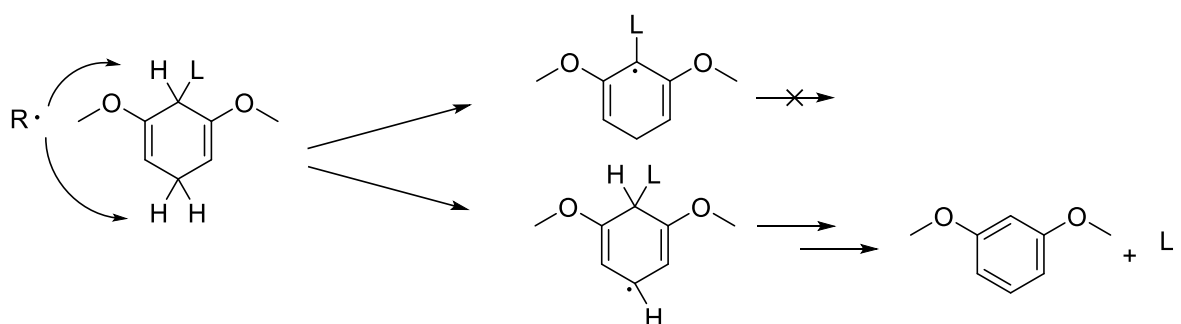
For addition of the methyl group the cyclohexadiene has to be lithiated again and then treated with a methylation reagent.
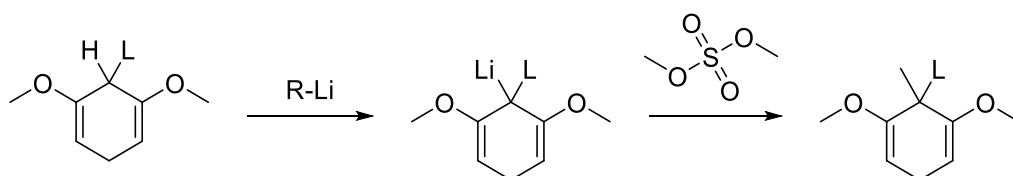
In this case, the radical can only abstract hydrogens from the para position of the leaving group and it is ensured that a leaving reactive radical is eliminated off the ring by aromatization.

To ensure efficient reinitiation of the propagation reaction the leaving group radical has to be reactive towards (meth)acrylates. The addition constants for silyl radicals is in the magnitude of 10^8 mol L^{-1} s^{-1} and for sulfonyl radicals around 10^9 mol L^{-1} s^{-1} which is sufficiently fast.[10, 182] Therefore, it was planned to synthesize silyl and sulfonyl dimethoxy cyclohexadienes.

2.2.1. Synthesis of 1,5-dimethoxy cyclohexa-1,4-diene (DCH)

As a precursor dimethoxy cyclohexadiene DCH had to be prepared via Birch reduction ident to literature and was further used for the synthesis of cyclohexadiene transfer agents.[181]
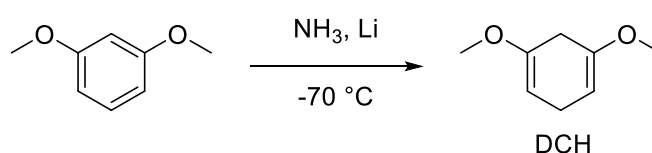
For the synthesis of 1,5-dimethoxy cyclohexa-1,4-diene 1 eq. dimethoxy benzene was dissolved in absolute diethyl ether under inert atmosphere and ammonia was condensed into the solution at -70 °C. 5 eq. lithium were added as metal wire and dissolved within minutes resulting in a deep blue solution of solvated electrons. After 2 h the reaction was quenched carefully with ethanol and the resulting mixture warmed up to room temperature. Afterwards it was extracted with saturated ammonium chloride solution. The dried organic phase was stripped of the solvent under vacuum and yielded 91% of theory, pure 1,5-dimethoxy cyclohexa-1,4-diene DCH as colorless liquid.

2.2.2. Synthesis of 1-(*t*-butyl dimethyl silyl)-1-methyl dimethoxy cyclohexadiene (SiDCH)

To compare the reactivity of simple alkyl silanes with electron rich TMS silanes it was planned to synthesize a cyclohexadiene with a trimethyl or triethyl silyl group. But from literature is known that only the *t*-butyl dimethyl silyl derivative of dimethoxy cyclohexadienes is stable, the trimethylsilyl derivative decomposes within hours. Therefore, the first synthesis attempt was used to obtain the stable of 1-(*t*-butyl dimethyl silyl)-1-methyl dimethoxy cyclohexadiene SiDCH in a one pot synthesis ident to literature.[180]
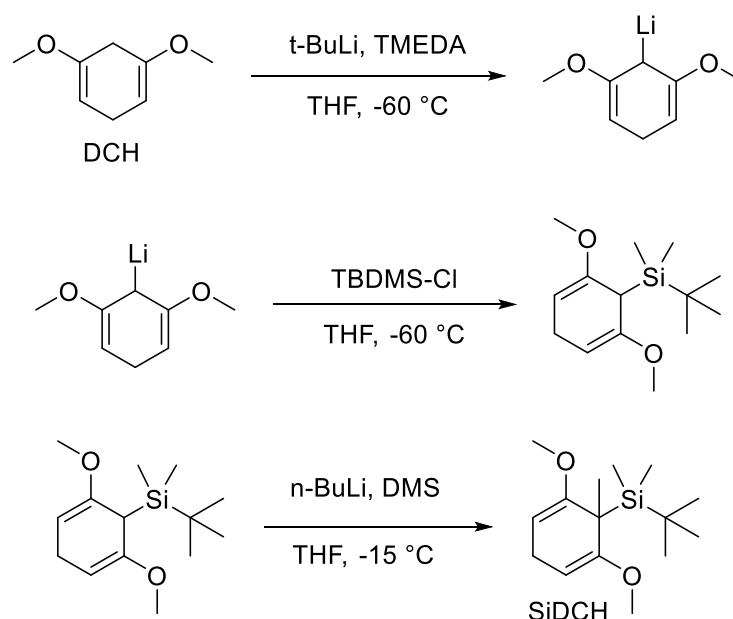
First dimethoxy cyclohexadiene DCH was dissolved in absolute THF under argon and cooled to -60 °C. Then the mixture was treated with 1.1 eq. *tert*-butyl lithium and tetramethylen diamine (TMEDA) resulting in a yellow solution. After 90 min 1.1. eq. of *tert*-butyl dimethyl chlorosilane was added and the mixture was allowed to warm up to RT and stirred for another 90 min. A precipitate of LiCl can be observed. In the last step, the solution was cooled to -15 °C and treated

with 1.1 eq. n-butyl lithium resulting in deep orange solution. For the methylation 1.1 eq. dimethyl sulfate (DMS) were added resulting in instant discoloration. After 30 min the reaction was quenched with water and extracted. The organic phase was washed twice with water and once with brine. After drying the organic phase the solvent was stripped off. Column chromatography and recrystallization of the product in MeOH afforded 51% of pure 1-(t-butyl dimethyl silyl)-1-methyl dimethoxy cyclohexadiene SiDCH as colorless crystals.

2.2.3. Synthesis of 3-tris(trimethylsilyl)silyl-3-methyl-2,4-dimethoxy-1,4-cyclohexadiene

As low steric hindered groups lead to instable products, a tris(trimethylsilyl)silyl (supersilyl) moiety should be introduced. It is known that super silyl radicals efficiently reinitiate the polymerization of acrylates and methacrylates.[171]
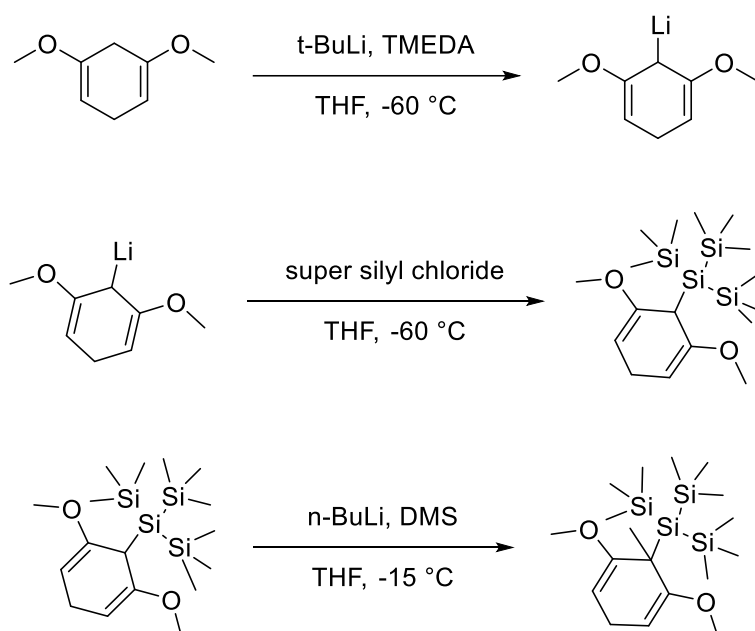
The procedure was the same as for the *tert*-butyl dimethyl derivative. After the first lithiation the 1.1 eq. supersilyl chloride was added and also a precipitate of LiCl could be seen. Reaction GC-MS confirmed the successful synthesis of the first step. The second lithiation also resulted in a dark orange mixture, which was decolorized by adding 1.1 eq. dimethyl sulfate (DMS). After aqueous workup and extraction with petrol ether, the solvent was removed by vacuum. Crude TLC showed five different products but 2D TLC first indicated sufficient stability on silica gel. After column chromatography, the fractions were concentrated in vacuum. Unfortunately, the product was not stable as expected and decomposed further resulting in multiple TLC spots in former clean fractions. Therefore, no further synthesis of silyl cyclohexadienes was done.

2.2.4. Synthesis of sulfonyl dimethoxy cyclohexadienes

Sulfonyl radicals are among the fastest radicals to add to (meth)acrylic double bonds. Therefore, a cyclohexadiene with a tosyl leaving group should be synthesized.
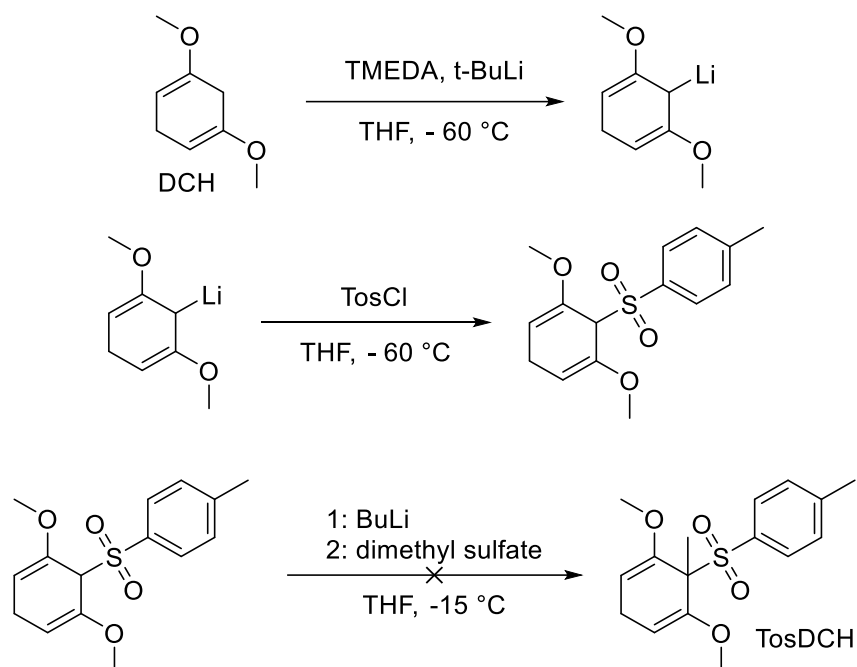
The same procedure was applied for this reaction as for the silyl derivative. After lithiation 1.1 eq. tosyl chloride was added to the lithium cyclohexadiene. After that the second lithiation and methylation was proceeded as described previously. After quenching with water, ethyl acetate was used for extraction as the product was expected to be more polar as the silylated cyclohexadienes. After drying with sodium sulfate the solvent of the organic phase was removed by vacuum distillation. The remaining oil was colorless until the rotary evaporator was vented with air. Then the oil turned deeply blue. When small portions were diluted in solvent the color was deeply violet and vanished after some hours. (Figure 67)

Figure 67. Solution of the violet product of the reaction with dimethoxy cyclohexadiene and tosyl chloride after dissolving and 30 min later. Complete discoloration occurred.

¹H-NMR showed various aromatic and aliphatic signals that could not be assigned to a specific structure. TLC also showed a violet spot among other products. Unfortunately, column chromatography was not possible as the product would move to the first third of the column and then fade. Therefore, the blue/violet species could not be isolated. The remaining oil discolored under argon at -18 °C over night. Exposing the oil to air would result in the same deep blue color. Probably stable radicals were formed under the exposure to oxygen, slowly disintegrating to other structures.
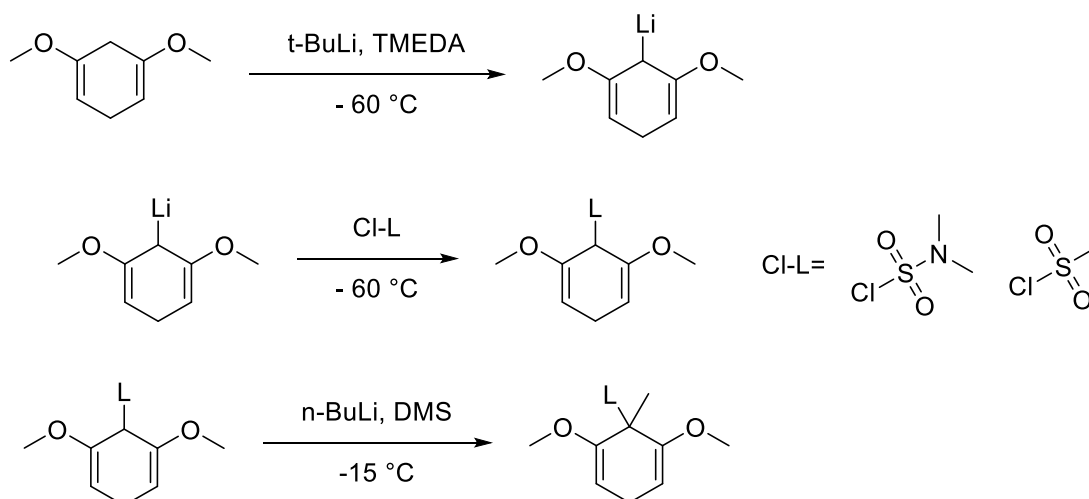
In the hope to find other stable sulfonyl modified cyclohexadienes also mesyl- and dimethyl sulfamoyl chloride was reacted in the exact same way as the tosyl derivative with dimethoxy cyclohexadiene. Again, no defined product could be isolated.

When 1.1 eq. dimethyl sulfamyl chloride were used for the introduction of the leaving group, the reaction did not turn orange but light yellow during the second lithiation. After usual addition of 1.1 eq. DMS and workup a slightly yellow crude product was obtained. Examination by NMR showed several aromatic products and various aliphatic signals. No double bond signals from the hexadiene were found. GC-MS showed mainly dimethoxy benzene and traces of sulfamyl substituted product from step 2.

The reaction product with mesyl chloride, which was conducted ident to the reaction with tosyl chloride, yielded a product with the same strange behavior as the reaction with tosyl chloride. Also in this case, a blue product was generated under air that lost its color with time at room temperature and could not be isolated as single substance. Storage under argon would decolorize the product, while contact to air caused instant blue coloration.

The *tert*-butyl dimethyl silyl dimethoxy cyclohexadiene SiDCH was the only stable derivative that could be synthesized. In Scheme 30 the proposed reaction with propagating chain and radicals, is shown.
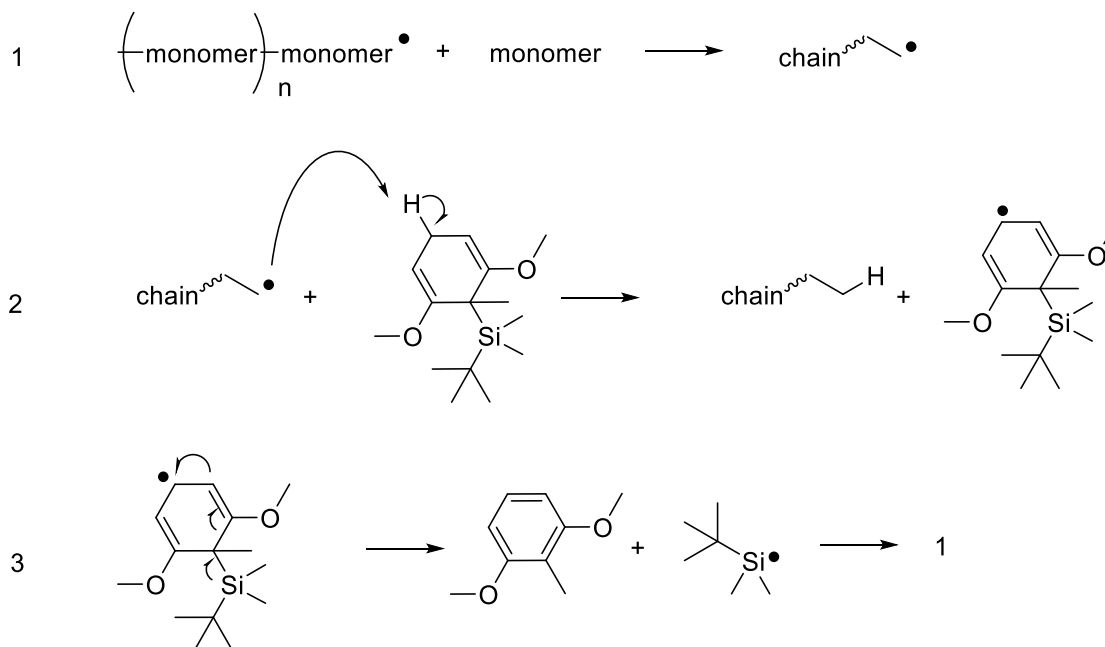
Scheme 30. Chain transfer reaction under exclusion of oxygen

In step 1 the normal chain growth reaction is taking place until it is terminated by abstraction of a hydrogen from the chain transfer reagent in step 2. The chain transfer reagent eliminates a radical tertbutyl dimethyl silyl radical by aromatization of the ring system in step three and this reactive radical should reinitiate chain growth of step one. As the ringstructure does not contain polymerizable groups the dimethoxy toluene remains in the network as volatile residue. For the proof of concept, these aromatic signals can be used as indicator of the aromatization reaction.

2.3. Testing HAFCT reagents in monofunctional systems

The new cyclohexdiane hydrogen abstraction fragmentation chain transfer (HAFCT) reagents should be tested under same conditions as AFCT reagents. Due to the challenging synthesis and low stability of the compounds, only one stable silyl cyclohexadiene, 1-(t-butyl dimethyl silyl)-1-methyl dimethoxy cyclohexadiene (SiDCH), could be tested. Like the AFCT reagents, the cyclohexadiene was first tested as chain transfer agent in a monofunctional benzyl methacrylate BMA. In addition, the precursor dimethoxy cyclohexadiene DCH carries abstractable hydrogens and was therefore tested as inactive reference to proof the concept of abstraction fragmentation chain transfer.
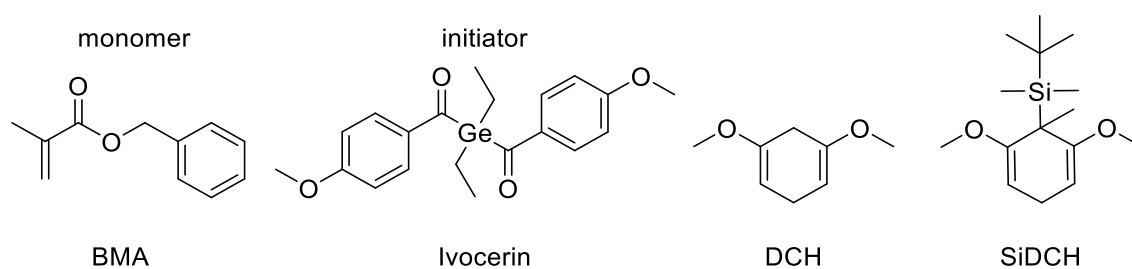
2.3.1. Photo-DSC

In a first study in monofunctional monomer, the reagents should be tested in a photo-DSC experiment. Monofunctional monomers form soluble linear polymers that can be further investigated by NMR and SEC studies. Benzyl methacrylate was selected as monomer as this compound has a high boiling pint of 276 °C and fewer disturbing NMR signals in the lower ppm scale.[142]

1 w% Ivocerin was used as photoinitiator and 20 mol% of additive were used to regulate the radical polymerization of BMA. After mixing chain transfer agents and initiator with the monomer, 12 ± 0.5 mg of sample were weighed into aluminum DSC pans and closed with a glass lid, to prevent monomer and additives from evaporation. The samples were irradiated at 1 W/cm^2 at the tip of the light guide twice for 300 s. The heat of polymerization was recorded against the time. The parameters were obtained and calculated according to chapter 3.

Already the resulting rate of polymerization R_P of the mixtures shows that both the unmodified cyclohexadiene DCH and the silyl hexadiene SiDCH slow down the propagation reaction of BMA. (Figure 68, left) unexpectedly the cyclohexadiene with a silyl leaving group showed the lowest rate of polymerization. At this point it is unclear if the mechanism works as predicted, but the significant drop in the rate of polymerization is not a positive sign. Both mixtures containing

cyclohexadienes exhibit a lower time to reach maximal R_P, so at least the start of the polymerization is not inhibited. (Figure 68, right)
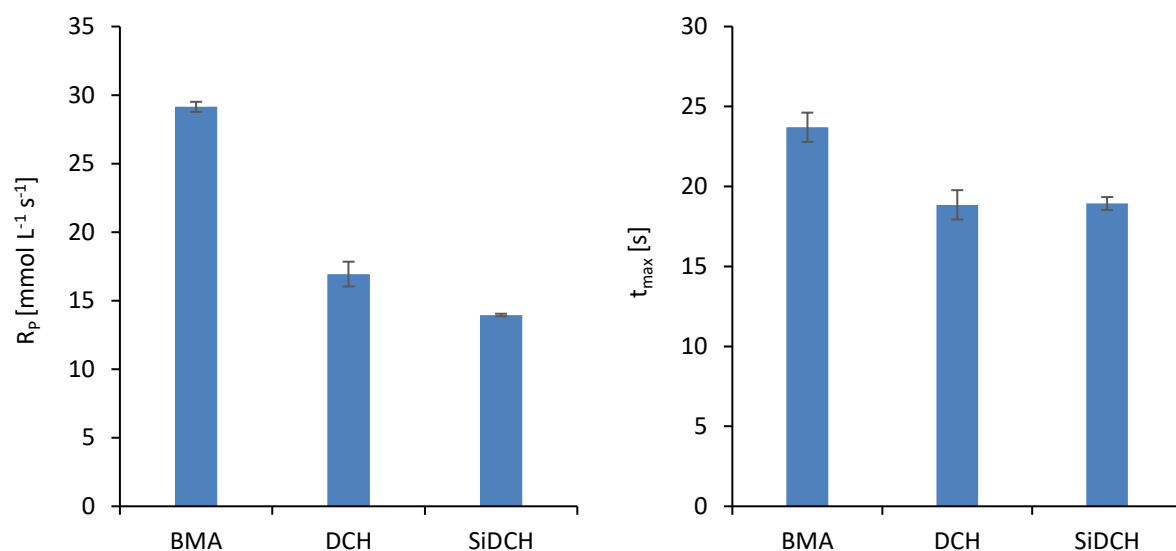
Figure 68. Rate of polymerization of BMA and mixtures with 20 db% additive (left) and time to maximal rate of polymerization (t_{max}) (right) of BMA and mixtures with 20 db% additive

In the left Figure 69 the time to reach 95% overall double bond conversion is shown, both mixtures with 20 db% cyclohexadiene DCH and silyl cyclohexadiene SiDCH exhibit lower t_{95} values than neat benzyl methacrylate BMA. On the other hand, visible on the right side of Figure 69, the double bond conversion DBC reached by the mixtures containing cyclohexadiene additive is massively reduced. It seems that there is no difference in the reactivity of the cyclohexadiene precursor DCH and the silylated product SiDCH. Benzyl methacrylate is a rather unreactive monomer and the process of hydrogen abstraction and elimination of the leaving group is time consuming. Therefore, it was expected that chain transfer by silyl cyclohexadiene SiDCH causes some retardation of the polymerization. It is surprising, that there is almost no difference observed when comparing the cyclohexadiene DCH with the "activated" silylhexadiene SiDCH.
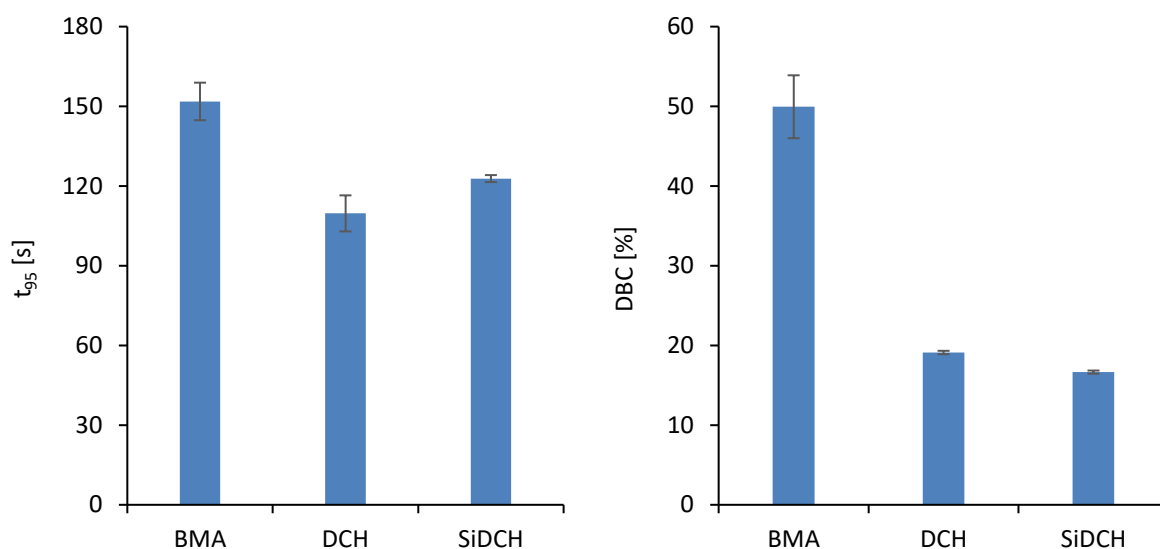
Figure 69. Time to 95% of overall double bond conversion (t$_{95}$) (left) and and Double bond conversion (DBC) of BMA and mixtures with 20 db% additive

2.3.2. NMR

To get a deeper understanding of the reaction, ^{1}H-NMR spectra were recorded from the un-irradiated mixtures and the irradiated samples from photo-DSC.
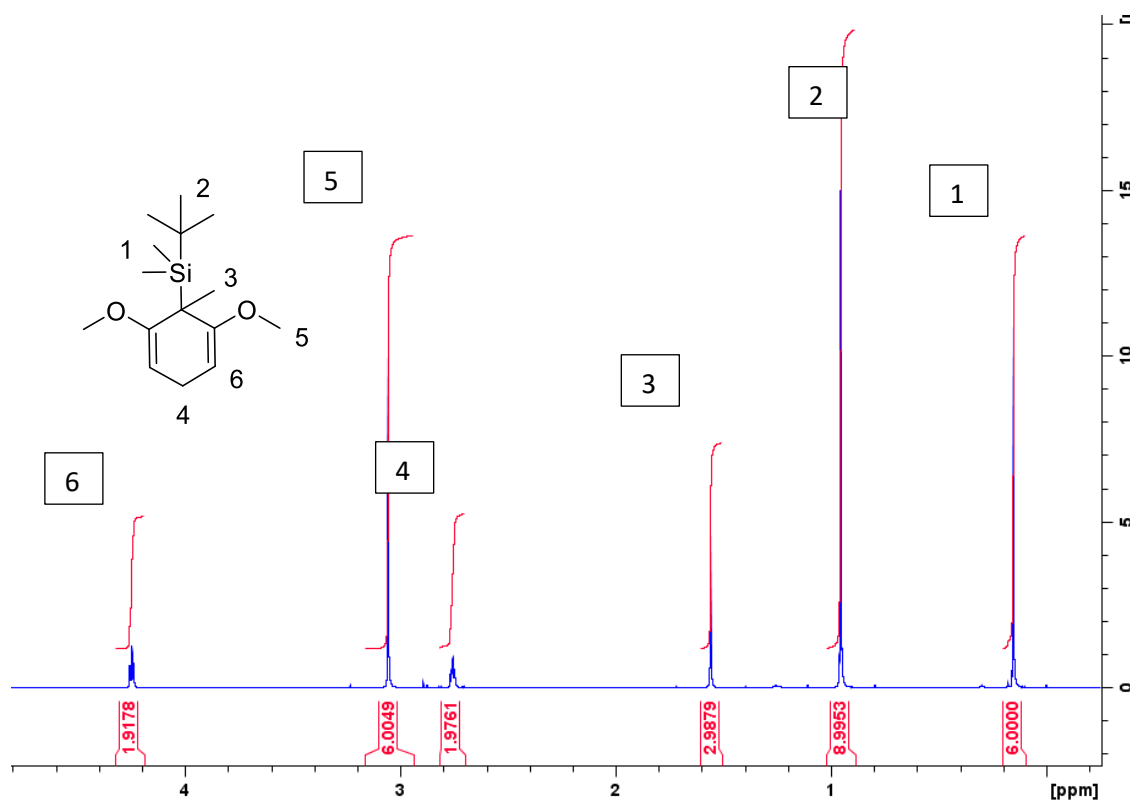
Figure 70. ^{1}H-NMR spectrum of silyl cyclohexadiene SiDCH in C$_6$D$_6$

The pure silyl hexadiene SiDCH is visible in Figure 70, showing the expected signals with corresponding integrals.
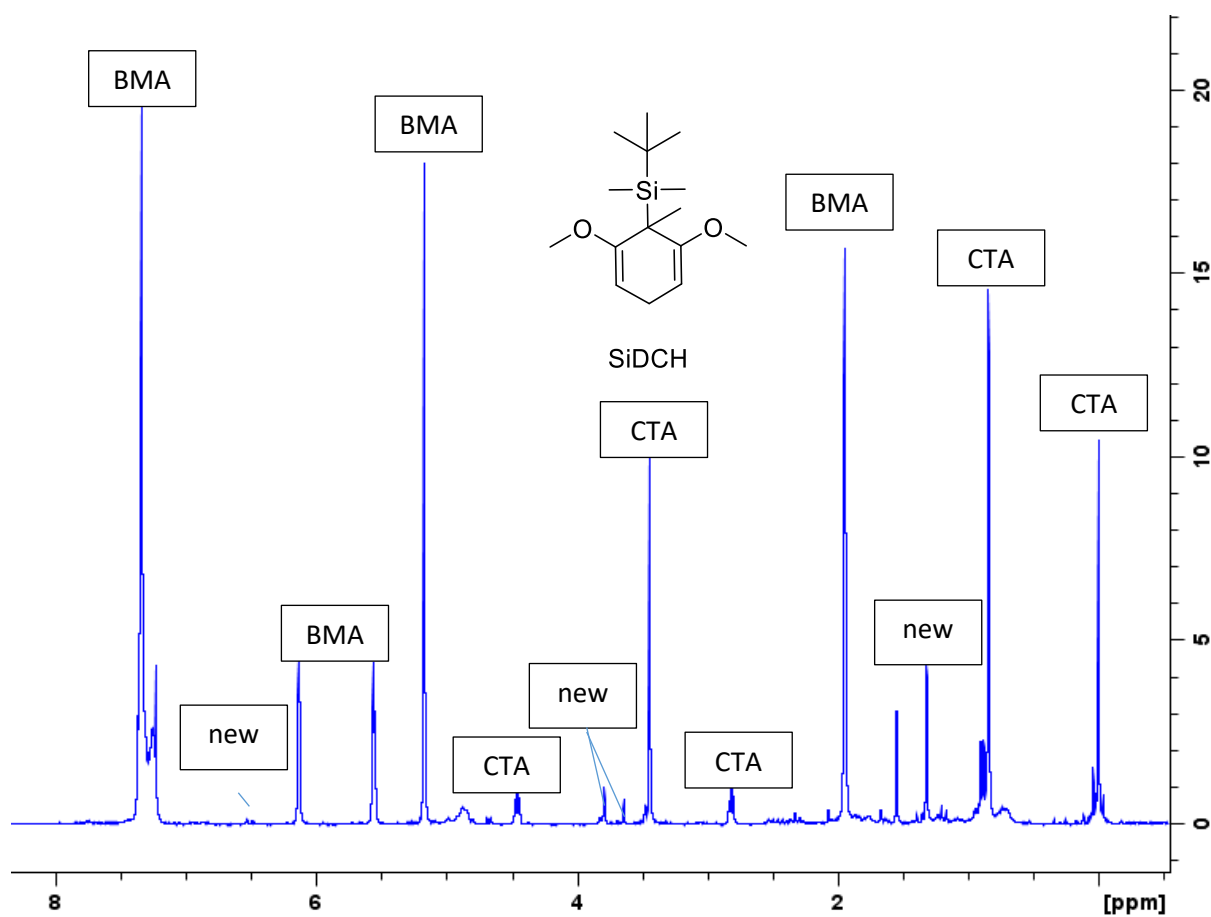
Figure 71. 1-H-NMR spectrum in CDCl₃ of BMA with 20 mol% silyl cyclohexadiene SiDCH and 1 wt% Ivocerin after 600 s irradiation at 1 W cm⁻² 400-500 nm

The silyl cyclohexadiene SiDCH showed some instability in CDCl₃ solution probably due to hydrochloric acid which is always present in chloroform, leading to new singlet peaks in the silyl area. The silyl hexadiene SiDCH was stable in monomer, but depending on the time between NMR sampling and recording of the spectra the CTA more and more decomposed. Therefore, measurements were conducted immediately after irradiation.

It is visible that still a lot of CTA was present after irradiation. Quantification of the conversion is possible by referencing the 6 H dimethyl silyl peak at 0 ppm which is not changed much by polymerization and comparing the integral to the ring hydrogen triplet signals. (Figure 71) The tert bultyl group at ~0.9 ppm is overlapping with broad polymer signals and also shows some additional singlet peaks as the dimethyl signal at 0 ppm. Due to the overlap the integral is higher. In Figure 72 this is shown in detail.
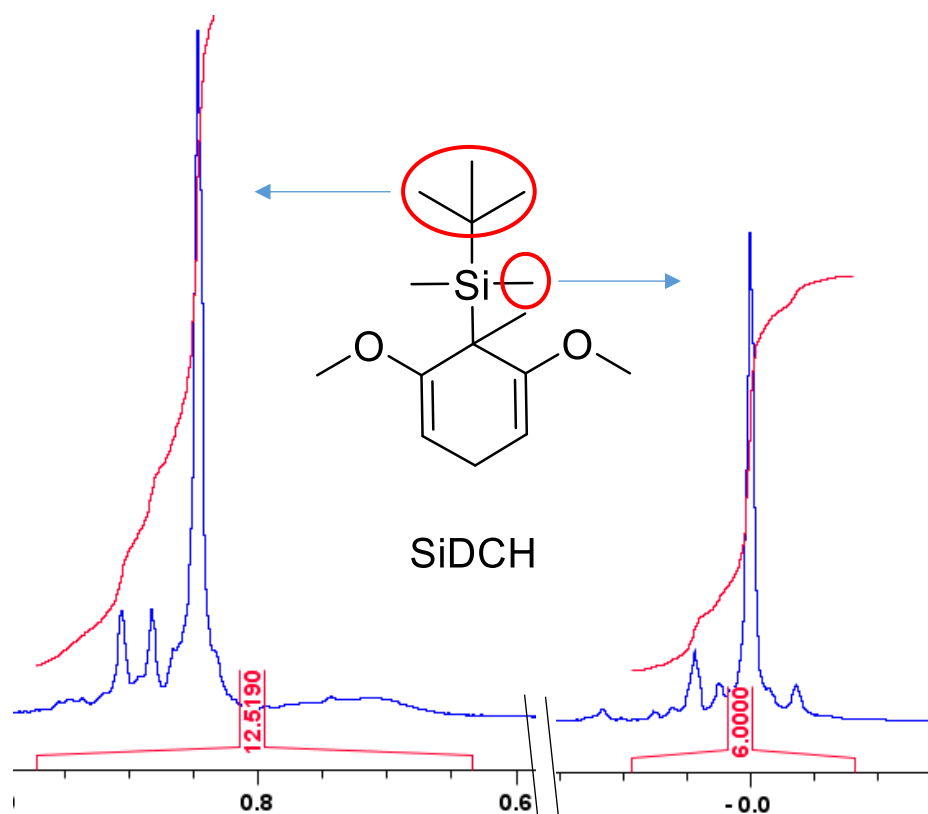
Figure 72. Zoomed view of the silyl signals after irradiation (x-axis ppm)

Luckily the triplet signals of the cyclohexadiene ring are well separated from other signals and quantifiable. (Figure 73) Indeed these signals decreased during polymerization and the conversion could be calculated accordingly.
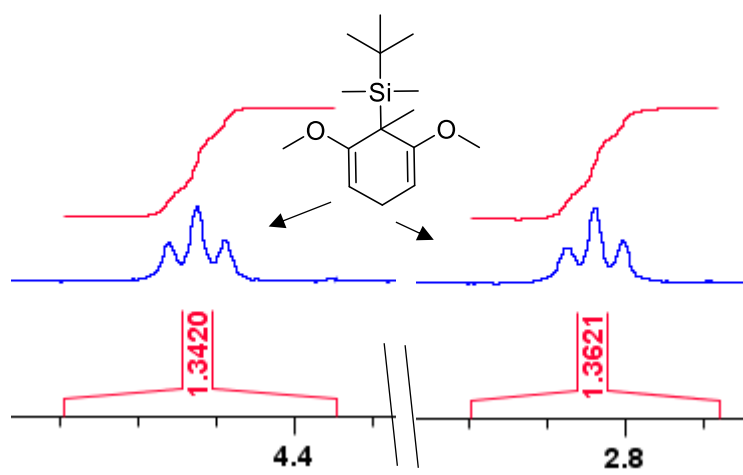
Figure 73. Triplet signals of the cyclohexadiene ring after irradiation (x-axis ppm)

By decrease of the triplet integrals the conversion of cyclohexadiene a conversion of 32.5% of the CTA SiDCH was reached. If the mechanism of hydrogen abstraction and fragmentation by aromatization of the ring is true, according aromatic signals should be visible. That means if the 2 H cyclohexadiene ring triplet signal decreases by 0.75 a new aromatic 2 H doublet signal of

about the same integral should appear at ~ 6.5 ppm. This was calculated by increment prediction. Indeed, there is a specific signal of resulting dimethoxy toluene when the mixture was irradiated visible in Figure 74 that shows some aromatization takes place. But the integral only sums up to 0.10. This indicates that hydrogen abstraction and subsequent aromatization is not the main pathway of the reaction in benzyl methacrylate.
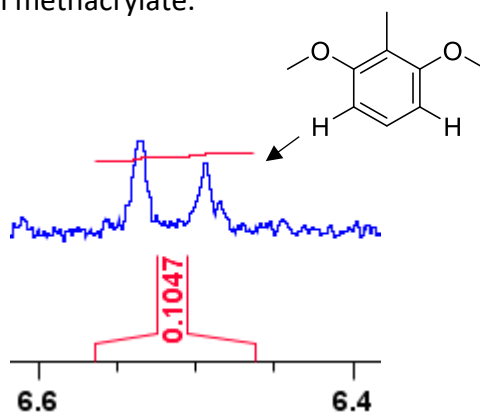
Figure 74. Specific aromatic signal of dimethoxy toluene (x-axis ppm)

Maybe, when hydrogen abstraction is not the main pathway, radicals directly add to the doublebonds. This could still lead to fragmentation. However, there is no energy gain by aromatization. Therefore, it is not clear if fragmentation would take place in this case. The resulting 1,3-cyclohexadiene would still carry abstractable hydrogens and doublebonds that would probably lead to inhibition of polymerization.
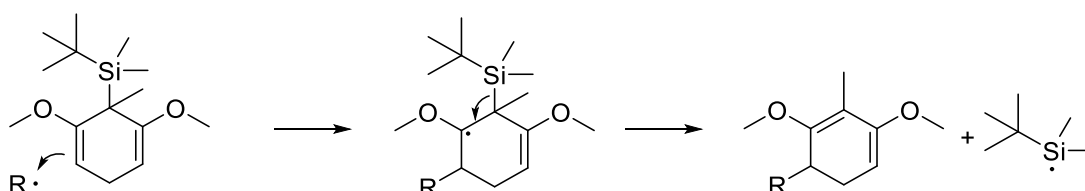
From the obtained NMR spectra, it is not possible to directly relate signals with the addition products although there are several overlapping new signals in the range of 1.5 − 4 ppm that could come from addition products.

The calculation of DBC of benzyl methacrylate shown in Figure 75 shows a bit higher values than that obtained by DSC measurements. The calculations deviate 3-4% which is either caused by a small endothermic effect or lies within the uncertainness of the measurements.
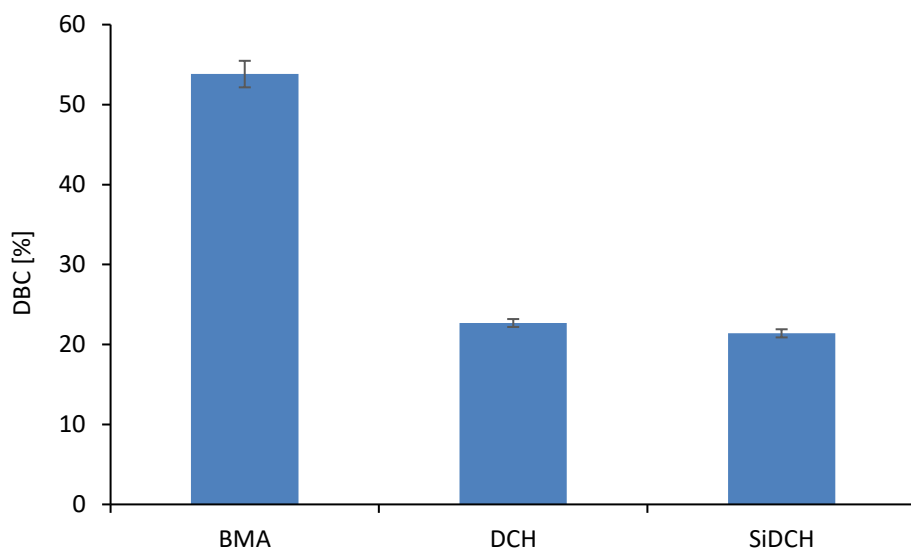
Figure 75. DBC of methacrylate BMA calculated by NMR

The calculation of DBC of benzyl methacrylate shown in Figure 75 shows a bit higher values than that obtained by DSC measurements. The calculations deviate 3-4% which is either caused by a small endothermic effect or lies within the uncertainness of the measurements.

2.3.3. Size exclusion chromatography (SEC)

After the NMR measurements the samples were diluted with THF and GPC chromatograms were recorded to determine the molecular weight and polydispersity of the polymers. (Figure 76)
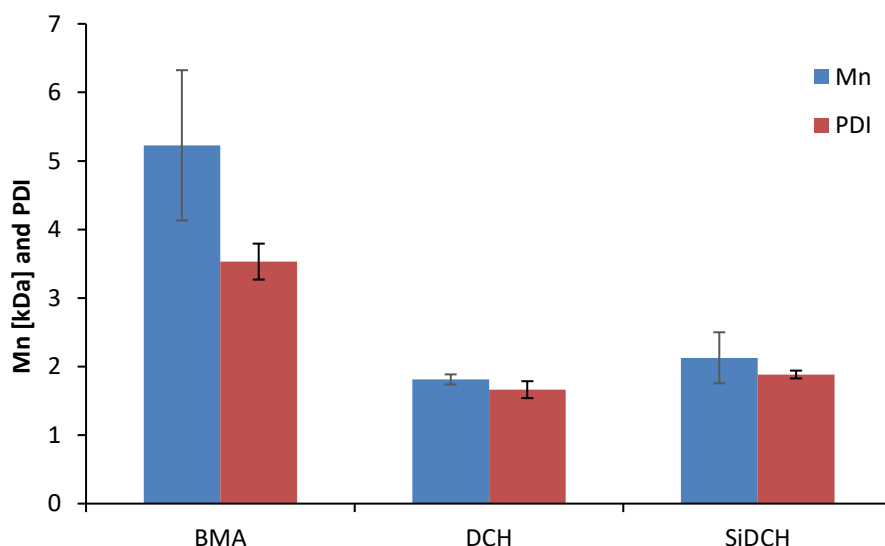
Figure 76. Number average molecular weight Mn and polydispersity index PDI of the resulting polymers from DSC measurements

As expected the neat monomer BMA reached an average Mn of about 5000 Da with a typical high PDI of 3.5. Both mixtures containing cyclohexadienes show very similar results. In both cases

the molecular weight is dramatically reduced to about 2000 Da and also the PDI is reduced below 2, which indicated regulation. The fact that there is no difference in the regulation between the dimethoxy cyclohexadiene DCH and the silylated version SiDCH is not very promising. It seems that both molecules rather inhibit the reaction, causing lower molecular weights and distributions and that the reinitiation by the silyl leaving group is not working properly.

2.4. Testing HAFCT reagents in difunctional systems

Although the results from the test in the monofunctional system with methacrylate BMA were not promising, the cyclohexadienes were also tested in a difunctional more reactive dental methacrylate mixture DMM. Photo rheology measurements with real time NIR were conducted a concentration of 20 db% and 10 db% respectively of CTA with 0.3 wt% Ivocerin as initiator. The initiator was used in low concentration to be able to properly follow the curing reaction. Therefore, also the lowest light intensity of 0.5 W/cm^2 supported by the Exfo OmniCure TM 2000 broadband Hg-lamp was used at 400-500 nm.

methacrylate system:

UDMA

D$_3$MA

1:1 molar mixture = DDM

Ivocerin
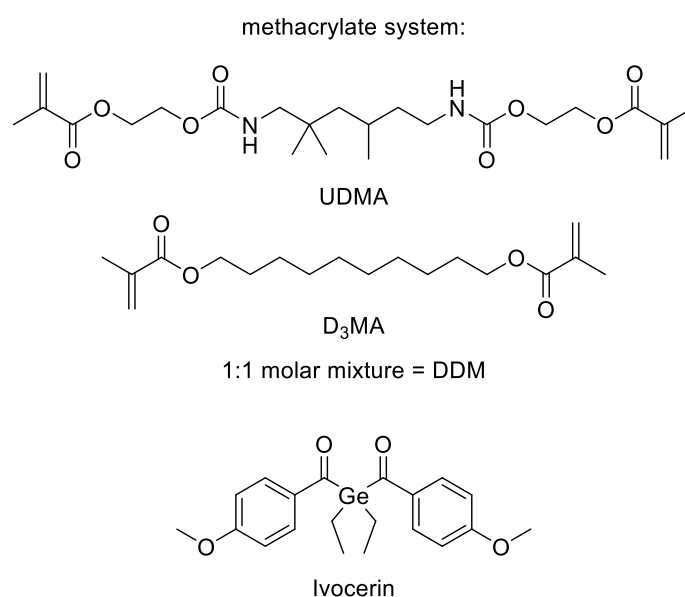
For the DMTA measurements, sample sticks (1.5 x 5 x 40 mm) were prepared in a silicon mold at 400-500 nm blue light irradiation, with 1 wt% initiator and samples containing 10 – 20 db% CTA were compared to the unmodified DMM network.

During DMTA measurements, the sample bars were heated from -100 °C to 200 °C while torsion strain of 1% at 1 Hz was applied to the material. The storage modulus G' and dissipation factor tan δ were recorded with temperature.

2.4.1. RT-NIR photorheology

For further investigation of the new HAFCT CTA, coupled RT-NIR-photorheology measurements were conducted.

Interestingly the measurements with the difunctional more reactive monomer DMM revealed different behavior of the HAFCT reagents than observed in the rather unreactive BMA mixtures. The mixture with 20 db% unmodified cyclohexadiene DCH showed typical inhibition and barely reaches 15% conversion in Figure 77. The mixture with 20 db% silylated cyclohexadiene SiDCH reached more than the double DBC of 44%. This is still a lot less than the neat monomer, which reaches a little more than 70%, and the polymerization is also much slower but a significant effect of the reinitiating group can be observed. In addition the sample was not a hard piece of plastic but more like an organo gel. Due to the release of dimethoxy toluene, the sample is softened as if it was swollen in solvent. In addition, the very distinct mint like odor of dimethoxy toluene was very present.

By lowering the amount of SiDCH to 10 db% a DBC 68% was reached and the polymerization was significantly faster as can be seen by comparison of the dark blue (20db% SiDCH) and the light blue line (10 db% SiDCH) in Figure 77.
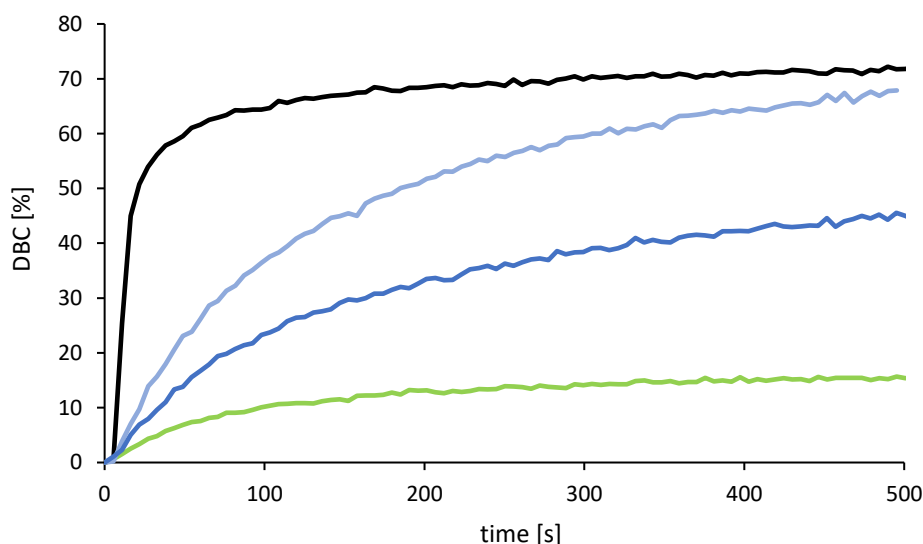
Figure 77. Double bond conversion DBC versus time of dimethacrylate DMM with hexadienes calculated from RT-IR:
— DMM neat, —DCH, —SiDCH 10 db%, —SiDCH 20 db%

In Figure 78 the time to gelation is shown. As expected the neat polymer reaches the gel point in around 4 s. Interestingly the cyclohexadiene DCH was so inhibiting that no gelpoint was reached and the mixture stayed liquid. The mixtures with silylated SiDCH reached the gelpoint in 37 s with

10 db% CTA and 43 s with 20 db% respectively. Interestingly the time to gelation is similar for both mixtures although the rate of polymerization is much lower for the mixture containing 20 db%.
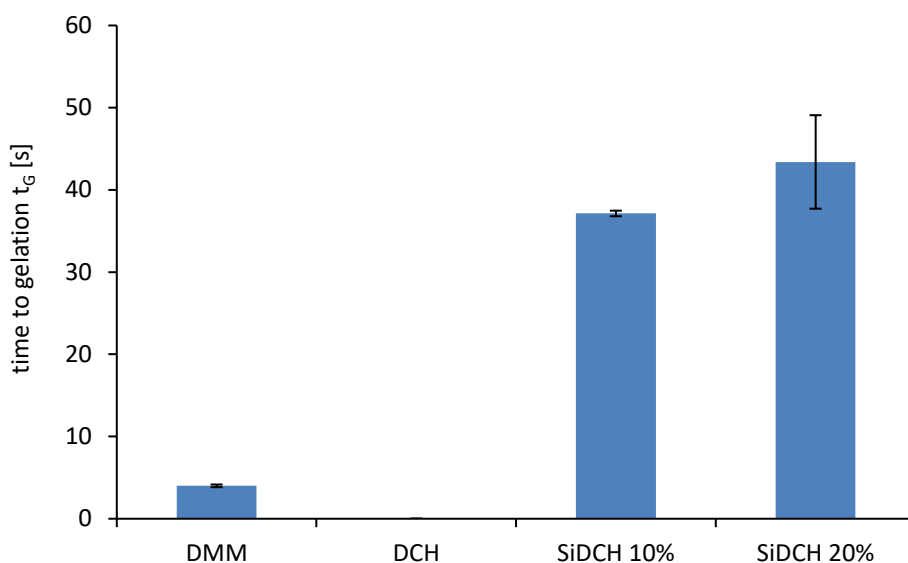
Figure 78. Time to reach the gelpoint t_G of the neat formulation DMM and the formulations containing cyclohexadienes

The 10 db% mixture of SiDCH showed higher conversion at the gel point than the neat monomer which reaches the gel point at 17% DBC. The DBC_G is significantly increased to over 20% by adding 10 db% silylated cyclohexadiene.
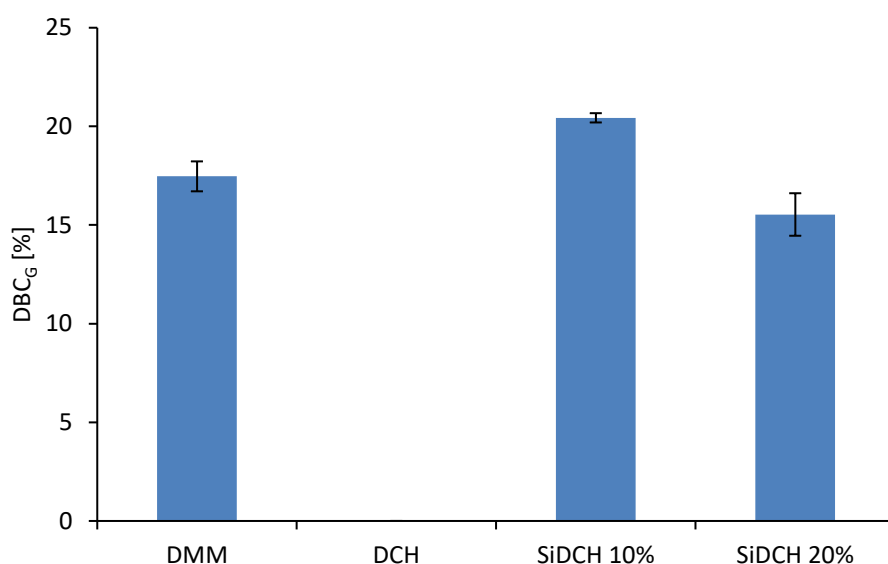
Figure 79. Double bond conversion at the gelpoint DBC_G of the neat formulation DMM and the formulations containing cyclohexadienes

Adding more HAFCT reagent shows no positive effect and the DBC_G decreases back to 16%. (Figure 79)

What was already visible in the conversion curves is also confirmed by measuring the time to 95% of reached DBC. (see Figure 80) All reagents cause significant retardation of polymerization. The mixture with 10 db% SiDCH reached a comparable DBC to the neat monomer system DMM but it takes more than the twofold amount of time to reach that conversion.
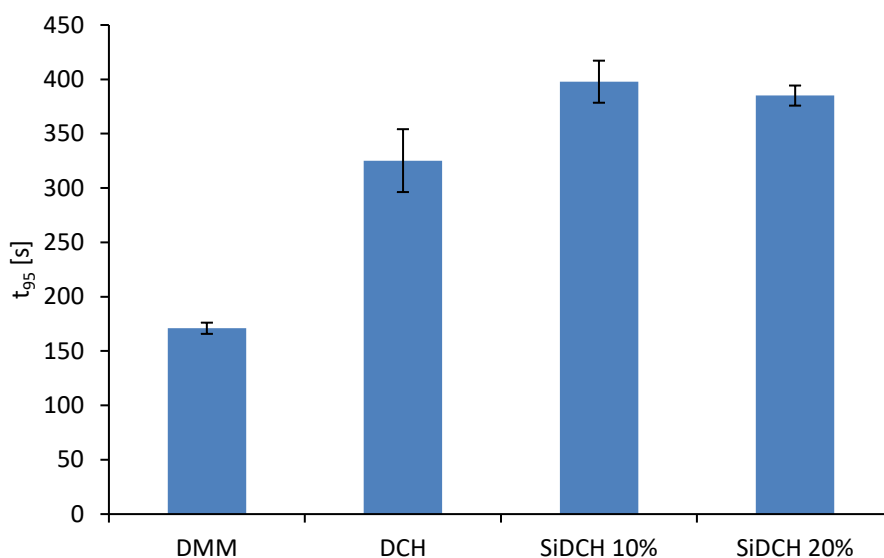
Figure 80. Time to 95% overall DBC t_{95} of the neat formulation DMM and the formulations containing 20 db% of dimethoxy cyclohexadienes DCH and silyl dimethoxy cyclohexadiene compound SiDCH in 10 and 20 db%.

Although the polymerization is slower, the 10 db% mixture of silyl compound SiDCH reached acceptable conversions and, as visible in the next graph Figure 81, the shrinkage force is reduced by 28%. As no gelation took place in case of the mixture containing 20 db% precursor DCH, no shrinkage was detected in this case. The 20 db% mixture with silyl compound SiDCH exhibits very low shrinkage force, but this was expected considering the low conversion and the slow polymerization.
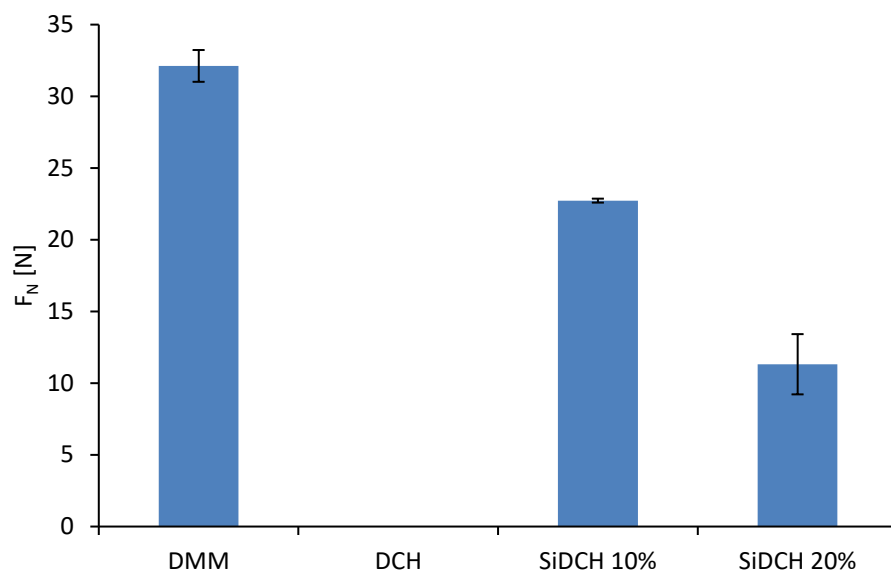
Figure 81. Maximal normal force F_N developed by the neat formulation DMM and the formulations containing cyclohexadienes

Interestingly the results of the storage modulus G' were surprisingly good. As can be seen in Figure 82, the mixture containing 10 db% of silyl compound SiDCH reaches a similar high modulus to the neat formulation DMM. Higher contents of the silyl CTA cause a significant reduction of modulus, which may be caused by the low conversion but also by the softening effect of evolving dimethoxy toluene. The green curve of precursor DCH clearly shoes that no polymerization takes place.
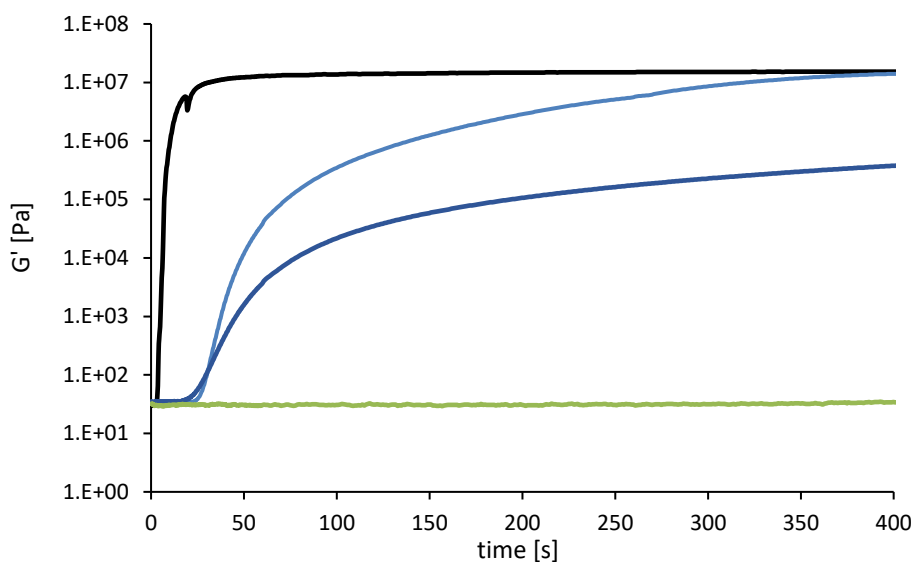
Figure 82. Storage modulus G' of the tested formulations — DMM neat, —DCH, —SiDCH 10 db%, —SiDCH 20 db%

2.4.2. Dynamic mechanical thermal analysis (DMTA)

Dynamic mechanical thermal analysis of duromeric networks can give a lot of information about the architecture of a network. Therefore, sample sticks (1.5 x 5 x 40 mm) were prepared in a silicon mold at 400-500 nm blue light irradiation, containing 20 db% respectively 10 db% regulator together with 1 wt% initiator and were compared to the unmodified DMM network. During DMTA measurements, the sample bars were heated from -100 °C to 200 °C while torsion strain of 1% at 1 Hz was applied to the material. The storage modulus G' and dissipation factor tan δ were recorded with temperature.

Also with 1 wt% photoinitiator and a curing time of 20 minutes the mixture containing 20 db% of precursor DCH did not cure at all. The other mixtures containing silyl cyclohexadiene SiDCH cured well, but the sample with a higher content of 20 db% was notable softer than the other sticks. Again, the distinct smell of dimethoxy toluene was observed in the case of the silyl CTA samples. As visible in Figure 83 the mixture containing 20 db% silyl compound SiDCH is indeed much softer than the neat DMM polymer. The material is so soft that the sample sticks break at 50 - 60 °C. The network modified by 10 db% SiDCH is also softer than the unmodified network, but the sticks withstand the stress applied and can therefore be measured again. It was already expected that the resulting dimethoxy toluene would act as softener. This could be proofed by a second DMTA run. It is clearly visible that the evaporation of the softener causes a significant increase of modulus at room temperature and also the glass transition is shifted to a higher temperature and much sharper. In the second run it can also be seen that the network regulation is not very good but at least the glass transition is sharper and lower than that of the neat polymer.
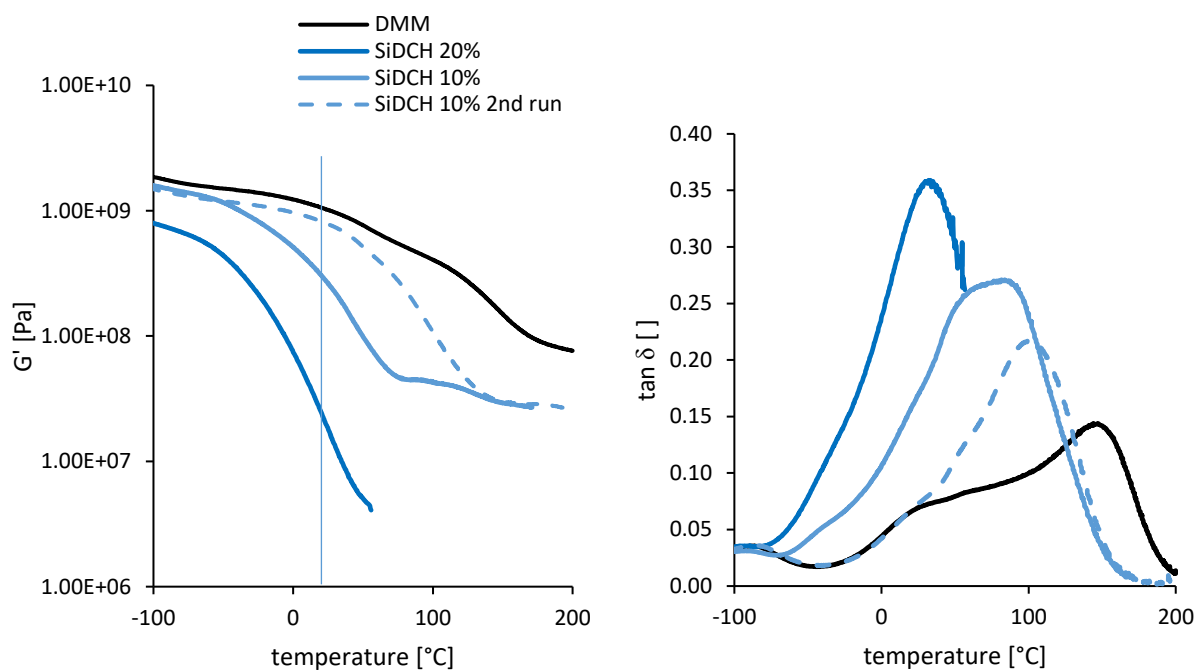
Figure 83. Storage modulus G' and loss factor tan δ of polymers, containing neat DMM and mixtures with silyl cyclohexadienes, plotted against temperature

After considering the results of all different measurements, it seems very likely that the system works as intended but not very efficiently. The conversion of CTA and monomer in monofunctional methacrylate BMA was not very high for both the unmodified and modified cyclohexadiene. The more reactive difunctional system DMM clearly showed that the unmodified dimethoxy cyclohexadiene is inhibiting the polymerization while the silyl compound exhibited higher reactivity of its formulations. With a reduced amount of 10 db% a high DBC was reached together with a higher DBC_G than the neat monomer and the shrinkage stress was significantly reduced. The rearomatization as driving force for the elimination of the leaving group could not be proved in the monofunctional methacrylate BMA. Surprisingly, in the mixtures with difunctional DMM the aromatization took most certainly place. This can be seen by the significant higher reactivity of activated silyl hexadiene SiDCH and the not activated precursor DCH, and also by the generation of very odorous dimethoxy toluene that acts as softener in the network.

2.5. Anti-oxygen inhibition - photoreactor tests

As the results were promising with 10 db% of silyl compound SiDCH also the activity of this substance as potential anti oxygen inhibition reagent was tested.

Hydrogen donors can be used to terminate unreactive peroxyl chain ends that inhibit radical polymerization under air.
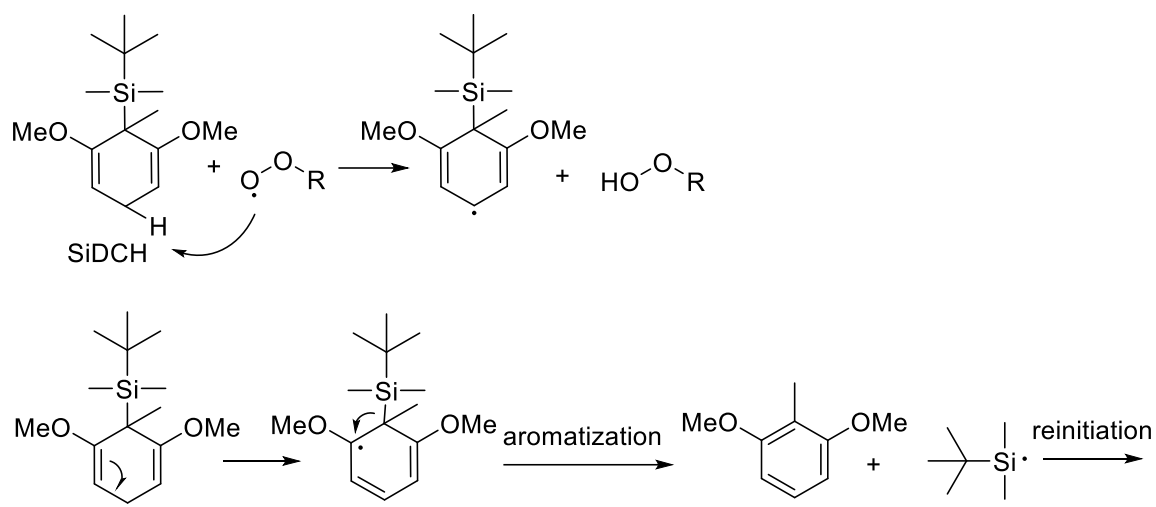
Scheme 31. Hydrogen donor mechanism of silyl compound SiDCH as antioxygen inhibition reagent.

As shown in Scheme 31 the donor hydrogen in para position to the leaving group gets abstracted and by the driving force of aromatization the leaving group is eliminated as radical to reinitiate polymerization. The mechanism of peroxyl radicals to abstract hydrogens from cyclohexadienes is already known from hydro silylation in organic chemistry.[183]

To see if the silyl cyclohexadiene SiDCH shows any activity against oxygen inhibition, photo-reactor studies were conducted in deuterated benzene. To prevent oxygen inhibition, hydrogen donors can be used in a threefold concentration of photoinitiator.[26]
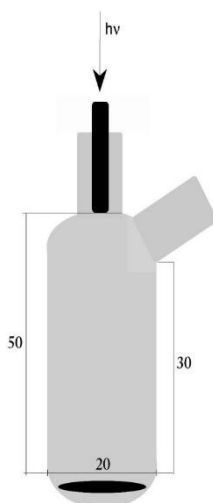
Figure 84. The photo reactor

For this purpose, a photo reactor with an OmniCure Hg-lamp with 400-500 nm filter as light source (Figure 84) was used to irradiate benzyl methacrylate in solution, after degassing with

argon or bubbling air through the solution. Ivocerin was used as photoinitiator in a concentration of 1 wt% and additives were used in 3 eq. to the initiator.

Samples were drawn before irradiation and every 500 s and subsequently ^{1}H-NMR spectra were recorded. In Figure 85 the conversion is plotted with the time. It is visible that neat BMA reaches 50.5% DBC after 1500 s under inert conditions. Under air the reaction stops at 42% DBC after 1000 s and does not further increase. Under inert conditions the cyclohexadiene additives cause a little lower rate of polymerization and therefore the dimethoxy cyclohexadiene DCH reaches only 43% DBC while the activated silyl compound reaches 47% DBC.
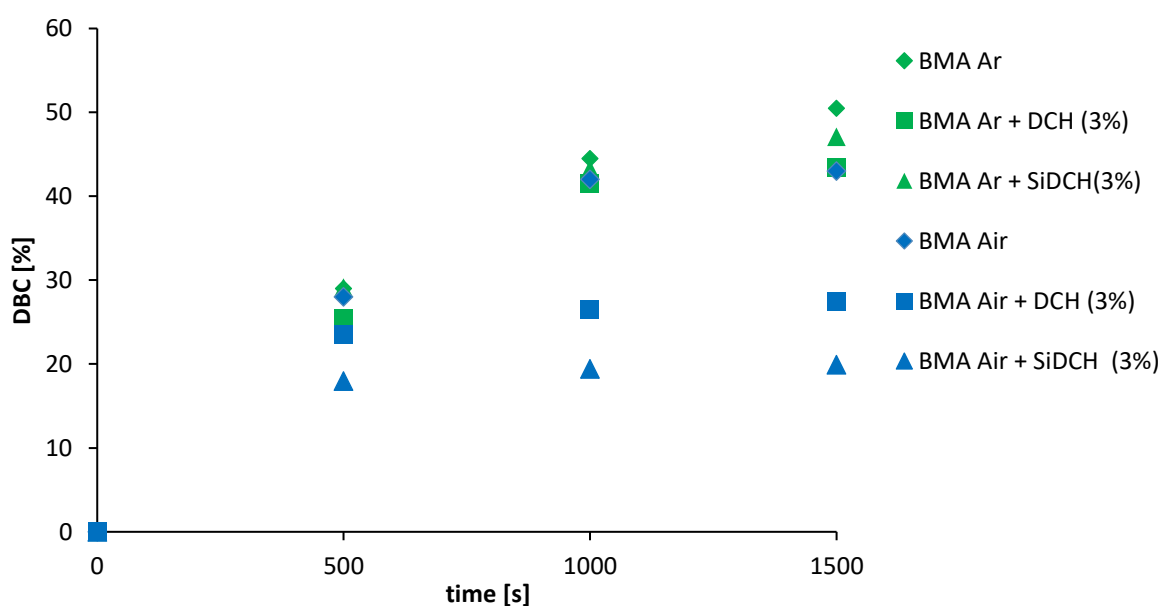
Figure 85. Photo reactor study in C$_6$D$_6$ with BMA as monomer under argon and air with cyclohexadiene DCH and silyl cyclohexadiene SiDCH as anti-oxygen inhibition reagent.

The polymerization under air is strongly inhibited by both cyclohexadienes, even though only around 3% are used. It seems that the proposed mechanism is not working under these conditions and the polymerization is additionally inhibited. The mixture with silyl activated cyclohexadiene only reaches 20% DBC and shows the lowest conversion. Also the conversion barely changes after 500 s.

Summary

Due to the frequent and gaining use of photopolymers for packages in food industry and medical applications from contact lenses to tissue engineering, the search for biocompatible and harmless photoinitiators is very important. The vast majority of applied industrial photoinitiators are based on aromatic ketone structures that are considered potentially harmful including their photoproducts. Therefore, new aliphatic compounds should be investigated on their suitability as photoinitiators in **Part I** of the thesis.

As a second task in **Part II** of the thesis, also the material properties of photopolymers have to be further improved. Therefore, the formation of brittle inhomogeneous photopolymer networks needs to be regulated. Regulation of radical bulk photopolymerization is a way to reach higher toughness and make photomaterials competitive with thermoplastic polymers. In this work, new addition fragmentation chain transfer (AFCT) reagents based on oxy-acrylates should be synthesized and tested. Additionally, a new concept of hydrogen abstraction fragmentation chain transfer agents (HAFCT) using cyclohexadienes with silyl and other leaving groups should be investigated.

In **Part I** first *simple aliphatic α-ketoesters* were examined in group a). Then by *modification of the ester moiety* in group b) the influence of the ester should be investigated. In group c) *modification of the α-carbonyl* the influence on the reactivity by introducing typical Type I initiator moieties was of interest. For curing at higher wavelengths, heteroatoms, planarization of the carbonyls and cross conjugation were investigated to find *long wavelength UV initiators (group d)* and *long wavelength visible initiators* (group e)*.

23 compounds with properties fitting to each group were selected to be tested. Nine of the substances were commercially available and another nine substances could be synthesized.

After preliminary initiation tests in hexanediol diacrylate, finally a selection of twelve compounds was found to be active as photoinitiator.

a) simple aliphatic ketoesters
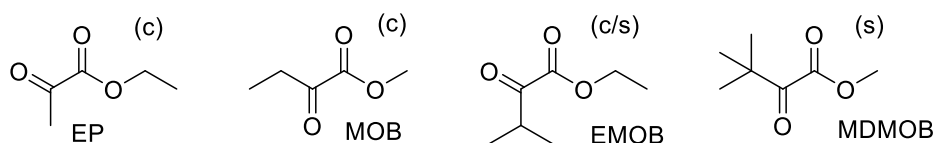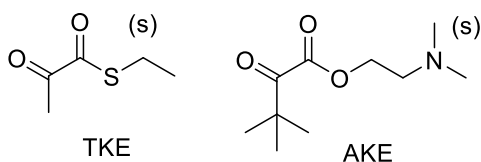
EP   MOB   EMOB   MDMOB

b) modification of the ester moiety

TKE   AKE

c) modification of the alpha carbonyl

BrKE   OHKE

d) long wavelength UV initiators

DDFD   DEKM   DEAP

e) long wavelength visible light initiators

SiKE

(c) commercial
(s) synthesized
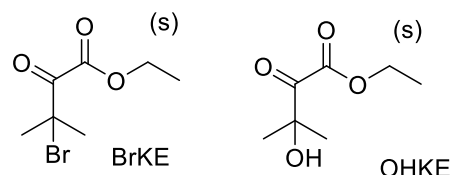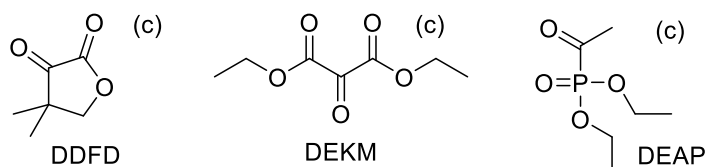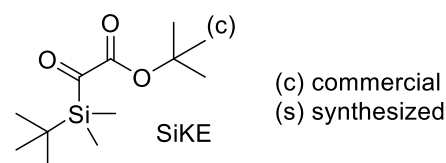
UV-Vis measurements in acetonitrile were conducted of the compounds and the spectra were evaluated to obtain n-π* absorption ranges and extinction coefficients.

Simple aliphatic ketoesters ethyl pyruvate EP, methyl oxobutanoate MOB, ethyl methyl oxobutanoate EMOB and methyl dimethyl oxobutanoate MDMOB showed absorption maxima from 311 to 331 nm with extinction coefficients between 17 and 25 L mol^{-1} cm^{-1}. The absorption of reference initiators e.g. benzophenone BP is in the same range (~330 nm) but the extinction coefficient with 140 L mol^{-1} cm^{-1}, is significantly higher. None of the compounds showed an absorption above 400 nm, so these initiators are limited to UV photopolymerization.

coinitiators

MDEA   EDB
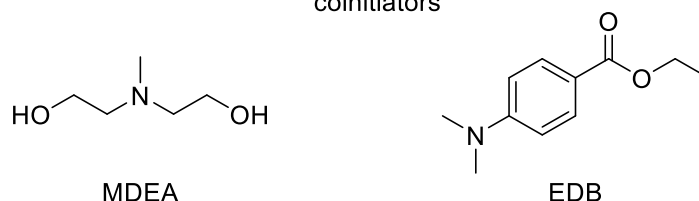
In acrylates and methacrylates, the *simple aliphatic α-ketoesters* showed good reactivity when used without coinitiators and could outperform benzophenone-based initiators BP and BMS with MDEA as coinitiator as well as phenyl glyoxylate PGO without coinitiator, even though the extinction coefficients of the industrial initiators were at least four times to three magnitudes higher. Generally, methyl esters were a little more reactive than ethyl esters, which can be explained by the higher reactivity of the methyl radical formed by intramolecular hydrogen

abstraction. When aliphatic amine MDEA is used as coinitiator, most ketoesters exhibit limited stability in the formulations due to aldol reactions. Aromatic amine coinitiator EDB known from dental composites was compatible with all ketoesters. The performance of most α-ketoesters was further improved.

Modification of the α-carbonyl by introducing a bromo or hydroxy group in β-position also lead to very reactive initiators. Bromo ketoester BRKE and hydroxy compound OHKE showed excellent reactivity. BrKE showed the highest reactivity of all ketoesters even though it could not be measured with amine coinitiators due to decomposition.

Modification of the ester side was unsuccessful, as ketoamides and thiono esters do not initiate at all. Introducing a tertiary amine as intramolecular coinitiator (AKE) lead to slow decomposition of the compound. In addition, thioketoester TKE showed poor reactivity only in the UV range.

Two compounds of the *long wavelength UV initiators*, cyclic ketoester DDFD and diethyl ketomalonate DEKM, showed significant absorption around 400 nm. The substances were tested under broadband and 400 nm LED conditions. Ketomalonate DEKM showed very poor results as the high sensitivity of ketomalonates towards moisture probably leads to fast degradation in technical grade monomers. Cyclic ketoester DDFD, however was very reactive at broadband and at 400 nm LED irradiation. Under this conditions ketoester DDFD showed better performance without coinitiator than state of the art visible light Type II thioxanthone initiator ITX with MDEA as coinitiator.

Acetophosphonate DEAP was surprisingly reactive in the UV range but did not absorb light above 390 nm. The compound also seemed to initiate via Norrish Type II mechanism as the performance could be significantly improved by coinitiator EDB.

No novel compounds suitable as *long wavelength visible initiators* (>410 nm) could be synthesized. Both, tosyl glyoxylates and phosphono glyoxylates were too instable to be isolated under normal conditions. Therefore, only already known aromat free dental initiator silyl glyoxylate SiKE was compared in dental methacrylates with a state of the art acyl germane Ivocerin. It revealed that silyl glyoxylates are a lot less reactive than acyl germanes.

Fortunately, FDA approved ethyl pyruvate and cyclic ketoester DDFD were water-soluble and could be tested in cell cultures and hydrogel formulations. Cytotoxicity tests proved that the compounds and their photoproducts are harmless to cells.

The initiators were tested in a PEG700 acrylic hydrogel formulation. Broadband DSC measurements showed that the ketoesters exhibit better reactivity than a state of the art water-

soluble Type II system (BPQ). Only simultaneously tested Type I initiator 2959 showed higher reactivity.

Photolysis studies with cyclic ketoester DDFD were conducted to reveal the initiation mechanism. From aliphatic α-ketoesters, it is known that they undergo a Norrish Type II reaction from the excited triplet state and initiate by intra/inter molecular hydrogen abstraction. This was also shown for cyclic DDFD but due to sterical reasons of the ring structure, no intra-molecular hydrogen abstraction was found.

The formulations used for DSC measurements were also used to determine discoloration of polymer specimens by UV aging. After irradiating the samples for 2 h with broadband UV light, the cured specimens were evaluated regarding their color. Generally, it can be said that all ketoesters lead to colorless polymer specimens, when no coinitiator was used. Mixtures with industrial Type II initiators benzophenone, benzophenone thioether BMS and thioxanthone ITX show significant yellowing, especially the mixture with ITX. The strongest yellowing was observed with aromatic amine coinitiator EDB. All polymer bars were visibly yellow. However, the formulations cured with aliphatic ketoesters were significantly less discolored.

With aliphatic α-ketoesters a new class of initiators was found, with surprisingly high reactivity. Simple ketoesters such as ethyl pyruvate show high potential as replacement for standard Type II initiators in UV curing. Together with the color stability of ketoester cured polymers this is a very promising new class of photoinitiators for industrial applications in various fields.

In **Part II** of the thesis it was tried to improve methacrylic networks with new addition fragmentation chain transfer agents (AFCT) and hydrogen abstraction fragmentation chain transfer agents (HAFCT), which were synthesized and tested.

The synthesis of chain transfer agents (CTAs) with boron and sulfenyl leaving groups was unsuccessful but new compounds with silyl and carbonate leaving groups could be synthesized. Further a phosphorus compound and a CTA with benzoyl leaving group were compared with the new compounds and also deeply investigated.

Photo-DSC studies with monofunctional benzyl methacrylate with subsequent NMR analysis and SEC measurements were conducted to gain deeper understanding of the polymerization kinetics and influence on the molecular weight of resulting polymers.

With a difunctional methacrylate mixture the CTAs were tested on a real-time NIR photorheometer to obtain information about the mechanics and chemical conversion curves at the same time.

TMSA SSA PCA

VP2 VE5
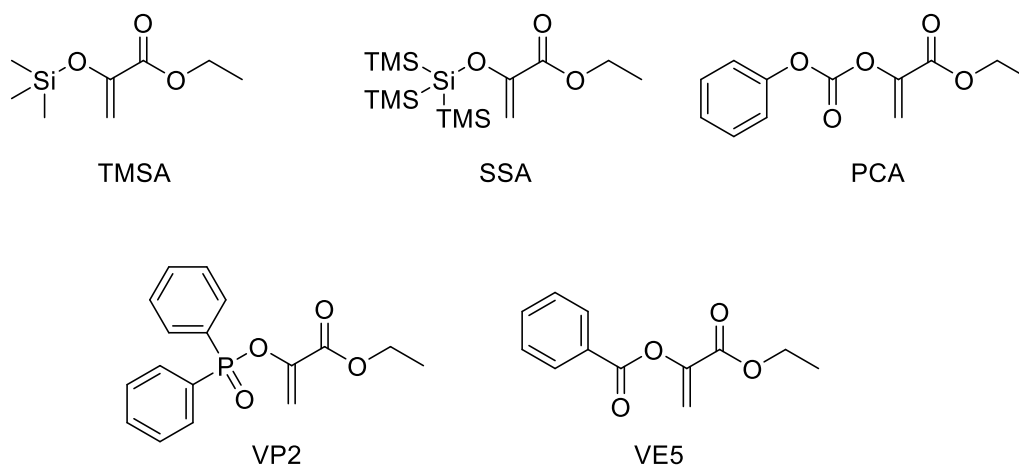
Finally, test bars were polymerized to obtain detailed thermal mechanical information about the formed networks by DMTA measurements.

The DSC tests with monofunctional methacrylate showed that mixtures with vinyl ester VE5 and vinyl carbonate PCA cause no retardation of the polymerization and that the double bond conversion is not negatively influenced. CTAs with silyl (TMSA) or phosphorus (VP2) leaving groups caused strong retardation of the polymerization and also lower conversions. Therefore, it is likely that the compounds are inhibiting the propagation. Bulky silyl compound SSA caused also strong retardation of polymerization but reached higher monomer conversions.

 SEC measurements showed that only the sample with supersilyl SSA achieved a lower molecular weight and a lower PDI.

The samples of smaller silyl CTA TMSA did not contain polymers at all, due to strong inhibition effects. In NMR studies self-consumption and homo polymerization of TMSA could be shown, explaining the strong polymerization inhibition of benzyl methacrylate.

Also in the difunctional monomer system the hetero atom CTAs caused massive retardation. Only supersilyl compound SSA could reach an acceptable DBC of 60%. The conversion at the gel point was not higher in any mixture of hetero CTAs, which is a clear sign that no efficient chain transfer took place.

The mixture with vinyl ester VE5 showed no change of polymerization kinetics and also the mechanical properties of the network remained unchanged. Surprisingly, vinyl carbonate PCA had a significant effect in the more reactive difunctional mixtures. The gel point was shifted in time and to higher conversions. Also the polymerization was significantly faster and reached

higher conversions than the unmodified reference. This is a clear sign that the compound is active as chain transfer agent in this system. This was further supported by the fact that the mixture with PCA was the only mixture with a significant lower and sharper glass transition than the neat network, while keeping the high modulus at RT of the unmodified network.

In the last approach the new mechanism of hydrogen abstraction fragmentation chain transfer (HAFCT) had to be proofed as concept. Therefore, cyclohexadienes with sulfonyl and silyl leaving groups should be synthesized.
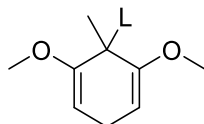
The synthesis of the new compounds was challenging, due to the low stability of the resulting compounds. Only the compound with t-butyl dimethyl silyl leaving group was stable. So, a proof of concept study was conducted with dimethoxy t-butyl dimethyl silyl cyclohexadiene (SiDCH). The leaving group activated compound was compared with not activated dimethoxy cyclohexadiene (DCH).

DCH   SiDCH
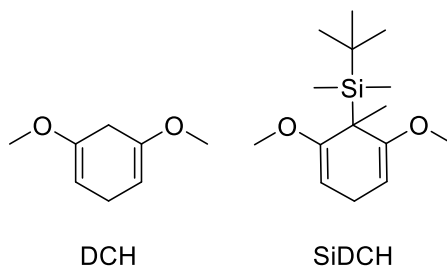
The compounds were tested in the same way as AFCT reagents in a concentration of 20 db%. In monofunctional monomer both cyclohexadiene compounds caused strong retardation and lower double bond conversion. SEC measurements revealed a significantly lower molecular weight but also a very low polydispersity. NMR measurements showed that silyl cyclohexadiene SiDCH is consumed to a similar extent as the monomer but only minor signs of aromatization were observed.

Real-time NIR photorheology in the more reactive difunctional monomer DMM showed significant different behavior between the activated and not activated hexadiene. The non-activated cyclohexadiene DCH inhibited the polymerization to an extent that no gelation was observed. When 10 db% of silyl hexadiene SiDCH were added, the conversion was still slower than that of the neat monomer but in the end nearly the same DBC of unmodified methacrylate DMM was reached. In case of the 10 db% mixture also the conversion at the gel point was higher,

which is a clear sign for regulation. Interestingly also the storage modulus was in the same range as the unmodified network, while the shrinkage force was significantly reduced. Both mixtures with silyl activated silyl hexadiene released the typical strong smell of 1,3-dimethoxy toluene during curing. Together with the observed effects this is a sign that the transfer mechanism with hydrogen abstraction and subsequent aromatization worked.

DMTA measurements revealed that the released dimethoxy toluene acts as softener. Therefore both mixtures with silyl hexadiene SiDCH were significantly softer than the reference material. Sample bars with 10 db% were investigated in a second run. Due to the evaporation of softener the bars exhibited a significantly higher modulus and showed a sharper and lower glass transition at 100 °C than the unmodified network. It seems that the proof of concept worked in a concentration of 10 db% with silyl cyclohexadiene SiDCH.

Experimental part

Part 1: Novel Photoinitiators based on aliphatic structures

1. Selection of compounds

For a first test of α-keto esters on their ability to initiate 1 wt% of keto compound was mixed with methacrylate DMM. Therefore, 10 mg of keto compound were weighed into brown glass vials and afterwards 1000 mg of monomer DMM were added. After 10 seconds mixing with the Vortex mixer at highest power, the sample was transferred into a silicon mold (2 x 1 x 0.15 cm) and put into the middle of an Intelliray 600 UV flood curing system. If a compound did not dissolve properly, mild heat was applied with a heat gun and mixed until a homogenous solution was achieved. The samples were irradiated on the middle tray for 100 s in an Intelliray broadband UV oven at 100% power of the mercury lamp. Afterwards the samples were categorized into cured, partly cured or uncured.

2. Synthesis and selection of α-keto compounds

2.1. Simple aliphatic α-ketoesters

2.1.1. Synthesis of dimethyl oxobutanoic acid (1)
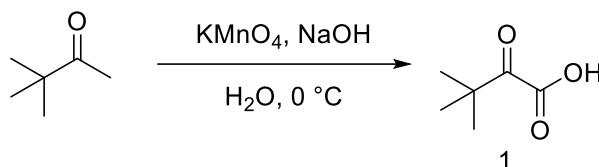
The synthesis of dimethyl oxobutanoic acid (1) was conducted according to literature.[59] Therefore, in a acetone/ice bath cooled 3 L three-necked flask 19.83 g pinacolone (0.198 mol, 1 eq.) were dissolved in 750 mL cold aqueous NaOH (0.396 mol, 2 eq.) and 62.58 g potassium permanganate (0.396 mol, 2 eq.) were added subsequently in small potions so that the temperature does not raise above -2 - 0 °C. After complete addition of permanganate within 4 h, the solution is allowed and warmed up to RT and stirring is continued overnight. The next day the precipitated manganese dioxide is filtered off and the solution is acidified with 35 mL conc. HCl to PH 2. The filtrate was extracted three times with 150 mL diethyl ether and the combined organic layers were washed with 150 mL brine. After drying the organic phase with anhydrous Na_2SO_4 the solvent was removed in vacuum. Distillation at 100 °C and 26 mbar afforded dimethyl oxobutanoic acid **1** in 78% of theory as colorless liquid. Small quantities of pivalic acid (8%) could not be removed.

bp.: 79-80 °C / 26 mbar, lit.: 78-80 °C / 19 Torr[184]

n_D^{20} = 1.421, lit.: n_D^{25} = 1.4222[185]

^{1}H NMR (400 MHz, CDCl$_3$, δ, ppm): 8.91 (s, 1 H, COO<u>H</u>), 1.11 (s, 9H, C(C<u>H</u>$_3$)$_3$).

^{13}C NMR (100 MHz, CDCl$_3$, δ (ppm): 200.8 (C4), 161.0 (C4), 42.6 (C4), 25.8 (C1).

2.1.2. Synthesis of methyl dimethyl oxobutanoate (MDMOB)
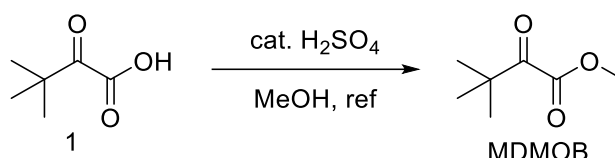
For the synthesis of methyl dimethyl oxobutanoate MDMOB, 13.01 g of dimethyl oxobutanoic acid (**1**) (0.10 mol, 1 eq.) is refluxed overnight in 100 mL freshly distilled methanol with 2 mL of sulfuric acid in a three-necked flask. The reaction mixture was poured in 100 mL ice water and extracted four times with 50 mL ethyl acetate. The combined organic phase was washed three times with 50 mL saturated sodium hydrogen carbonate solution and once with 40 mL brine. After evaporation of the solvent in vacuum, 10.90 g the crude product was distilled in vacuum at 100 °C and 20 mbar to remove side product pivalic acid methyl ester. Finally 5.51 g (38% of theory) of pure methyl dimethyl oxobutanoate were obtained as colorless liquid with fruity odor.

bp.: 60 °C / 20 mbar, lit.: 59-60 °C / 18 Torr[186]

n_D^{20} = 1.412, lit.: n_D^{25} = 1.413[187]

^{1}H NMR (400 MHz, C$_6$D$_6$, δ, ppm): 3.83 (s, 3H, C<u>H</u>$_3$), 1.24 (s, 9H, 3C<u>H</u>$_3$)

^{13}C NMR (100 MHz, CDCl$_3$, δ (ppm): 201.2 (C4), 163.9 (C4), 52.1 (C1), 42.4 (C4), 25.3 (C1),

2.1.3. Synthesis of ethyl methyl oxobutanoate (EMOB)
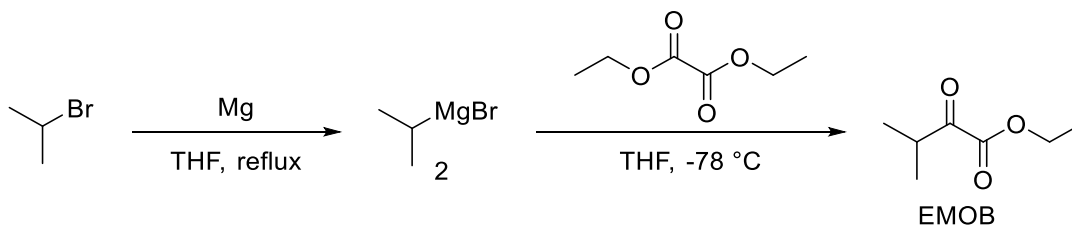
For the synthesis of ethyl methyl oxobutanoate EMOB a Grignard reaction between diethyl oxalate and isopropyl magnesium bromide (**2**) was chosen as convenient preparation pathway.[64, 65]

For the preparation of the Grignard reagent, 3.26 g magnesium flakes (0.134 mol, 1.1 eq.) were placed in a 250 mL three-necked flask and heated with a heat gun under vacuum. The flakes were

cooled to RT under argon and 20 mL of dry THF were added. Then 15.01 g 2-bromo propane (0.122 mol, 1 eq.) were diluted in 100 mL dry THF and attached to the flask in a dropping funnel. 2ml of the bromo mixture was added to the magnesium and heated to reflux with a heat gun. The remaining solution of bromo propane was added dropwise so that the reflux temperature was maintained. After full addition, the mixture was heated to reflux for another 35 min.

For the next step 26.7 g (0.183 mol, 1.5 eq.) freshly distilled diethyl oxalate, dried with CaH$_2$ was dissolved in 30 mL THF and cooled to -80 °C under argon atmosphere. The Grignard solution (**2**) from the first step was added dropwise over one hour. After the addition the mixture was allowed to warm up to -15 °C and quenched with 100 mL saturated ammonium chloride solution. After three times extraction with 100 mL ether the combine organic phase was washed with 100 mL brine and dried with Na$_2$SO$_4$. The solvent was stripped off in vacuum and the raw ketoester was distilled at 100 °C and 12 mbar. Three fractions with a boiling point between 60 °C and 67 °C were obtained. All of them contaminated with remaining oxalate. Column chromatography with PE:EE = 20:1 yielded 6.39 g (36% of theory) ethyl methyl oxobutanoate EMOB as colorless oil with a distinct smell of pineapple.

bp.: 64-67 °C / 12 mbar, lit.: 63-70 °C /12 Torr[188]

n_D^{20} = 1.412, lit.: n_D^{20} = 1.413[64]

^{1}H NMR (400 MHz, C$_6$D$_6$, δ, ppm): 4.29 (q, J = 7.1 Hz, 2H, O-C<u>H$_2$</u>-CH$_3$), 3.20 (h, J = 7.0 Hz, 1H, -<u>CH</u>-(CH$_3$)$_2$), 1.33 (t, J = 7.1 Hz, 3H, O-CH$_2$-<u>CH$_3$</u>); 1,12 (d, J = 7.0 Hz, 6H, -CH-<u>(CH$_3$)$_2$</u>)

2.2. Modification of the ester moiety

2.2.1. Synthesis of N,N-dibutyl-2-oxopropanamide (KEA)

As pyruvates showed instability under basic conditions, the amide should be prepared via the acid chloride according to literture.[68, 69]
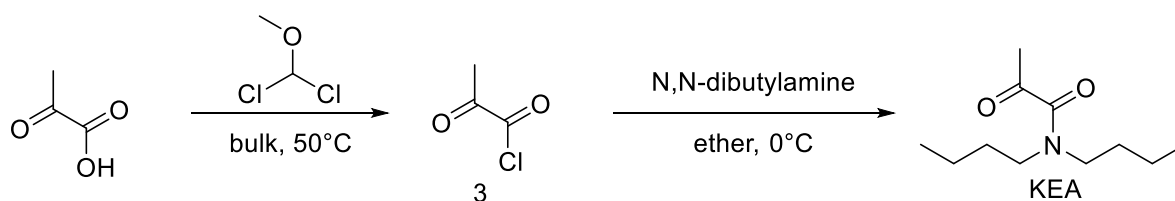
For the synthesis of N,N-dibutyl-2-oxopropanamide (KEA) first 6.16 g (70 mmol, 1 eq.) pyruvic acid and five drops of dry DMF were put into a 100 mL three-necked flask under argon atmosphere. 8.05 g (70 mmol, 1 eq.) of dichloromethyl methylether were added slowly under inert conditions and heated to 50 °C for 30 min after completion of addition. Then the mixture was stirred overnight at room temperature. After evaporation of all volatile residues in vacuum,

the acid chloride **3** was used as is. In the next step, 2.13 g (20 mmol, 1 eq.) acid chloride diluted in 10 mL dry ether and added to a 5.43 g (42 mmol, 2.1 eq.) of dibutyl amine dissolved in 30 mL dry diethyl ether at 0 °C. During the addition of acid chloride the reaction turned orange and hydrochloric smoke was visible. The reaction was stirred for 1 h while cooling and quenched with 45 mL 1N HCl. After phase separation, the aqueous phase was extracted with another 50 mL ether and the combined organic phase was dried with 50 mL brine and Na_2SO_4. After evaporation of the solvent, 42% of raw product were received as red oil. Flash chromatography over 100 g silica (PE:EE = 5:1) yielded 830 mg (21% of theory) of N,N-dibutyl-2-oxopropanamide (KEA) as clear liquid.

DC: PE:EE (5:1) Rf: 0.68

^{1}H NMR (400 MHz, C_6D_6, δ, ppm): 3.15 (t, J = 7.5 Hz, 2H, C$\underline{H}_2$), 2.91 (t, J = 7.6 Hz, 2H, C$\underline{H}_2$), 2.12 (s, 3H, C$\underline{H}_3$), 1.36(qi, J = 7.4 Hz, 2H, CH$_2$), 1.25 (qi, J = 7.5 Hz, 2H, C$\underline{H}_2$), 1.13 (s, J = 7.6 Hz, 2H, C$\underline{H}_2$), 0.98 (s, J = 7.6 Hz, 2H, C$\underline{H}_2$), 0.80 (t, J = 7.3 Hz, 3H, C$\underline{H}_3$), 0.72 (t, J = 7.3 Hz, 3H, C$\underline{H}_3$)

^{13}C NMR (100 MHz, C_6D_6, δ (ppm): 198.8 (C4), 166.9 (C4), 47.4 (C2), 44.8 (C2), 33.3 (C2), 31.1 (C2), 27.8 (C1), 20.2 (C2), 19.9 (C2), 13.8 (C1), 13.7 (C1)

GC-MS: 199.27 [M+], 156.21 [M - C_2H_5], 100.11 [M - C_2H_5-C_4H_9], 57.13 [M - N-C_4H_9-COCOCH$_3$]

2.2.2. Synthesis of O-methyl S-ethyl 2-oxopropanethioate (TKE)

TKE
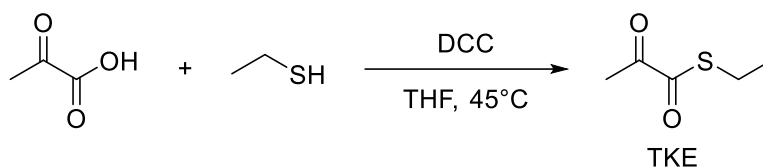
Direct reaction of pyruvic acid and ethane thiol with DCC was chosen for synthesis of O-methyl S-ethyl 2-oxopropanethioate TKE.[73]

Therefore, 19.6 g (98 mmol, 1eq.) DCC were dissolved 200 mL dry THF. After the addition of 5.90 g (98 mmol, 1 eq.) ethane thiol, 8.37 g (98 mmol, 1 eq.) pyruvic acid were added dropwise diluted in 25 mL THF. Instant formation of solid urea was visible and the whole reaction mixture turned deeply yellow. After refluxing for 5 min the mixture was cooled and filtrated. After evaporation of the solvent under vacuum, the yellow residual oil was distillated twice, yielding 4.3 g (34% of theory) O-methyl S-ethyl 2-oxopropanethioate TKE as yellow extremely smelly oil. The compound has to be handled very carefully as the unbearable smell is causing nausea and can be hardly removed from any surface.

bp.: 59 °C / 13 mbar, lit.: 62-64 °C / 10 Torr[189]

^{1}H NMR (400 MHz, C$_6$D$_6$, δ, ppm): 2.51 (q, *J* = 7.3 Hz, 2H, C$\underline{H}_2$-CH$_3$), 1.78 (s, 3H, C$\underline{H}_3$), 0.89 (t, *J* = 7.4 Hz, 3H, CH$_2$-C$\underline{H}_3$)

^{13}C NMR (100 MHz, C$_6$D$_6$, δ (ppm): 193.2 (C4), 191.6 (C4), 23.9 (C1), 23.2 (C2), 14.2 (C1)

2.2.3. Synthesis of O-methyl 3,3-dimethyl-2-oxobutanethioate (TBTKE)

For the synthesis of O-methyl thiolate TBTKE a direct onepot synthesis from pinacolone with thionyl chloride and methanol as reagent was chosen. [74]
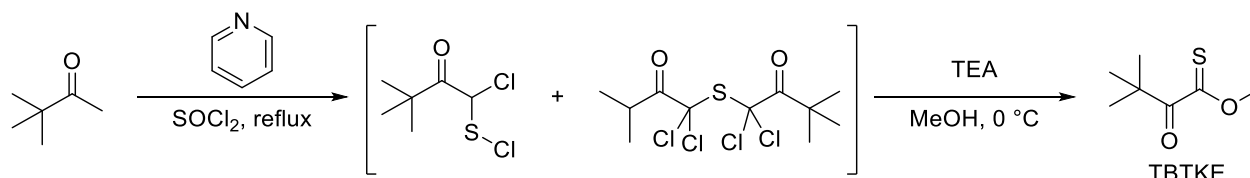
To 88 g (0.75 mol, 15 eq.) thionyl chloride, 5.01 g (50 mmol, 1 eq.) pinacolone was added dropwise while stirring at RT together with 2 mol% of pyridine as catalyst. Instantly a lot of gas formation and the reaction turning deeply red was observed. After two hours the excess of thionyl chloride was distilled off under vacuum. The crude intermediate was redissolved in 100 mL methanol and 20 g (200 mmol, 4 eq.) triethylamine were added dropwise at 0 °C. After complete addition, the reaction was allowed to warm up to RT overnight. The next day the reaction was acidified with 50 mL 1 N HCl and extracted three times with 50 mL ether. After drying the organic phase with Na$_2$SO$_4$ the solvent was stripped off in vacuum and 1.73 g of yellow very smelly raw product was obtained. Further purification with MPLC (PE:EE = 5:1) and subsequent ball pipe distillation afforded 582 mg (8% of theory) pure O-methyl 3,3-dimethyl-2-oxobutanethioate (TBTKE) as yellow oil with unbearable smell.

bp.: 124 °C / 0.9 mbar, lit.: na

^{1}H NMR (400 MHz, C$_6$D$_6$, δ, ppm): 3.43 (s, 3H, O-C$\underline{H}_3$), 1.11 (s, 9H, C-(C$\underline{H}_3$)$_3$)

2.2.4. Synthesis of 2-(dimethylamino)ethyl 2-oxopropanoate (AKE)
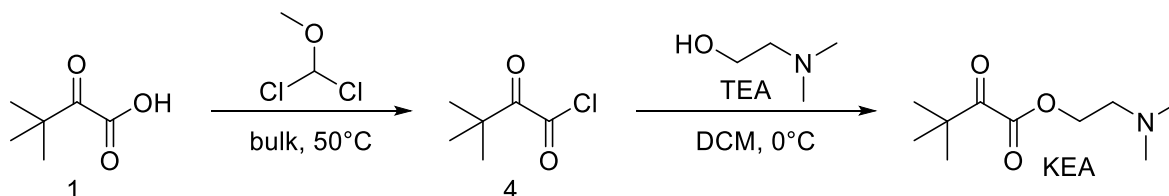
For the synthesis of 2-(dimethylamino)ethyl 2-oxopropanoate KEA, dimethyl oxobutanioc acid chloride (**4**) had to be prepared first.[69]

Therefore, 4.55 g (35 mmol, 1 eq.) dimethyl oxobutanoic acid (**1**) and five drops DMF were dissolved in 30 mL dry DCM under argon atmosphere. While stirring at RT, 4.39 g (38.5 mmol, 1.1

eq.) dichloro methyl methylether were added dropwise and the mixture was stirred for two hours.

Then the volatile residues were removed by vacuum and the residues were distilled at 60 °C and 95 mbar (bp.: 40 °C). The acid chloride 4 was obtained as clear liquid in a low yield of 10%. α-oxo acid chlorides are sensitive and it seems that distillation causes some decomposition.

In the next step 0.54 g (3.7 mmol, 1 eq.) of acid chloride 4 were dissolved in 10 mL DCM under argon. To the solution 0.81 g (9.1 mmol, 2.5 eq.) dimethyl ethanolamine were added dropwise while cooling with ice.[190] The mixture was stirred for 48 h. Then the solvent was removed in vacuum. The crude oil was redissolved in ether to remove insoluble hydrochloride. Due to water solubility and the ability of the product to form ammonium salts, aqueous extraction with hydrochloric acid was not possible. Therefore, the product was purified with ball pipe distillation (bp.: 94 °C / 1.2 mbar).

Only 122 mg (17% of theory) could be isolated as colourless oil with an amine like smell.

The product was metastable as the basic amino group slowly decomposed the ketoester!

R_f: 0.10, PE:EE (1:1)

^{1}H NMR (400 MHz, C_6D_6, δ, ppm): 4.11 (t, J= 6.5 Hz, 2H, O-C$\underline{H}_2$-CH$_2$-), 2.29 (t, J= 5.9 Hz, 2H, CH$_2$-C$\underline{H}_2$-N), 2.02 (s, 6H, N-(C$\underline{H}_3$)$_2$), 1.16 (s, 9H, C-(C$\underline{H}_3$)$_3$)

2.3. Modification of the alpha carbonyl – Type I cleavage

2.3.1. Synthesis of ethyl 3-bromo-3-methyl-2-oxobutanoate (BrKE)

EMOB → BrKE
Br$_2$
CCl$_4$ / 10 % AcOH
RT
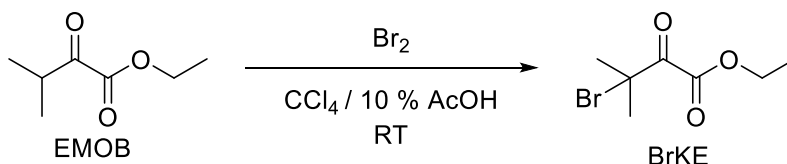
For the synthesis[191] of the bromo ketoester BrKE 1.44 g (10 mmol, 1 eq.) of ethyl 3-methyl-2-oxobutanoate (EMOB) were dissolved in 10 mL CCl$_4$ together with 1 mL of acetic acid. 1.60 g (10 mmol, 1 eq.) of bromine were added via syringe and the mixture was stirred in darkness for 1.5 h. 50 mL chloroform were added and the reaction was quenched with 50 mL saturated NaHCO$_3$ solution. After extraction in a separation funnel the organic phase was dried with 10 g Na$_2$SO$_4$ and the solvent was removed by rotary evaporator (10 mbar, 40 °C) to yield 2.09 g (94% of theory) BrKE as slightly yellow oil with fruity smell.

R_f = 0.48, PE:Et$_2$O = 9 : 1

n_D^{25} = 1.449, lit.: na

^{1}H-NMR (400 MHz, CDCl3, ppm): 4.38 (q, 2 H, J= 7.05 Hz, <u>CH$_2$</u>-CH$_3$); 2.01 (s, 6 H, Br-C-<u>(CH$_3$)$_2$</u>); 1.39 (t, 3H, J= 7.05 Hz, CH$_2$-<u>CH$_3$</u>).

2.3.2. Synthesis of ethyl hydroxymethyl butanoate (OHKE)
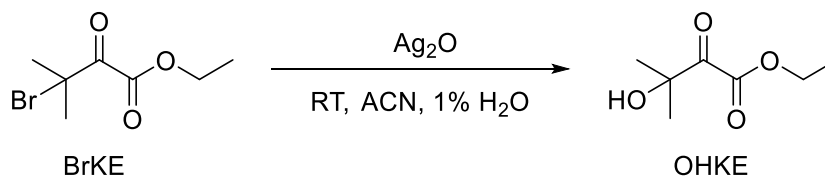
For the synthesis of ethyl hydroxymethyl butanoate OHKE 4.46 g (20 mmol, 1 eq.) bromomethyl oxobutanoate (BrKE) is dissolved in 30 mL acetonitrile with 0.3 mL water.[78] Then 2.32 g (10 mmol, 0.5 eq.) Ag$_2$O are added. The suspension is stirred 16 h at RT under exclusion of light. During the reaction the suspension changes from black coarse particles to grey and fine. Afterwards the grey solid is filtered off. The filtrate is diluted with 10 mL water and extracted with 100 mL diethyl ether. After drying the combined organic phases, the solvent is stripped off in vacuum (100 mbar). Subsequent ball pipe distillation affords 1.50 g (94%) desired hydroxyl ketoester in 93% purity as clear oil. The impurities consist of precursor BrKE.

R$_f$: 0.5, PE:EE = 3:1

n_D^{20} = 1.417, lit.: n_D^{20} = 1.4176[192]

bp.: 120 °C / 25 mbar, 80-90 °C / 12 Torr[192]

^{1}H-NMR (400 MHz, C$_6$D$_6$, ppm): 3.85 (q, 2 H, J= 7.2 Hz, <u>CH$_2$</u>-CH$_3$), 2.94 (bs, 1H, <u>-OH</u>), 1.30 (s, 6 H, HO-C-<u>(CH$_3$)$_2$</u>).

2.4. Modification of the alpha carbonyl – Long wavelength UV initiators

2.4.2. Synthesis of ethyl 3-methyl-2-oxobut-3-enoate (MAKE)
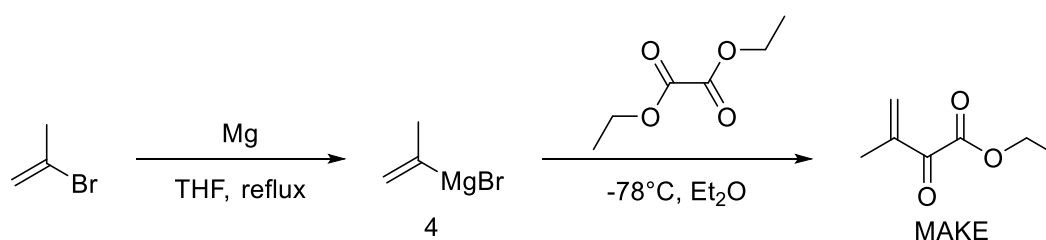
For the synthesis of 3-methyl-2-oxobut-3-enoate 1.5 eq. the Grignard reagent isopropenyl magnesium bromide (**4**) had to be prepared first ident to literture.[64, 193] Therefore, 1.09 g (45 mmol, 1.5 eq.) magnesium flakes where moisturized with 2 mL dry THF. After diluting 4.36 g (36 mmol, 1.3 eq.) isopropenyl bromide in 37 mL of dry THF, 2 mL of the solution were added to

the magnesium and heated with a heat gun. After the reaction started, reflux temperature was maintained by dropwise addition of isopropenyl bromide solution.

After the Grignard reaction was finished the resulting solution was added dropwise to a solution of 4.38 g (30 mmol, 1 eq.) dry diethyl oxalate in 60 mL 1:1 dry ether and THF at -80 °C. As the Grignard reagent **4** can react multiple times with the substrate, TLC monitoring was crucial. After adding ¾ of the solution, subsequent TLCs showed no more diethyl oxalate so the addition of magnesium bromide **4** was stopped and the reaction was quenched with 15 mL 2 N H_2SO_4. After three times extraction with 30 mL ether, the combined organic phases were dried with 50 mL brine and Na_2SO_4, then the solvent was removed in vacuum. The resulting yellow oil shows some remaining diethyl oxalate and impurities in NMR. After ball pipe distillation at 12 mbar and 100 °C, a clear oil was obtained. NMR still showed some precursor. 1.46 g (34% of theory) of 3-methyl-2-oxobut-3-enoate (MAKE) was finally obtained by column chromatography with PE:EE = 19:1.

The conversion of diethyl oxalate is hard to follow by TLC as the compound is not visible under UV and hardly stains with any staining reagent. After NMR it was clear that diethyl oxalate was not fully consumed, therefore the yield is lower than expected.

In literature, the compound is described as yellow which made this product especially interesting as the double bond was expected to cause a bathochromic shift.[93, 94] Nevertheless, the color is caused by impurities of diketone, which results from double attack by the Grignard reagent. The yellow very apolar compound can be separated by column chromatography. The pure ethyl 3-methyl-2-oxobut-3-enoate (MAKE) is almost colorless.

R_f: 0.3, PE:EE = 19:1

n_D^{25} = 1.434, lit.: n_D^{20} = 1.4325[64]

^{1}H-NMR (400 MHz, CDCl$_3$, ppm): 6.17 (s, 1H, C=C$\underline{H_2}$), 6.09 (s, 1H, C=C$\underline{H_2}$), 4.35 (q, J= 7.2 Hz, 2H, O-C$\underline{H_2}$-CH$_3$), 1.93 (s, 3H, CH$_3$), 1.37 (t, J= 7.2 Hz, 3H, O-CH$_2$-C$\underline{H_3}$).

^{13}C NMR (100 MHz, CDCl$_3$, δ (ppm): 188.8 (C4, C=O), 164.2 (C4, C=O), 140.7 (C4, $\underline{C}$=CH$_2$), 132.4 (C2, C=$\underline{CH_2}$), 62.1 (C2, O-$\underline{CH_2}$-CH$_3$), 16.2 (C1, CH$_3$), 14.1 (C1, O-CH$_2$-$\underline{CH_3}$)

2.5. Modification of the alpha carbonyl – Long wavelength visible light initiators

2.5.1. Synthesis of trimethyl silylglyoxylate (TMSi)
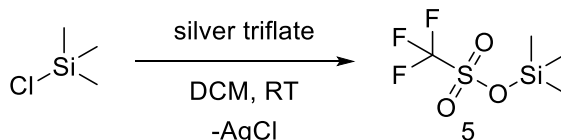
For the synthesis of the ethyl trimethyl silylglyoxylate, the triflate compound **5** had to be synthesized first from trimethyl chloro silane ident to literature.[96] Therefore, 0.71 g (6.5 mmol, 1eq.) trimethyl chloro silane was added at once to 1.67 g (6.5 mmol, 1 eq.) silver triflate suspended in 4 mL abs. DCM under argon. The suspension is stirred overnight under exclusion of light and filtrated.
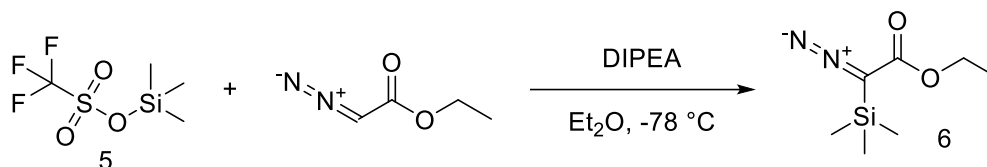
The solution of TMS-triflate **5** (smoking) was then added dropwise to 0.85 g (6.5 mmol, 1 eq.) ethyl diazo acetate and 0.84 g (6.5 mmol, 1 eq.) ethyl diisopropyl amine in 30 mL dry ether under argon at -78 °C.[194] After 20 min the mixture was warmed up to room temperature and stirred overnight. After filtration of the resulting ammonium salt the solvent was stripped off in vacuum and the crude ethyl diazo(trimethylsilyl)acetate (**6**) was obtained as deep yellow oil. Further purification was not conducted due to stability concerns of the product. The product **6** shows a specific ATR-IR signal of C=N$_2$ at 2080 cm^{-1} which is consistent with literature.[195]
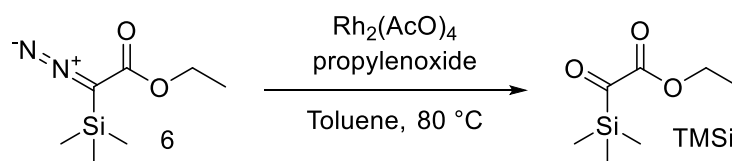
The diazo compound **6** was immediately redissolved in 20 mL toluene and 5.2 g (78 mmol, 12 eq.) of propylene oxide were added. Then 66 mg (2 mol%) rhodium acetate was added while stirring. Instant formation of gas was observed. The reaction was then heated to 40 °C overnight and the solvent was stripped of in vacuum.

The crude product was flashed over silica with PE/EE 25:1 and after evaporation of the solvent 350 mg (31% of theory) ethyl trimethyl silylglyoxylate TMSi was obtained as brilliant yellow oil.

R$_f$: 0.4, PE:EE = 25:1

^{1}H-NMR (400 MHz, CDCl$_3$, ppm): 3.87 (q, J= 7.14 Hz, 2H, O-C$\underline{H_2}$-CH$_3$), 0.87 (t, J= 7.14 Hz, 3H, O-CH$_2$-C$\underline{H_3}$), 0.12 (s, 9 H, Ge(CH$_3$)$_3$)

^{13}C NMR (100 MHz, CDCl$_3$, ppm): 230.2 (C4, C=O), 161.1 (C4, C=O), 61.7 (C2, C$\underline{H_2}$-CH$_3$), 13.8 (C1, CH$_2$-C$\underline{H_3}$), -3.5 (C1, Si$\underline{(CH_3)_3}$)

GC-MS: calculated: 174.07, found: 175.14 [M +H], 159.07 [M –CH$_3$], 131.11 [M –Et, -CH$_3$], 101.01 [M –COOEt], 73.13 [(CH$_3$)$_3$Si]

2.5.2. Synthesis of ethyl trimethyl germylglyoxylate (TMGe)

For the synthesis of trimethyl germylglyoxylate (TMGe) the exact same procedure as in 2.5.1. was conducted but with trimethyl chloro germane.
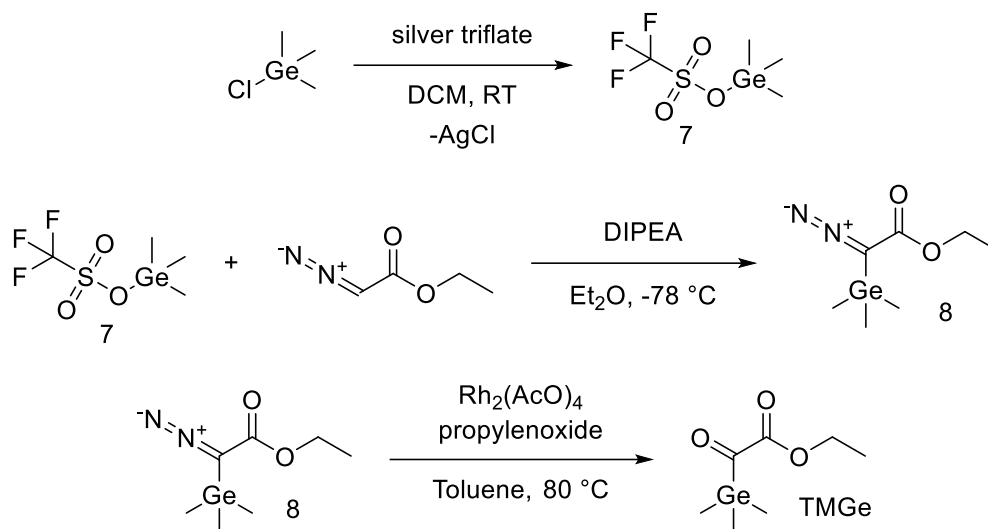
The diazo intermediate **8** shows a specific ATR-IR signal of C=N$_2$ at 2077 cm^{-1} which is also found in literature.[195]

Column chromatography with Et$_2$O : PE = 5:95 afforded 500 mg (35% of theory) of ethyl trimethyl germyl glyoxylate TMGe as brilliant yellow oil.

R$_f$: 0.26, PE:Et$_2$O = 95:5

^{1}H-NMR (400 MHz, CDCl$_3$, ppm): 3.9 (q, J= 7.14 Hz, 2H, O-C$\underline{H_2}$-CH$_3$), 0.9 (t, J= 7.14 Hz, 3H, O-CH$_2$-C$\underline{H_3}$), 0.32 (s, 9 H, Ge(CH$_3$)$_3$).

^{13}C NMR (100 MHz, CDCl$_3$, ppm): 184.8 (C4, C=O), 160.1 (C4, C=O), 59.8 (C2, O-C$\underline{H_2}$-CH$_3$), 13.4 (C1, O-CH$_2$-C$\underline{H_3}$), -4.3 (C1, Ge$\underline{(CH_3)_3}$)

GC-MS: calculated: 220.02, found: 221.02 [M +H], 204.86 [M −CH$_3$], 146.98 [M −COOEt], 118.98 [(CH$_3$)$_3$Ge]

2.5.3. Synthesis of triethyl phosphono glyoxylate (PKE)

2.5.3.1. Synthesis of tosyl azide (9)

For the preparation of phosphono glyoxylate PKE tosyl azide had to be prepared first.
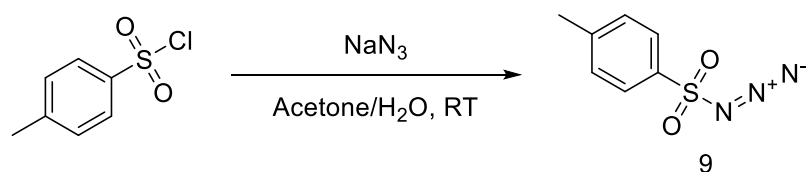
For the preparation of tosyl azide (**9**) ident to literature, 4.88 g (75 mmol, 1.5 eq.) sodium azide is dissolved in 20 mL water and stirred.[102] Then 9.53 g (50 mmol, 1 eq.) tosyl chloride is dissolved in 20 mL acetone and added dropwise to the stirred sodium azide solution cooled to 0 °C. After 1 h the precipitate of NaCl is filtered and the filtrate is extracted with 100 mL ether. After drying the organic phase with Na_2SO_4, the solvent is stripped off carefully (RT) in vacuum to afford 9.8 g (99% of theory) tosyl azide (**9**) quantitatively as colorless oil. Heating should be avoided as tosyl azide can be explosive. During storage in the fridge tosyl azide crystalizes as colorless needles, which rapidly melt at RT.

mp.: 21 °C, lit.: 22°C[196]

^{1}H-NMR (400 MHz, CDCl$_3$, ppm): 7.76 (d, J = 8.6 Hz, 2H, Ar), 7.34 (d, J = 8.4 Hz, 2H, Ar), 2.40 (s, 3H, CH$_3$).

2.5.3.2. Synthesis of ethyl 2-diazo-2-(diethoxyphosphoryl)acetate (10)
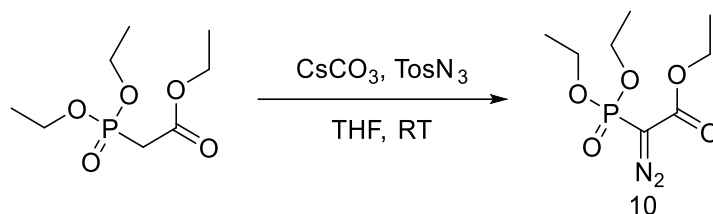
In the next step 100 mL abs. THF were charged with 2.47 g (11 mmol, 1 eq.) triethyl phosphono acetate and 3.58 g (11 mmol, 1 eq.) cesium carbonate. Then 2.17 g (11 mmol, 1 eq.) tosyl azide (**9**) are added quickly and the mixture is stirred at RT for 2 h according to literature.[103] Afterwards the reaction is filtered over hyflow to remove the precipitated tosyl amide and the solvent stripped off in vacuum to afford crude triethyl phosphono diazo acetate as yellow oil. NMR analysis showed remaining tosyl amide so the compound is redissolved in a small amount of diethyl ether and the same amount of petrol ether is added to precipitate remaining tosyl amide. After filtration and removal of the solvent in vacuum, 1.34 g (49% of theory) phosphor diazo compound (**10**) is received as yellow oil. Small amounts tosyl amide are still present but due to the instability of the compound 92% purity was acceptable.

^{1}H-NMR (400 MHz, CDCl$_3$, ppm): 4.29 - 4.01 (m, 6H), 1.36 – 1.15 (m, 9H)

^{13}C NMR (100 MHz, CDCl$_3$, ppm): 161.5 (d, J$_{C-P}$= 12.1 Hz, C4), 63.7 (d, J$_{C-P}$= 5.8 Hz, C2), 61.7 (C2) 16.1 (d, J$_{C-P}$= 7.2 Hz, C1), 14.3 (C1)

GC-MS: calculated: 250.07, found: 250.05 [M+], 223.11 [M -N$_2$, +H], 177.04 [M –COOEt], 137.08 [PO(OEt)$_2$]

2.5.4. Synthesis of ethyl tosyl glyoxylate (SKE)

2.5.4.1. Synthesis of ethyl tosyl acetate (11)
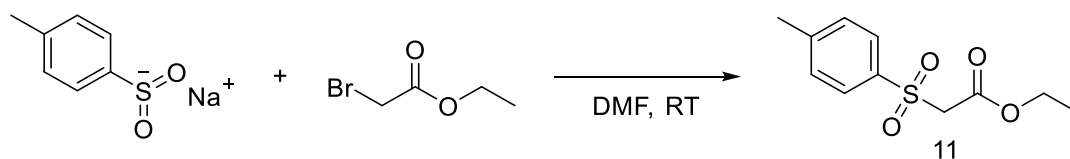
For the synthesis of ethyl tosyl glyoxylate SKE, ethyl tosyl acetate (**11**) had to be prepared first according to literature.[105] Therefore, 2.67 g (15 mmol, 1 eq.) sodium toluene sulfinate was dispersed in100 mL DMF and 2.51 g (15 mmol, 1 eq.) ethyl bromo acetate were added at once. The suspension gets warm and the solid dissolves quickly. After stirring overnight, the mixture is diluted with half the volume water and extracted with 50 mL ethyl acetate. The solvent is then stripped off the organic phase dried with Na_2SO_4. To remove the remaining DMF the oil was redissolved in 50 mL diethyl ether and extracted three times with the 200ml water. After drying and evaporating the organic phase, 2.53 g (70% of theory) of tosyl ethyl acetate (**11**) crystallized as colorless needles.

mp.: 31-33 °C, lit.: 32-33 °C[197]

^{1}H-NMR (400 MHz, CDCl$_3$, ppm): 7.75 (d, J= 8.1 Hz, 2H, Ar), 7.30 (d, J= 8.1 Hz, 2H, Ar), 4.09 (q, J= 7.0 Hz, 2H, O-C$\underline{H}_2$-CH$_3$), 4.02 (s, 2H, S-CH$_2$-COO-), 2.39 (s, 3H, Ar-CH$_3$), 1.13 (t, J= 7.3 Hz, 3H, CH$_2$-C$\underline{H}_3$)

GC-MS: calculated: 242.06, found: 243.19 [M +H], 197.05 [M –COOEt], 155.13 [Tol-SO$_2$]

2.5.4.2. Synthesis of ethyl tosyl diazoacetate (12)
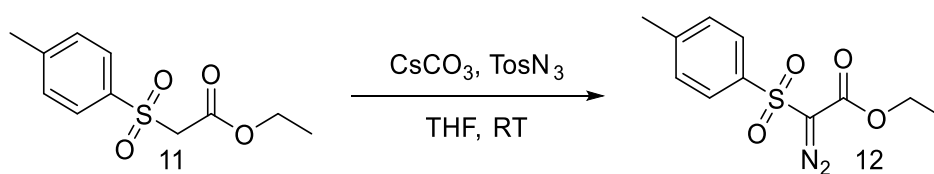
In the next step 1.79 g (7.4 mmol, 1 eq.) tosyl acetate (**11**) were suspended with 2.41 (7.4 mmol, 1 eq.) of cesium carbonate in 70 mL THF under argon. An equimolar amount of tosyl azide was added after 30 min stirring at RT and stirred overnight analogue to literature.[106] The next day the deeply orange solution was filtered off the colorless precipitate and the solvent was stripped off in vacuum. The resulting orange oil was filtered over 50 g silica gel with 1:1 EE/PE as eluent. The solvent was removed again by vacuum and the resulting lemon-yellow oil crystallized. Recrystallization from CHCl$_3$ affords 1.75 g (88% of theory) of ethyl tosyl diazoacetate (**12**), with

small amounts of remaining tosyl amide, as yellow needles. Melting point and NMR perfectly fit literature values.[198]

mp.: 64-65 °C, lit.: 65 °C[198]

^{1}H-NMR (400 MHz, CDCl$_3$, ppm): 7.83 (d, J= 8.1 Hz, 2H, Ar), 7.28 (d, J= 8.1 Hz, 2H, Ar), 4.15 (q, J= 7.4 Hz, 2H, O-C̲H̲$_2$-CH$_3$), 2.38 (s, 3H, Ar-CH$_3$), 1.18 (t, J= 7.1 Hz, 3H, CH$_2$-C̲H̲$_3$)

3. Preliminary curing tests with α-keto compounds

To test α-keto compounds on their ability to initiate polymerization 1 wt% of keto compound was mixed with the diacrylate HDDA. Therefore, 10 mg of keto compound were weighed into brown glass vials and afterwards 1000 mg of monomer were added. After 10 seconds mixing with the Vortex mixer at highest power. If compounds would not dissolve, mild heat was applied by heat-gun and longer mixing times were used until a homogenous solution was obtained. The sample was transferred into a silicon mold (2 x 1 x 0.15 cm) and put into the middle tray of an Intelliray 600 UV flood curing system. The samples were irradiated for 100 s at 100% power of the mercury lamp. If no curing occurred another 200 s of irradiation were added. Afterwards the samples were categorized into cured, partly cured or uncured.

4. UV-Vis measurements

For the UV-Vis experiments samples were dissolved in pure acetonitrile and measured in 10 mm quartz cells on a Lambda 750 UV-Vis photometer (scanning mode) from 250 to 450 nm at a slit width of 2 nm.

The concentration was chosen so that the absorption is not higher than 1.2 AU and Lambert Beer's law can be applied. Aliphatic α-ketoesters were measured at 10^{-2} mol L^{-1}, benzophenone and phenyl glyoxylate at 10^{-3} mol L^{-1} and high absorbing benzophenone derivative BMS and thioxanthone ITX were measured at 10^{-5} and 10^{-4} mol L^{-1} respectively.

5. Photo-DSC measurements with α-keto compounds

Initiators that showed curing activity in the preliminary tests were further tested in photo-DSC measurements.

Hexanediol diacrylate HDDA was used as received. Methacrylate mixture DMM was prepared from 1 eq. 7,7,9-Trimethyl-4,13-dioxo-3,14-dioxa-5,12-diazahexadecan-1,16-diyl-bis(2-methyl-acrylate) (UDMA, 470.56 g mol^{-1}) and 1 eq. 1,10-decanediol dimethacrylate (D3MA, 338.49 g mol^{-1}). The monomers were mixed for one minute after warming the mixture to reduce the viscosity.

The hydrogel acrylate mixture was prepared from polyethyleneglycol diacrylate (Mn = 700 Da) with 50 wt% water.

The theoretical heat of polymerization for diacrylates (161 kJ mol^{-1}) was found in literature[199] and used to calculate the heat of polymerization for HDDA ($\Delta H_{0,HDDA}$ = 711 J g^{-1}) and the PEG700DA for the hydrogel formulation ($\Delta H_{0,HDDA}$ = 230 J g^{-1}). For methacrylate mixture DMM ($\Delta H_{0,DMM}$ = 299.54 J g^{-1}) the known value from literature was used.[37]

Measurements at 320-500 nm and general procedure

To ensure a constant molar ratio of initiators to monomer for all tested compounds, ethyl pyruvate (EP) as smallest molecule was used as benchmark. For the photo-DSC measurements, 10 mg (1 wt%, 0,086 mmol) of EP was weighed into a brown glass vial with 1000 mg monomer. All other (co)initiators were weighed into the monomer equimolar to the amount of 1 wt% ethyl pyruvate. All samples were thoroughly mixed on a Vortex mixer at highest power for 10 seconds. If the (co)initiator would not dissolve easily, mild heat was applied by heat-gun and longer mixing times were used until a homogenous solution was obtained.

The Photo-DSC measurements were conducted on a Netzsch DSC 204 F1 with auto-sampler at 25 °C under nitrogen atmosphere. Photoreactivity of the monomers was tested by weighing accurately 10 to 11 mg of the sample into an aluminium DSC pan with an Eppendorf pipette, which was subsequently placed in the DSC chamber after closing it with a glass lid. The sample chamber was purged with a N$_2$ flow (~ 20 mL min-1) for 4 min. Afterwards the samples were irradiated with filtered UV-light (320 – 500 nm) from an Exfo OmniCure S2000 broadband Hg-lamp with a light intensity of 1 W cm^{-2} at the end of the light guide. The samples were exposed to light for 2 × 300 s, and the heat flow was recorded as a function of time.

After subtracting the baseline calorigram of the second irradiation period from the first, a baseline corrected calorigram was obtained. From the area under the curve, the total heat evolved during polymerization was given. With the theoretical heat of polymerization the maximal rate of polymerization (R$_P$) and double bond conversion DBC was calculated according to Equation 4 and 5.

$$R_P = \frac{q \times \delta \times 1000}{\Delta H_0} \qquad \text{Equation 4}$$

R_P .... *rate of polymerization in mM s-1*
q .... *maximum heat flow mJ s-1 mg-1*
δ .... *density of the sample in g L-1*
ΔH_0 .... *theoretical heat of polymerization in kJ mol-1*

$$DBC = 100 \times \frac{\Delta H_P}{\Delta H_0}$$
<div align="right">Equation 5</div>

ΔH_P..............measured heat of polymerization J g^{-1}
ΔH_0..............theoretical heat of polymerization in J g^{-1}

All measurements were conducted as triplicates. To ensure the stability of the measuring device the lamps were calibrated before each measurement and a reference sample of HDDA with SC73 as initiator was measured before, in the middle and at the end of each series.

For each value the average deviation was determined to find an acceptable range of error. The obtained values were accepted with maximal the double average relative deviation. (Table 25)

Table 25. Average relative standard deviation of determined values from DSC measurements in %

	Rp	t_{max}	t_{95}	DBC
determined	2.5	2.0	6.6	0.8
accepted	5	4	14	2

Measurements with errors above the accepted deviation were repeated.

Measurements at 400-500 nm

The mixtures were prepared, sampled and measured according to the general procedure.

As light source for the DSC-measurements an Exfo OmniCure S2000 broadband Hg-lamp with filtered UV-light (400 – 500 nm) and a light intensity of 1 W cm^{-2} at the end of the light guide was used.

Long wavelength experiments at 400 nm

The mixtures were prepared, sampled and measured according to the general procedure.

As light source for the DSC-measurements, a 400 nm OmniCure® LX400+ LED spot curing system was used and coupled into the device light guide by an aluminum passive cooler. To prevent overheating of the LED a second aluminum passive cooler was attached to the tail of the LED and a USB fan was used for cooling. (Figure 86)
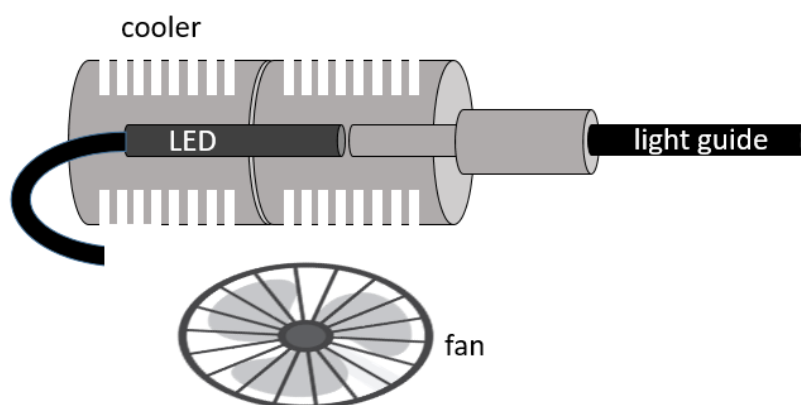
Figure 86. LED coupling with DSC light guide and active cooling

With an ocean optics photometer a light intensity of 0.38 W cm^{-2} was measured 1 cm from the tip of the light guide at 100% power of the LED.

Measurements at same absorption and 365 nm

In the case of measurements at same absorption the concentrations of initiators were calculated to fit the absorption of 1 wt% of benzophenone at 365 nm with Equation 6 and 7.

$$F = \frac{\varepsilon_{365,ini}}{\varepsilon_{365,BP}}$$ **Equation 6**

F .... extinction factor at 365 nm
$\varepsilon_{365,ini}$ ....extinction coefficient of initiator at 365 nm
$\varepsilon_{365,BP}$ ....extinction coefficient of benzophenone at 365 nm

$$m_{ini,eq.abs.} = \frac{mol_{BP} \times M_{ini}}{F}$$ **Equation 7**

$m_{ini,eq.abs.}$ ....equiabsorbent mass of initiator in 1000 mg monomer

mol_{BP} ....molar equivalent of 10 mg benzophenone

M_{ini} ....molar mass of initiator

F .... extinction factor at 365 nm

Table 26. Calculated (co)initiator mass for 1000 mg monomer at same absorption

Initiator	Conc. mol*L^{-1}	A$_{365}$	ε_{365} L*mol^{-1}*s*cm^{-1}	Factor F	Eq Abs. mg	EDB mg
BP	0.001	0.060	59.90	1.000	10.00	10.61
EP	0.01	0.071	7.08	0.118	53.92	89.74
BrKE	0.01	0.228	22.78	0.380	32.20	x
DDFD	0.01	0.253	25.32	0.423	16.63	25.09

The mixtures were according to Table 26, sampled and measured according to the general procedure.

As light source for the DSC-measurements an Exfo OmniCure S2000 broadband Hg-lamp with filtered UV-light (365 nm) and a light intensity of 1 W cm^{-2} at the end of the light guide was used.

6. UV-Aging of Polymers

500 mg of mixtures used for the DSC measurements were cured in a silicon mold (2 x 1 x 0.15 cm) and afterwards aged in the Intelliray 600 UV flood curing system in one step. The samples were exposed to the UV light for 2 h and afterwards the discoloration was documented by digital photography.

7. Photolysis studies

^{1}H-NMR spectra were recorded on a 200 MHz Bruker AVANCE DPX spectrometer. Irradiation of the solutions in CD_3CN was carried out using 365 nm LEDs (100 mW) and spectra recorded after 0, 30 and 60 min.

8. Cytotoxicity

Mouse fibroblast cell line L929 were purchased from Sigma-Aldrich and cultured in Dulbecco's Modified Eagle's medium (DMEM, Sigma-Aldrich) supplemented with 10% fetal bovine serum (Sigma) and 1% of 10 000 units penicillin and 10 mg mL^{-1} streptomycin (Sigma-Aldrich).

Cells were cultivated in incubator in humid atmosphere with 5% carbon dioxide at 37 ºC. Medium was refreshed every second day.

To evaluate the cytocompatibility of photoinitiators PrestoBlue cell viability reagent (Thermo Fisher) was used. For this test ten 96-well plates were seeded with 5 000 cells per well and left in the incubator overnight for cells to attach. Next day, the cells were incubated with 100 µL of different dilutions of PI in DMEM, each plate in duplicate, one to evaluate cytotoxicity of substance only and another to cytotoxicity after exposure to UV for 10 min in a Boekel Scientific UV crosslinker at 365 nm. All plates had wells with non-treated cells as a control samples, every concentration had at least 6 repetitions.

After 24 h incubation period with photoinitiators, culture medium was exchanged twice to remove residues of photoinitiator and cell viability was evaluated. Resazurin-based reagent PrestoBlue was diluted 1:10 with medium and 100 µL were applied per well and incubated for 1 hour. Because of the reducing environment of viable cells, this reagent is transformed and turns

red, while becoming highly fluorescent. The fluorescence was then measured with a plate reader (Synergy BioTek, excitation 560 nm, emission 590 nm). After correction for background fluorescence, the results of the cells exposed to different concentrations of photoinitiators were compared to each other and to the controls (non-stimulated cells) using One Way ANOVA Dunnett's Multiple Comparisons Test. It was assumed that metabolic activity of the 24h control not exposed to photoinitiators is 100%. Statistical evaluation of data was performed using software package IBM SPSS Statistic 25.0 and Excel 2016 (Microsoft Office).

Part 2: Improving network properties with chain transfer reagents

1. Addition fragmentation chain transfer (AFCT)

1.2. Selection and synthesis of AFCT compounds

1.2.1. Synthesis of silanoxy ethyl acrylates

1.2.1.1. Synthesis of trimethylsilanoxy ethyl acrylate (TMSA)
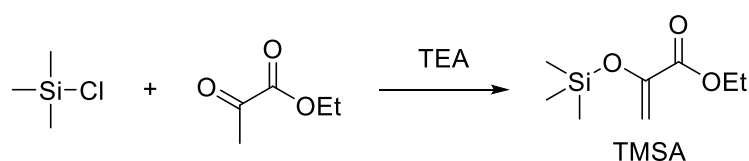
For the preparation of TMS oxyacrylate according to literature, 13.93 g (120 mmol, 1 eq.) of ethyl pyruvate are enolised by 13.36 g (132 mmol, 1.1 eq.) trimethylamine in 120 mL dichloromethane under argon while cooling to 0 °C. Then 14.34 g (132 mmol, 1.1 eq.) freshly distilled trimethyl chlorosilane is added dropwise diluted in 20 mL DCM.[146] The mixture is allowed to warm up to room temperature and stirred for another hour. After filtration the solvent was removed by vacuum. Distillation at 100 °C and 50 mbar afforded 15.0 g (67% of theory) TMS oxyacrylate TMSA as clear fluid liquid with an intense smell.

bp.: 92 °C / 50 mbar, lit.: 90-92 °C / 38 Torr[200]

^{1}H-NMR (400 MHz, CDCl$_3$, ppm): 5.28 (s, 1H, C=C$\underline{H_2}$), 4.64 (s, 1H, C=C$\underline{H_2}$), 3.98 (q, J= 7.0 Hz, 2H, -C$\underline{H_2}$-CH$_3$), 3.56 (t, J= 7.2 Hz, 3H, CH$_2$-C$\underline{H_3}$), 0.00 (s, 9H, Si$\underline{(CH_3)_3}$).

^{13}C NMR (100 MHz, CDCl$_3$, ppm): 164.3 (C4), 147.2 (C4), 103.7 (C2), 61.1 (C2), 14.1 (C1), -0.2 (C1).

GC-MS: calculated: 188.09, found: 189.05 [M +H], 173.06 [M –CH$_3$], 115.21 [M –COOEt], 73.45 [(CH$_3$)$_3$Si]

1.2.1.2. Synthesis of supersilyl oxyacrylate (SSA)

For the synthesis of supersilyl oxyacrylate SSA a more reactive triflate had to be prepared from the chlorosilane identical to literature.[147]
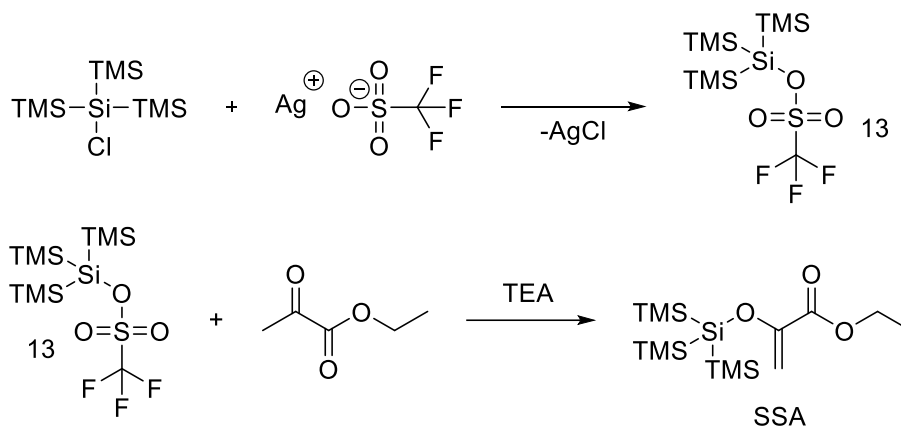
Therefore, 1.00g (3.55 mmol, 1 eq.) chloro supersilane was stirred overnight with 0.91 (3.55 mmol, 1 eq.) silver triflate in 3.5 mL absolute DCM under argon and exclusion of light. The suspension was decanted the next day and tris(trimethylsilyl)silyl triflate (**13**) was added without further purification to 0.41 g (3.55 mmol, 1 eq.) ethyl pyruvate in dry dichloromethane under argon with 0.36 g (3.55 mmol, 1 eq.) trimethylamine as base.[147] After stirring for 6 h at RT the mixture was filtrated and extracted with 20 mL 1N HCl, 20 mL saturated $NaHCO_3$ solution and 20 mL brine. After drying the organic phase with sodium sulfate and removal of the solvent in vacuum, column chromatography with PE:EE = 92:8 afforded 700 mg (54% of theory) supersilyl oxyacrylate SSA as viscous oil.

R_f = 0.23, PE:EE = 92:8

^{1}H-NMR (400 MHz, $CDCl_3$, ppm): 5.21 (s, 2H, $=CH_2$), 4.51 (s, 2H, $=CH_2$), 3.98 (q, J= 7.2 Hz, 2H, O-CH$_2$-CH$_3$), 1.08 (t, J= 7.1 Hz, 3H, O-CH$_2$-CH$_3$), 0.00 (s, 27H, Si(TMS)$_3$).

^{13}C NMR (100 MHz, $CDCl_3$, ppm): 174.0 (C4), 164.1 (C4), 101.1 (C2), 60.9 (C2), 14.1 (C1), -0.1 (C1).

GC-MS: calculated: 362.16; found: 363.02 [M +H], 347.03 [M -CH$_3$], 289.02 [M −COOEt], 263.11 [(TMS)$_3$SiO]

Elemental analysis: Calculated: C, 46.35; H, 9.45; O, 13.23 Found: C, 40.74;* H, 9.52; O, 13.09*

*formation of SiC and SiO_2

1.1.2. Synthesis of boron oxy ethyl acrylates
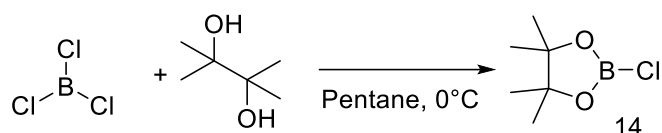
For the synthesis of pinacolo chloroborane 14 according to literature, 3.55 g (30 mmol, 1 eq.) dry pinacol was dissolved in 100 mL dry pentane at 0 °C in argon atmosphere, afterwards 30 mL of a commercial solution of boron trichloride in hexane (30 mmol, 1eq.) was added carefully.[151] The unavoidable sideproduct of diborane was filtered off and the filtrate was distilled quickly under inert conditions at 60 °C and 10 mbar affording 1.80 g (37% of theory) pinacolo chloroborane 14 as highly sensitive liquid. Pinacolo chloroborane 14 is meta stable and can be kept at -80 °C for two days under slow decomposition. To avoid decomposition the afforded distillate was kept in action ice slurry at – 80 °C under argon and was directly used for further synthesis.

bp.: 40 °C / 10 mbar, lit.: 31-33 °C / 3.8 Torr[201]

1.1.3. Synthesis of sulphur oxy ethyl acrylates

For synthesis of phenyl sulfenyl chloride (15), to 10.0 g (46 mmol, 1 eq.) diphenyl disulphane 12.4 g (92 mmol, 2 eq.) sulfuryl chloride were added dropwise while stirring.[155]
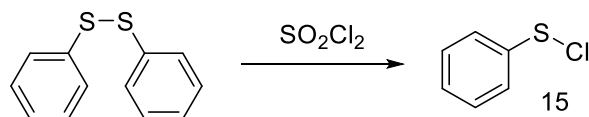
After removal of excessive sulfuryl chloride in vacuum with a cooling trap, sulfenyl chloride 15 can be distilled as blood red metastable liquid at 100 °C and 15 mbar. Decomposition of the distillate takes place if the receiver flask is not cooled. This can lead to a violent explosion, as well as warming up the substance from the freezer. The compound has to be freshly prepared and cannot be stored.

Distillation under vacuum with cooled receiver affords 4.3 g (32% of theory) phenyl sulfenyl chloride (15) as red liquid with suffocating smell.

bp.: 75 °C / 15 mbar, lit.: 80-81 °C / 20 Torr[202]

1.1.4. Synthesis of phenyl oxycarbonyl ethyl acrylate (PCA)
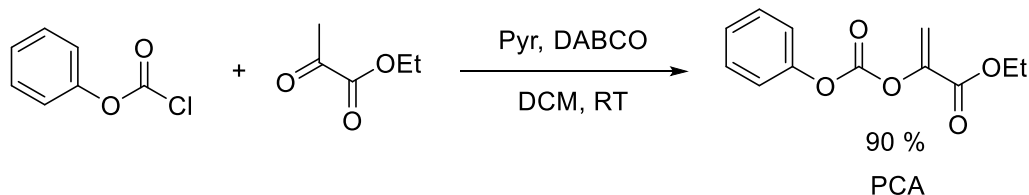
To synthesize phenyl oxycarbonyl ethyl acrylate PCA a three-necked flask was charged with 20 mL dry DCM under argon. Then 3.1 mL (28 mmol, 1 eq.) ethyl pyruvate were added together with 3.39 mL (42 mmol, 1.5 eq.) dry pyridine. 4.82 g (31 mmol, 1.1 eq.) phenyl chloroformate were added dropwise diluted in 10 mL DCM while cooling with a water bath. Another 15 mL of DCM were added to dilute the precipitating pyridine hydrochloride. After 18 h the reaction was not finished so 4.7 g (42 mmol, 1.5 eq.) DABCO were added. After 2 h complete conversion was observed by TLC. Therefore, the mixture was subsequently extracted with 2x 60 mL 1N HCl, 60 mL saturated NaHCO$_3$ solution and 80 mL brine. The combined organic phase was dried with Na$_2$SO$_4$ and the solvent stripped off in vacuum. Column chromatography with PE:Et$_2$O = 1:1 afforded 5.8 g (88% of theory) phenyl oxycarbonyl ethyl acrylate PCA as slightly yellow oil after removal of solvent in vacuum.

R$_f$ = 0.6, PE:Et$_2$O = 1:1

mp.: ~8 °C

^{1}H-NMR (400 MHz, CDCl$_3$, ppm): 7.40-7.10 (m, 5H, Ar-H), 6.04 (s, 1H, =CH$_2$), 5.60 (s, 1H, =CH$_2$), 4.24 (q, J=7,22 Hz, 2H, O-C$\underline{H}_2$-CH$_3$), 1.27 (t, J=7,22 Hz, 3H, O-CH$_2$-C$\underline{H}_3$)

^{13}C NMR (100 MHz, CDCl$_3$, ppm): 161.0 (C4), 151.3 (C4), 150.9 (C4), 144.7 (C4), 129.6 (C3), 126.5 (C3), 120.8 (C3), 113.9 (C2), 62.1 (C2), 14.1 (C1).

Elemental analysis: Calculated: C, 61.02; H, 5.12; O, 33.86; Found: C, 61.59;* H, 5.16; O, 32.49

1.3. Testing AFCT Reagents in Monofunctional Systems

1.3.1. Photo-DSC

For the DSC measurements 20 mol% of chain transfer reagent and 1wt% of Ivocerin as photoinitiator were mixed with 1000 mg benzyl methacrylate BMA on a Vortex mixer in brown glass vials.

The Photo-DSC measurements were conducted on a Netzsch DSC 204 F1 with auto-sampler at 25 °C under nitrogen atmosphere. Photoreactivity of the monomers was tested by weighing accurately 10 to 11 mg of the sample into an aluminum DSC pan with an Eppendorf pipette, which was subsequently placed in the DSC chamber after closing it with a glass lid. The sample chamber was purged with a N$_2$ flow (~ 20 mL min-1) for 4 min. Afterwards the samples were irradiated with filtered UV-light (400 – 500 nm) from an Exfo OmniCure S2000 broadband Hg-lamp with a light intensity of 1 W cm^{-2} at the end of the light guide. The samples were exposed to light twice for 300 s, and the heat flow was recorded as a function of time.

The rate of polymerization and DBC was calculated with the theoretical heat for benzyl methacrylate of 56 kJ/mol, taken from literature[142] according to the general procedure in chapter 5, page 177.

1.3.2. NMR

Directly after DSC measurements the aluminum pans with polymer sample were transferred from the autosampler into 2 mL glass vials and 0.7 mL of deuterated chloroform were added. The polymer samples were dissolved by shaking and transferred to brown NMR tubes with a syringe. ^{1}H-NMR spectroscopic analysis of conversions were recorded with a Bruker AC 400 spectrometer at 400 MHz, using $CDCl_3$ as a solvent (deuteration > 99.5%). The solvent signal was used as internal reference for shifts.

The resulting spectra were evaluated by integration of the double bond peaks of the CTAs and monomer. (Figure 87) The O-CH$_2$-Ph signal of benzyl methacrylate at 5.2 ppm was used as internal standard. For determination of the consumption of monomer the double bond signals at 6.2 ppm (s, 1H, =CH$_2$) and 5.6 ppm (s, 1H, =CH$_2$) were used. The consumption of CTA was determined the same way by integration of the corresponding double bonds signals.
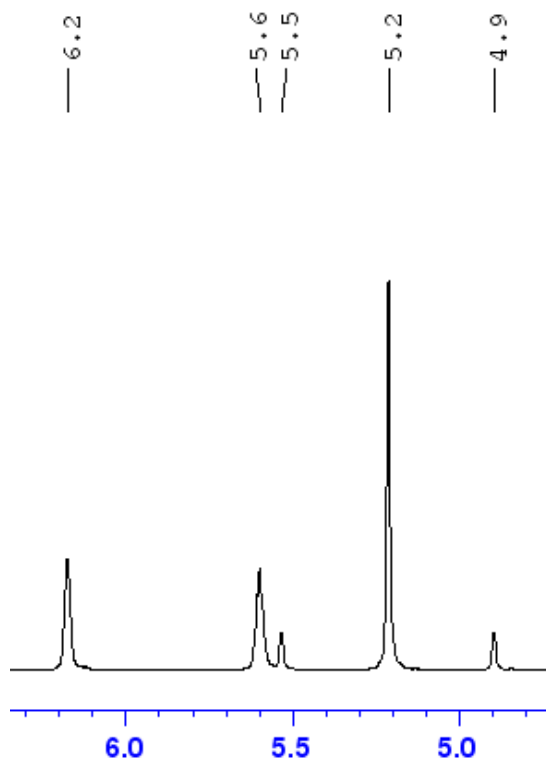
Figure 87. NMR of BMA with 20 mol% trimethylsilane oxyacrylate TMSA

Spectra were measured before and after polymerization. Double bond conversion could be easily determined by the integrals of the double bonds before (I_0) and after curing (I) as shown in equation 8.

$$DBC\% = (1 - \frac{I}{I_0}) \times 100 \quad \text{Equation 8}$$

1.3.3. Size exclusion chromatography (SEC)

Size exlusion chromatography (GPC) was performed with a Waters GPC using three columns connected in series (Styragel HR 0.5, Styragel HR 3 and a Styragel HR 4) and a Waters 2410 RI detector. The columns and detector were maintained at 40 °C and a flow rate of 1.0 mL min^{-1} was used. Polystyrene standards were used for molecular weight calibration and abs. THF stabelized with BHT was used as solvent.

For the sample preparation 0.5 mL of the NMR samples were transferred to a SEC analysis vial and diluted with 1.5 mL THF.

The baseline was set from a stable plateau before the polymer peak to the stable plateau before the injection peak. Then the area for automatic integration was set to the beginning and end of the polymer peak. The molecular weight and distribution was automatically calculated by the OmniSEC operating software.

1.4. Testing AFCT Reagents in Difunctional Systems

1.4.1. RT-NIR Photorheology

Sample mixtures were prepared with dimethacrylate monomer DMM containing 0.3 wt% of Ivocerin as photoinitiator and 10 db% or 20 db% chain transfer agent respectively. Double bond percent (db%) are mol% calculated on the total molar amount of doublebonds.

Real-Time-NIR-Photorheology experiments were conducted on an Anton Paar MCR 302 WESP with a P-PTD 200/GL Peltier glass plate and a PP25 measuring system. A Bruker Vertex 80 FTIR spectrometer is additionally coupled with the rheometer.
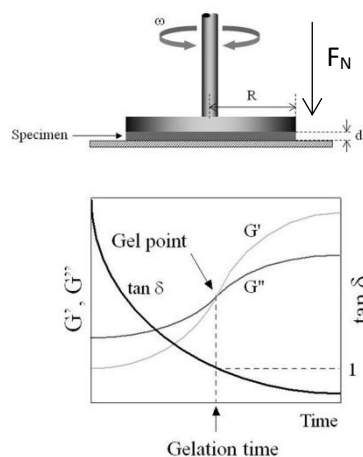
Figure 88. Determination of the gel point by intersection of G' and G''

For the experiments, 130 µl of sample mixture were transferred to the center of the glass plate. The head of the rheometer is lowered to a measuring position of 200 µm. The formulations were subjected to an oscillatory stress with an angular strain of 1% and a frequency of 1 Hz. Photopolymerization was started by blue light (300 s, 400-500 nm, 0.5 W/cm^2) guided to the sample from underneath by a waveguide using an Exfo OmniCure TM 2000 broadband Hg-lamp light source with 400-500 nm filter. The IR beam passes through the sample and is reflected by the rheology head before returning to an external MCT detector. During the measurements, the storage modulus G', the loss modulus G'' and the normal force F_N were recorded. The double bond conversion (DBC) was determined by recording a set of single spectra (time interval = 0.47s) and then integrating the respective double bond bands at ~6160 cm^{-1}. All spectra were exported into ACII-format using the software OPUS from Bruker. The area of the double bond signal at the start and during the measurement were used to calculate the DBC with time. DBC at the point of gelation is defined by the time at which the storage and loss modulus intersect. (Figure 88)

1.4.2. Dynamic mechanical thermal analysis (DMTA)

For the DMTA measurements mixtures with dimethacrylate DMM were prepared containing 10 or 20 db% CTA and 1 wt% Ivocerin as photoinitiator. The samples were mixed on a vortex mixer until a homogenous formulation was obtained. Afterwards the mixture was filled into a transparent silicone mold (Elastosil RT 601, 4 x 0.5 x 0.2 cm) and the samples were irradiated twice at RT for 10 min in an Ivoclar Lumamat light oven (400-500 nm). Between the irradiations the samples were turned upside down to ensure homogenous curing.

Afterwards the cured sample sticks were grinded to perfect geometry with grinding paper (grade 1000). The samples were placed into an Anton Paar MCR 301 DMTA device with a CTD 450 oven

188

and a SRF 12 measuring system. The samples were cooled to -100 °C and heated to 200 °C with 2 °C min^{-1} while 1% torsion stress is applied at a frequency of 1 Hz.

The storage-, loss modulus and dissipation factor tan δ was obtained as function of temperature. The glass transition was defined as maximum of tan δ and the sharpness described by the full width at half maximum (FWHM)

2. Hydrogen abstraction fragmentation chain transfer (HAFCT)

2.2. Selection and synthesis of HAFCT compounds

2.2.1. Synthesis of 1,5-dimethoxy cyclohexa-1,4-diene (DCH)

Dimethoxy cyclohexadiene DCH had to be prepared via Birch reduction according to literature as a precursor and was further used for the synthesis of cyclohexadiene transfer agents.[181]
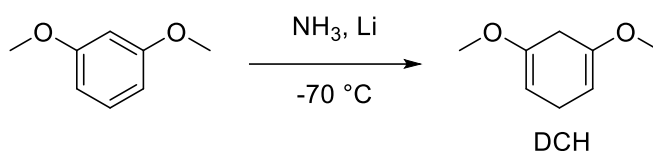
For the synthesis of 1,5-dimethoxy cyclohexa-1,4-diene DCH 6.0 g (43.4 mmol, 1 eq.) dimethoxy benzene was dissolved in 16 mL dry diethyl ether under inert atmosphere and 180 mL ammonia was condensed into the solution at -70 °C. Then 1.51 g (217 mmol, 5 eq.) lithium were added as metal wire and dissolved within minutes resulting in a deep blue solution of solvated electrons. After 2 h the reaction was quenched carefully over 30 min with 20 mL ethanol and the resulting decolorized was mixture warmed up to room temperature. Afterwards it was extracted with 140 mL saturated ammonium chloride solution. The organic phase was dried twice with 30 mL brine and Na$_2$SO$_4$. Then the solvent is stripped off under vacuum and yielded 5.53 g (91% of theory) pure 1,5-dimethoxy cyclohexa-1,4-diene DCH as colourless liquid.

R$_f$= 0.27, PE:EE =98:2

^{1}H-NMR (400 MHz, CDCl$_3$): 4.31 (m, 2H, CH), 3.51 (s, 6H, CH$_3$), 2.65 (m, 4H, CH$_2$).

GC-MS: 140.09 [M+], 139.21 [M-H], 124.20 [M-CH$_3$], 110.21 [M-2CH$_3$], 109.23 [M-OCH$_3$], 94.25 [M-CH$_3$-OCH$_3$]

2.2.2. Synthesis of 1-(*t*-butyl dimethyl silyl)-1-methyl dimethoxy cyclohexadiene (SiDCH)

For the synthesis of 1-(*t*-butyl dimethyl silyl)-1-methyl dimethoxy cyclohexadiene SiDCH, a one pot synthesis ident to literature was conducted.[180]
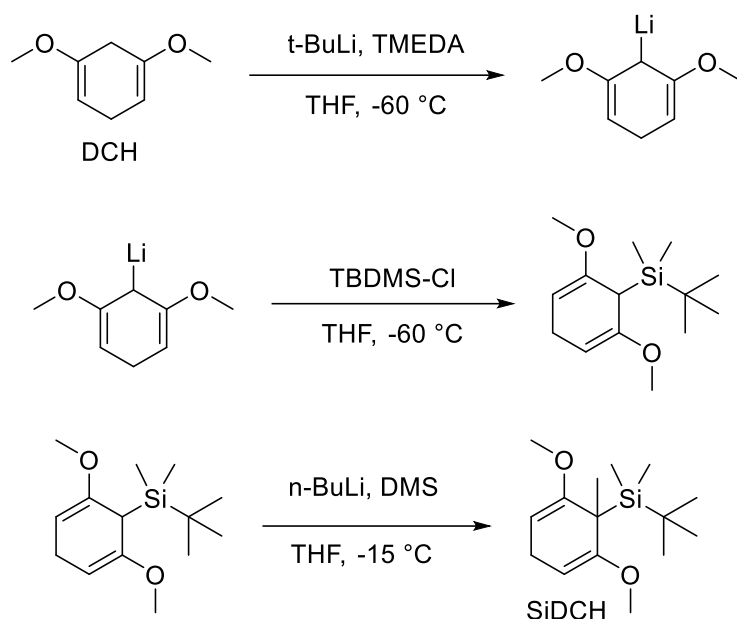
First 4.91 g (35 mmol, 1 eq.) dimethoxy cyclohexadiene DCH was dissolved in 100 mL absolute THF under argon and cooled to -60 °C. Then the mixture was treated with 22.6 mL (38.5 mmol, 1.1 eq.) *tert*-butyl lithium (1.7 M in pentane) over 30 min. Then 4.5 g (38.5 mmol, 1.1 eq.) tetramethylene diamine (TMEDA) were added dropwise within 5 min. The resulting yellow solution was stirred 90 min. Then 12.9 mL (38.5 mmol, 1.1. eq.) of a 3 M *tert*-butyl dimethyl chlorosilane solution in THF was added dropwise at -60 °C over 10 min. Next the mixture was allowed to warm up to RT and stirred for another 90 min.

A precipitate of LiCl can be observed. In the last step, the solution was again cooled to -15 °C and treated with 15.4 mL (38.5 mmol, 1.1. eq.) of a n-butyl lithium solution in hexane over 15 min, resulting in deep orange solution. The reaction was stirred for another 60 min at -15 °C. For the methylation 4.74 g (38.5 mmol, 1.1. eq.) dimethyl sulfate (DMS) were added within 5 min resulting in instant fade of color. After 30 min at RT the reaction was quenched with 40 mL water and extracted. The organic phase was washed twice with 40 mL H_2O and 40 mL brine. After drying the organic phase with Na_2SO_4 the solvent was stripped off in vacuum. The crude oil was purified by column chromatography (PE:EE = 98:2). To further improve the purity the compound was recrystallized from 10 mL MeOH twice and afforded 4.77 g (51% of theory) pure 1-(t-butyl dimethyl silyl)-1-methyl dimethoxy cyclohexadiene SiDCH as colorless crystals.

R_f= 0.49, PE:EE = 98:2

mp.: 34.3 - 34.9 °C, lit.: 32-33 °C [203]

^{1}H-NMR (400 MHz, CDCl$_3$): 4.36 (t, J_{HH} = 3.7 Hz, 2H, C=C<u>H</u>), 3.12 (s, 6H, O-C<u>H</u>$_3$), 2.88-2.86 (m, 2<u>H</u>, CH-C<u>H</u>$_2$), 1.67 (s, 3H, C=C-C-C<u>H</u>$_3$), 1.07 (s, 9H, Si-C-C<u>H</u>$_3$), 0.27 (s, 6H, Si-C<u>H</u>$_3$)

^{13}C NMR (100 MHz, CDCl$_3$, ppm): 158.9 (C4), 88.7 (C3), 53.2 (C1), 35.8 (C4), 27.5 (C1), 24.7 (C2), 20.3 (C1), 19.4 (C4), -4.5 (C1).

GC-MS: 269.99 [M+H], 268.02 [M+], 253.16 [M-CH$_3$], 212.10 [M-t-Butyl], 195.12 [M-t-Butyl,-CH$_3$], 179.15 [M-t-Butyl,-OCH$_3$], 153.16 [M-(Si-R)], 152.16 [M-(Si-R),-H], 138.18 [M-(Si-R),-CH$_3$], 121.21 [M-(Si-R),-OCH$_3$], 107.19 [M-(Si-R),-OCH$_3$,-CH$_3$], 91.19 [M-(Si-R),-OCH$_3$,-2CH$_3$]

2.3. Testing HAFCT reagents in monofunctional systems

2.3.1. Photo-DSC

Photo-DSC measurements were conducted according the general procedure and with 400-500 nm at 1 W cm^{-2}. See chapter 1.3.1, page 185.

2.3.2. NMR

Sample preparation and evaluation of monomer conversion see exp. chapter 1.3.2, page 186. Evaluation of HAFCT reagent conversion see chapter 2.3.2, page 144.

2.3.3. Size exclusion chromatography (SEC)

SEC measurements were conducted and evaluated as described in chapter 1.3.3, page 187.

2.4. Testing HAFCT reagents in difunctional systems

2.4.1. RT-NIR Photorheology

Rheometry measurements were conducted and evaluated as described in exp. chapter 1.4.1, page 187.

2.4.2. Dynamic mechanical thermal analysis (DMTA)

DMTA measurements were prepared and conducted as described in exp. chapter 1.4.2, page 188.

2.5. Anti-oxygen inhibition - photoreactor tests

The polymerization of benzyl methacrylate BMA under air or argon in deuterated benzene was performed in a light reactor seen in Figure 89.
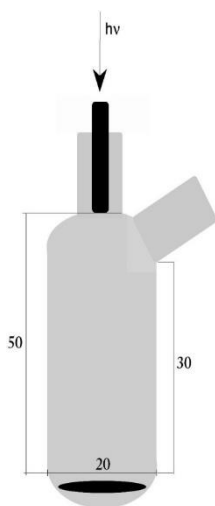
Figure 89. Dimensions of the glass photoreactor

For the polymerization of benzyl methacrylate BMA, 2 mL deuterated benzene were put into the reactor together with a 4 mm magnetic stirrer under exclusion of light. After 3 mol% of Ivocerin as photoinitiator and anti oxygen inhibition reagent were added, the solution was purged over a septum with argon or air for ten minutes. Irradiation was performed with a 400-500 nm filtered OmniCure mercury lamp system at a low light intensity of 3 mW/cm^2 on the sample.

Irradiation was performed in a "stop and go" method. Therefore the irradiation time was set to 500s and samples were drawn after every exposure. This was repeated for three times. After each irradiation 0.6 mL of sample were transferred into a brown glass NMR tubes and measured subsequently after finishing the series of exposure.

Evaluation of conversion was performed by integration of the double bond peaks of BMA at 6.2 ppm and 5.6 ppm respectively in the same way as for the DSC-NMR samples in chapter 1.3.2, page 186.

Material and Methods

Chemicals

All chemicals not synthesized were purchased from different chemical suppliers and used as received unless otherwise noted. (Table 27)

THF was received in absolute quality. Dichloromethane (DCM) used for synthesis was of high purity grade from an absolution device.

Urethane dimethacrylate (UDMA M44311), 1,10-decanediol dimethacrylate (D$_3$MA N01688) and bis(4-methoxy phenoyl)diethyl germanium (Ivocerin©) were obtained from Ivoclar Vivadent and used as received.

Hexanediol diacrylate HDDA and polyethyleneglycol diacrylate PEG700DA were received form Sigma Aldrich and used as received.

All chemicals that were light sensitive were handled under exclusion of light (orange light).

Table 27: Applied reagents for synthesis

Substance	Distrubutor
2-Hydroxy-2-methylpropiophenone (SC73)	Lambson
2-Hydroxy-4'-(2-hydroxyethoxy)-2-Methylpropiophenone (2959)	Ciba
3-(4-Benzoylphenoxy)-2-hydroxy-N,N,N-Trimethyl-1-propanaminium chloride (BPQ)	Rahn
4,4-Dimethyldihydrofuran-2,3-dione	Sigma Aldrich
4-Benzoyl-4'-methyldiphenyl sulphide	Lambson
Acetone	Donau Chem
Acetonitrile 99.9%	Acros
Benzophenone	TCI
Bromine	Merk
BMS	Lambson
Chlorotris(trimethylsilyl)silan	TCI
DABCO 98%	TCI
Dichloromethane	Fluka
Dichloromethyl methyl ether	ABCR
Diethylether	Donau Chem
Diethyloxalate	Sigma Aldrich
Diethyl acetylphosphonate	TCI
Dimethyl ethanolamine	Sigma Aldrich
Dicyclohexylcarbodiimide	Sigma Aldrich
Diphenyldisulfide	Fluka
Ethanol, denatured	AUSTRALCO
Ethanediol	Sigma Aldrich
Ethyl 3-methyl-2-oxobutyrate	Sigma Aldrich
Ethyl acetate	Donau Chem
Ethyl diazoacetate	Sigma Aldrich
Ethyl pyruvate	TCI
Isopropylbromid	Sigma Aldrich
Methyl diethanolamine	Fluka
Methanol	Donau Chem
N,N-dibutylamine	Fluka
Pinacolone	Sigma Aldrich
Pinacol	TCI
Phenylglyoxylate	na

Phenylchloroformate	TCI
Pyruvic acid	TCI
Silver triflate	TCI
Silver(I) oxide	Sigma Aldrich
Sodium p-toluenesulfinate	Fluka
Sulfuric acid	na
THF	Merk
Thionyl chloride 99.7%	Acros
Triethyl phosphono acetate	TCI
Trimethyl chlorogermane	TCI
Trimethyl chlorosilane	Acros
Toluene	Fluka
Tosyl chloride	Sigma Aldrich
Triethylamine 99%	Sigma Aldrich

All solvents and chemicals were applied in a quality common for organic synthesis.

TLC

(TLC) aluminum foils, coated with silica gel 60 F254 from Merck were used.

Melting points

Melting points were obtained from an Optimelt MPA100 automated melting point apparatus.

GC-MS

Measurments were conducted on a Thermo Scientific GC–MS DSQ II using a BGB 5 column (l = 30 m, d = 0.32 mm, 1.0 µm film, achiral) with the following temperature method (injection volume: 1 µL): 2 min at 80 °C, 20 °C min^{-1} until 280 °C, 2 min at 280 °C.

NMR

Spectra (400 MHz for ^{1}H and 100 MHz for ^{13}C, respectively) were recorded with a Bruker AC 400 spectrometer, using CDCl$_3$ or C$_6$D$_6$ as a solvent (deuteration > 99.5%). The solvent signal was used as internal reference.

Photo differential scanning calorimetry (Photo-DSC)

The photo differential scanning calorimetry (photo DSC) is a powerful and easy method to characterize a photopolymerizable system.
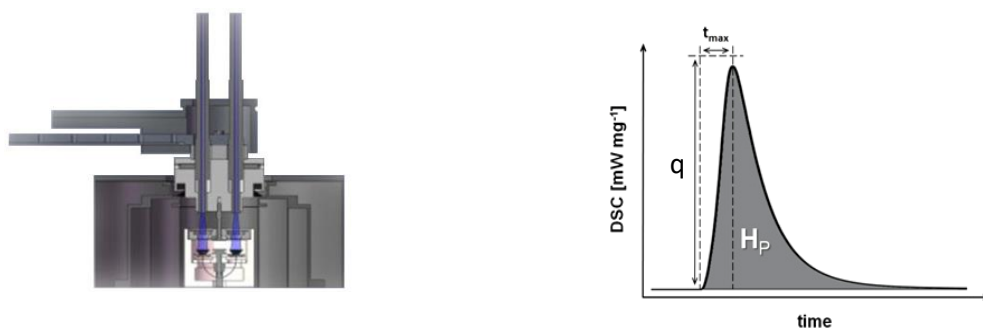
Figure 90. Cross-sectional drawing of a photo-DSC measuring device and resulting calorigram

During polymerization heat is generated by the chain reaction of double bonds. The difference in heat flow to a non-reactive reference, the exothermic reaction during polymerization, is detected and delivers several important parameters. (Figure 90) The time to maximal rate of polymerization (t_{max}) shows how quick the reaction is in the beginning. The height of the peak maximum (q) is used to calculate the maximum rate of polymerization R_P. The faster t_{max} and the higher R_P is the more reactive is a system. The area of the peak (H_p) displays the total energy yield of the reaction. With the theoretical heat of polymerization of a monomer, the conversion can by determined by H_p. Time to attain 95% conversion (t_{95}) is defined as the time required for conversion to equal 95% of total DBC. The higher t_{95} is, the longer full curing takes.

RT-NIR Photorheology

Experiments were conducted on an Anton Paar MCR 302 WESP with a P-PTD 200/GL Peltier glass plate and a PP25 measuring system. A Bruker Vertex 80 FTIR spectrometer is additionally coupled with the rheometer.

DMTA

Anton Paar MCR 301 DMTA device with a CTD 450 oven and a SRF 12 measuring system

Viscoelasticity is the characteristic that polymers, if they are exposed to an external load, show frequency and temperature dependent mechanical properties.

Dynamic mechanical thermal analysis (DMTA) measures the storage and loss modulus as a function of temperature. This is achieved by applying a sinusoidal mechanical stress $\sigma(t)$ to the sample to produce a sinusoidal strain $\varepsilon(t)$ of preselected amplitude. The sinusoidal strain is delayed by a phase angle δ from the applied stress, because of the viscoelastic manners of the material. (Figure 91)

The complex modulus E* is defined by the ratio between stress and deformation, with the real component E' and the imaginary component E''.
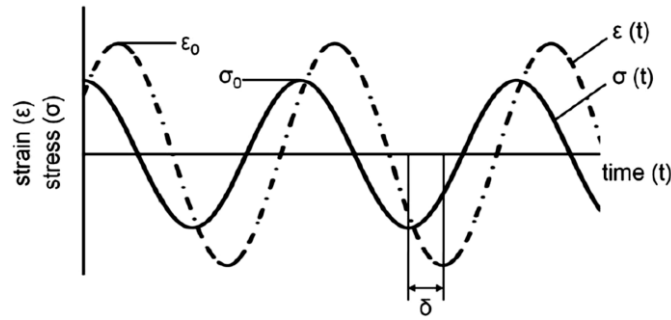
Figure 91. Schematic plots for stress and strain during DMA experiment for viscoelastic behavior[204]

These two moduli characterize the mechanical properties of materials. E' is called the storage modulus and describes the elastic behavior of materials like rigidity and stiffness. E'' is called the loss modulus. It defines the viscous behavior of a material, how fluid or rubbery a material is. By the ratio of the two moduli the parameter tan δ is defined (tan δ = E''/E'). It shows the ratio of energy loss and energy storage in each deformation cycle.[205] The viscous behavior, the dissipated energy during deformation, is represented by the loss modulus and the elastic behavior, the quantity of stored energy during deformation, is represented by the storage modulus (equates the Young's modulus). The phase shift between them is the so called loss factor (tan δ). In the range of the Tg a decrease of the storage modulus can be observed which is typical for (semi)crystalline materials. (Figure 92)
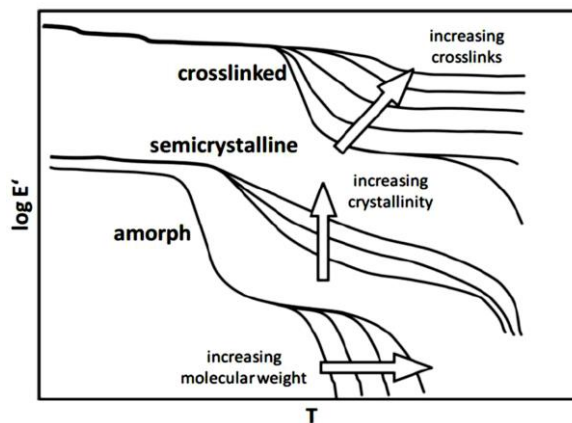
Figure 92. Temperature dependency of the storage modulus[204]

The value of the loss modulus runs through a relative maximum at the glass transition temperature. It is possible to obtain the T_g from the inflection point of the storage modulus ($T_{g,}$ storage modulus) and from the relative maximum of the loss modulus ($T_{g,}$ loss modulus) and the loss factor ($T_{g,}$ tanδ). All three values differ slightly from each other. [204] In this study T_g was defined as the maximum tan δ.

196

References

1.   Group, S. P. The Future of Radiation Curing Print Markets to 2022. https://www.smitherspira.com/industry-market-reports/printing/radiation-curing-for-print-markets-to-2022

2.   Sebastian Koltzenburg, M. M., Oskar Nuyken, *Polymere: Synthese, Eigenschaften und Anwendungen.* 2014; 145-168.

3.   Schwalm, R., *UV Coatings: Basics, Recent Developments and New Applications.* Elsevier Science: 2007; 112.

4.   Fouassier, J.-P., *Photoinitiation, Photopolymerization, and Photocuring: Fundamentals and Applications.* Hanser: 1995.

5.   Hunt, E. K., *Health Effect Assessments of the Basic Acrylates.* Taylor & Francis: 1993; 104-109.

6.   Crivello, J. V.; Dietliker, K.; Bradley, G., *Photoinitiators for Free Radical Cationic & Anionic Photopolymerisation.* Wiley: 1999.

7.   Perkampus, H. H.; Grinter, H. C.; Threlfall, T. L., *UV-VIS Spectroscopy and Its Applications.* Springer Berlin Heidelberg: 2013.

8.   Bayrakçeken, F. Triplet–triplet optical energy transfer from benzophenone to naphthalene in the vapor phase. *Spectrochimica Acta Part A: Molecular and Biomolecular Spectroscopy* **2008,** 71 (2), 603-608.

9.   Randy, Jablonski Diagram. For Diagrams, 2015.

10.   Fouassier, J. P. L., Jacques, *Photoinitiators for Polymer Synthesis.* Wiley-VCH Verlag GmbH & Co. KGaA: 2012; 225-228.

11.   Dietliker, K., *A Compilation of Photoinitiators Commercially Available for UV Today.* SITA Technology Ltd.: London, 2002.

12.   Green, W. A., *Industrial photoinitiators : a technical guide.* CRC Press, Taylor & Francis Group: 2010; 86-87.

13.   Fouassier, J. P.; Ruhlmann, D.; Graff, B.; Morlet-Savary, F.; Wieder, F. Excited state processes in polymerization photoinitiators. *Prog. Org. Coat.* **1995,** 25 (3), 235-271.

14.   Hult, A.; Ranby, B., *Primary and Secondary Reactions in Photoinitiated Free-Radical Polymerization of Organic Coatings.* American Chemical Society: 1985; Vol. 266, 457-472.

15.   Gatlik, I.; Rzadek, P.; Gescheidt, G.; Rist, G.; Hellrung, B.; Wirz, J.; Dietliker, K.; Hug, G.; Kunz, M.; Wolf, J. P. Structure-reactivity relationships in radical reactions: A novel method for the simultaneous determination of absolute rate constants and structural features. *J. Am. Chem. Soc.* **1999,** 121 (36), 8332-8336.

16.   Eibel, A.; Radebner, J.; Haas, M.; Fast, D. E.; Freißmuth, H.; Stadler, E.; Faschauner, P.; Torvisco, A.; Lamparth, I.; Moszner, N.; Stueger, H.; Gescheidt, G. From mono- to tetraacylgermanes: extending the scope of visible light photoinitiators. *Polym. Chem.* **2018,** 9 (1), 38-47.

17.   Mitterbauer, M.; Knaack, P.; Naumov, S.; Markovic, M.; Ovsianikov, A.; Moszner, N.; Liska, R. Acylstannanes: Cleavable and Highly Reactive Photoinitiators for Radical Photopolymerization at Wavelengths above 500 nm with Excellent Photobleaching Behavior. *Angew Chem Int Edit* **2018,** 57 (37), 12146-12150.

18.   Purbrick, M. D. Photoinitiation, photopolymerization and photocuring. J.-P. Fouassier. Hanser Publishers, Munich, 1995. pp. xii + 375, price DM198.00, sFr175.00, öS1466.00, US$138.00, £84.00. ISBN 3-446-17069-3. *Polym. Int.* **1996,** 40 (4), 315-315.

19.   Santini, A.; Gallegos, I. T.; Felix, C. M. Photoinitiators in Dentistry: A Review. *Primary Dental Journal* **2013,** 2 (4), 30-33.

20.   Vapenka, L.; Vavrous, A.; Votavova, L.; Kejlova, K.; Dobias, J.; Sosnovcova, J. Contaminants in the paper-based food packaging materials used in the Czech Republic. *J Food Nutr Res-Slov* **2016,** 55 (4), 361-373.

21.   Crivello, J. V.; Reichmanis, E. Photopolymer Materials and Processes for Advanced Technologies. *Chem. Mater.* **2014,** 26 (1), 533-548.

22.   Fouassier, J. P.; Allonas, X.; Burget, D. Photopolymerization reactions under visible lights: principle, mechanisms and examples of applications. *Prog. Org. Coat.* **2003,** 47 (1), 16-36.

23.   Dendukuri, D.; Panda, P.; Haghgooie, R.; Kim, J. M.; Hatton, T. A.; Doyle, P. S. Modeling of Oxygen-Inhibited Free Radical Photopolymerization in a PDMS Microfluidic Device. *Macromolecules* **2008,** 41 (22), 8547-8556.

24.   Harbourn, D., AN UPDATE ON THE CURRENT MARKET SITUATION FOR UV/EBCURING AND AN INSIGHT INTO THE DEVELOPMENT OF NEW MARKETS FOR UV/EB PROCESSING In *RadTech Asia*, 2013.

25.   Ligon, S. C.; Husár, B.; Wutzel, H.; Holman, R.; Liska, R. Strategies to Reduce Oxygen Inhibition in Photoinduced Polymerization. *Chem. Rev.* **2014,** 114 (1), 557-589.

26.   Husar, B.; Ligon, S. C.; Wutzel, H.; Hoffmann, H.; Liska, R. The formulator's guide to anti-oxygen inhibition additives. *Prog. Org. Coat.* **2014,** 77 (11), 1789-1798.

27.   Belon, C.; Allonas, X.; Croutxe-Barghorn, C.; Lalevee, J. Overcoming the Oxygen Inhibition in the Photopolymerization of Acrylates: A Study of the Beneficial Effect of Triphenylphosphine. *J Polym Sci Pol Chem* **2010,** 48 (11), 2462-2469.

28.   Gorsche, C.; Koch, T.; Moszner, N.; Liska, R. Exploring the benefits of beta-allyl sulfones for more homogeneous dimethacrylate photopolymer networks. *Polym. Chem.* **2015,** 6 (11), 2038-2047.

29.   Gorsche, C. Synthesis and characterization of monomers and additives for photopolymer-based dental restoratives. TU Wien, 2015.

30.   Ligon-Auer, S. C.; Schwentenwein, M.; Gorsche, C.; Stampfl, J.; Liska, R. Toughening of photo-curable polymer networks: a review. *Polym. Chem.* **2016,** 7 (2), 257-286.

31.   Ligon, S. C.; Liska, R.; Stampfl, J.; Gurr, M.; Mülhaupt, R. Polymers for 3D Printing and Customized Additive Manufacturing. *Chem. Rev.* **2017,** 117 (15), 10212-10290.

32.   Nicolas, J.; Guillaneuf, Y.; Lefay, C.; Bertin, D.; Gigmes, D.; Charleux, B. Nitroxide-mediated polymerization. *Prog. Polym. Sci.* **2013,** 38 (1), 63-235.

33.   Moad, G.; Rizzardo, E. Alkoxyamine-Initiated Living Radical Polymerization: Factors Affecting Alkoxyamine Homolysis Rates. *Macromolecules* **1995,** 28 (26), 8722-8728.

34.   Patten, T. E.; Matyjaszewski, K. Atom Transfer Radical Polymerization and the Synthesis of Polymeric Materials. *Adv. Mater.* **1998,** 10 (12), 901-915.

35.   Moad, G.; Rizzardo, E.; Thang, S. H. Radical addition–fragmentation chemistry in polymer synthesis. *Polymer* **2008,** 49 (5), 1079-1131.

36.   Gauss, P. RAFT and AFCT in Debonding on Demand of Dental Materials. TU Wien, Vienna, 2014.

37.   Gorsche, C.; Griesser, M.; Gescheidt, G.; Moszner, N.; Liska, R. beta-Allyl Sulfones as Addition-Fragmentation Chain Transfer Reagents: A Tool for Adjusting Thermal and Mechanical Properties of Dimethacrylate Networks. *Macromolecules* **2014,** 47 (21), 7327-7336.

38.   Ligon, S. C.; Seidler, K.; Gorsche, C.; Griesser, M.; Moszner, N.; Liska, R. Allyl Sulfides and alpha-Substituted Acrylates as Addition-Fragmentation Chain Transfer Agents for Methacrylate Polymer Networks. *J Polym Sci Pol Chem* **2016,** 54 (3), 394-406.

39.   Gorsche, C.; Seidler, K.; Knaack, P.; Dorfinger, P.; Koch, T.; Stampfl, J.; Moszner, N.; Liska, R. Rapid formation of regulated methacrylate networks yielding tough materials for lithography-based 3D printing. *Polym. Chem.* **2016,** 7 (11), 2009-2014.

40.   Hoyle, C. E.; Bowman, C. N. Thiol-Ene Click Chemistry. *Angewandte Chemie-International Edition* **2010,** 49 (9), 1540-1573.

41.   Chatgilialoglu, C.; Newcomb, M., *Hydrogen Donor Abilities of the Group 14 Hydrides*. Academic Press: 1999; Vol. 44, 67-112.

42.   Schlecht, C.; Klammer, H.; Jarry, H.; Wuttke, W. Effects of estradiol, benzophenone-2 and benzophenone-3 on the expression pattern of the estrogen receptors (ER) alpha and beta, the estrogen receptor-related receptor 1 (ERR1) and the aryl hydrocarbon receptor (AhR) in adult ovariectomized rats. *Toxicology* **2004,** 205 (1-2), 123-30.

43.   Angel Lago, M.; Rodriguez, A.; Sendón, R.; Bustos, J.; Teresa Nieto, M.; Paseiro, P. Photoinitiators: a food safety review. **2015,** 32, 780-798.

44.   EFSA. Opinion of the Scientific Panel on food additives, flavourings, processing aids and materials in contact with food (AFC) related to 2-Isopropyl thioxanthone (ITX) and 2-ethylhexyl-4-dimethylaminobenzoate (EHDAB) in food contact materials. *EFSA Journal* **2005,** 3 (12), 293.

45.   IACR. Benzophenone. *IARC Monogr. Eval. Carcinog. Risks Hum.* **2013,** 101, 284-304.

46.   Nakagawa, Y.; Tayama, K. Benzophenone-induced estrogenic potency in ovariectomized rats. *Arch. Toxicol.* **2002,** 76 (12), 727-731.

47.   Nakagawa, Y.; Tayama, K. Estrogenic potency of benzophenone and its metabolites in juvenile female rats. *Arch. Toxicol.* **2001,** 75 (2), 74-79.

48.   Suzuki, T.; Kitamura, S.; Khota, R.; Sugihara, K.; Fujimoto, N.; Ohta, S. Estrogenic and antiandrogenic activities of 17 benzophenone derivatives used as UV stabilizers and sunscreens. *Toxicol. Appl. Pharmacol.* **2005,** 203 (1), 9-17.

49.   Baro, J. P., W.; Raulfs, F.-W. Water-Based UV Inkjet - Novel Chemistry Approach for Food Packaging Applications *Tech. Conf. Proc., RadTech Europe 11* **2011**, i.d. 9.3.

50.   Liu, R.; Mabury, S. A. First Detection of Photoinitiators and Metabolites in Human Sera from United States Donors. *Environ. Sci. Technol.* **2018,** 52 (17), 10089-10096.

51.   Bouzrati-Zerelli, M.; Kirschner, J.; Fik, C. P.; Maier, M.; Dietlin, C.; Morlet-Savary, F.; Fouassier, J. P.; Becht, J. M.; Klee, J. E.; Lalevee, J. Silyl Glyoxylates as a New Class of High Performance Photoinitiators: Blue LED Induced Polymerization of Methacrylates in Thin and Thick Films. *Macromolecules* **2017,** 50 (17), 6911-6923.

52.   Hammond, G. S.; Turro, N. J.; Leermakers, P. A. Direct and Sensitized Photolysis of Ethyl Pyruvate. *J. Am. Chem. Soc.* **1961,** 83 (10), 2395-2396.

53.   Leermakers, P. A.; Warren, P. C.; Vesley, G. F. Photochemistry of Alpha-Keto Acids + Alpha-Keto Esters .2. Solution Phase Photodecomposition of Alpha-Keto Esters. *J. Am. Chem. Soc.* **1964,** 86 (9), 1768-1771.

54.   Evans, T. R.; A., L. P. Norrish Type 2 Process in Alpha-Keto Acids Photolysis of Alpha-Ketodecanoic Acid in Benzene. *J. Am. Chem. Soc.* **1968,** 90 (7), 1840-1842.

55.   Nakadair.Y; Hirota, Y.; Nakanish.K. Photochemical Reactions of Non-Enolizable Alpha-Keto-Esters Derived from Dehydroginkgolide A. *Journal of the Chemical Society D-Chemical Communications* **1969,** (24), 1469-&.

56.   Samuni, A.; Behar, D.; Fessenden, R. W. Electron spin resonance study of radicals produced in the photolysis of .alpha.-keto acids and esters. *The Journal of Physical Chemistry* **1973,** 77 (6), 777-780.

57.   Davidson, R. S.; Goodwin, D.; de Violet, P. F. The mechanism of the norrish type II reaction of α-keto-acids and esters. *Tetrahedron Lett.* **1981,** 22 (26), 2485-2486.

58.   Rochat, S.; Minardi, C.; de Saint Laumer, J.-Y.; Herrmann, A. Controlled Release of Perfumery Aldehydes and Ketones by Norrish Type-II Photofragmentation of α-Keto Esters in Undegassed Solution. *Helv Chim Acta* **2000,** 83 (7), 1645-1671.

59.   Nitsch, D.; Huber, S. M.; Poethig, A.; Narayanan, A.; Olah, G. A.; Prakash, G. K. S.; Bach, T. Chiral propargylic cations as intermediates in SN1-type reactions: Substitution pattern, nuclear magnetic resonance studies, and origin of the diastereoselectivity. *J. Am. Chem. Soc.* **2014,** 136 (7), 2851 - 2857.

60.   Dubois, J. E.; Bauer, P. Metathetical transposition of bis-tert-alkyl ketones. 1. A model for a study of group migration. *J. Am. Chem. Soc.* **1976,** 98 (22), 6993 - 6999.

61.   Fouassier, J. P.; Lalevée, J., *Radical Photoinitiating Systems*. Wiley-VCH Verlag GmbH & Co. KGaA: 2012; 123-125.

62.   Hu, S. K.; Wu, X. S.; Neckers, D. C. Methyl phenylglyoxylate as a photoinitiator. *Macromolecules* **2000,** 33 (11), 4030-4033.

63.   Dietlin, C.; Schweizer, S.; Xiao, P.; Zhang, J.; Morlet-Savary, F.; Graff, B.; Fouassier, J. P.; Lalevee, J. Photopolymerization upon LEDs: new photoinitiating systems and strategies. *Polym. Chem.* **2015,** 6 (21), 3895-3912.

64.   Rambaud, M.; Bakasse, M.; Duguay, G.; Villieras, J. A One-Step Synthesis of Alkyl 2-Oxo-3-alkenoates from Alkenyl Grignard Reagents and Dialkyl Oxalates. *Synthesis* **1988,** (7), 564 - 566.

65.   Imoto, H.; Imamiya, E.; Momose, Y.; Sugiyama, Y.; Kimura, H.; Sohda, T. Studies on non-thiazolidinedione antidiabetic agents. 1. Discovery of novel oxyiminoacetic acid derivatives. *Chem. Pharm. Bull.* **2002,** 50 (10), 1349 - 1357.

66.   Adiwidjaja, G.; Günther, H.; Voß, J. Entstehen bei der Reaktion von Methylketonen mit Thionylchlorid α-Oxo-thiocarbonsäurechloride? *Angew. Chem.* **1980,** 92 (7), 559-561.

67.   Gathergood, N.; Juhl, K.; Poulsen, T. B.; Thordrup, K.; Jorgensen, K. A. Direct catalytic asymmetric aldol reactions of pyruvates: scope and mechanism. *Org. Biomol. Chem.* **2004,** 2 (7), 1077-1085.

68.   Staben, S. F., Jianwen; Loke, Pui Leng; Montalbetti, Christian A. G. N. Preparation of heterocyclic propargylic alcohol compounds as NF-κB inducing kinase inhibitors for treating inflammations. US20120214762A1 2012.

69.   Kashiwabara, T.; Tanaka, M. Rhodium-catalyzed addition of alpha-keto acid chlorides with terminal alkynes. *Adv. Synth. Catal.* **2011,** 353 (9), 1485 - 1490.

70.   Min, S.; More, S. V.; Park, S. Y.; Choi, D.-K.; Park, J.-Y.; Yoon, S.-H.; Jeon, S.-B.; Park, E.-J. EOP, a newly synthesized ethyl pyruvate derivative, attenuates the production of inflammatory mediators via p38, ERK and NF-kappaB pathways in lipopolysaccharide-activated BV-2 microglial cells. *Molecules* **2014,** 19 (12), 19361 - 19375.

71.   Heaney, F.; Fenlon, J.; McArdle, P.; Cunningham, D. alpha-Keto amides as precursors to heterocycles-generation and cycloaddition reactions of piperazin-5-one nitrones. *Organic and Biomolecular Chemistry* **2003,** 1 (7), 1122 - 1132.

72.   Ishibashi, H.; Kobayashi, T.; MacHida, N.; Tamura, O. A new efficient route to (?)-physostigmine and (?)-physovenine by means of 5-exo selective aryl radical cyclization of o-bromo-N- acryloylanilides. *Tetrahedron* **2000,** 56 (11), 1469 - 1473.

73.   Huse, K. B., Gerd; Birkenmeier, Monika; Substances and Pharmaceutical Compositions for the Inhibition of Glyoxalases and Their Use As Anti-Fungal Agents. US2008/300303, 2008.

74.   Adiwidjaja, G.; Guenther, H.; Voss, J. Entstehen bei der Reaktion von Methylketonen mit Thionylchlorid alpha-Oxo-thiocarbonsaeurechloride? *Angew. Chem.* **1980,** 92 (7), 559 - 561.

75.   Gonz?lez, L.; Jim?nez, R.; Mart?nez De, B.; Gar?n; Orduna; Villacampa; Blesa. Using functionalized nonlinear optical chromophores to prepare NLO-active polycarbonate films. *Dyes and Pigments* **2015,** 119, 30 - 40.

76.   De Kimpe, N.; De Buyck, L.; Verhé, R.; Schamp, N. Facile Synthesis of 2-Alkoxy-2-aryloxiranes. *Chem. Ber.* **1983,** 116 (11), 3631-3636.

77.   Cope; Graham. *J. Am. Chem. Soc.* **1951,** 73, 4702,4705.

78.   Cavicchioni. Bromoamides as starting materials in the synthesis of alpha-hydroxy- and alpha-alkoxy derivatives. *Synth. Commun.* **1994,** 24 (16), 2223 - 2227.

79.   YOSHIHIRO, M. T. Y. T. A. H. T. PIPERIDINE COMPOUND AND PROCESS FOR PREPARING THE SAME. WO2006/4195, 2006.

80.   Fujihara; Hirakura; Mizoguchi; Kawanishi; Sugihara; Ohshiro. Synthesis and evaluation of the local anesthetic activity of a series of aliphatic amino acid anilides. *Yakugaku zasshi : Journal of the Pharmaceutical Society of Japan* **1969,** 89 (1), 88 - 97.

81.   Goswami, P. C.; Swanton, D. J.; Henry, B. R. Evidence for vibronic coupling contributions to overtone intensities in alkyl phenyl ketones. *J. Chem. Phys.* **1987,** 86 (10), 5281 - 5287.

82.   Blanco, L.; Amice, P.; Conia, J.-M. Reaction of Chloromethylcarbene with Trimethylsilyl Enol Ethers; Preparation of alpha-Methylene Ketones and alpha-Methyl-alpha,beta-unsaturated Ketones and Aldehydes. *Synthesis* **1981,** (4), 291 - 293.

83.   Leonard, N. J.; Mader, P. M. The Influence of Steric Configuration on the Ultraviolet Absorption of 1,2-Diketones. *J. Am. Chem. Soc.* **1950,** 72 (12), 5388-5397.

84.   Calvin, M.; Wood, C. L. Conjugation of Carbonyl Groups and the Absorption Spectrum of Triketopentane. *J. Am. Chem. Soc.* **1940,** 62 (11), 3152-3155.

85.   Yamazaki, T.; Takizawa, T.; Oohama, T.; Doiuchi, T. Studies on Cyclic Vic-Polyketones .1. Syntheses and Characterization of 1,2-Disubstituted Cyclopentenetriones. *Chem. Pharm. Bull. (Tokyo)* **1972,** 20 (2), 238-+.

86.   DULIN, M. B. W. X. D. S. Z. F. Y. Preparation method for phosphorus-containing alpha-keto ester. CN105175443 2015.

87.   Schnermann, M. J.; Romero, F. A.; Hwang, I.; Nakamaru-Ogiso, E.; Yagi, T.; Boger, D. L. Total Synthesis of Piericidin A1 and B1 and Key Analogues. *J. Am. Chem. Soc.* **2006,** 128 (36), 11799-11807.

88.   ARRIMAN GERALDINE, C. M., CRAIG E; HARWOOD, JAMES ; BHAT, SATHESH; GREENWOOD, JEREMY ROBERT ACC INHIBITORS AND USES THEREOF 2013.

89.   Ma, B. W., Xiaoguang; Du, Shenghua; Zeng, Fanliang; Yin, Dulin A phosphorus-containing alpha-keto ester preparation method of the (by machine translation). CN105175443, 2017.

90.   Schnermann, M. J.; Romero, F. A.; Hwang, I.; Nakamaru-Ogiso, E.; Yagi, T.; Boger, D. L. Total synthesis of piericidin A1 and B1 and key analogues. *J. Am. Chem. Soc.* **2006,** 128 (36), 11799 - 11807.

91.   Taylor, P. G.; University, T. O.; Clark, G.; Smart, L. E., *Mechanism and Synthesis.* Royal Society of Chemistry: 2007; 85.

92.   Wang, X.-j.; Zhang, L.; Sun, X.; Xu, Y.; Krishnamurthy, D.; Senanayake, C. H. Addition of Grignard Reagents to Aryl Acid Chlorides: An Efficient Synthesis of Aryl Ketones. *Org. Lett.* **2005,** 7 (25), 5593-5595.

93.   Marsini, M. A.; Reeves, J. T.; Desrosiers, J.-N.; Herbage, M. A.; Savoie, J.; Li, Z.; Fandrick, K. R.; Sader, C. A.; McKibben, B.; Gao, D. A.; Cui, J.; Gonnella, N. C.; Lee, H.; Wei, X.; Roschangar, F.; Lu, B. Z.; Senanayake, C. H. Diastereoselective Synthesis of alpha-Quaternary Aziridine-2-carboxylates via Aza-Corey-Chaykovsky Aziridination of N-tert-Butanesulfinyl Ketimino Esters. *Org. Lett.* **2015,** 17 (22), 5614 - 5617.

94.   Evans, D. A.; Kvaerno, L.; Dunn, T. B.; Beauchemin, A.; Raymer, B.; Mulder, J. A.; Olhava, E. J.; Juhl, M.; Kagechika, K.; Favor, D. A. Total synthesis of (+)-azaspiracid-1. An exhibition of the intricacies of complex molecule synthesis. *J. Am. Chem. Soc.* **2008,** 130 (48), 16295 - 16309.

95.   Klee, J. E. S., Florian; Maier, Maximilian; Ritter, Helmut; Lalevee, Jacques; Fouassier, Jean Pierre; Morlet-Savary, Fabrice; Dietlin, Celine; Bouzrati-Zerelli, Mariem; Fik, Christoph P. Dental composition comprising polymn. initiator system with acylsilyl-or acylgermanyl-group containing compd. 2017.

96.   Drake, J. E.; Khasrou, L. N.; Majid, A. Trimethylgermyl-methane and -trifluoromethane-sulfonates. *J. Inorg. Nucl. Chem.* **1981,** 43 (7), 1473-1478.

97.   Mckenna, C. E.; Levy, J. N. Alpha-Keto Phosphonoacetates. *Journal of the Chemical Society-Chemical Communications* **1989,** (4), 246-247.

98.   Kreutzkamp, N.; Mengel, W. Darstellung einiger γ- und α-Dicarbonyl-phosphonsäure-ester. 10. Mitt. über Carbonyl- und Cyan-phosphonester. *Arch. Pharm.* **1967,** 300 (5), 389-392.

99.   De Nanteuil, F.; Waser, J. Catalytic [3+2] annulation of aminocyclopropanes for the enantiospecific synthesis of cyclopentylamines. *Angewandte Chemie - International Edition* **2011,** 50 (50), 12075 - 12079.

100.   Prasad, K.; Kneussel, P.; Schulz, G.; Stuetz, P. A NEW METHOD OF CARBON EXTENSION AT C-4 OF AZETIDINONES. *Tetrahedron Lett.* **1982,** 23 (12), 1247 - 1250.

101.   Lee; Yuk. An improved and efficient method for diazo transfer reaction of active methylene compounds. *Synth. Commun.* **1995,** 25 (10), 1511 - 1515.

102.   Ghosh, A. K.; Bischoff, A.; Cappiello, J. Asymmetric total synthesis of the gastroprotective microbial agent AI-77-B. *Eur. J. Org. Chem.* **2003,** (5), 821 - 832.

103.   Lee, J. C.; Yuk, J. Y. An Improved and Efficient Method for Diazo Transfer-Reaction of Active Methylene-Compounds. *Synth. Commun.* **1995,** 25 (10), 1511-1515.

104.   McKenna, C. E. K., B.A., *New Aspects in Phosphorus Chemistry I.* 2002.

105.   Kunugi, A.; Abe, K. The Cathodic Desulfonylation of 1-Ethoxycarbonyl- and 1-Cyano-1-(p-tolylsulfonyl)-2-phenylethenes at the Mercury Electrode in Nonaqueous Solvents. *Bull. Chem. Soc. Jpn.* **1988,** 61, 3329 - 3331.

106.   Davis, O. A.; Croft, R. A.; Bull, J. A. Synthesis of diversely functionalised 2,2-disubstituted oxetanes: fragment motifs in new chemical space. *Chem. Commun.* **2015,** 51 (84), 15446-15449.

107.   Anschütz, R.; Parlato, E. Ueber den Oxomalonsäureäthylester. *Berichte der deutschen chemischen Gesellschaft* **1892,** 25 (2), 3614-3617.

108.   Dalton, J. C.; Bourque, R. A. Mechanistic photochemistry of acylsilanes. 2. Reaction with electron-poor olefins. *J. Am. Chem. Soc.* **1981,** 103 (3), 699-700.

109.   Brook, A. G., *The Photochemistry of Organosilicon Compounds*. 1998.

110.   Taraban, M. V., Olga; Kruppa Alexander I.; Leshina, Tatyana V. , *Radical Reaction Mechanisms of and at Organic Germanium, Tin and Lead.* 2009; 589 - 594.

111.   Arnett, J. F.; Newkome, G.; Mattice, W. L.; McGlynn, S. P. Excited electronic states of the .alpha.-dicarbonyls. *J. Am. Chem. Soc.* **1974,** 96 (14), 4385-4392.

112.   Hyatt, J. L.; Wadkins, R. M.; Tsurkan, L.; Hicks, L. D.; Hatfield, M. J.; Edwards, C. C.; Ross, C. R.; Cantalupo, S. A.; Crundwell, G.; Danks, M. K.; Guy, R. K.; Potter, P. M. Planarity and Constraint of the Carbonyl Groups in 1,2-Diones Are Determinants for Selective Inhibition of Human Carboxylesterase 1. *J. Med. Chem.* **2007,** 50 (23), 5727-5734.

113.   Page, P. C. M., M. J.; Klair, S. S.; Rosenthal, S., *Acyl Silanes*. 2003.

114.   www.petrochemistry.eu Acrylic monomers. https://www.petrochemistry.eu/sector-group/acrylic-monomers/ (23.01.2019),

115.   ECHA Hexamethylen diacrylate. https://echa.europa.eu/substance-information/-/substanceinfo/100.032.641

116.   Hu, S. K.; Neckers, D. C. Alkyl phenylglyoxylates as radical photoinitiators creating negative photoimages. *J. Mater. Chem.* **1997,** 7 (9), 1737-1740.

117.   Bryant, S. J.; Nuttelman, C. R.; Anseth, K. S. Cytocompatibility of UV and visible light photoinitiating systems on cultured NIH/3T3 fibroblasts in vitro. *J. Biomater. Sci. Polym. Ed.* **2000,** 11 (5), 439-57.

118.   Peutzfeldt, A.; Asmussen, E. Hardness of restorative resins: effect of camphorquinone, amine, and inhibitor. *Acta Odontol. Scand.* **1989,** 47 (4), 229-31.

119.   Davidson, R. S. The chemistry of photoinitiators — some recent developments. *J. Photochem. Photobiol. A: Chem.* **1993,** 73 (2), 81-96.

120.   Lissi, E. A.; Encina, M. V. Polymerization Photosensitized by Carbonyl-Compounds. *J Polym Sci Pol Chem* **1979,** 17 (9), 2791-2803.

121.   Florio, J. J.; Miller, D. J., *Handbook Of Coating Additives*. Taylor & Francis: 2004.

122.   Misra, H.; Mehta, B.; Jain, d. c., *Optimization of Extraction Conditions and HPTLC - UV Method for Determination of Quinine in Different Extracts of Cinchona species Bark*. 2008; Vol. 2.

123.   Bryce-Smith, D., *Photochemistry*. Chemical Society.: 1971; 548.

124.   Bouzrati-Zerelli, M.; Kirschner, J.; Fik, C. P.; Maier, M.; Dietlin, C.; Morlet-Savary, F.; Fouassier, J. P.; Becht, J.-M.; Klee, J. E.; Lalevée, J. Silyl Glyoxylates as a New Class of High Performance Photoinitiators: Blue LED Induced Polymerization of Methacrylates in Thin and Thick Films. *Macromolecules* **2017,** 50 (17), 6911-6923.

125.   Caló, E.; Khutoryanskiy, V. V. Biomedical applications of hydrogels: A review of patents and commercial products. *Eur. Polym. J.* **2015,** 65, 252-267.

126.   Hult, A.; Rånby, B. Photo-stability of photo-cured organic coatings: Part II—Yellowing and photo-oxidation of thioxanthone/amine photo-cured organic coatings. *Polym. Degradation Stab.* **1984,** 8 (2), 89-105.

127.   Sehnal, P.; Harper, K.; T. Rose, A.; G. Anderson, D.; A. Green, W.; Husár, B.; Griesser, M.; Liska, R., *Novel Phosphine Oxide Photoinitiators*. 2014.

128.   Segurola, J.; Allen, N. S.; Edge, M.; McMahon, A.; Wilson, S. Photoyellowing and discolouration of UV cured acrylated clear coatings systems: influence of photoinitiator type. *Polym. Degradation Stab.* **1999,** 64 (1), 39-48.

129.   Scaiano, J. C.; Encinas, M. V.; Lissi, E. A.; Zanocco, A.; Das, P. K. Photochemistry of Alkyl Pyruvates. *J Photochem* **1986,** 33 (2), 229-236.

130.   Zanocco, A. L.; Soto, E. A.; Lissi, E. A.; Scaiano, J. C. Photochemistry of Ethyl-Esters of Alpha-Oxo-Carboxylic Acids. *J Photoch Photobio A* **1990,** 53 (1), 77-85.

131.   Meijs, G. F.; Rizzardo, E. Chain Transfer by an Addition-Fragmentation Mechanism - the Use of Alpha-Benzyloxystyrene for the Preparation of Low-Molecular-Weight Poly(Methyl Methacrylate) and Polystyrene. *Makromol Chem-Rapid* **1988,** 9 (8), 547-551.

132. Meijs, G. F.; Rizzardo, E.; Thang, S. H. Preparation of Controlled Molecular-Weight, Olefin-Terminated Polymers by Free-Radical Methods - Chain Transfer Using Allylic Sulfides. *Macromolecules* **1988,** 21 (10), 3122-3124.

133. Park, H. Y.; Kloxin, C. J.; Scott, T. F.; Bowman, C. N. Stress Relaxation by Addition-Fragmentation Chain Transfer in Highly Cross-Linked Thiol-Yne Networks. *Macromolecules* **2010,** 43 (24), 10188-10190.

134. Moad, G.; Rizzardo, E.; Thang, S. H. Radical addition -fragmentation chemistry in polymer synthesis. *Polymer* **2008,** 49 (5), 1079-1131.

135. Colombani, D.; Chaumont, P. Addition-fragmentation processes in free radical polymerization. *Progress in Polymer Science* **1996,** 21 (3), 439-503.

136. Meijs, G. F.; Rizzardo, E. The use of activated benzyl vinyl ethers to control molecular weight in free radical polymerizations. *Die Makromolekulare Chemie* **1990,** 191 (7), 1545-1553.

137. Rizzardo, E.; Chong, Y. K.; Evans, R. A.; And, G. M.; Thang, S. H. Control of polymer structure by chain transfer processes. *Macromolecular Symposia* **1996,** 111 (1), 1-11.

138. Busfield, W. K.; Zayas-Holdsworth, C. I.; Thang, S. H. End-functionalized copolymers prepared by the addition–fragmentation chain-transfer method: Vinyl acetate/methacrylonitrile system. *J. Polym. Sci., Part A: Polym. Chem.* **2001,** 39 (17), 2911-2919.

139. Seidler, K. Photopolymer Networks with Homogeneous Polymer Architectures. TU Wien, Vienna, 2016.

140. Chaumont, P.; Colombani, D. Chain Transfer by Addition Substitution Mechanism .4. Alkyl Permethacrylates - a New Class of Polymerization Regulators. *Macromol. Chem. Phys.* **1995,** 196 (3), 947-955.

141. Cramer, N. B.; Couch, C. L.; Schreck, K. M.; Carioscia, J. A.; Boulden, J. E.; Stansbury, J. W.; Bowman, C. N. Investigation of thiol-ene and thiol-ene-methacrylate based resins as dental restorative materials. *Dent. Mater.* **2010,** 26 (1), 21-28.

142. Gauss, P.; Ligon-Auer, S. C.; Griesser, M.; Gorsche, C.; Svajdlenkova, H.; Koch, T.; Moszner, N.; Liska, R. The Influence of Vinyl Activating Groups on beta-Allyl Sulfone-Based Chain Transfer Agents for Tough Methacrylate Networks. *J Polym Sci Pol Chem* **2016,** 54 (10), 1417-1427.

143. Seidler, K.; Griesser, M.; Kury, M.; Harikrishna, R.; Dorfinger, P.; Koch, T.; Svirkova, A.; Marchetti-Deschmann, M.; Stampfl, J.; Moszner, N.; Gorsche, C.; Liska, R. Vinyl Sulfonate Esters: Efficient Chain Transfer Agents for the 3D Printing of Tough Photopolymers without Retardation. *Angew Chem Int Edit* **2018,** 57 (29), 9165-9169.

144. Taylor, G. E.; Gosling, M.; Pearce, A. Low level determination of p-toluenesulfonate and benzenesulfonate esters in drug substance by high performance liquid chromatography/mass spectrometry. *J. Chromatogr.* **2006,** 1119 (1), 231-237.

145. Glowienke, S.; Frieauff, W.; Allmendinger, T.; Martus, H.-J.; Suter, W.; Mueller, L. Structure–activity considerations and in vitro approaches to assess the genotoxicity of 19 methane-, benzene- and toluenesulfonic acid esters. *Mutation Research/Genetic Toxicology and Environmental Mutagenesis* **2005,** 581 (1), 23-34.

146. Barton, D. H. R.; Chern, C.-Y.; Jaszberenyi, J. C. The invention of radical reactions. Part XXXIV. Homologation of carboxylic acids to α-keto carboxylic acids by Barton-ester based radical chain chemistry. *Tetrahedron* **1995,** 51 (7), 1867-1886.

147. Albert, B. J.; Yamamoto, H. A Triple-Aldol Cascade Reaction for the Rapid Assembly of Polyketides. *Angew. Chem. Int. Ed.* **2010,** 49 (15), 2747-2749.

148. Lalevee, J.; Tehfe, M. A.; Allonas, X.; Fouassier, J. P. Boryl Radicals as a New Photoinitiating Species: A Way to Reduce the Oxygen Inhibition. *Macromolecules* **2008,** 41 (23), 9057-9062.

149. Fyfe, J. W. B.; Watson, A. J. B. Recent Developments in Organoboron Chemistry: Old Dogs, New Tricks. *Chem* **2017,** 3 (1), 31-55.

150. Sana, M.; Leroy, G.; Wilante, C. Enthalpies of Formation and Bond-Energies in Lithium, Beryllium, and Boron Derivatives - a Theoretical Attempt for Data Rationalization. *Organometallics* **1991,** 10 (1), 264-270.

151. Bettinger, H. F.; Filthaus, M.; Bornemann, H.; Oppel, I. M. Metal-free conversion of methane and cycloalkanes to amines and amides by employing a borylnitrene. *Angewandte Chemie - International Edition* **2008,** 47 (25), 4744 - 4747.

152. Kuwajima, I.; Nakamura, E. Reactive enolates from enol silyl ethers. *Acc. Chem. Res.* **1985,** 18 (6), 181-187.

153. Pattenden, G., *General and Synthetic Methods*. Royal Society of Chemistry: 2007.

154. Baechler, R. D.; Filippo, L. J. S.; Schroll, A. STRUCTURAL EFFECTS UPON COMPETITIVE DECOMPOSITION PATHWAYS OF THIOSULFOXIDE INTERMEDIATES. *Tetrahedron Lett.* **1981,** 22 (52), 5247 - 5250.

155. Tuladhar, S. M.; Fallis, A. G. Phenylsulfenyl chloride/N,N-diisopropylethylamine: A useful reagent for cyclic ether formation (sulfenyletherification). *Tetrahedron Lett.* **1987,** 28 (5), 523-526.

156.   Braverman, S.; Pechenick, T.; Gottlieb, H. E. Tandem sigmatropic rearrangements and cyclizations of propargylic dialkoxy disulfides. *Tetrahedron Lett.* **2003,** 44 (4), 777-780.
157.   Tardif, S. L.; Williams, C. R.; Harpp, D. N. Diatomic sulfur transfer from stable alkoxy disulfides. *J. Am. Chem. Soc.* **1995,** 117 (35), 9067 - 9068.
158.   Chiral diphosphorus compounds and transition metal complexes thereof. EP1400527, 2004.
159.   Houlihan, F.; Bouchard, F.; Frechet, J. M. J.; Willson, C. G. Phase-Transfer Catalysis in the Tert-Butyloxycarbonylation of Alcohols, Phenols, Enols, and Thiols with Di-Tert-Butyl Dicarbonate. *Canadian Journal of Chemistry-Revue Canadienne De Chimie* **1985,** 63 (1), 153-162.
160.   Lu, H.; Carioscia, J. A.; Stansbury, J. W.; Bowman, C. N. Investigations of step-growth thiol-ene polymerizations for novel dental restoratives. *Dental Materials* **2005,** 21 (12), 1129-1136.
161.   Cramer, N. B.; Bowman, C. N. Investigation into the kinetics of thiol-ene and thiol-acrylate photopolymerizations using real-time FTIR. *Abstr Pap Am Chem S* **2001,** 222, U284-U284.
162.   Gautier, A.; Garipova, G.; Dubert, O.; Oulyadi, H.; Piettre, S. R. Efficient and practical aerobic radical addition of thiophosphites to alkenes. *Tetrahedron Lett.* **2001,** 42 (33), 5673-5676.
163.   Guterman, R.; Kenaree, A. R.; Gilroy, J. B.; Gillies, E. R.; Ragogna, P. J. Polymer Network Formation Using the Phosphane-ene Reaction: A Thiol-ene Analogue with Diverse Postpolymerization Chemistry. *Chem. Mater.* **2015,** 27 (4), 1412-1419.
164.   Smirnova, L. A.; Semchikov, Y. D.; Kamyshenkova, L. I.; Sveshnikova, T. G.; Yegorochkin, A. N.; Kalinina, G. S.; Yegorov, B. A. Features of the chain-transfer reaction of group IV B organo-metal compounds. *Polymer Science U.S.S.R.* **1982,** 24 (5), 1127-1138.
165.   Bouzrati-Zerelli, M.; Maier, M.; Dietlin, C.; Fabrice, M.-S.; Fouassier, J. P.; Klee, J. E.; Lalevée, J. A novel photoinitiating system producing germyl radicals for the polymerization of representative methacrylate resins: Camphorquinone/R3GeH/iodonium salt. *Dent. Mater.* **2016,** 32 (10), 1226-1234.
166.   El-Roz, M.; Lalevée, J.; Allonas, X.; Fouassier, J.-P. The Silane-ene and Silane-Acrylate Polymerization Process: A New Promising Chemistry? *Macromol. Rapid Commun.* **2008,** 29 (10), 804-808.
167.   El-Roz, M.; Lalevee, J.; Allonas, X.; Fouassier, J. P. Mechanistic Investigation of the Silane, Germane, and Stannane Behavior When Incorporated in Type I and Type II Photoinitiators of Polymerization in Aerated Media. *Macromolecules* **2009,** 42 (22), 8725-8732.
168.   Chatgilialoglu, C.; Guerrini, A.; Lucarini, M. The trimethylsilyl substituent effect on the reactivity of silanes. Structural correlations between silyl radicals and their parent silanes. *The Journal of Organic Chemistry* **1992,** 57 (12), 3405-3409.
169.   Chatgilialoglu, C. Structural and Chemical-Properties of Silyl Radicals. *Chem. Rev.* **1995,** 95 (5), 1229-1251.
170.   Chatgilialoglu, C.; Timokhin, V. I. Silyl radicals in chemical synthesis. *Advances in Organometallic Chemistry, Vol 57* **2008,** 57, 117-181.
171.   Steindl, J.; Koch, T.; Moszner, N.; Gorsche, C. Silane-Acrylate Chemistry for Regulating Network Formation in Radical Photopolymerization. *Macromolecules* **2017,** 50 (19), 7448-7457.
172.   Steindl, J.; Svirkova, A.; Marchetti-Deschmann, M.; Moszner, N.; Gorsche, C. Light-Triggered Radical Silane-Ene Chemistry Using a Monosubstituted Bis(trimethylsilyl)silane. *Macromol. Chem. Phys.* **2017,** 218 (9).
173.   Zaborovskiy, A. B.; Lutsyk, D. S.; Prystansky, R. E.; Kopylets, V. I.; Timokhin, V. I.; Chatgilialoglu, C. A mechanistic investigation of (Me3Si)3SiH oxidation. *J. Organomet. Chem.* **2004,** 689 (18), 2912-2919.
174.   Chatgilialoglu, C., *Organosilanes in Radical Chemistry*. Wiley: 2004; 70.
175.   Chatgilialoglu, C.; Guarini, A.; Guerrini, A.; Seconi, G. Autoxidation of Tris(Trimethylsilyl)Silane. *J. Org. Chem.* **1992,** 57 (8), 2207-2208.
176.   Amrein, S. J. Silylierte Cyclohexadiene als neue Reagenzien in der Radikalchemie. ETH Zürich, 2002.
177.   Sparling, B. A.; Moebius, D. C.; Shair, M. D. Enantioselective total synthesis of hyperforin. *J. Am. Chem. Soc.* **2013,** 135 (2), 644 - 647.
178.   Zimmerman, H. E.; Wang, P. A. The regioselectivity of the Birch reduction. *J. Am. Chem. Soc.* **1993,** 115 (6), 2205-2216.
179.   Studer, A.; Amrein, S.; Schleth, F.; Schulte, T.; Walton, J. C. Silylated cyclohexadienes as new radical chain reducing reagents: Preparative and mechanistic aspects. *J. Am. Chem. Soc.* **2003,** 125 (19), 5726-5733.
180.   Amrein Stephan Johannes , S. A., Silylierte Cyclohexadiene als neue Reagenzien in der Radikalchemie. Zürich, E., Ed. 2002; p 86.
181.   Studer, A.; Amrein, S. Silylated Cyclohexadienes: New Alternatives to Tributyltin Hydride in Free Radical Chemistry. *Angew. Chem. Int. Ed.* **2000,** 39 (17), 3080-3082.
182.   Anderson, W. G. S. S. P. Polymer Testing, 2nd edition. **2005**.
183.   Oestreich, M. Transfer Hydrosilylation. *Angew Chem Int Edit* **2016,** 55 (2), 494-499.

184. Hudlicky, M. SYNTHESIS OF FLUORINATED alpha-DIKETONES AND SOME INTERMEDIATES. *J. Fluorine Chem.* **1981,** 18, 383 - 406.

185. Rabjohn, N.; Harbert, C. A. Decarboxylation and rearrangement of 3,3-dialkyl-2-oxocarboxylic acids. *J. Org. Chem.* **1970,** 35 (11), 3726 - 3729.

186. Ohno, A.; Ikeguchi, M.; Kimura, T.; Oka, S. Reduction by a model of NAD(P)H. 25. A chiral model which induces high asymmetry. *J. Am. Chem. Soc.* **1979,** 101 (23), 7036-7040.

187. Bauer, P.; Dubois, J. E. Metathetical transposition of bis-tert-alkyl ketones. 2. Structural effects on alkyl migration. Existence of linear relation networks. *J. Am. Chem. Soc.* **1976,** 98 (22), 6999-7007.

188. Eliel, E. L.; Hartmann, A. A. Convenient synthesis of .alpha.-keto esters. *The Journal of Organic Chemistry* **1972,** 37 (3), 505-506.

189. Wladislaw, B.; Marzorati, L.; Donnici, C. L.; Biaggio, F. C.; Neves, R. M. A.; Claro Jr, N. F. PTC sulfanylation of some carboxylic acids derivatives activated by alpha-sulfonyl or alpha-sulfinyl group, in solid-liquid system. *Phosphorus, Sulfur and Silicon and Related Elements* **1997,** 123, 197 - 208.

190. Tehrani, B.; Holmberg. Cationic ester-containing gemini surfactants: Physical-chemical properties. *Langmuir* **2010,** 26 (12), 9276 - 9282.

191. Seifert, P.; Vogel, E.; Rossi, A.; Schinz, H. Einige Reaktionen an Derivaten von α-Ketosäuren und α-Ketosäureestern. *Helv Chim Acta* **1950,** 33 (3), 725-736.

192. Wisaksono, W. W.; Arens, J. F. Chemistry of acetylenic ethers. LIII: Conversion of acetylenic ethers into α-ketoesters. *Recl. Trav. Chim. Pays-Bas* **1961,** 80, 846 - 848.

193. Pinard, E.; Burner, S.; Cueni, P.; Montavon, F. o.; Zimmerli, D. A short and efficient synthesis of the NMDA glycine site antagonist: (3R,4R)-3-amino-1-hydroxy-4-methyl pyrrolidin-2-one (L-687,414). *Tetrahedron Lett.* **2008,** 49 (42), 6079 - 6080.

194. Ioannou, M.; Porter, M. J.; Saez, F. Conversion of 1,3-oxathiolanes to 1,4-oxathianes using a silylated diazoester. *Tetrahedron* **2005,** 61 (1), 43-50.

195. Schöllkopf, U.; Bánhidai, B.; Scholz, H.-U. Metallsubstituierte Carbene und C-metallierte Diazoalkane, V. Trimethylgermyl-, Trimethylstannyl- und Trimethylplumbyl-äthoxycarbonylcarben aus Trimethylmetallyl-diazoessigsäureäthylestern. *Justus Liebigs Ann. Chem.* **1972,** 761 (1), 137-149.

196. Azeez, S.; Chaudhary, P.; Sureshbabu, P.; Sabiah, S.; Kandasamy, J. Tert -Butyl nitrite mediated nitrogen transfer reactions: Synthesis of benzotriazoles and azides at room temperature. *Organic and Biomolecular Chemistry* **2018,** 16 (37), 6902 - 6907.

197. Dressler, H.; Graham, J. E. *J. Org. Chem.* **1967,** 32, 985 - 990.

198. Chowdhry; Westheimer. p-Toluenesulfonyldiazoacetates: reagents for photoaffinity labeling. *Bioorg. Chem.* **1978,** 7 (2), 189 - 205.

199. Brandrup, J.; Immergut, E. H.; Grulke, E. A., *Polymer handbook, 4th edition.* 4th ed.; Wiley: New York ; Chichester, 2004; 368.

200. Sugimura, H.; Yoshida, K. A New Synthetic Method for alpha-Oxo-beta,gamma-unsaturated Esters. *Bull. Chem. Soc. Jpn.* **1992,** 65 (11), 3209 - 3211.

201. Herberich, G. E.; Fischer, A. Borylcyclopentadienides. *Organometallics* **1996,** 15 (1), 58 - 67.

202. Ivanov, I. K.; Parushev, I. D.; Christov, V. C. Bifunctionalized allenes, part XI: Competitive electrophilic cyclization and addition reactions of 4-phosphorylated allenecarboxylates. *Heteroat. Chem* **2014,** 25 (1), 60 - 71.

203. Amrein, S.; Studer, A. Silylated cyclohexadienes in radical chain hydrosilylations. *Helv Chim Acta* **2002,** 85 (10), 3559-3574.

204. Grellmann, W.; Seidler, S., *Polymer testing.* 2nd edition. ed.; 2005.

205. Menczel, J. D.; Prime, R. B., *Thermal analysis of polymers : fundamentals and applications.* John Wiley: Hoboken, N.J., 2009; 387-430.

Abbreviations

Δ	difference
°C	degree(s) Celcius
AFCT	addition fragmentation chain transfer
ATRP	atom transfer radical polymerization
AU	absorption units
BMA	benzyl methacrylate
CO	carbon monoxide
C_T	chain transfer constant

CTA	chain transfer agent
CTA	chain transfer agent
D3MA	decandiol dimethacrylate
DABCO	1,4-diazabicyclo[2.2.2]octane
DB	double bond
db%	double bond percent
DBC	double bond conversion
DBC_g	double bond conversion at gelpoint
DBPO	dibenzoylperoxide
DCM	methylene chloride
DIPEA	diisopropyl ethyl amine
DMAP	4-(dimethylamino)pyridine
DMF	dimethyl formamide
DMM	dental methacrylate mixture
DMTA	dynamical mechanical thermo analysis
DSC	differential scanning calorimetry
EDB	ethyl-4-dimethylaminobenzoate
EE	ethyl acetate
EP	ethyl pyruvate
eq.	equivalent
F_N	normal force
FT-IR	Fourier transformed infrared
G'	storage modulus
G''	loss modulus
GC-MS	gas chromatography-mass spectrometry
HAFCT	hydrogen abstraction chain transfer
HAFCT	hydrogen abstraction fragmentation chain transfer
HDDA	hexanediol diacrylate
HDDMA	hexanediol dimethacrylate
HOMO	highest occupied molecular orbital
IARC	International Agency of Cancer Research
LED	light emitting diode
LUMO	lowest unoccupied molecular orbital
mbar	millibar
MDEA	methyl diethanolamine
min	minutes
mL	milliliter
mM	millimolar
mmol	millimol
Mn	number average molecular weight
mol%	mole percent
Mp	melting point
MPa	mega Pascal

MPLC	medium pressure liquid chromatography
N	Newton
n_D^{20}	refractive index at 20 °C
n_D^{25}	refractive index at 25 °C
NIR	near infrared
nm	nanometer
NMP	nitroxide mediated polymerization
NMR	nuclear-magnetic-resonance
Pa	Pascal
PDI	polydispersity index
PE	petrolether
PEG	polyethylene glycol
Ph	phenyl group
PI	photoinitiator
PI	photo initiator
ppm	parts per million
q	evolved heat at maximum rate of polymerization
RAFT	reversible addition fragmentation chain transfer
R_f	relate to front
R_P	maximal rate of polymerization
RT	room temperature
RT	room temperature
RT-NIR	real time near infrared
s	seconds
SEC	size exclusion chromatography
t_{95}	time to 95% of total conversion
tan δ	dissipation factor
TEA	triethylamine
t_g	time to gelation
THF	tetrahydrofuran
TLC	thin layer chromatography
t_{max}	time to maximum rate of polymerization
tmax	time to maximal rate of poymerization
UDMA	urethane dimethacrylate
UV	ultra violet
Vis	visible light
VOC	volatile organic compound
w%	weight percent
ΔH_p	heat of polymerization
ε	molar extinction coefficient
λ	wavelength